

RADIOLOGY
AND
ONCOLOGY

vol.51 no.2
june 2017



NOVO



Cilja na 2 procesa nastanka CINV* v 1 odmerku
Zagotavlja učinkovito 5-dnevno preprečevanje CINV¹⁻⁵

En odmerek Dvojno delovanje 5-dnevno preprečevanje¹⁻⁵

Akynzeo[®]
netupitant/palonosetron

* CINV: Chemotherapy-induced nausea and vomiting
[Slabost in bruhanje povzročena s kemoterapijo]

1. Aapro M et al. Ann Oncol. 2014 Jul;25(7):1328-33.
2. Hesketh et al. Ann Oncol. 2014 Jul;25(7):1340-46.
3. Gralla RJ et al. Ann Oncol. 2014 Jul;25(7):1333-39.
4. Rojas C et al. Eur J Pharmacol. 2014 Jan 5;572:26-37.
5. Akynzeo SmPC, junij 2016

SKRAJŠAN POVZETEK GLAVNIH ZNAČILNOSTI ZDRAVILA

▼ Za to zdravilo se izvaja dodatno spremljanje varnosti. Tako bodo hitreje na voljo nove informacije o njegovi varnosti. Zdravstvene delavce naprošamo, da poročajo o katerem koli domnevnem neželenem učinku zdravila.

Akynzeo 300 mg/0,5 mg trde kapsule (netupitant/palonosetron)

TERAPEVTSKE INDIKACIJE Pri odraslih za preprečevanje akutne in zakasnjene navzee in bruhanja, povezanih z zelo emetogeno kemoterapijo na osnovi cisplatina za zdravljenje raka ter z zmerno emetogeno kemoterapijo za zdravljenje raka. **ODMERJANJE IN NAČIN UPORABE** Eno 300 mg/0,5 mg kapsulo je treba dati približno eno uro pred začetkom vsakega cikla kemoterapije. Trdo kapsulo je treba pogoltniti celo. Kapsulo je mogoče vzeti s hrano ali brez nje. Priporočeni peroralni odmerek deksametazona je treba ob sočasni uporabi z Akynzeom zmanjšati za približno 50 %. Prilagoditev odmerka pri starejših bolnikih ni potrebna. Pri uporabi tega zdravila pri bolnikih, starejših od 75 let, je potrebna previdnost zaradi daljšega razpolovnega časa zdravilnih učinkovin in omejenih izkušenj s to populacijo. Varnost in učinkovitost Akynzeo pri pediatrični populaciji nista bili dokazani. Prilagoditev odmerka pri bolnikih z blago do hudo okvaro ledvic predvidoma ni potrebna. Potrebno se je izogibati uporabi Akynzeo pri bolnikih s končnim stadijem bolezni ledvic, ki potrebujejo hemodializo. Pri bolnikih z blago ali zmerno okvaro jeter (stopnje 5-8 po lestvici Child-Pugh) prilagoditev odmerka ni potrebna. Pri bolnikih s hudo okvaro jeter (stopnja ≥ 9 po lestvici Child-Pugh) je treba Akynzeo uporabljati previdno. **KONTRAINDIKACIJE** Preobčutljivost na zdravilni učinkovini ali katero koli pomožno snov, nosečnost. **POSEBNA OPOZORILA IN PREVIDNOSTNI UKREPI** Ker lahko palonosetron podaljša čas prehoda skozi debelo črevo, je treba bolnike z anamnezo zaprtja ali znaki subakutne zapore črevesa po dajanju zdravila spremljati. Pri uporabi antagonistov 5-HT₃ samih ali v kombinaciji z drugimi serotonergičnimi zdravili (vključno s selektivnimi zaviralci ponovnega privzema serotonina (SSRI) in zaviralci ponovnega privzema serotonina in noradrenalina (SNRI)) so poročali o serotoninskem sindromu. Priporočamo ustrezno opazovanje bolnikov glede simptomov, podobnih kot pri serotoninskem sindromu. Ker Akynzeo vsebuje antagonist receptorjev 5-HT₃, je potrebna previdnost pri sočasni uporabi z zdravili, ki podaljšujejo interval QT, ali pri bolnikih, ki so razvili podaljšan interval QT, oziroma je verjetno, da ga bodo. Tega zdravila ne smemo uporabljati za preprečevanje navzee in bruhanja v dneh po kemoterapiji, razen v povezavi z dajanjem naslednjega cikla kemoterapije. Ne smemo ga uporabljati za zdravljenje navzee in bruhanja po kemoterapiji. Pri bolnikih s hudo okvaro jeter je potrebna previdnost, saj je za te bolnike na voljo malo podatkov. To zdravilo je treba uporabljati previdno pri bolnikih, ki sočasno peroralno prejemajo zdravilne učinkovine, ki se primarno presnavljajo prek CYP3A4 in imajo ozko terapevtsko območje. Netupitant je zmeren zaviralec CYP3A4 in lahko poveča izpostavljenost kemoterapevtskim zdravilom, ki so substrati za CYP3A4, npr. docetakselu. Zaradi tega je treba bolnike spremljati glede povečane toksičnosti kemoterapevtskih zdravil, ki so substrati za CYP3A4, vključno z irinotekanom. Poleg tega lahko netupitant vpliva tudi na učinkovitost kemoterapevtskih zdravil, pri katerih je potrebna aktivacija prek presnove s CYP3A4. Akynzeo vsebuje sorbitol in saharozo. Bolniki z redko dedno intoleranco za fruktozo, malabsorpcijo glukoze/galaktoze ali pomanjkanjem saharoza-izomaltaze ne smejo jemati tega zdravila. Poleg tega lahko vsebuje tudi sledi lecitina, pridobljenega iz soje. Zaradi tega je treba bolnike z znano preobčutljivostjo na arašide

ali sojo skrbno spremljati glede znakov alergijske reakcije. Ženske v rodni dobi ne smejo biti noseče ali zanosit med zdravljenjem z Akynzeom. Pred začetkom zdravljenja je treba opraviti test nosečnosti pri vseh ženskah, ki še niso imele menopavze. Ženske v rodni dobi morajo uporabljati učinkovito kontracepcijo med zdravljenjem in še do en mesec po njem. Akynzeo je kontraindiciran med nosečnostjo. Med zdravljenjem z Akynzeom in še 1 mesec po zadnjem odmerku je treba prenehati z dojenjem. **INTERAKCIJE** Ob sočasni uporabi Akynzeo z drugim zaviralcem CYP3A4 lahko pride do zvišanja plazemskih koncentracij netupitanta. Pri sočasni uporabi Akynzeo in zdravil, ki spodbujajo delovanje CYP3A4, lahko pride do znižanja plazemskih koncentracij netupitanta, kar lahko privede do zmanjšane učinkovitosti. Akynzeo lahko zviša plazemske koncentracije sočasno uporabljenih zdravil, ki se presnavljajo prek CYP3A4. Ob sočasnem dajanju deksametazona z Akynzeom je treba peroralni odmerek deksametazona zmanjšati za približno 50 %. Ob sočasnem dajanju z Akynzeom se je izpostavljenost docetakselu in etopozidu povečala za 37 % oziroma 21 %. Pri ciklofosfamidu po sočasnem dajanju netupitanta niso opazili konsistentnih učinkov. Pri eritromicinu, midazolamu ali drugih benzodiazepinih, ki se presnavljajo prek CYP3A4 (alprazolam, triazolam), je treba ob sočasnem dajanju Akynzeo upoštevati možne učinke njihovih zvišanih plazemskih koncentracij. Pri sočasnem dajanju Akynzeo z močnimi zaviralci CYP3A4 (npr. ketokonazol) je potrebna previdnost, sočasnemu dajanju z močnimi spodbujevalci CYP3A4 (npr. rifampicin) pa se je treba izogibati. Priporočamo previdnost pri uporabi netupitanta v kombinaciji s peroralnim substratom encima UGT2B7 (npr. zidovudin, valprojska kislina, morfin), ker *in vitro* podatki kažejo, da netupitant zavira UGT2B7. Priporočamo previdnost pri kombiniranju netupitanta z digoksinom ali drugimi substrati P-gp, kot sta dabigatran ali kolhicin, ker podatki *in vitro* kažejo, da je netupitant zaviralec P-gp. **NEŽELENI UČINKI** Pogosti ($\geq 1/100$ do $< 1/10$): glavobol, zaprtje, utrujenost. Občasni ($\geq 1/1.000$ do $< 1/100$): nevtropenija, levkocitoza, zmanjšan apetit, nespečnost, omotica, vrtoglavica, atrijski blok prve stopnje, kardiomiopatija, motnja prevajanja, hipertenzija, kolcanje, bolečina v trebuhu, driska, dispneja, naperjanje, navzea, alopecija, urtikarija, astenija, zvišane jetrne transaminaze, zvišana alkalna fosfataza v krvi, zvišan kreatinin v krvi, podaljšanje QT na elektrokardiogramu. Redki ($\geq 1/10.000$ do $< 1/1.000$): cistitis, levkopenija, limfocitoza, hipokalemija, akutna psihoza, sprememba razpoloženja, motnja spanja, hipestezija, konjunktivitis, zamegljen vid, aritmija, atrijski blok druge stopnje, kračni blok, popuščanje mitralne zaklopke, miokardna ishemija, ventrikularne extrasistole, hipotenzija, disgagija, obložen jezik, bolečina v hrbtu, občutek vročine, nekardialna bolečina v prsnem košu, nenormalen okus zdravila, zvišan bilirubin v krvi, zvišana kreatin fosfokinaza MB v krvi, depresija segmenta ST na elektrokardiogramu, nenormalen segment ST-T na elektrokardiogramu, zvišan troponin. **Vrsta ovojnine in vsebina:** Škatla z eno kapsulo v prebršenem omotu iz aluminija. **Režim izdaje:** Rp Imetnik dovoljenja za promet: Helsinn Birex Pharmaceuticals Ltd, Damastown, Mulhuddart, Dublin 15, Irska AKY-062016

Pred predpisovanjem in uporabo zdravila prosimo preberite celoten povzetek glavnih značilnosti zdravila!

Samo za strokovno javnost!
AKY0816-01, avgust 2016

 **PharmaSwiss**
Choose More Life

Odgovoren za trženje v Sloveniji:
PharmaSwiss d.o.o., Brodšiče 32, 1236 Trzin
telefon: +386 1 236 47 00, faks: +386 1 283 58 10

 **HEL SIN N**
Building quality cancer care together



Publisher

Association of Radiology and Oncology

Affiliated with

Slovenian Medical Association – Slovenian Association of Radiology, Nuclear Medicine Society,
Slovenian Society for Radiotherapy and Oncology, and Slovenian Cancer Society
Croatian Medical Association – Croatian Society of Radiology
Societas Radiologorum Hungarorum
Friuli-Venezia Giulia regional groups of S.I.R.M.
Italian Society of Medical Radiology

Aims and scope

Radiology and Oncology is a journal devoted to publication of original contributions in diagnostic and interventional radiology, computerized tomography, ultrasound, magnetic resonance, nuclear medicine, radiotherapy, clinical and experimental oncology, radiobiology, radiophysics and radiation protection.

Editor-in-Chief

Gregor Serša, Institute of Oncology Ljubljana,
Department of Experimental Oncology, Ljubljana,
Slovenia

Executive Editor

Viljem Kovač, Institute of Oncology Ljubljana,
Department of Radiation Oncology, Ljubljana, Slovenia

Deputy Editors

Andrej Čör, University of Primorska, Faculty of
Health Science, Izola, Slovenia

Maja Čemažar, Institute of Oncology Ljubljana,
Department of Experimental Oncology, Ljubljana,
Slovenia

Igor Kocijančič, University Medical Centre
Ljubljana, Institute of Radiology, Ljubljana, Slovenia

Karmen Stanič, Institute of Oncology Ljubljana,
Department of Radiation Oncology, Ljubljana, Slovenia

Primož Strojjan, Institute of Oncology Ljubljana,
Department of Radiation Oncology, Ljubljana, Slovenia

Editorial Board

Sotirios Bisdas, National Hospital for Neurology
and Neurosurgery, University College London
Hospitals, London, UK

Karl H. Bohuslavizki, Facharzt für
Nuklearmedizin, Hamburg, Germany

Serena Bonin, University of Trieste, Department of
Medical Sciences, Trieste, Italy

Boris Brkljačić, University Hospital "Dubrava",
Department of Diagnostic and Interventional
Radiology, Zagreb, Croatia

Luca Campana, Veneto Institute of Oncology
(IOV-IRCCS), Padova, Italy

Christian Ditttrich, Kaiser Franz Josef - Spital,
Vienna, Austria

Metka Filipič, National Institute of Biology,
Department of Genetic Toxicology and Cancer Biology,
Ljubljana, Slovenia

Maria Gódeny, National Institute of Oncology,
Budapest, Hungary

Janko Kos, University of Ljubljana, Faculty of
Pharmacy, Ljubljana, Slovenia

Robert Jeraj, University of Wisconsin, Carbone
Cancer Center, Madison, Wisconsin, USA

Advisory Committee

Tullio Girdali, University of Trieste, Faculty of
Medicine and Psychology, Trieste, Italy

Vassil Hadjidekov, Medical University,
Department of Diagnostic Imaging, Sofia, Bulgaria

Tamara Lah Turnšek, National Institute of
Biology, Ljubljana, Slovenia

Damijan Miklavčič, University of Ljubljana,
Faculty of Electrical Engineering, Ljubljana, Slovenia

Luka Milas, UT M. D. Anderson Cancer Center,
Houston, USA

Damir Miletić, Clinical Hospital Centre Rijeka,
Department of Radiology, Rijeka, Croatia

Håkan Nyström, Skandionkliniken,
Uppsala, Sweden

Maja Osmak, Ruder Bošković Institute,
Department of Molecular Biology, Zagreb, Croatia

Dušan Pavčnik, Dotter Interventional Institute,
Oregon Health Science University, Oregon,
Portland, USA

Geoffrey J. Pilkington, University of
Portsmouth, School of Pharmacy and Biomedical
Sciences, Portsmouth, UK

Ervin B. Podgoršak, McGill University,
Montreal, Canada

Matthew Podgorsak, Roswell Park Cancer
Institute, Departments of Biophysics and Radiation
Medicine, Buffalo, NY, USA

Marko Hočevar, Institute of Oncology Ljubljana,
Department of Surgical Oncology, Ljubljana, Slovenia

Miklós Kásler, National Institute of Oncology,
Budapest, Hungary

Csaba Polgar, National Institute of Oncology,
Budapest, Hungary

Dirk Rades, University of Lubeck, Department of
Radiation Oncology, Lubeck, Germany

Mirjana Rajer, Institute of Oncology Ljubljana,
Department of Radiation Oncology, Ljubljana, Slovenia

Luis Souhami, McGill University, Montreal,
Canada

Borut Štabuc, University Medical Centre Ljubljana,
Department of Gastroenterology, Ljubljana, Slovenia

Katarina Šurlan Popovič, University Medical
Center Ljubljana, Clinical Institute of Radiology,
Ljubljana, Slovenia

Justin Teissié, CNRS, IPBS, Toulouse, France

Gillian M. Tozer, University of Sheffield,
Academic Unit of Surgical Oncology, Royal
Hallamshire Hospital, Sheffield, UK

Andrea Veronesi, Centro di Riferimento
Oncologico - Aviano, Division of Medical Oncology,
Aviano, Italy

Branko Zakotnik, Institute of Oncology Ljubljana,
Department of Medical Oncology, Ljubljana, Slovenia

Stojan Plesničar, Institute of Oncology Ljubljana,
Department of Radiation Oncology, Ljubljana, Slovenia

Tomaž Benulič, Institute of Oncology Ljubljana,
Department of Radiation Oncology, Ljubljana, Slovenia

Editorial office

Radiology and Oncology

Zaloška cesta 2

P. O. Box 2217

SI-1000 Ljubljana

Slovenia

Phone: +386 1 5879 369

Phone/Fax: +386 1 5879 434

E-mail: gsera@onko-i.si

Copyright © Radiology and Oncology. All rights reserved.

Reader for English

Vida Kološa

Secretary

Mira Klemenčič

Zvezdana Vukmirović

Design

Monika Fink-Serša, Samo Rovar, Ivana Ljubanović

Layout

Matjaž Lužar

Printed by

Tiskarna Ozimek, Slovenia

Published quarterly in 400 copies

Beneficiary name: DRUŠTVO RADIOLOGIJE IN ONKOLOGIJE

Zaloška cesta 2

1000 Ljubljana

Slovenia

Beneficiary bank account number: SI56 02010-0090006751

IBAN: SI56 0201 0009 0006 751

Our bank name: Nova Ljubljanska banka, d.d.,

Ljubljana, Trg republike 2,

1520 Ljubljana; Slovenia

SWIFT: LJBASIX

Subscription fee for institutions EUR 100, individuals EUR 50

The publication of this journal is subsidized by the Slovenian Research Agency.

Indexed and abstracted by:

- *Celdes*
- *Chemical Abstracts Service (CAS)*
- *Chemical Abstracts Service (CAS) - SciFinder*
- *CNKI Scholar (China National Knowledge Infrastructure)*
- *CNPIEC*
- *DOAJ*
- *EBSCO - Biomedical Reference Collection*
- *EBSCO - Cinahl*
- *EBSCO - TOC Premier*
- *EBSCO Discovery Service*
- *Elsevier - EMBASE*
- *Elsevier - SCOPUS*
- *Google Scholar*
- *J-Gate*
- *JournalTOCs*
- *Naviga (Softweco)*
- *Primo Central (ExLibris)*
- *ProQuest - Advanced Technologies Database with Aerospace*
- *ProQuest - Health & Medical Complete*
- *ProQuest - Illustrata: Health Sciences*
- *ProQuest - Illustrata: Technology*
- *ProQuest - Medical Library*
- *ProQuest - Nursing & Allied Health Source*
- *ProQuest - Pharma Collection*
- *ProQuest - Public Health*
- *ProQuest - Science Journals*
- *ProQuest - SciTech Journals*
- *ProQuest - Technology Journals*
- *PubMed*
- *PubsHub*
- *ReadCube*
- *SCImago (SJR)*
- *Summon (Serials Solutions/ProQuest)*
- *TDOne (TDNet)*
- *Thomson Reuters - Journal Citation Reports/Science Edition*
- *Thomson Reuters - Science Citation Index Expanded*
- *Ulrich's Periodicals Directory/ulrichsweb*
- *WorldCat (OCLC)*

This journal is printed on acid-free paper

On the web: ISSN 1581-3207

<http://www.degruyter.com/view/j/raon>

<http://www.radioloncol.com>

contents

radiology

- 121 **Diffusion kurtosis imaging of gliomas grades II and III - a study of perilesional tumor infiltration, tumor grades and subtypes at clinical presentation**
Anna F. Delgado, Markus Fahlström, Markus Nilsson, Shala G. Berntsson, Maria Zetterling, Sylwia Libardó, Irina Alafuzoff, Danielle van Westen, Jimmy Lätt, Anja Smits, Elna-Marie Larsson
- 130 **Breast dynamic contrast enhanced MRI: fibrocystic changes presenting as a non-mass enhancement mimicking malignancy**
Zorica C. Milosevic, Mirjan M. Nadrljanski, Zorka M. Milovanovic, Nina Z. Gusic, Slavko S. Vucicevic, Olga S. Radulovic
- 137 **Evaluation of brain edema formation defined by MRI after LINAC-based stereotactic radiosurgery**
Maciej Harat, Andrzej Lebioda, Judyta Lasota, Roman Makarewicz

clinical oncology

- 142 **Genetic factors affecting intraoperative 5-aminolevulinic acid-induced fluorescence of diffuse gliomas**
Kiyotaka Saito, Toshinori Hirai, Hideo Takeshima, Yoshihito Kadota, Shinji Yamashita, Asya Ivanova, Kiyotaka Yokogami
- 151 **Single nucleotide polymorphisms in genes *MACC1*, *RAD18*, *MMP7* and *SDF-1a* as prognostic factors in resectable colorectal cancer**
Matej Horvat, Uros Potocnik, Katja Repnik, Rajko Kavalari, Vesna Zadnik, Stojan Potrc, Borut Stabuc
- 160 **MRI reduces variation of contouring for boost clinical target volume in breast cancer patients without surgical clips in the tumour bed**
Noora Al-Hammadi, Palmira Caparrotti, Saju Divakar, Mohamed Riyas, Suparna Halsnad Chandramouli, Rabih Hammoud, Jillian Hayes, Maeve Mc Garry, Satheesh Prasad Paloor, Primoz Petric
- 169 **The influence of the distal resection margin length on local recurrence and long-term survival in patients with rectal cancer after chemoradiotherapy and sphincter-preserving rectal resection**
Jan Grosek, Vaneja Velenik, Ibrahim Edhemovic, Mirko Omejc
- 178 **Clinical outcomes of 130 patients with primary and secondary lung tumors treated with Cyberknife robotic stereotactic body radiotherapy**
Zsolt Levente Janvary, Nicolas Jansen, Veronique Baart, Magali Devillers, David Dechambre, Eric Lenaerts, Laurence Seidel, Nicole Barthelemy, Patrick Berkovic, Akos Gulyban, Ferenc Lakosi, Zsolt Horvath, Philippe A. Coucke

- 187 **Genetic counselling, BRCA1/2 status and clinico-pathologic characteristics of patients with ovarian cancer before 50 years of age**
Mirjam Cvelbar, Marko Hocevar, Srdjan Novakovic, Vida Stegel, Andraz Perhavec, Mateja Krajc
- 195 **Insulin-like growth factor 1 receptor expression in advanced non-small-cell lung cancer and its impact on overall survival**
Mojca Humar, Izidor Kern, Gregor Vlacic, Vedran Hadzic, Tanja Cufer
- 203 **Carotid artery stiffness, digital endothelial function, and coronary calcium in patients with essential thrombocytosis, free of overt atherosclerotic disease**
Matjaz Vrtovec, Ajda Anzic, Irena Preloznik Zupan, Katja Zaletel, Ales Blinc
- 211 **Perioperative increase in neutrophil CD64 expression is an indicator for intra-abdominal infection after colorectal cancer surgery**
Milena Kerin Povsic, Bojana Beovic, Alojz Ihan
- 221 **Treatment-related cardiovascular toxicity in long-term survivors of testicular cancer**
Jasenska Gugic, Lorna Zadavec Zaletel, Irena Oblak

radiophysics

- 228 **Dosimetric predictors of treatment-related lymphopenia induced by palliative radiotherapy: predictive ability of dose-volume parameters based on body surface contour**
Tetsuo Saito, Ryo Toya, Tomohiko Matsuyama, Akiko Semba, Natsuo Oya
- 235 **Excess of radiation burden for young testicular cancer patients using automatic exposure control and contrast agent on whole-body computed tomography imaging**
Hannele Niiniviita, Jarmo Kulmala, Tuukka Pölönen, Heli Määttänen, Hannu Järvinen, Eeva Salminen

| *slovenian abstracts*

Diffusion kurtosis imaging of gliomas grades II and III - a study of perilesional tumor infiltration, tumor grades and subtypes at clinical presentation

Anna F. Delgado^{1,2}, Markus Fahlström¹, Markus Nilsson³, Shala G. Berntsson⁴, Maria Zetterling⁵, Sylwia Libard⁶, Irina Alafuzoff⁶, Danielle van Westen⁷, Jimmy Lätt⁸, Anja Smits⁴, Elna-Marie Larsson¹

¹ Department of Surgical Sciences, Radiology, Uppsala University, Uppsala, Sweden

² Department of Clinical Neuroscience, Karolinska Institute, Stockholm, Sweden

³ Bioimaging Center, Lund University, Lund, Sweden

⁴ Department of Neuroscience, Neurology, Uppsala University, Uppsala, Sweden

⁵ Department of Neuroscience, Neurosurgery, Uppsala University, Uppsala, Sweden

⁶ Department of Immunology, Genetics and Pathology, Section of pathology, Uppsala University Hospital and Uppsala University, Uppsala, Sweden

⁷ Clinical Sciences Lund, Diagnostic Radiology, Lund University, Lund, Sweden

⁸ Department of Imaging and Function, Skåne University Healthcare, Lund, Sweden

Radiol Oncol 2017; 51(2): 121-129.

Received 15 August 2016

Accepted 8 January 2017

Correspondence to: Dr. Anna Falk Delgado, Department of Surgical Sciences, Radiology, Uppsala University, Uppsala, Sweden.
Phone: +46 8517 70000; Fax +46 8 311101; E-mail: anna.falk-delgado@karolinska.se

Disclosure: No potential conflicts of interest were disclosed.

Background. Diffusion kurtosis imaging (DKI) allows for assessment of diffusion influenced by microcellular structures. We analyzed DKI in suspected low-grade gliomas prior to histopathological diagnosis. The aim was to investigate if diffusion parameters in the perilesional normal-appearing white matter (NAWM) differed from contralateral white matter, and to investigate differences between glioma malignancy grades II and III and glioma subtypes (astrocytomas and oligodendrogliomas).

Patients and methods. Forty-eight patients with suspected low-grade glioma were prospectively recruited to this institutional review board-approved study and investigated with preoperative DKI at 3T after written informed consent. Patients with histologically proven glioma grades II or III were further analyzed (n=35). Regions of interest (ROIs) were delineated on T2FLAIR images and co-registered to diffusion MRI parameter maps. Mean DKI data were compared between perilesional and contralateral NAWM (student's *t*-test for dependent samples, Wilcoxon matched pairs test). Histogram DKI data were compared between glioma types and glioma grades (multiple comparisons of mean ranks for all groups). The discriminating potential for DKI in assessing glioma type and grade was assessed with receiver operating characteristics (ROC) curves.

Results. There were significant differences in all mean DKI variables between perilesional and contralateral NAWM ($p < 0.000$), except for axial kurtosis ($p = 0.099$). Forty-four histogram variables differed significantly between glioma grades II (n=23) and III (n=12) ($p = 0.003-0.048$) and 10 variables differed significantly between ACs (n=18) and ODs (n=17) ($p = 0.011-0.050$). ROC curves of the best discriminating variables had an area under the curve (AUC) of 0.657-0.815.

Conclusions. Mean DKI variables in perilesional NAWM differ significantly from contralateral NAWM, suggesting altered microstructure by tumor infiltration not depicted on morphological MRI. Histogram analysis of DKI data identifies differences between glioma grades and subtypes.

Key words: diffusion kurtosis imaging (DKI); glioma; perilesional; tumor infiltration; grade, subtype

Introduction

Gliomas are neoplasms arising from neuroglial or precursor cells. Neuropathological classification is based on dominant cell type, malignancy grade atypia (I–IV), cell density, mitosis, endothelial proliferation, necrosis and genetic tumor properties.^{1,2} Astrocytomas (ACs) and oligodendrogliomas (ODs) are the most prevalent histological glioma subtypes. Neuropathologically glioma grade II differs from grade III primarily based on cell density and proliferation and may present with similar imaging patterns on morphological Magnetic resonance imaging (MRI), showing high signal intensity on T2-weighted images. Grade II and III gliomas typically do not display necrosis or ring-like contrast enhancement as do gliomas grade IV.^{3–5}

Imaging is an important tool in the preoperative evaluation of suspected low-grade gliomas as well as monitoring of treatment response and follow-up. MRI, that is non-invasive except for administration of contrast agent, is used to assess tumor extension but also to evaluate tumor heterogeneity and to identify higher-grade areas within low-grade tumors, preoperatively or as a sign of progression. Low-grade gliomas are associated with a more indolent clinical course compared to high-grade gliomas. The clinical course varies within the group of low-grade gliomas where ODs have a slower growth than ACs.^{6,7} Accurate preoperative radiological diagnosis is of special interest when tumors are located in or adjacent to eloquent areas because the time to surgery and neuropathological diagnosis might be prolonged in such cases. MRI also plays an important role in the follow-up of gliomas that are primarily not suitable for gross tumor resection.⁸

Gliomas have an infiltrating growth pattern in the white matter^{9,10}, exemplified by their ability to grow in cranial nerves.¹¹ Tumor infiltration is commonly assessed by morphological T2-weighted images where the high tumor signal defines the outer borders of the tumor.¹² This concept of evaluating glioma growth through morphological MRI has been challenged by studies showing infiltrative growth in gliomas not perceived on T2-weighted images.^{13,14} Studies have shown tumor growth up to several centimeters outside the morphological T2-boundary on MRI.^{14–16} Jenkinson *et al.*, found that ODs with intact 1p19q were more likely to show an infiltrating growth pattern despite having more sharp edges towards the surrounding brain on T2-weighted MRI.¹³ Perilesional microscopic tumor infiltration that is not visualized on mor-

phological MRI may give rise to local tumor recurrence also in patients operated with radiologically radical tumor resection. Therefore, a better method for preoperative glioma border evaluation than T2-weighted signal changes is warranted.

Water diffusivity, the random motion of water molecules, in particular non-Gaussian, reflects tissue microstructure, in for example cellularity and edema.¹⁷ Diffusion kurtosis imaging (DKI) is an extension of diffusion tensor imaging (DTI) and provides quantitative information about how tissue water diffusion deviates from a normally distributed diffusion.^{18,19} DKI quantifies excess kurtosis, but also directional diffusivities from DTI and as such gives a more comprehensive analysis of tissue diffusion properties.²⁰ Recently, histological evaluation and quantitative microscopy was used to show that high kurtosis in tumors is associated to both intra-voxel heterogeneity in cell density and high cell eccentricity.²¹

A limited number of studies have investigated DKI in gliomas (grade I–IV).^{17,22–25} Previous DKI studies have focused on the evaluation of differences in mean DKI parameters between low-grade gliomas (grade I–II) and high-grade gliomas (grade III–IV)^{22–25}, while comparisons between specific grades or glioma subtypes have been limited. Glioma grade has also been evaluated by perfusion MRI with only a few studies showing differences between glioma grade II and grade III, and that by applying a histogram based approach.^{26–28}

The aim of this prospective study is to investigate if diffusion parameters in the perilesional normal-appearing white matter (NAWM) differ from contralesional NAWM, and to investigate the role of DKI histogram analysis in discrimination between glioma malignancy grades (grade II *vs.* grade III) and glioma subtypes (AC *vs.* OD) in a cohort of patients with suspected low-grade gliomas.

Patients and methods

Forty-eight patients (> 18 years) with clinical and radiological suspected low-grade gliomas were prospectively recruited during 2010–2014. A patient suspected of having a low-grade glioma had an intra-axial brain lesion with high signal intensity on T2-weighted images with none or minimal contrast enhancement on morphological MRI. Ring-like contrast enhancement or areas of necrosis were exclusion criteria. The study was approved by the local ethics committee (regional ethical review board in Uppsala (Dnr 2010/015)) and

was therefore performed in accordance with the ethical standards laid down in the 1964 Declaration of Helsinki and its later amendments. All patients (n = 48) gave written informed consent before taking part in the study.

Imaging was performed preoperatively on a 3 T MRI scanner with a 32-channel head coil (Achieva, Philips Healthcare, Best, the Netherlands) with morphological and diffusion sequences (Figure 1).

Morphological MRI included axial T2FLAIR (TR/TE 11,000/125ms; 90 degree flip angle; 512 x 512 matrix; 0.45 x 0.45 x 6.00 mm³ voxel size) and T1-weighted spin echo sequences (TR/TE 600/10ms; 70 degree flip angle; 512 x 512 matrix; 0.45 x 0.45 x 5.00 mm³ voxel size) before and after gadobutrol contrast agent administration (Gadovist®, Bayer Schering Pharma, Berlin-Wedding, Germany). Morphological MRI sequences not assessed in this study were sagittal and axial T2-weighted turbo spin echo, coronal T2FLAIR, and sagittal T1-weighted 3D turbo field echo after contrast agent injection.

DKI was acquired with a SE-EPI sequence, and the following scan parameters were used: TR/TE 5,400 ms/76 ms; 27 slices with a thickness of 2 mm; SENSE = 2; 128 x 128 matrix; FoV 256 x 256 mm²; 15 diffusion encoding directions, with b = 0, 500, 1,000, 2,500, and 2,750 s/mm², for a total scan time of 6 minutes. Selection of b-values was based on the protocol optimized by Poot *et al.*²⁹ Post-processing was performed using in-house developed software, implemented in Matlab (The Mathworks, Natick, MA, USA). Motion and eddy current distortions were corrected by an extrapolation-based procedure that has superior performance for high b-value dMRI compared to the conventional method of registering to the volume acquired with b = 0³⁰, available at <https://github.com/markus-nilsson/md-dmri>. In this process, images were smoothed using 3D Gaussian kernel with a FWHM of 2 mm. This smoothing was performed to reduce the number of model misfits. The spatial smoothing was kept to a minimum by the conservative choice of kernel width. DTI parameter maps of mean diffusivity (MD) and fractional anisotropy (FA) were calculated based on volumes acquired with b ≤ 1,000 s/mm². The mean of the kurtosis tensor (MK) was calculated as described by Latt *et al.*³¹, and Hansen *et al.*³²

Axial T2FLAIR images were co-registered to Mean Diffusivity maps with the SPM8 toolbox (www.fil.ion.ucl.ac.uk/spm) using normalized mutual information with 7th-order B-spline interpolation. Co-registered images were visually as-

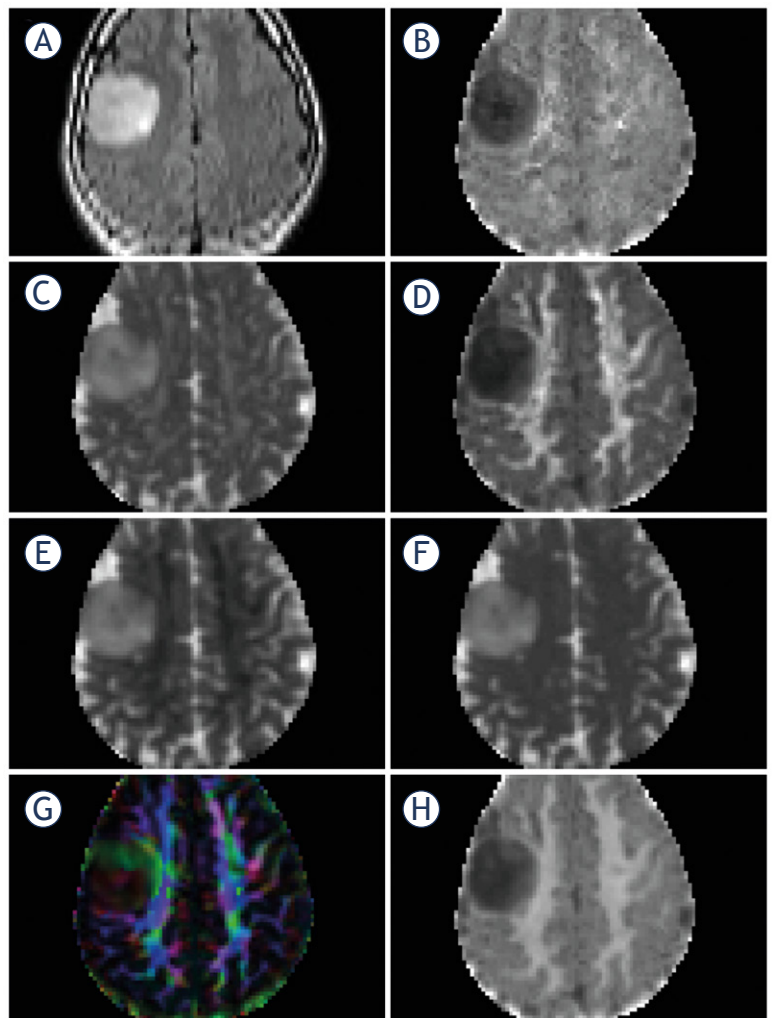


FIGURE 1. MRI in a patient with an oligodendroglioma grade II in the right frontal lobe, non-smoothed images. (A) T2FLAIR, (B) Axial Kurtosis, (C) Axial Diffusivity, (D) Radial Kurtosis, (E) Radial Diffusivity, (F) Mean Diffusivity, (G) Fractional Anisotropy, color coded, (H) Mean Kurtosis. Mean, axial and radial diffusivity 10⁻³ mm²/sec, fractional anisotropy, mean, axial and radial kurtosis and fractional anisotropy are dimensionless.

essed for correct re-alignment to source images. Manual Regions of interest (ROIs) placement was performed blinded to histopathological diagnosis on non-smoothed T2FLAIR images using in-house developed software. Increased signal intensity on T2FLAIR was regarded as tumor.³³ To avoid artifacts, the most superior and the most inferior slice were excluded from analysis; also chemical shift artifacts were excluded. Perilesional volume ROIs were delineated in NAWM one voxel outside the suspected tumor area on T2FLAIR on three consecutive slices, avoiding bulk tumor and gray matter (74 ± 43 voxels (mean ± SD)). NAWM ROIs were delineated in the contralateral hemisphere white mat-

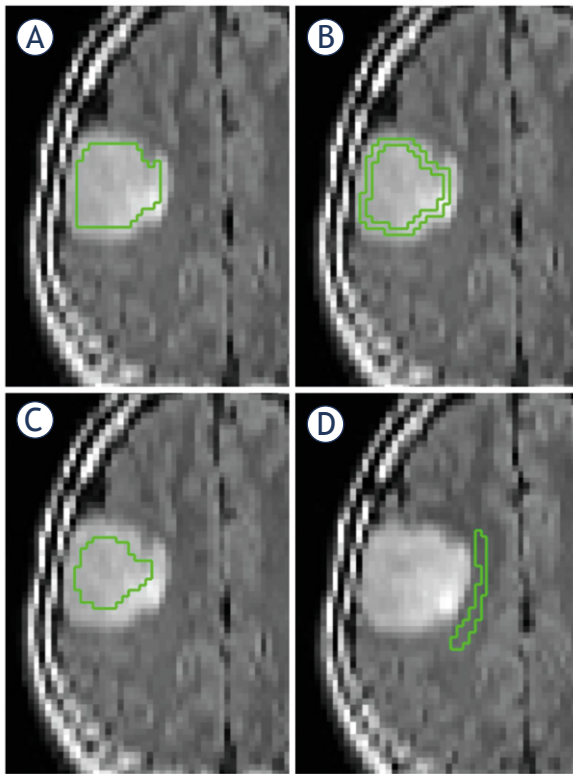


FIGURE 2. ROIs in a patient with an oligodendroglioma grade II. (A) Total tumor ROI. (B) Peripheral tumor ROI. (C) Central tumor ROI. (D) Perilesional ROI. All ROIs were drawn on non-smoothed images to increase the precision. ROI = region of interest

ter, lateral to the lateral ventricle (corona radiata) on four consecutive slices (131 ± 37 voxels (mean \pm SD)). Three tumor volume ROIs (total tumor, central tumor, and peripheral tumor) were delineated on T2FLAIR as depicted in Figure 2 A–D. Total tumor ROIs were delineated 1 voxel inside the outer border of the increased signal on T2FLAIR images ($3,087 \pm 2,102$ voxels (mean \pm SD)) on all slices with tumor. Peripheral tumor ROIs ($1,153 \pm 595$ voxels (mean \pm SD)) were delineated one voxel inside the increased signal on T2FLAIR, one voxel wide on all slices with tumor. Central tumor ROIs were delineated with a margin of two voxels to the border of the FLAIR signal changes ($1,491 \pm 1,384$ voxels (mean \pm SD)). ROIs were then transferred to the co-registered diffusion maps and diffusion parameters (axial, radial and mean kurtosis; axial, radial and mean diffusivity; and FA) were extracted.

Statistical analysis

Data distribution was analyzed using the normal probability plot and Shapiro-Wilks W test. Non-normally distributed data were analyzed with

non-parametric tests and normally distributed data were analyzed with parametric tests. Statistical analysis was performed with Statistica 12 (Statsoft, Tulsa, OK, USA) software. A p value < 0.05 after correction for multiple comparisons was regarded as statistically significant. To test for differences between mean DKI histogram variables in perilesional compared to NAWM, the Student's t test for dependent samples was used for normally distributed data and Wilcoxon matched pairs test for non-normally distributed data. Descriptive data of mean DKI variables for tumor grades and subtypes were calculated with mean and SD. Histograms with mean, standard deviation, skewness, kurtosis, peak height, peak position, 10th, 50th and 90th percentiles were calculated for all DKI variables in all ROIs. To adjust for interindividual differences between patients, ratios were calculated between tumor ROIs, perilesional ROIs and contralateral NAWM ROIs. To test for differences in relative DKI histogram variables between glioma grades II and III and between glioma subtypes ACs and ODs, a non-parametric test for multiple comparisons of mean ranks for all groups was performed with correction for multiple comparisons with Dunn's test in each histogram group (mean, standard deviation, skewness, kurtosis, peak height, peak position, 10th, 50th and 90th percentiles). From the multiple comparisons analysis, receiver-operating characteristics (ROC) curves were calculated for variables with the lowest p -values. The area under the curve (AUC) and the diagnostic performance were calculated from ROC.

Results

Forty-eight patients were included in the study. Thirty-five patients had a postoperative neuropathological diagnosis of AC or OD grades II or III and data from these 35 patients are presented. Diagnosis was obtained by neuronavigation-guided needle biopsy ($n = 4$), open biopsy ($n = 5$), or resection sample ($n = 26$). The neuropathological diagnoses followed the 2007 WHO classification of brain tumors³⁴, based on dominant cell type (AC or OD), cell density and proliferation (grade II *vs.* grade III). Included patients had a neuropathological diagnosis of AC II ($n = 10$), AC III ($n = 8$), OD II ($n = 13$) and OD III ($n = 4$). Mean age at diagnostic imaging was 48 ± 15 years (mean \pm SD).

Significant differences in mean DKI variables were observed between perilesional white matter and contralateral NAWM ($p = < 0.0000$ – 0.0002) for

TABLE 1. Results from analysis of perilesional and contralateral normal-appearing white matter

Diffusion histogram parameter	Perilesional NAWM	Contralateral NAWM	p
	Mean (SD) (n = 35)	Mean (SD) (n = 35)	
Axial diffusivity	1.26 (0.14)	1.38 (0.13)	0.000182
Radial diffusivity	0.67 (0.10)	0.53 (0.06)	0.000001
Fractional anisotropy	0.40 (0.11)	0.55 (0.09)	< 0.000000
Axial kurtosis	0.76 (0.07)	0.73 (0.08)	0.099422
Radial kurtosis	1.29 (0.24)	1.63 (0.16)	< 0.000000
Mean diffusivity	0.87 (0.07)	0.82 (0.04)	0.000009
Mean kurtosis	0.95 (0.09)	1.06 (0.05)	< 0.000000

Student's t-test for dependent samples (normally distributed data) and Wilcoxon matched pairs test (non-normally distributed data). NAWM = Normal appearing white matter. Mean, axial and radial diffusivity 10^{-3} mm²/sec, fractional anisotropy, mean, axial and radial kurtosis and fractional anisotropy are dimensionless.

all variables but axial kurtosis ($p = 0.0994$), with lower mean and radial kurtosis in perilesional white matter (Table 1). Fractional anisotropy and axial diffusivity were lower in the perilesional NAWM compared to contralateral white matter, while the mean diffusivity and radial diffusivity were higher in the perilesional NAWM.

Mean DKI parameters from whole tumor (total tumor ROIs) are presented in table 2. Mean DKI variables did not differ significantly between glioma grades II ($n = 23$) and III ($n = 12$) or between ACs ($n = 18$) and ODs ($n = 17$) ($p = 0.10$ – 0.96).

The DKI histogram analysis identified 44 (out of 252) histogram variables (supplementary Table 1A) that significantly differed between glioma grades II and III ($p = 0.0025$ – 0.0476). Ten variables were statistically different between ACs and ODs (supplementary Table 1B) ($p = 0.0110$ – 0.0496). All results were adjusted for multiple comparisons.

The best discriminating DKI histogram variables between glioma grades II and III and between ACs

grade II and III were derived from radial kurtosis in the peripheral tumor ROI (Table 3). The best discriminating variable between ODs grades II and III was derived from fractional anisotropy in the peripheral tumor ROI (Table 3). The best discriminating variables between ACs and ODs were derived from MD in central and perilesional ROIs (Table 3).

Results from ROC calculations of the best discriminating DKI variable are presented in Table 3 with ROC figures presented in Figure 3. A full analysis of the discriminating properties of these variables is presented in supplementary Table 2.

Discussion

We investigated preoperative DKI in patients with suspected low-grade gliomas to analyze differences in DKI parameters between perilesional and contralateral NAWM and between malignancy grades and histological subtypes.

TABLE 2. Mean diffusion kurtosis imaging variables in tumor regions of interest (ROI) (mean (SD))

Glioma subgroups:	Grade II	Grade III	p	Astrocytoma	Oligodendroglioma	p
	n = 23	n = 12		n = 18	n = 17	
Axial diffusivity (mean (SD))	1.72 (0.19)	1.81 (0.35)	0.19	1.76 (0.28)	1.74 (0.24)	0.78
Radial diffusivity (mean (SD))	1.44 (0.20)	1.50 (0.34)	0.52	1.47 (0.31)	1.46 (0.17)	0.71
Fractional anisotropy (mean (SD))	0.12 (0.03)	0.13 (0.04)	0.22	0.13 (0.04)	0.12 (0.03)	0.10
Axial kurtosis (mean (SD))	0.47 (0.08)	0.48 (0.06)	0.47	0.46 (0.06)	0.49 (0.08)	0.68
Radial kurtosis (mean (SD))	0.53 (0.09)	0.53 (0.08)	0.77	0.52 (0.09)	0.54 (0.09)	0.54
Mean diffusivity (mean (SD))	1.54 (0.19)	1.60 (0.34)	0.71	1.56 (0.30)	1.55 (0.19)	0.96
Mean kurtosis (mean (SD))	0.50 (0.08)	0.50 (0.07)	0.50	0.49 (0.07)	0.51 (0.09)	0.66

All values are expressed as ratios normalized against contralateral normal appearing white matter. Mean, axial and radial diffusivity 10^{-3} mm²/sec, fractional anisotropy, mean, axial and radial kurtosis and fractional anisotropy are dimensionless.

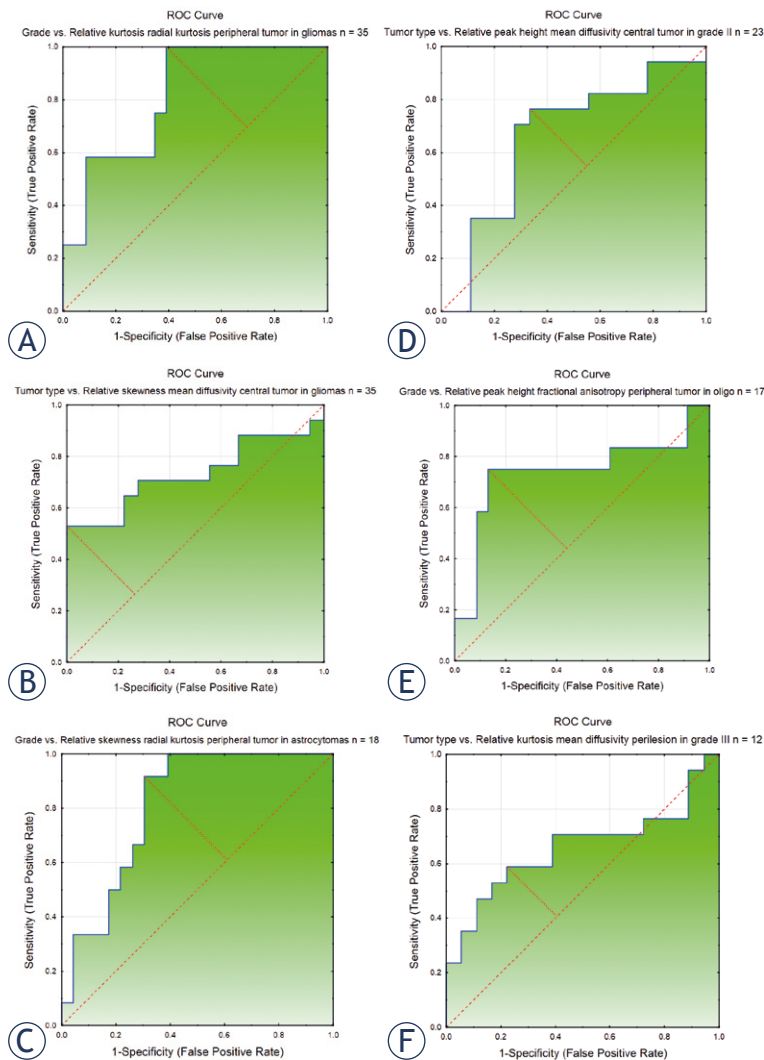


FIGURE 3. ROC curves presenting the best discriminating relative DKI histogram variables between glioma grades (II and III) and subtypes (astrocytomas and oligodendrogliomas). (A) Discrimination between glioma grades II and III with the kurtosis of radial kurtosis in peripheral tumor ROI, AUC = 0.815. (B) Discrimination between glioma subtypes astrocytoma and oligodendroglioma with the skewness of mean diffusivity in central tumor ROI, AUC = 0.732. (C) Discrimination between glioma grades II and III in astrocytomas with the skewness of radial kurtosis in peripheral tumor ROI, AUC = 0.812. (D) Discrimination between glioma subtypes astrocytoma and oligodendroglioma in gliomas grade II with the peak height of mean diffusivity in central tumor ROI, AUC = 0.660. (E) Discrimination between glioma grades II and III in oligodendrogliomas, with the peak height of fractional anisotropy in peripheral tumor ROI, AUC = 0.739. (F) Discrimination between glioma subtypes astrocytoma and oligodendroglioma in gliomas grade III with the kurtosis of mean diffusivity in perilesional ROI, AUC = 0.657.

AUC = area under the curve; ROC = receiver operating characteristic; ROI = region of interest

DKI parameters in perilesional NAWM differed significantly from contralesional NAWM. A higher mean diffusivity and lower fractional anisotropy is a characteristic diffusional pattern for white matter tumor infiltration.³⁵ A lower kurtosis in the perile-

sional white matter supports the rearrangement of white matter microstructure associated with tumor infiltration. Lower axial diffusivity reflects a less organized structure in gliomas compared to normal white matter structure, and a higher radial diffusivity reflects the non-demyelinating nature of tumor infiltration.³⁶

The perilesional NAWM was defined as the area outside of the high signal intensity tumor on T2-weighted images. The high T2-signal correlates to the area of the tumor but is an inefficient method to describe less dense cell concentration present in the periphery of diffusely infiltrating gliomas.^{9,12,14,16} Since pure vasogenic edema is rare in suspected low-grade gliomas we believe that the risk of misclassifying tumor infiltration edema for pure vasogenic edema in this cohort is small.¹²

Our findings that DKI parameters in the perilesional NAWM differ from contralateral NAWM can be interpreted as the presence of peritumoral infiltration.¹⁴ This advantage of DKI over morphological T2-weighted images allows for a more exact appreciation of the tumor invasion into the brain parenchyma prior to the planning of surgery and/or radiation therapy.¹² There is accumulating evidence that the extent of tumor resection in low-grade gliomas correlates with improved survival.³⁷ The presence of perilesional infiltration supports the concept of supratotal tumor resection.³⁸ DKI parameters from the preoperative MRI would thus potentially be helpful in the pre-surgical/radiation planning.

We identified 44 histogram variables with significant differences between glioma grades II and III (supplementary Table 1A). Variables with the lowest *p*-value and highest AUC from ROC-analysis were all derived from the peripheral tumor ROIs and two out of the three best discriminating variables were derived from histogram parameters of radial kurtosis (Table 3). The differences in radial kurtosis between glioma grades II and III may be related to structural re-arrangements in micro-architecture when grade II tumors progress into malignant gliomas. Our results are in agreement with those by Raab *et al.*¹⁷, who found no difference in mean FA between ACs grade II and III. Our results are also in line with a report by Murakami *et al.*³⁹, who reported no significant differences in minimum, average or maximum ADC (MD) between ACs grades II and III.³⁹ Our data differs from the recent paper by Jiang *et al.*²⁴, who found significant differences in mean kurtosis between glioma grades II and III using a semiautomatic process. This discrepancy could be attributed to the fact that the patient cohort in our study only include

TABLE 3. Results from multiple comparison test and receiver operating characteristics curves in groups and subgroups of gliomas

	p	AUC
Discrimination between glioma grades II (n = 23) and III (n = 12)		
The kurtosis of radial kurtosis in peripheral tumor ROI	0.0025	0.8152
Discrimination between astrocytoma grades II (n = 10) and III (n = 8)		
The skewness of radial kurtosis in peripheral tumor ROI	0.0034	0.8116
Discrimination between oligodendroglioma grades II (n = 13) and III (n = 4)		
The peak height of fractional anisotropy in peripheral tumor ROI	0.0066	0.7391
Discrimination between glioma types astrocytomas (n = 18) and oligodendrogliomas (n = 17)		
The skewness of mean diffusivity in central tumor ROI	0.0191	0.7320
Discrimination between glioma types astrocytomas grade II (n = 10) and oligodendrogliomas grade II (n = 13)		
The peak height of mean diffusivity in central tumor ROI	0.0110	0.6601
Discrimination between glioma types astrocytomas grade III (n = 8) and oligodendrogliomas grade III (n = 4)		
The kurtosis of mean diffusivity in perilesion ROI	0.0174	0.6569

Multiple comparison of mean ranks between groups of glioma grades and types of gliomas with Dunn's correction for multiple comparisons. AUC = area under the curve. ROI = region of interest. All values are expressed as ratios normalized against contralateral normal appearing white matter.

suspected low-grade gliomas, possibly selecting cases of grade III gliomas more similar in radiologic appearance and biology than a non-selected group of gliomas including all four glioma grades (WHO grade I-IV). In our study cohort, none of the included patients showed ring like contrast enhancement with central necrosis on conventional MRI, and therefore we were unlikely to include any cases of gliomas grade IV neuropathologically misdiagnosed as grade III.

The partition of ROIs into peripheral and central zones is based on the concept of glioma growth. Gliomas show infiltrating growth outside the outer tumor boundaries appreciated on T2-weighted MRI but tend to recur centrally after radiation therapy, where the cell density is highest.¹⁰ Infiltration length outside the T2-hyperintensity has been estimated mathematically and confirmed through biopsy series¹⁰ and by en-bloc resections outside the radiological tumor borders.¹⁴ Our data confirm both the concept of differences in biological structure in the central and peripheral tumor portion of gliomas, but also the presence of biological microstructural changes outside the boundaries appreciated on morphological T2-weighted images.

Ten histogram variables differed significantly between ACs with ODs (supplementary Table 1B). The best discriminating variable was derived from the MD, which showed different skewness, peak height and kurtosis between astrocytic and oligodendroglial tumors. MD measures the average diffusion between several directions without di-

rectional information. While ACs and ODs share a common histogenetic origin they differ in their histological appearances. ACs are recognized through their neoplastic astrocytes with slightly elongated nuclei on a background of multiple fibrillary dendrites expressing glial fibrillary acidic protein (GFAP) while ODs display higher cell density with monomorphic cells with uniformly round nuclei and perinuclear halos.^{34,40} These differences in extracellular space composition may explain differences in MD between ACs and ODs.

MD histograms have previously been used to discriminate ACs from ODs. In 2007, Tozer *et al.*⁴¹, differentiated glioma subtypes in a cohort of 27 gliomas grade II by ADC histogram analysis. They performed the MRI post-biopsy, and in agreement with our study, mean ADCs could not alone separate the different subtypes. In 2009 Bian *et al.*⁴², and Khayal *et al.*⁴³, reported on a group of gliomas grade II analyzing ADC histograms in non-enhancing tumor regions and found significant differences between ODs and ACs for histogram variables. Our results that the peak height of MD in central tumor ROI differ between ACs and ODs grade II are in agreement with Khayal *et al.*⁴³ who found significant differences in the 75th percentile of ADC between ACs and ODs grade II. Also in agreement with our study, Lam *et al.*⁴⁴, when assessing 17 glioma patients reported no difference in mean ADCs between ODs and non-OD. If glial subtypes could be assessed without the need for surgery, patients deemed inoperable due to tumor

location could have a higher probability of receiving adequate treatment, since ODs have shown better prognosis and clinical effect when receiving chemotherapeutics.⁴⁵

One limitation to our study is the manual definition of tumor and perilesional ROIs. We minimized the risk of bias in ROI-delineation by choosing a method that could easily be standardized between patients. Therefore we analyzed the whole tumor area seen as high signal intensity on T2FLAIR. Our methodology strives to assess the major diffusional properties of gliomas and minimize the risk of selection bias that may be introduced when small ROIs are selected. In addition, analyzing small ROIs may result in large inter-observer variations. Further, a manually defined ROI reflects a clinical setting. Another limitation to our study might be attributed to the limited number of included patients. Despite this, our cohort of gliomas grades II and III is equal to or larger than in previously published DKI studies.^{17,22}

In summary, we investigated histogram DKI analysis in a prospectively gathered cohort of patients with suspected low-grade gliomas. We conclude that DKI variables in perilesional NAWM differ significantly from contralesional NAWM, suggesting an altered microstructure not depicted on morphological MRI. Further, histogram analysis of DKI data identifies differences between glioma grades II and III and between astrocytomas and oligodendrogliomas not apparent through comparisons of mean DKI parameters. Future glioma studies should analyze the extent of tumor cell infiltration outside the high signal intensity on T2FLAIR and correlate DKI-data with co-localized neuropathological data.

Acknowledgement

Uppsala county council has provided financial support for the study. Grant from Swedish cancer society.

References

- Ostrom QT, Gittleman H, Farah P, Ondracek A, Chen Y, Wolinsky Y, et al. CBTRUS statistical report: Primary brain and central nervous system tumors diagnosed in the United States in 2006-2010. *Neuro Oncol* 2013; **Suppl 2**: 1-56. doi: 10.1093/neuonc/not151
- Louis DN, Perry A, Reifenberger G, von Deimling A, Figarella-Branger D, Cavenee WK, et al. The 2016 World Health Organization classification of tumors of the central nervous system: a summary. *Acta Neuropathol* 2016; **131**: 803-20. doi: 10.1007/s00401-016-1545-1
- Fan GG, Deng QL, Wu ZH, Guo QY. Usefulness of diffusion/perfusion-weighted MRI in patients with non-enhancing supratentorial brain gliomas: a valuable tool to predict tumour grading? *Br J Radiol* 2006; **79**: 652-8. doi:10.1259/bjr/25349497
- Schafer ML, Maurer MH, Synowitz M, Wustefeld J, Marnitz T, Streitparth F, et al. Low-grade (WHO II) and anaplastic (WHO III) gliomas: differences in morphology and MRI signal intensities. *Eur Radiol* 2013; **23**: 2846-53. doi: 10.1007/s00330-013-2886-y
- Law M, Yang S, Wang H, Babb JS, Johnson G, Cha S, et al. Glioma grading: sensitivity, specificity, and predictive values of perfusion MR imaging and proton MR spectroscopic imaging compared with conventional MR imaging. *AJNR Am J Neuroradiol* 2003; **24**: 1989-98.
- Okamoto Y, Di Patre PL, Burkhard C, Horstmann S, Jourde B, Fahey M, et al. Population-based study on incidence, survival rates, and genetic alterations of low-grade diffuse astrocytomas and oligodendrogliomas. *Acta Neuropathol* 2004; **108**: 49-56. doi: 10.1007/s00401-004-0861-z
- Gupta M, Djalilvand A, Brat DJ. Clarifying the diffuse gliomas: an update on the morphologic features and markers that discriminate oligodendroglioma from astrocytoma. *Am J Clin Pathol* 2005; **124**: 755-68. doi: 10.1309/6JNX-4PA6-0TQ5-USVG
- Ius T, Angelini E, Thiebaut de Schotten M, Mandonnet E, Duffau H. Evidence for potentials and limitations of brain plasticity using an atlas of functional resectability of WHO grade II gliomas: towards a "minimal common brain". *Neuroimage* 2011; **56**: 992-1000. doi: 10.1016/j.neuroimage.2011.03.022
- Smits A, Zetterling M, Lundin M, Melin B, Fahlstrom M, Grabowska A, et al. Neurological impairment linked with cortico-subcortical infiltration of diffuse low-grade gliomas at initial diagnosis supports early brain plasticity. *Front Neurol* 2015; **6**: 137. doi: 10.3389/fneur.2015.00137
- Unkelbach J, Menze BH, Konukoglu E, Dittmann F, Ayache N, Shih HA. Radiotherapy planning for glioblastoma based on a tumor growth model: implications for spatial dose redistribution. *Phys Med Biol* 2014; **59**: 771-89. doi: 10.1088/0031-9155/59/3/771
- Mabray MC, Glastonbury CM, Mamlouk MD, Punch GE, Solomon DA, Cha S. Direct cranial nerve involvement by gliomas: case series and review of the literature. *AJNR Am J Neuroradiol* 2015; **36**: 1349-54. doi: 10.3174/ajnr.A4287
- Kelly PJ, Dumas-Duport C, Scheithauer BW, Kall BA, Kispert DB. Stereotactic histologic correlations of computed tomography- and magnetic resonance imaging-defined abnormalities in patients with glial neoplasms. *Mayo Clin Proc* 1987; **62**: 450-9.
- Jenkinson MD, du Plessis DG, Smith TS, Joyce KA, Warnke PC, Walker C. Histological growth patterns and genotype in oligodendroglial tumours: correlation with MRI features. *Brain* 2006; **129**: 1884-91. doi: 10.1093/brain/awl108
- Zetterling M, Roodakker KR, Berntsson SG, Edqvist PH, Latini F, Landtblom AM, et al. Extension of diffuse low-grade gliomas beyond radiological borders as shown by the coregistration of histopathological and magnetic resonance imaging data. *J Neurosurg* 2016; **125**: 1155-66. doi: 10.3171/2015.10.JNS15583
- Pallud J, Varlet P, Devaux B, Geha S, Badoual M, Deroulers C, et al. Diffuse low-grade oligodendrogliomas extend beyond MRI-defined abnormalities. *Neurology* 2010; **74**: 1724-31. doi: 10.1212/WNL.0b013e3181e04264
- Price SJ, Jena R, Burnet NG, Hutchinson PJ, Dean AF, Pena A, et al. Improved delineation of glioma margins and regions of infiltration with the use of diffusion tensor imaging: an image-guided biopsy study. *AJNR Am J Neuroradiol* 2006; **27**: 1969-74.
- Raab P, Hattingen E, Franz K, Zanella FE, Lanfermann H. Cerebral gliomas: diffusional kurtosis imaging analysis of microstructural differences. *Radiology* 2010; **254**: 876-81. doi: 10.1148/radiol.09090819
- Basser PJ, Mattiello J, LeBihan D. MR diffusion tensor spectroscopy and imaging. *Biophys J* 1994; **66**: 259-67. doi: 10.1016/S0006-3495(94)80775-1
- Jensen JH, Helpert JA, Ramani A, Lu H, Kaczynski K. Diffusional kurtosis imaging: the quantification of non-gaussian water diffusion by means of magnetic resonance imaging. *Magn Reson Med* 2005; **53**: 1432-40. doi: 10.1002/mrm.20508
- Cheung MM, Hui ES, Chan KC, Helpert JA, Qi L, Wu EX. Does diffusion kurtosis imaging lead to better neural tissue characterization? A rodent brain maturation study. *Neuroimage* 2009; **45**: 386-92. doi: 10.1016/j.neuroimage.2008.12.018

21. Szczepankiewicz F, van Westen D, Englund E, Westin CF, Stahlberg F, Latt J, et al. The link between diffusion MRI and tumor heterogeneity: Mapping cell eccentricity and density by diffusional variance decomposition (DIVIDE). *Neuroimage* 2016; **142**: 522-3. doi: 10.1016/j.neuroimage.2016.07.038
22. Van Cauter S, Veraart J, Sijbers J, Peeters RR, Himmelreich U, De Keyser F, et al. Gliomas: diffusion kurtosis MR imaging in grading. *Radiology* 2012; **263**: 492-501. doi: 10.1148/radiol.12110927
23. Van Cauter S, De Keyser F, Sima DM, Sava AC, D'Arco F, Veraart J, et al. Integrating diffusion kurtosis imaging, dynamic susceptibility-weighted contrast-enhanced MRI, and short echo time chemical shift imaging for grading gliomas. *Neuro Oncol* 2014; **16**: 1010-21. doi: 10.1093/neuonc/not304
24. Jiang R, Jiang J, Zhao L, Zhang J, Zhang S, Yao Y, et al. Diffusion kurtosis imaging can efficiently assess the glioma grade and cellular proliferation. *Oncotarget* 2015; **6**: 42380-93. doi: 10.18632/oncotarget.5675
25. Tietze A, Hansen MB, Ostergaard L, Jespersen SN, Sangill R, Lund TE, et al. Mean diffusional kurtosis in patients with glioma: initial results with a fast imaging method in a clinical setting. *AJNR Am J Neuroradiol* 2015; **36**: 1472-8. doi: 10.3174/ajnr.A4311
26. Arevalo-Perez J, Peck KK, Young RJ, Holodny AI, Karimi S, Lyo JK. Dynamic Contrast-enhanced perfusion mri and diffusion-weighted imaging in grading of gliomas. *J Neuroimaging* 2015; **25**: 792-8. doi: 10.1111/jon.12239
27. Falk A, Fahlstrom M, Rostrop E, Berntsson S, Zetterling M, Morell A, et al. Discrimination between glioma grades II and III in suspected low-grade gliomas using dynamic contrast-enhanced and dynamic susceptibility contrast perfusion MR imaging: a histogram analysis approach. *Neuroradiol* 2014; **56**: 1031-8. doi: 10.1007/s00234-014-1426-z
28. Emblem KE, Due-Tonnessen P, Hald JK, Bjørnerud A, Pinho MC, Scheie D, et al. Machine learning in preoperative glioma MRI: survival associations by perfusion-based support vector machine outperforms traditional MRI. *J Magn Reson Imaging* 2014; **40**: 47-54. doi: 10.1002/jmri.24390
29. Poot DH, den Dekker AJ, Achten E, Verhoye M, Sijbers J. Optimal experimental design for diffusion kurtosis imaging. *IEEE Trans Med Imaging* 2010; **29**: 819-29. doi: 10.1109/TMI.2009.2037915
30. Klein S, Staring M, Murphy K, Viergever MA, Pluim JP. Elastix: a toolbox for intensity-based medical image registration. *IEEE Trans Med Imaging* 2010; **29**: 196-205. doi: 10.1109/TMI.2009.2035616
31. Lätt J, Nilsen M, Brockstedt S, Wirestam R, Ståhlberg F. Bias free estimates of the diffusional kurtosis in two minutes: avoid solving the kurtosis tensor. *Proc Intl Soc Mag Reson Med* 2010; **18**: 3972
32. Hansen B, Lund TE, Sangill R, Jespersen SN. Experimentally and computationally fast method for estimation of a mean kurtosis. *Magn Reson Med* 2013; **69**: 1754-60. doi: 10.1002/mrm.24743
33. Gerin C, Pallud J, Deroulers C, Varlet P, Oppenheim C, Roux FX, et al. Quantitative characterization of the imaging limits of diffuse low-grade oligodendrogliomas. *Neuro Oncol* 2013; **15**: 1379-88. doi: 10.1093/neuonc/not072
34. Louis DN, Ohgaki H, Wiestler OD, Cavenee WK, Burger PC, Jouvet A, et al. The 2007 WHO classification of tumours of the central nervous system. *Acta Neuropathol* 2007; **114**: 97-109. doi: 10.1007/s00401-007-0243-4
35. Wang S, Zhou J. Diffusion tensor magnetic resonance imaging of rat glioma models: a correlation study of MR imaging and histology. *J Comput Assist Tomogr* 2012; **36**: 739-44. doi: 10.1097/RCT.0b013e3182685436
36. Karlsgodt KH, Rosser T, Lutkenhoff ES, Cannon TD, Silva A, Bearden CE. Alterations in white matter microstructure in neurofibromatosis-1. *PLoS One* 2012; **7**: e47854. doi: 10.1371/journal.pone.0047854
37. Jakola AS, Myrmet KS, Kloster R, Torp SH, Lindal S, Unsgard G, et al. Comparison of a strategy favoring early surgical resection vs a strategy favoring watchful waiting in low-grade gliomas. *JAMA* 2012; **308**: 1881-8. doi: 10.1001/jama.2012.12807
38. Yordanova YN, Moritz-Gasser S, Duffau H. Awake surgery for WHO Grade II gliomas within "noneloquent" areas in the left dominant hemisphere: toward a "supratotal" resection. Clinical article. *J Neurosurg* 2011; **115**: 232-9. doi: 10.3171/2011.3.JNS101333
39. Murakami R, Hirai T, Sugahara T, Fukuoka H, Toya R, Nishimura S, et al. Grading astrocytic tumors by using apparent diffusion coefficient parameters: superiority of a one- versus two-parameter pilot method. *Radiology* 2009; **251**: 838-45. doi: 10.1148/radiol.2513080899
40. Kinjo S, Hirato J, Nakazato Y. Low grade diffuse gliomas: shared cellular composition and morphometric differences. *Neuropathology* 2008; **28**: 455-65. doi: 10.1111/j.1440-1789.2008.00897.x
41. Tozer DJ, Jager HR, Danchavijitr N, Benton CE, Tofts PS, Rees JH, et al. Apparent diffusion coefficient histograms may predict low-grade glioma subtype. *NMR Biomed* 2007; **20**: 49-57. doi: 10.1002/nbm.1091
42. Bian W, Khayal IS, Lupo JM, McGue C, Vandenberg S, Lamborn KR, et al. Multiparametric characterization of grade 2 glioma subtypes using magnetic resonance spectroscopic, perfusion, and diffusion imaging. *Transl Oncol* 2009; **2**: 271-80.
43. Khayal IS, McKnight TR, McGue C, Vandenberg S, Lamborn KR, Chang SM, et al. Apparent diffusion coefficient and fractional anisotropy of newly diagnosed grade II gliomas. *NMR Biomed* 2009; **22**: 449-55. doi: 10.1002/nbm.1357
44. Lam WW, Poon WS, Metreweli C. Diffusion MR imaging in glioma: does it have any role in the pre-operation determination of grading of glioma? *Clin Radiol* 2002; **57**: 219-25. doi: 10.1053/crad.2001.0741
45. Ramirez C, Bowman C, Maurage CA, Dubois F, Blond S, Porchet N, et al. Loss of 1p, 19q, and 10q heterozygosity prospectively predicts prognosis of oligodendroglial tumors—towards individualized tumor treatment? *Neuro Oncol* 2010; **12**: 490-9. doi: 10.1093/neuonc/nop071

Breast dynamic contrast enhanced MRI: fibrocystic changes presenting as a non-mass enhancement mimicking malignancy

Zorica C. Milosevic^{1,2}, Mirjan M. Nadrljanski^{1,2}, Zorka M. Milovanovic³, Nina Z. Gusic⁴, Slavko S. Vucicevic¹, Olga S. Radulovic⁵

¹ Clinic for Radiation Oncology and Radiology, Institute of Oncology and Radiology of Serbia, Belgrade, Serbia

² Faculty of Medicine, University of Belgrade, Belgrade, Serbia

³ Department for Pathology, Institute of Oncology and Radiology of Serbia, Belgrade, Serbia

⁴ Primary Health Center Zvezdara, Belgrade, Serbia

⁵ Institute for Biological Research 'Sinisa Stankovic', Belgrade, Serbia

Radiol Oncol 2017; 51(2): 130-136.

Received 18 October 2016

Accepted 20 February 2017

Correspondence to: Zorica Milošević, M.D., Clinic for Radiation Oncology and Radiology, Institute of Oncology and Radiology of Serbia, Pasterova 14, 11000 Belgrade, Serbia and Faculty of Medicine, University of Belgrade, Dr Subotića 8, 11000 Belgrade, Serbia. Phone: +381 11 206 7214; Fax: +381 11 268 53 00; E-mail: pipa011@ptt.rs

Disclosure: No potential conflicts of interest were disclosed.

Background. We aimed to analyse the morphokinetic features of breast fibrocystic changes (nonproliferative lesions, proliferative lesions without atypia and proliferative lesions with atypia) presenting as a non-mass enhancement (NME) in dynamic contrast-enhanced magnetic resonance imaging (DCE-MRI) examination.

Patients and methods. Forty-six patients with histologically proven fibrocystic changes (FCCs) were retrospectively reviewed, according to Breast Imaging Reporting and Data System (BI-RADS) lexicon. Prior to DCE-MRI examination, a unilateral breast lesion suspicious of malignancy was detected clinically, on mammography or breast ultrasonography.

Results. The predominant features of FCCs presenting as NME in DCE-MRI examination were: unilateral regional or diffuse distribution (in 35 patients or 76.1%), heterogeneous or clumped internal pattern of enhancement (in 36 patients or 78.3%), plateau time-intensity curve (in 25 patients or 54.3%), moderate or fast wash-in (in 31 patients or 67.4%). Nonproliferative lesions were found in 11 patients (24%), proliferative lesions without atypia in 29 patients (63%) and lesions with atypia in six patients (13%), without statistically significant difference of morphokinetic features, except of the association of clustered microcysts with proliferative dysplasia without atypia.

Conclusions. FCCs presenting as NME in DCE-MRI examination have several morphokinetic features suspicious of malignancy, therefore requiring biopsy (BI-RADS 4). Nonproliferative lesions, proliferative lesions without atypia and proliferative lesions with atypia predominantly share the same predefined DCE-MRI morphokinetic features.

Key words: breast; magnetic resonance imaging; fibrocystic changes

Introduction

Fibrocystic changes (FCCs) are the most frequent benign conditions of breast, diagnosed in 50% of women examined clinically and in 90% of women in histopathological studies. These benign disorders have two important implications from the point of view of breast cancer diagnosis and man-

agement. First, FCCs can mimic breast cancer on clinical examination, mammography and breast ultrasonography, leading to unnecessary breast biopsies and patient anxiety. Second, some types of FCCs represent a risk factor for the subsequent development of breast cancer.¹ Based on a classification system of FCCs proposed by Dupont and Page and according to other studies, women with

histologically confirmed nonproliferative lesions have no increased breast cancer risk. On the contrary, women whose breast biopsies show proliferative lesions with or without atypia are at risk of developing cancer, with relative risk ranging from 3.9–13.0 and 1.3–1.9 respectively.²⁻⁴

Combining morphological and enhancement kinetics features of the breast lesions, dynamic contrast-enhanced MRI (DCE-MRI) shows the highest sensitivity of all imaging methods in detecting breast diseases, up to 100%. Nevertheless, the specificity in the differentiation between benign and malignant lesions is lower, up to 75%.⁵ The major cause of false positive findings in DCE-MRI examination and consecutive unnecessary biopsies are the lesions with non-mass enhancement (NME). NME refers to the lesion that is seen only on post-contrast DCE-MRI sequences and does not have space-occupying effect. The enhancement pattern of NME is distinct from normal surrounding breast parenchyma and may contain interspersed fat. On the contrary, a mass enhancement is a three-dimensional space-occupying lesion.^{6,7} The causes of NME include FCCs, inflammatory benign lesions, *in situ* ductal carcinoma (DCIS), invasive lobular carcinoma and some cases of oestrogen receptor-negative invasive ductal carcinoma. The mass enhancement is usually confined to malignant or benign tumors.⁸⁻¹¹

Our study of pathologically confirmed FCCs presenting as NME in DCE-MRI examination has two goals: 1) to analyse morphological and enhancement kinetics features of FCCs, 2) to compare these features between nonproliferative lesions, proliferative lesions without atypia and proliferative lesions with atypia.

Patients and methods

Patients

In the period of two years (January 2010 to January 2012) a total of 947 patients were examined by two radiologists (MZC and NMM) using the standardized breast DCE-MRI full diagnostic protocol. From this group, 46 patients with FCCs presenting as NME were selected and retrospectively reviewed. The study was performed in accordance with the Declaration of Helsinki and was approved by the Institutional Review Board Committee (No. 4502-01/2011). All patients gave written informed consent to participate in DCE-MRI examination. The age of the patients was 50.78 ± 8.99 years. In all premenopausal women DCE-MRI was performed

in the second and third week of the menstrual cycles. None of the patients had previous breast biopsy, breast surgery or current hormone replacement therapy. All patients initially had unilateral breast lesion suspicious of malignancy either on clinical examination, mammography or ultrasonography. The lesions were presented as calcifications or asymmetric tissue on mammography and hypoechoic non-mass lesions on ultrasonography (BI-RADS 4a to BI-RADS 4c categories according to the ACR BI-RADS lexicon).^{6,12} The indication for breast DCE-MRI prior to biopsy was to evaluate the local extent of the lesion in the dense breast on mammography (32 patients) or suspected multifocal lesions on mammography and/or ultrasonography (14 patients).¹³ After the pathological confirmation of FCCs, the patients were examined biannually by physical examination and mammography. During the predefined follow-up period, no ipsilateral or contralateral breast cancer was detected.

Methods

The DCE-MRI examinations were performed with a 1.5 Tesla MRI unit (Magnetom Avanto, Siemens Medical Solutions, Erlangen, Germany) with dedicated bilateral breast coil and the patient in the prone position. The standard protocol was used for the axial-plane images with the slice thickness of 2 mm (Table 1).¹⁴ The contrast medium was gadopentetate dimeglumine (Magnevist, Bayer Schering Pharma, Berlin, Germany) applied as the bolus injection of 0.1 mmol/kg body weight injected with the automatic injector (Mississippi, Ulrich Medical,

TABLE 1. Standard dynamic contrast-enhanced magnetic resonance imaging (DCE-MRI) protocol for axial-plane images for T1-weighted FLASH 3D precontrast and five postcontrast series

	T2-weighted	T2-weighted	T1-weighted	T1-weighted
MRI sequence/parameters	TIRM	TSE	TSE	FLASH 3D
Echo time (ms)	60	70	12	4.8
Repetition time (ms)	7690	5900	910	9.1
Inversion time (ms)	180			
Flip angle (°)	150	180	90	25
Field of view (mm×mm)	340×340	340×340	340×340	340×340
Image matrix	320×256	384×319	320×234	576×564

3D = three-dimensional; DCE-MRI = dynamic contrast-enhanced magnetic resonance imaging; FLASH = fast low-angle shot pulse sequence; TIRM = turbo inversion recovery magnitude; TSE = turbo spin-echo

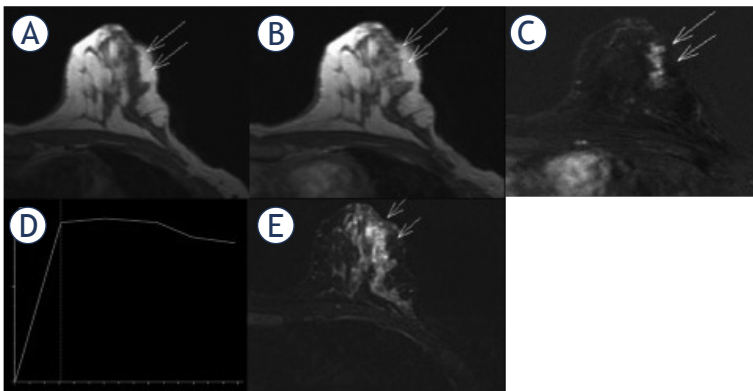


FIGURE 1. DCE-MRI findings of proliferative fibrocystic changes. Axial T1-weighted images, precontrast image (A) and contrast-enhanced image 1 min 23 s after administration of gadolinium (B) with corresponding subtraction image (C), show the segmental, non-mass enhancement (long arrows), measured 2.5x1x2.5 cm, with clumped internal pattern of enhancement. Time-intensity curve is plateau (type 2) with fast wash-in (D). Turbo inversion recovery magnitude (TIRM) sequence (E) show clustered microcysts (short arrows).

Ulm, Germany) at the rate of 2 mL/s, followed by the flush of 20 mL saline. Contrast-enhanced dynamic sequences were acquired five times every 1 min 23 s. The postprocessing methods, including a creation of time intensity curves (TICs), *i.e.* enhancement (%) against time (s), were performed on the workstation Leonardo, using the image processing software Syngo (Syngo, Siemens Medical Solutions).

Two experienced radiologists in breast MRI, ZCM, 20 yr. and MMN, 7 yr., reviewed the DCE-MRI examinations. Based on the fifth edition of the BI-RADS lexicon, published in 2013, the following morphokinetic features of NME were analysed: distribution of enhancement (focal, linear, segmental, regional, multiple regions, diffuse), internal enhancement pattern (homogeneous, heterogeneous, clumped, clustered ring enhancement, stippled), type of TICs (persistent curve or type 1, plateau curve or type 2, wash out curve or type 3), wash-in *i.e.* the enhancement rate 90 s after intravenous contrast application (slow, medium, rapid), and signal intensity on T2-weighted (T2W) images.⁶

A surgical biopsy was performed in all patients. Among them, 21 patients with nonpalpable lesions, prior to the biopsy underwent a radioguided occult lesion localization (ROLL) procedure with Technetium-99m, under stereotactic or ultrasonographic guidance.¹⁵ Haematoxylin and eosin stained slides of formalin-fixed and paraffin-embedded tissue blocks were assessed by a pathologist, experienced in breast pathology. According to

the classification system of Dupont and Page, the lesions were classified as nonproliferative lesions, proliferative lesions without atypia, and proliferative lesions with atypia (atypical ductal and lobular hyperplasia).²

Statistical analysis

Following DCE-MRI features of NME were analysed: distribution of postcontrast enhancement, internal enhancement pattern, type of TICs, wash-in, and signal intensity on T2W images. These distinctive DCE-MRI features of NME were compared for three groups of FCCs: nonproliferative lesions, proliferative lesions without atypia, and proliferative lesions with atypia. Frequencies were used to describe the distribution of categorical variables. The difference between investigated variables in three groups of FCCs was analysed using χ^2 test. P values less than 0.05 were considered statistically significant. SPSS for Windows, Statistics version 16.0. (SPSS Inc., Chicago, USA) was used to perform statistical analyses.

Results

The lesions were detected clinically in 25 patients (54.3%), on mammography in 43 patients (93.5%) and by breast ultrasonography in 30 patients (65.2%).

Out of 46 biopsies, nonproliferative lesions were found in 11 patients (24%), proliferative lesions without atypia in 29 patients (63%) and proliferative lesions with atypia in six patients (13%). On DCE-MRI examination, all cases were presented as unilateral non-mass enhancement of BI-RADS 4 category (Figure 1).

Forty-three lesions (93.5%) were equal to or larger than 1 cm in size and three lesions were smaller than 1 cm and larger than 0.5 cm in size (6.5%). The distribution of the postcontrast enhancement was segmental in 11 patients (23.9%) and regional or diffuse in 35 patients (76.1%). The other types of distribution (focal, linear enhancement and multiple regions) were not found. The internal enhancement pattern was homogeneous in two patients (4.3%), heterogeneous and clumped in 36 patients (78.3%), and stippled in eight patients (17.4%). Clustered ring enhancement was not detected. The types of time-intensity curves were persistent (type 1) in 17 patients (37.0%), plateau (type 2) in 25 patients (54.3%), and wash out (type 3) in four patients (8.7%). The initial postcontrast signal in-

TABLE 2. Nonproliferative lesion, proliferative lesions without atypia and proliferative lesions with atypia: dynamic contrast-enhanced magnetic resonance imaging (DCE-MRI) morphological and enhancement kinetics features, based on BI-RADS lexicon

Statistical difference	Proliferative lesions without atypia (N = 6)	Proliferative lesions with atypia (N = 29)	Non proliferative lesions (N = 11)	The DCE-MRI features of fibrocystic changes	
p = 0.454	1	1	1	0.5 < d < 1 cm	Size
	5	28	10	d ≥ 1 cm	
p = 0.168	3	7	1	Segmental	NME distribution
	3	22	10	Regional or diffuse	
p = 0.722	0	2	0	Homogeneous	NME internal enhancement
	1	4	3	Stippled	
	5	23	8	Heterogeneous or clumped	
p = 0.097	3	8	6	Persistent	TIC
	3	19	3	Plateau	
	0	2	2	Wash out	
p = 0.752	2	8	5	Slow	Wash-in
	1	10	3	Moderate	
	3	11	3	Fast	
p = 0.014	1	18	2	Present	Microcysts (T2W images)
	5	11	9	Absent	

d = longest diameter; DCE-MRI = dynamic contrast-enhanced magnetic resonance imaging; NME = non-mass enhancement; TIC = time-intensity curve; T2W = T2-weighted

tensity enhancement (enhancement rate, wash-in) was slow in 15 patients (32.6%), moderate in 14 patients (30.4%), and fast in 17 patients (37.0%). On T2W images FCCs were associated with clustered microcysts in 25 cases (54.3%).

As shown in Table 2, the features of nonproliferative lesions, proliferative lesions without atypia and proliferative lesions with atypia on DCE-MRI examination did not show statistically significant difference in the term of the size ($p = 0.454$), the distribution of postcontrast enhancement ($p = 0.168$), the internal enhancement pattern ($p = 0.722$), the types of time-intensity curves ($p = 0.097$) and the initial postcontrast signal intensity enhancement ($p = 0.752$). Presence of microcysts on T2W images in these three groups of FCCs was statistically significant compared to the lack of the feature ($p = 0.014$).

Discussion

Numerous studies have demonstrated the clinical importance of FCCs, related to the high prevalence of the condition, the considerable impact on quality of life and the increased breast cancer risk for women with proliferative lesions.^{2-4,16-18}

Nevertheless, only few studies analysed features of FCCs on DCE-MRI, based on the limited number of cases. Chen *et al.* reported two studies with 31 patients and 11 patients, analysing FCCs in DCE-MRI examination and MR spectroscopy for choline detection.^{19,20} Van den Bosch *et al.* and Kiyak *et al.* reported morphological and kinetic features of FCCs on DCE-MRI in the group of 14 patients and 27 patients, respectively.^{21,22}

Our study included 46 symptomatic patients with pathologically confirmed FCCs presenting as NME, mimicking malignancy in DCE-MRI examination. Chen *et al.* reported that FCCs on DCE-MRI had characteristics of NME in 39% of cases, mass enhancement in 35% of cases, while 26% of cases were nonenhancing lesions.¹⁹ According to the published data, breast DCE-MRI has the potential to distinguish benign from malignant mass lesions effectively. Nevertheless, DCE-MRI is inferior in discriminating benign from malignant NME lesions.²³ Hence, a meticulous analysis of the multiple, standardized parameters from BI-RADS lexicon is crucial to achieve a higher diagnostic performance of DCE-MRI in the case of FCCs presenting as NME, including the distribution of enhancement, the internal enhancement pattern, the

type of TICs, the wash-in, and the signal intensity on T2W images.

In our study the postcontrast enhancement of FCCs was unilateral in all patients. The most frequent types of the distribution of NME were regional - involving more than 25% of a breast quadrant, and diffuse - involving the entire breast (35 patients or 76.1%). Segmental distribution, reflecting the ductal distribution, was detected in 11 patients (23.9%). Thomassin-Naggara *et al.* emphasize that „the more extensive distribution of enhancement is, the less suspicious for malignancy it is“.⁸ Agrawal *et al.* showed that the diffuse enhancement was highly suggestive of benign lesions.²⁴ On the other hand, segmental NME was considered the most suspicious, with the positive predictive value (PPV) for malignancy from 76% to 100%, confirmed with the study by Tozaki and Fukuda.²⁵ Our results show that FCCs mainly show the more extensive distribution - regional and diffuse, suggesting benign aetiology of the condition.

The internal pattern of enhancement in our study was heterogeneous and clumped in 36 cases (78.3%). The stippled enhancement was noted in eight patients (17.4%) and homogeneous in two patients (4.3%). According to the previous studies (Thomassin-Naggara *et al.*, Tozaki and Fukuda), when the enhancement is heterogeneous or clumped the risk of malignancy is considered high, with the PPV of 53–58%, while the homogenous enhancement has low PPV for malignancy, up to 5%. The stippled enhancement represents the normal breast parenchymal enhancement.^{8,25} Since almost 80% of the cases in our study showed heterogeneous or clumped enhancement on DCE-MRI, the internal pattern can be one of the most important reasons for mimicry of the breast cancer by FCCs.

Kinetic curve enhancement reflects functional aspects of blood vessel permeability in normal and pathological breast tissue after intravenous gadolinium contrast application. According to the published data, the permanent enhancement (type 1 time-intensity curve) is seen in benign lesions in 85% of cases, the plateau (type 2) curve is seen in 36% of malignant cases and the washout (type 3) curve in 57% of malignant cases.²⁶ In our study the majority of patients have type 2 curve (25 or 54.3%), followed by type 1 curve in 17 patients (37%) and type 3 in four patients (8.7%). Generally, the published data about the kinetic curve enhancement of NME significantly differ. In the study of FCCs by Chen *et al.* 90% of NME lesions had the type 1 curve.¹⁹ Bartella *et al.* reported predominantly the type 2 curve in cases of malignant NME.²⁷ Goto *et*

al. did not find any differences in the kinetic curve enhancement between benign and malignant NME lesions.²⁸ These differences may be partly due to the fact that the time-intensity curves are based on the semiquantitative analysis of gadolinium contrast uptake with the free-hand selected region of interest (ROI) on the heterogeneous areas of NME. Some recent studies suggested that the quantitative analysis using automated computer-aided diagnosis (CAD) can overcome subjectivity of the free-hand selection of ROI.²⁹ The postcontrast enhancement rate types in our study were slow in 15 patients (32.6%), moderate in 14 patients (30.4%) and fast in 17 patients (37.0%). Based on the published data, slow wash-in indicates benign lesions, medium wash-in may indicate lesions like mastitis, fresh scar, FCCs or DCIS, while the fast initial enhancement is suggestive of malignancy, especially when combined with the type 2 or the type 3 enhancement curve.³⁰

NME lesions in our study of FCCs were associated with microcysts on T2W images in 54.3% of cases, which was suggestive of benign conditions.⁸

Additionally, we investigated DCE-MRI morphokinetic features of three distinct histological types of FCCs: nonproliferative lesions (11 cases or 24%), proliferative lesions without atypia (29 cases or 63%) and proliferative lesions with atypia (6 cases or 13%). Our results show that nonproliferative lesions, proliferative lesions without atypia and proliferative lesions with atypia have similar morphokinetic features (distribution of NME, internal pattern of enhancement, type of TICs and wash-in) with the exception of the significant association of microcysts with proliferative hyperplasia without atypia. To our knowledge, our study is the first, which analyses the morphokinetic features of distinct histological types of FCCs on MRI examination. Our study was prompted by the report from Hartman *et al.* published in 2015, which anticipated a potentially important role of DCE-MRI in case of atypical hyperplasia.³¹ Hartman *et al.* showed that in women with atypical hyperplasia a lifetime risk of breast cancer approaches 30% at 25 years. This high cumulative incidence is not widely recognized, and thus screening DCE-MRI is not routinely recommended for these patients.^{13,32} Hartman *et al.* suggested more intensive screening of women with atypical hyperplasia, with DCE-MRI added to mammography, as well as the use of selective oestrogen-receptor modulators and aromatase inhibitors to prevent breast cancer in women with atypical hyperplasia. We hypothesized that the differentiation of atypical hyperplasia by DCE-MRI

examination from other types of FCCs could be helpful in DCE-MRI screening. Our study was limited by the low number of proliferative lesions with atypia, thus necessitating further investigation.

Our study has some limitations. We did not analyse incidental findings of FCCs on DCE-MRI. Our analysis was conducted in the selected group of symptomatic patients: the lesions were suspicious of malignancy on clinical examination, mammography or ultrasonography and larger than 1 cm in DCE-MRI examination in 93.5% of cases. These facts may have influenced the interpretation and results of DCE-MRI examination.

In conclusion, the profile of FCCs presented as NME in DCE-MRI examination predominantly includes: unilateral regional or diffuse distribution (76.1% of cases), heterogeneous or clumped internal pattern of enhancement (78.3% of cases), plateau (type 2) time-intensity curve (54.3% of cases) with moderate or fast wash-in (67.4% of cases), and associated clustered microcysts (54.3% of cases). Although these findings do not have the classic appearance of malignancy, they are sufficiently suspicious to recommend the biopsy, as final BI-RADS 4 category. In case of NME, proliferative lesions without atypia are the most frequent type of FCCs (63%), followed by nonproliferative lesions (24%), and proliferative lesions with atypia (13%). DCE-MRI cannot show the subtle histological differences between nonproliferative lesions, proliferative lesions without atypia and proliferative lesions with atypia. According to some novel data, MR diffusion-weighted imaging (DWI), related to tissue cellularity and thermal motion of water molecules instead of permeability of blood vessels after the contrast uptake, may be more specific than DCE-MRI to define the benign nature of FCCs.^{33,34}

References

- Guray M, Sahin AA. Benign breast diseases: classification, diagnosis, and management. *Oncologist* 2006; **11**: 435-49. doi: 10.1634/theoncologist.11-5-435
- Dupont WD, Page DL. Risk factors for breast cancer in women with proliferative breast disease. *N Engl J Med* 1985; **312**: 146-51. doi: 10.1056/NEJM198501173120303
- Dupont WD, Parl FF, Hartmann WH, Brinton LA, Winfield AC, Worrell JA, et al. Breast cancer risk associated with proliferative breast disease and atypical hyperplasia. *Cancer* 1993; **71**: 1258-65.
- Ellis IO. Intraductal proliferative lesions of the breast: morphology, associated risk and molecular biology. *Modern Pathology* 2010; **23(Suppl 2)**: S1-7. doi: 10.1038/modpathol.2010.56
- O'Flynn EAM. Diagnosis of primary breast cancer. In: Luna A, Vilanova JC, Celso Hygino Da Cruz Jr. LC, Rossi SE, editors. *Functional imaging in oncology: clinical applications*. Berlin Heidelberg: Springer-Verlag; 2014. p. 816-37.
- D'Orsi CJ, Sickles EA, Mendelson EB, Morris EA. *ACR BI-RADS atlas, breast imaging reporting and data system*. Reston, VA: American College of Radiology; 2013.
- Millet I, Pages E, Hoa D, Merigeaud S, Curros Doyon F, Prat X, et al. Pearls and pitfalls in breast MRI. *Br J Radiol* 2012; **85**: 197-207. doi: 10.1259/bjr/47213729
- Thomassin-Naggara I, Salem C, Darai E, Bazot M, Uzan S, Marsault C, et al. Non-masslike enhancement on breast MRI: interpretation pearls. *J Radiol* 2009; **90**: 269-75. doi: JR-04-2009-90-4-0221-0363-101019-200904045
- Yabuuchi H, Matsuo Y, Kamitani T, Setoguchi, Okafuji T, Soeda H, et al. Non-mass-like enhancement on contrast-enhanced breast MR imaging: lesion characterization using combination of dynamic contrast-enhanced and diffusion-weighted MR images. *Eur J Radiol* 2010; **75**: 126-32. doi: 10.1016/j.ejrad.2009.09.013
- Nadriljanski M, Markovic BB, Milosevic ZC. Breast ductal carcinoma in situ (DCIS): morphologic and kinetic MRI findings. *Iran J Radiol* 2013; **10**: 99-102. doi: 10.5812/iranradiol.4876
- Nadriljanski M, Milošević ZČ, Plešinc-Karapandžić V, Goldner B. Značaj magnetne rezonancije dojki u dijagnostici duktalnog karcinoma *in situ*. *Srp Arh Celok Lek* 2013; **141**: 402-8. doi: 10.2298/SARH1306402N
- Japan Association of Breast and Thyroid Sonology. *Guideline for breast ultrasound: management and diagnosis*. Tokyo: Nankodo Co.; 2004. p. 35-7.
- Sardanelli F, Boetes C, Borisch B, Decker T, Federico M, Gilbert FJ, et al. Magnetic resonance imaging of the breast: Recommendations from the EUSOMA working group. *Eur J Cancer* 2010; **46**: 1296-316. doi: 10.1016/j.ejca.2010.02.015
- Nadriljanski MM, Milošević ZC, Plešinc-Karapandžić V, Maksimovic R. MRI in the evaluation of breast cancer patient response to neoadjuvant chemotherapy: predictive factors for breast conservative surgery. *Diagn Interv Radiol* 2013; **19**: 463-70. doi: 10.5152/dir.2013.13201
- Povoski SP, Neff RL, Mojzsis CM, O'Malley DM, Hinkle GH, Hall NC, et al. A comprehensive overview of radioguided surgery using gamma detection probe technology. *World J Surg Oncol* 2009; **7**: 7-11. doi: 10.1186/1477-7819-7-11
- Santen RJ, Mansel R. Benign Breast Disorders. *N Engl J Med* 2005; **353**: 275-85. doi: 10.1056/NEJMra035692
- Goehring C, Morabia A. Epidemiology of benign breast disease, with special attention to histologic types. *Epidemiol Rev* 1997; **19**: 310-27.
- Wu C, Ray RM, Lin MG, Gao DL, Horner NK, Nelson ZC, et al. A case-control study of risk factors for fibrocystic breast conditions. *Am J Epidemiol* 2004; **160**: 945-60. doi: 10.1093/aje/kwh318
- Chen JH, Liu H, Baek HM, Nalcioğlu O, Su MY. MR imaging features of fibrocystic change of the breast. *Magn Reson Imaging* 2008; **26**: 1207-14. doi: 10.1016/j.mri.2008.02.004
- Chen JH, Nalcioğlu O, Su MY. Fibrocystic change of the breast presenting as a focal lesion mimicking breast cancer in MR imaging. *J Magn Reson Imaging* 2008; **28**: 1499-505. doi: 10.1002/jmri.21455
- van den Bosch MA, Daniel BL, Mariano MN, Nowels KN, Birdwell RL, Fong KJ, et al. Magnetic resonance imaging characteristics of fibrocystic change of the breast. *Invest Radiol* 2005; **40**: 436-41.
- Kiyak G, Asik E, Yazgan A. Magnetic resonance imaging characteristics of fibrocystic change of the breast. *Bratisl Lek Listy* 2011; **112**: 506-9.
- Jansen SA, Fan X, Karczmar GS, Abe H, Schmidt RA, Giger M, et al. DCE MRI of breast lesions: Is kinetic analysis equally effective for both: mass and nonmass-like enhancement? *Med Phys* 2008; **35**: 3102-9. doi: 10.1118/1.2936220
- Agrawal G, Su MY, Nalcioğlu O, Feig SA, Chen JH. Significance of breast lesion descriptors in the ACR BIRADS MRI lexicon. *Cancer* 2009; **115**: 1363-80. doi: 10.1002/cncr.24156
- Tozaki M, Fukuda K. High-spatial-resolution MRI of non-masslike breast lesions: interpretation model based on BI-RADS MRI descriptors. *AJR Am J Roentgenol* 2006; **187**: 330-7. doi: 10.2214/ajr.187.3.w330
- Rahbar H, Partridge SC. Multiparametric MR imaging of breast cancer. *Magn Reson Imaging Clin N Am* 2016; **24**: 223-38. doi: 10.1016/j.mric.2015.08.012

27. Bartella L, Liberman L, Morris EA, Dershaw DD. Nonpalpable mammographically occult invasive breast cancers detected by MRI. *AJR Am J Roentgenol* 2006; **186**: 865-70. doi: 10.2214/AJR.04.1777
28. Goto M, Ito H, Akazawa K, Kubota T, Kizu O, Yamada K, et al. Diagnosis of breast tumors by contrast-enhanced MR imaging: comparison between the diagnostic performance of dynamic enhancement patterns and morphologic features. *J Magn Reson Imaging* 2007; **25**: 104-12. doi: 10.1002/jmri.20812
29. Newell D, Nie K, Chen JH, Hsu CC, Yu HJ, Nalcioglu O, et al. Selection of diagnostic features on breast MRI to differentiate between malignant and benign lesions using computer-aided diagnosis: differences in lesions presenting as mass and non-mass-like enhancement. *Eur Radiol* 2010; **20**: 771-81. doi: 10.1007/s00330-009-1616-y
30. Kaiser WA. *Signs in MR-Mammography*. Berlin Heidelberg: Springer-Verlag; 2008.
31. Hartmann LC, Degnim AC, Santen RJ, Dupont WD, Ghosh K. Atypical hyperplasia of the breast - risk assessment and management options. *N Engl J Med* 2015; **372**: 78-9. doi: 10.1056/NEJMs1407164
32. Saslow D, Boetes C, Burke W, Harms S, Leach MO, Lehman CD, et al. American Cancer Society guidelines for breast screening with MRI as an adjunct to mammography. *CA Cancer J Clin* 2007; **57**: 75-89.
33. Ochi M, Kuroiwa T, Sunami S, Murakami J, Murakami J, Miyahara S, Nagaie T, et al. Diffusion-weighted imaging (b value = 1500 s/mm (2)) is useful to decrease false-positive breast cancer cases due to fibrocystic changes. *Breast Cancer* 2013; **20**: 137-44. doi: 10.1007/s12282-011-0319-9
34. Nadrljanski MM, Gusic N, Milovanovic Z, Plesinac-Karapandzic V, Radulovic O, Milosevic ZC. Fibrocystic changes of the breast: lesion characterization using dynamic contrast-enhanced and diffusion-weighted MR images. *ECR 2013, EPOS*. Available at: <http://dx.doi.org/10.1594/ecr2013/C-0868>.

Evaluation of brain edema formation defined by MRI after LINAC-based stereotactic radiosurgery

Maciej Harat¹, Andrzej Lebioda^{2,4}, Judyta Lasota³, Roman Makarewicz^{2,4}

¹ Department of Radiotherapy, The Franciszek Lukaszczyk Oncology Center, Bydgoszcz, Poland

² Department of Oncology and Brachytherapy, Nicolaus Copernicus University, Ludwik Rydygier Collegium Medicum, Bydgoszcz, Poland

³ Department of Medical Physics, The Franciszek Lukaszczyk Oncology Centre, Bydgoszcz, Poland

⁴ Department of Oncology and Brachytherapy, The Franciszek Lukaszczyk Oncology Center, Bydgoszcz, Poland

Radiol Oncol 2017; 51(2): 137-141.

Received 28 August 2016

Accepted 2 March 2017

Correspondence to: Maciej Harat, 85-796 Bydgoszcz, Romanowskiej 2 St., Poland. Phone: +48 52 374 3479; E-mail: haratm@co.bydgoszcz.pl

Disclosure: No potential conflicts of interest were disclosed.

Background. Peri-lesional edema is a serious and well-known complication of stereotactic radiosurgery (SRS). Here we evaluated edema risk after SRS and assessed its formation and resolution dynamics.

Patients and methods. 107 patients underwent SRS for heterogeneous diagnoses: 34 (29%) with arteriovenous malformations, 38 (35%) with meningiomas, 16 (15%) with metastatic tumors, 16 (15%) with acoustic neuromas, 3 with (3%) cavernomas, and 2 (2%) each with anaplastic astrocytomas and anaplastic oligoastrocytomas. Edema area was delineated in MRI T2-FLAIR sequences 0, 6, 12, 18, 24, 30, and 38 months after treatment. Lesion location was defined as either above ($n = 80$) or below ($n = 32$) the "Frankfurt modified line" (FML).

Results. 17% of patients developed or had worsening post-treatment edema. Edema volume was maximal at 6 months (mean 7.2, SD 1.2) post radiosurgery. Post-SRS edema was 5.1 (1.06 – 24.53) times more likely in patients with lesions above the FML. There was no association between edema development and age, PTV size, number of beams, and diagnosis ($p = 0.07$).

Conclusions. Radiosurgery-associated edema develops within 6 months of treatment and decreases over time. Edema occurrence is strongly related to lesion location, and its presence is much more likely when the treated lesions are situated above the Frankfurt line.

Key words: brain edema; LINAC; radiosurgery; stereotactic

Introduction

Intracranial stereotactic radiosurgery (SRS) is a radiotherapy technique used to treat patients unsuitable for surgery or after partial resection of meningiomas, neuromas, brain metastases, and vascular malformations. Typical eligibility criteria are patients with tumors not exceeding 3.5 cm and those who can cooperate during the procedure.^{1,2}

Brain edema is a common radiosurgery-related side effect³⁻⁷ that often requires symptomatic treat-

ment since untreated it can impair quality of life or even cause death. For many years, the most effective edema treatments have been corticosteroids (dexamethasone) and mannitol.

The exact pathophysiology of edema formation after radiotherapy remains unclear but may be related to cerebrovascular impairment, disruption of the blood-brain barrier, or radiation-induced damage to microglia and astrocytes.⁸ Aquaporin 4 and other mediators have been implicated in edema formation including inflammatory cytokines, an-

giogenesis factors (VEGF), hypoxia-related factors (HIF-1), cyclooxygenases, and markers of glial activation.^{5,9-11}

Current evidence suggests that radiosurgery-related brain edema is associated with tumor size, location of the lesion, the prescribed radiotherapy dose, and the presence of edema before treatment.^{12,13} Some data show that brain edema, even in homogenous clinical groups, is unrelated to the maximum dose or the surrounding conformity index.¹⁴ It should be noted that most existing research concerns edema related to meningioma radiosurgery.^{5,12,13}

We have observed edema after radiosurgery in patients with various clinical and histopathologic diagnoses in our practice, the significance of which remains uncertain. We therefore sought to identify factors that predispose to edema formation after SRS and assess edema formation and resolution dynamics.

Patients and methods

One hundred and three patients undergoing 111 SRS procedures were treated in the Oncology Centre in Bydgoszcz between January 2008 and October 2012. The study population had a heterogeneous set of histopathological diagnoses: 34 (29%) arteriovenous malformations (AVMs), 38 (35%) meningiomas, 16 (15%) metastatic tumors, 16 (15%) neuromas, 3 (3%) cavernous angiomas, 2 (2%) anaplastic astrocytomas, and 2 (2%) anaplastic oligoastrocytomas. The baseline patient characteristics are shown in Table 1.

Patients were treated with a 6 MV photon beam provided by a linear accelerator (Varian, USA) and a micromultileaf collimator with 3mm width leaves at the isocenter (Brainlab, Germany). The median prescribed doses at the lesion margin (isodose line) was 16 Gy for all lesions apart from for neuromas (12 Gy). Patient immobilization and target volume definition were achieved using a stereotactic frame or thermoplastic mask. After mask/frame fixation, three-dimensional computed tomography (3D-CT) was performed and then fused with non-stereotactic gadolinium-enhanced T1-weighted magnetic resonance imaging (MRI) sequences.

All patients with radiological signs of brain edema during follow-up examinations were included. Edema volume was delineated on T2-weighted axial MRI/FLAIR scans with a 1 mm slice thickness using the Oncentra Brachy (Nucletron) treatment planning workstation. Edema analysis was performed on MRI scans prior to treatment and 3, 6, 9, 12, 18, 24, 30, and 36 months after treatment. An example is shown in Figure 1.

To analyze lesion location, lesions were separated into occurrence above ($n = 80$) and below ($n = 32$) a plane separating the top and bottom of the skull extending from frontal to parietal (protuberantia frontalis to protuberantia occipitalis) and situated 3 cm above the Frankfurt line¹⁴ (referred to here as the Frankfurt modified line (FML)) (Figure 2). All infratentorial tumors (number), lesions localized in the central brain structures (*e.g.*, hippocampus, caudate nucleus), lesions localized to the temporal and inferior parts of the frontal lobes, and meningiomas of the tentorium and sella turcica were regarded as “below” FML lesions and all others as “above” FML lesions. The study was performed in accordance with the principles of the Helsinki Declaration and was approved by the Ethics Committee of Collegium Medicum of Nicolaus Copernicus University.

TABLE 1. Baseline patient characteristics

Characteristic	Number of patients
Total number of lesions	111
Sex	
Male	40
Female	63
Age (mean)	51
Histopathological diagnosis	
Arteriovenous malformation	34
Meningioma	38
Metastasis	16
Neuroma	16
Cavernous angioma	3
Anaplastic astrocytoma	2
Anaplastic Oligoastrocytoma	2
Lesion location	
Ponto-cerebellar angle	24
Cerebellum	7
Parietal lobe	16
Frontal lobe	17
Subcortical nucleus/hippocampus	12
Convexity	2
Petroclival	1
Temporal lobe	8
Falx	13
Tentorium	3
Occipital lobe	4
More than one SRS treatment	8
Mean V_{12}	6.3 cm ³

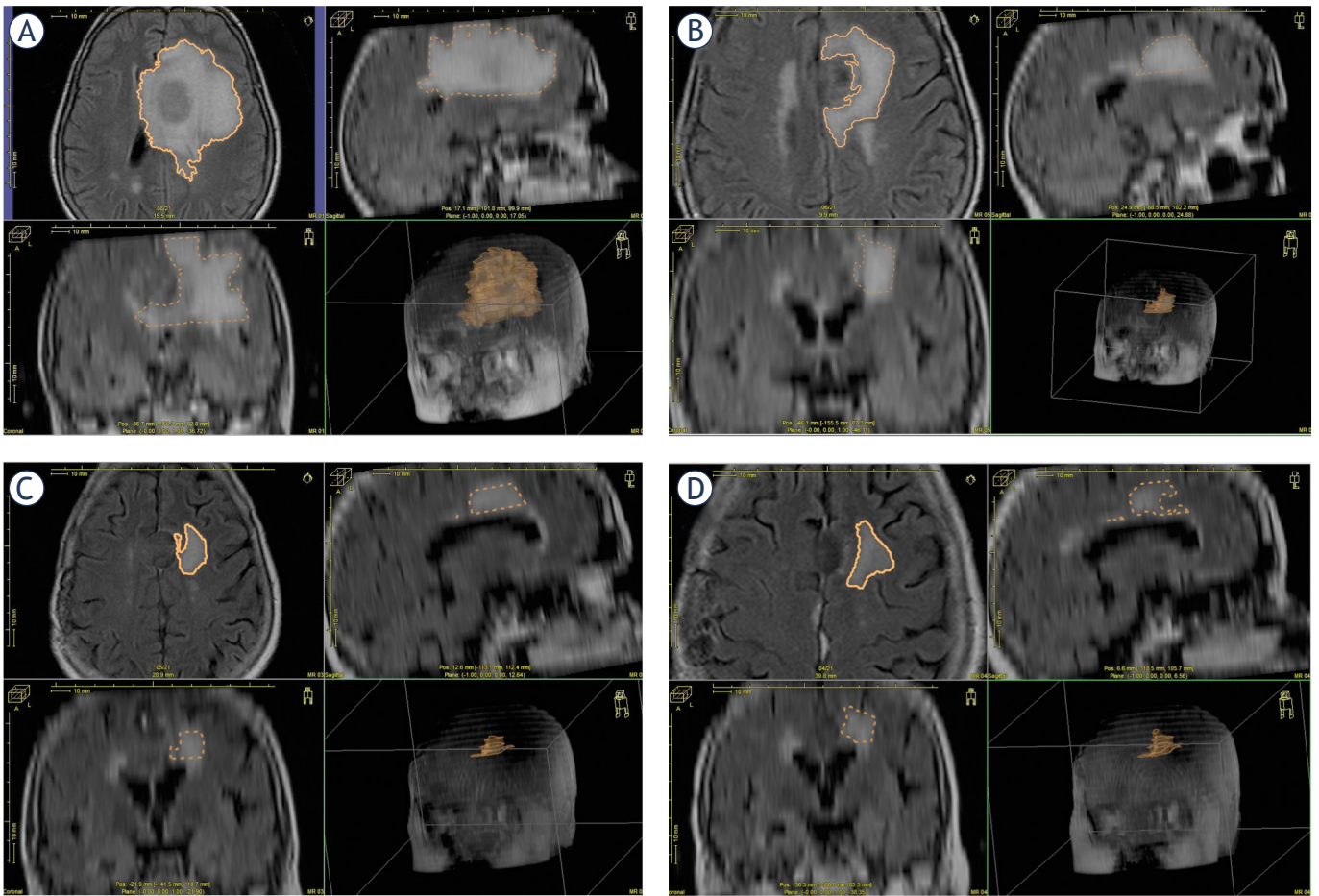


FIGURE 1. MRI scans performed after treatment showing delineation of area with decreasing edema. (A) 6 months; (B) 12 months; (C) 18 months; (D) 24 months.

All statistical analyses were performed using Statistica v.10 (Dell Inc., Austin, TX).

Results

Five patients did not attend for follow-up studies and were excluded from further analysis. SRS-associated edema occurred in 17 patients, of whom one patient was diagnosed with a meningioma located in the pontocerebellar angle with edema prior to SRS and that increased in volume in the six months after treatment. The initial MRI did not reveal edema in the other patients. SRS-related edema occurred in 2/16 (12.5%) metastatic tumors, 5/34 (14.7%) AVMs and 10/38 (26.3%) meningiomas.

The dynamics of edema formation over time (log-normal distribution) are shown in Figure 3. There were no associations between edema development and age, size of irradiated area, volume of

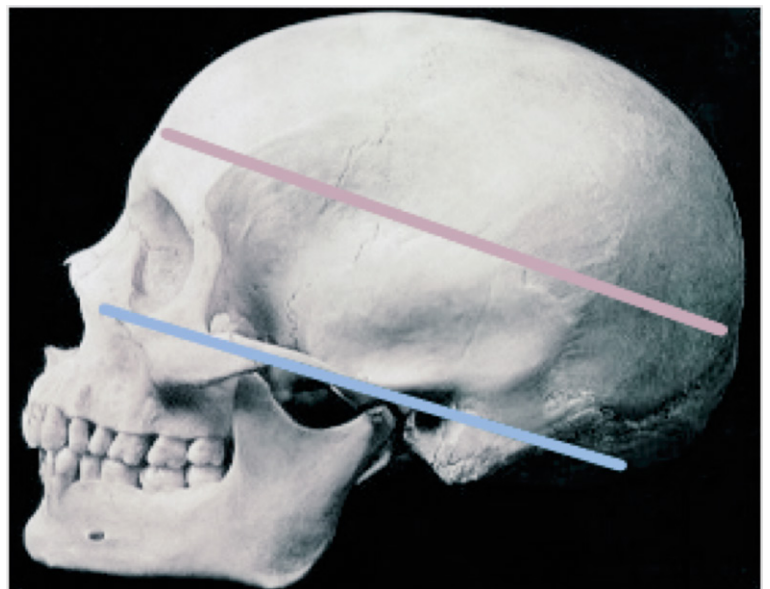


FIGURE 2. The Frankfurt Line (blue line) and the Frankfurt modified line (FML; red line).

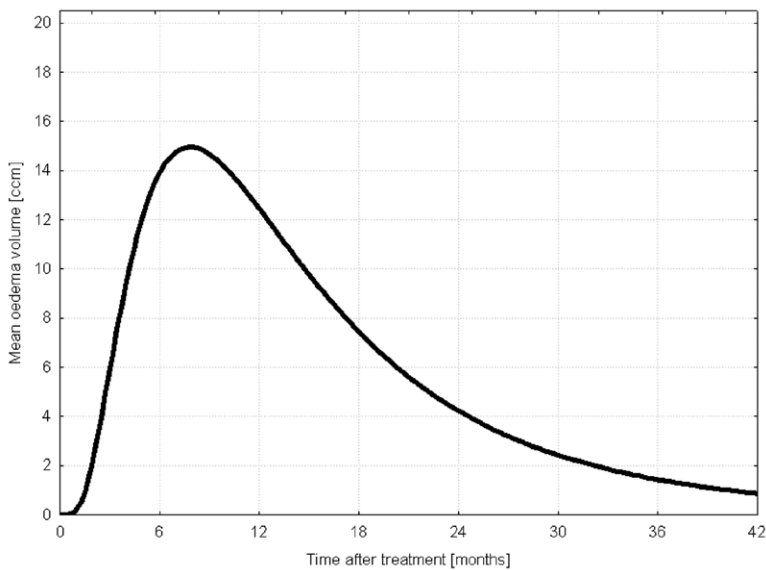


FIGURE 3. The largest volume of edema was observed at 6 months (mean 7.2 months, S.D. 1.2 months) after radiosurgery and decreased thereafter.

normal brain covered by 12 Gy isodose (V_{12}), number of beams, type of tumor ($p = 0.07$), or the type of immobilization applied.

With respect to lesion location, edema occurred in 2/32 lesions below the FML and in 15/80 lesions above the FML, representing a 5.1-times (1.06 – 24.53) increased incidence of edema after radiosurgery for lesions above the FML.

There was no association between edema development after secondary radiosurgery in the same patients if no edema formed after the initial treatment.

Discussion

Radiosurgery-related peri-lesional edema is a well-known but rarely described complication of SRS. Here we present the relationship between edema occurrence and lesion location in a population of patients with heterogeneous diagnoses.

The incidence of edema in this cohort (17%) is consistent with the published literature, recognizing that most data relates to edema occurring after radiosurgery for meningiomas. Chang *et al.* observed edema in 26.3% of patients with meningiomas after radiosurgery, about 40% of whom presented with symptoms of increased intracranial pressure.¹⁵ Kobayashi *et al.* reported edema in 13.8% of patients with benign meningiomas after radiosurgery.¹⁶ With respect to radiosurgery-relat-

ed edema in patients with other histopathological diagnoses, Hallemeier *et al.* reported edema after radiosurgery in 44% of patients with astrocytoma, which was effectively treated with oral or intravenous steroid therapy¹⁷, while Williams *et al.* described a case of steroid-resistant edema treated with bevacizumab that developed 9 months after radiosurgery for a vascular malformation.¹⁸

Cai *et al.* found that the risk of edema increased with greater tumor-brain contact interface area, supporting the observed differing incidence of edema according to location: the decreased incidence of edema below the FML may be associated with the amount of brain surrounding the lesion, since the lesion-brain contact interface above the FML is greater than below the FML.¹⁹

We found no association between the presence of edema and lesion size, dose escalation, or histopathological diagnosis. Although this finding may be due to the small number of patients in each group, these parameters need to be taken into account when assessing edema risk after radiosurgery.²⁰

The lack of an association between the histopathological diagnosis and lesion size suggests a common pathway for post-SRS edema formation, most likely related to impaired blood flow surrounding the intracranial lesion and explaining why the incidence of edema is lower in locations with better blood supply. For instance, with respect to tumors occurring in the parasagittal region, a higher edema risk may be present due to an unfavorable location (above the FML) and a histopathological diagnosis of meningioma. In this area, numerous veins carry blood to the superior sagittal sinus and the lower and deep vein (Galena vein), and numerous vessels at the tumor border drain blood from the tumor to normal brain vessels. Radiosurgery may impair flow in these vessels, similar to the mechanism seen when vessels in an AVM are obliterated. This leads to regional impairment of venous drainage from the brain and, as a consequence, edema.

We observed an increase in edema volume over the first 6 – 9 months and a decrease thereafter. In one retrospective multi-center study, the average duration of edema after radiosurgery was estimated to be 15 months (range 5 – 18 months)²¹, with maximum accumulation after 6 – 8 months, consistent with the results presented here. Not all brain edema is symptomatic or requires treatment, but if edema is observed radiologically at follow-up 3 months after treatment even in the absence of symptoms, a short regimen of steroids may be ap-

appropriate to avoid the natural dynamics of edema formation occurring.

Patients treated with multiple rounds of radiosurgery to more than one lesion are a valuable study group for assessing the prevalence of complications. Here, this patient subgroup did not develop edema at follow up after both the first and subsequent treatments. This may suggest that resistance to edema formation depends on host or individual factors, but this hypothesis would require further clinical validation.

The study has several limitations. The FML plane was arbitrarily selected by the investigators from personal observations and does not represent an anatomical border that may explain differences in edema formation. Due to the retrospective nature of the analysis, we were unable to examine steroid treatment and its influence on edema formation and resolution. Nevertheless, to our knowledge, this is one of the largest studies of SRS-related edema formation.

Conclusions

Peri-lesional cerebral edema is a temporary intracranial complication after radiosurgery. The most severe MRI changes can be observed in the first six to nine months after treatment. The occurrence of cerebral edema is dependent on the intracranial location. Localization of lesion above the FML is a strong predictor of the emergence of this treatment complication.

Acknowledgements

We gratefully acknowledge Nextgenediting (www.nextgenediting.com) for editorial assistance.

References

- Chin L, Regine W. *Principles and practice of stereotactic radiosurgery*. New York: Springer; 2008.
- Bakay RA. Stereotactic radiosurgery in the treatment of brain tumors. *Clin Neurosurg* 1992; **39**: 292-313.
- Nakamura S, Hiyama H, Arai K, Nakaya K, Sato H, Hayashi M, et al. Gamma knife radiosurgery for meningiomas: four cases of radiation-induced edema. *Stereotact Funct Neurosurg* 1996; **66**: 142-5. doi: 10.1159/000099804
- Ganz JC, Schrottner O, Pendl G. Radiation-induced edema after gamma knife treatment for meningiomas. *Stereotact Funct Neurosurg* 1996; **66**: 129-33. doi: 10.1159/000099778
- Kan P, Liu JK, Wendland MM, Shrieve D, Jensen RL. Peritumoral edema after stereotactic radiosurgery for intracranial meningiomas and molecular factors that predict its development. *J Neurooncol* 2007; **83**: 33-8. doi: 10.1007/s11060-006-9294-y
- Morimoto M, Yoshioka Y, Shiomi H, Isohashi F, Konishi K, Kotsuna T, et al. Significance of tumor volume related to peritumoral edema in intracranial meningioma treated with extreme hypofractionated stereotactic radiation therapy in three to five fractions. *Jpn J Clin Oncol* 2011; **41**: 609-16. doi: 10.1093/jjco/hyr022
- Unger KR, Lominska CE, Chanyasulkit J, Randolph-Jackson P, White RL, Aulisi E, et al. Risk factors for posttreatment edema in patients treated with stereotactic radiosurgery for meningiomas. *Neurosurgery* 2012; **70**: 639-45. doi: 10.1227/NEU.0b013e3182351ae7
- Papadopoulos MC, Saadoun S, Binder DK, Manley GT, Krishna S, Verkman AS. Molecular mechanisms of brain tumor edema. *Neuroscience* 2004; **129**: 1011-20. doi: 10.1016/j.neuroscience.2004.05.044
- Saadoun S, Papadopoulos MC. Aquaporin-4 in brain and spinal cord oedema. *Neuroscience* 2010; **168**: 1036-46.
- Moore AH, Olschowka JA, Williams JP, Paige SL, O'Banion MK. Radiation-induced edema is dependent on cyclooxygenase 2 activity in mouse brain. *Radiat Res* 2004; **161**: 153-60.
- Khan RB, Krasin MJ, Kasow K, Leung W. Cyclooxygenase-2 inhibition to treat radiation-induced brain necrosis and edema. *J Pediatr Hematol Oncol* 2004; **26**: 253-5.
- Chang JH, Chang JW, Choi JY, Park YG, Chung SS. Complications after gamma knife radiosurgery for benign meningiomas. *J Neural Neurosurg Psychiatry* 2003; **74**: 226-30.
- Kalapurakal JA, Silverman CL, Akhtar N, Laske DW, Braitman LE, Boyko OB, et al. Intracranial meningiomas: factors that influence the development of cerebral edema after stereotactic radiosurgery and radiation therapy. *Radiology* 1997; **204**: 461-5. doi: 10.1148/radiology.204.2.9240536
- F. Łabiszewska-Jaruzelska *Ortodoncja: zasady i praktyka*. Warszawa: PZWL; 1995. p. 57.
- Chang JH, Chang JW, Choi JY, Park YG, Chung SS. Complications after gamma knife radiosurgery for benign meningiomas. *J Neural Neurosurg Psychiatry* 2003; **74**: 226-30.
- Kobayashi T, Kida Y, Mori Y. Long-term results of stereotactic gamma radiosurgery of meningiomas. *Surg Neurol* 2001; **55**: 325-31.
- Hallemeier CL, Pollock BE, Schomberg PJ, Link MJ, Brown PD, Stafford SL. Stereotactic radiosurgery for recurrent or unresectable pilocytic astrocytoma. *Int J Radiat Oncol Biol Phys* 2012; **83**: 107-12. doi: 10.1016/j.ijrobp.2011.05.038
- Williams BJ, Park DM, Sheehan JP. Bevacizumab used for the treatment of severe, refractory perilesional edema due to an arteriovenous malformation treated with stereotactic radiosurgery. *J Neurosurg* 2012; **116**: 972-7. doi: 10.3171/2012.1.JNS111627
- Cai R, Barnett GH, Novak E, Chao ST, Suh JH. Principal risk of peritumoral edema after stereotactic radiosurgery for intracranial meningioma is tumor-brain contact interface area. *Neurosurgery* 2010; **66**: 513-22. doi: 10.1227/01.NEU.0000365366.53337.88
- Unger KR, Lominska CE, Chanyasulkit JBA, Randolph-Jackson P, White RL, Aulisi E, et al. Risk factors for posttreatment edema in patients treated with stereotactic radiosurgery for meningiomas. *Neurosurgery* 2012; **70**: 639-45. doi: 10.1227/NEU.0b013e3182351ae7
- Kondziolka D, Flickinger JC, Perez B. Judicious resection and/or radiosurgery for parasagittal meningiomas: outcomes from a multicenter review-Gamma Knife Meningioma Study Group. *Neurosurgery* 1998; **43**: 405-14.

Genetic factors affecting intraoperative 5-aminolevulinic acid-induced fluorescence of diffuse gliomas

Kiyotaka Saito¹, Toshinori Hirai², Hideo Takeshima¹, Yoshihito Kadota², Shinji Yamashita¹, Asya Ivanova¹, Kiyotaka Yokogami¹

¹ Department of Neurosurgery, Division of Clinical Neuroscience, Faculty of Medicine, University of Miyazaki, Japan

² Department of Radiology, Division of Pathophysiological Diagnosis and Therapy, Faculty of Medicine, University of Miyazaki, Japan

Radiol Oncol 2017; 51(2): 142-150.

Received 15 December 2016

Accepted 13 March 2017

Correspondence to: Kiyotaka Saito, M.D., Department of Neurosurgery, Division of Neuroscience, Faculty of Medicine, University of Miyazaki, 5200 Kihara, Kiyotake, Miyazaki, 889-1692, Japan. Phone: +81-985-85-3128; Fax: +81-985-84-4571; E-mail: kiyotaka_saitou@med.miyazaki-u.ac.jp

Disclosure: No potential conflicts of interest were disclosed.

This study was supported by a Grant-in-Aid for Clinical Research from Miyazaki University Hospital.

Background. In patients operated for malignant glioma, 5-aminolevulinic acid (5-ALA)-induced fluorescence guidance is useful. However, we occasionally experience instances of non-visible fluorescence despite a histopathological diagnosis of high-grade glioma. We sought to identify factors that influence the intraoperative visualization of gliomas by their 5-ALA-induced fluorescence.

Patients and methods. We reviewed data from 60 patients with astrocytic or oligodendroglial tumors who underwent tumor removal under 5-ALA-induced fluorescence guidance between January 2014 and December 2015. Their characteristics, preoperative magnetic resonance imaging (MRI) findings, histological diagnosis, and genetic profile were analyzed and univariate and multivariate statistical analyses were performed.

Results. In 42 patients (70%) we intraoperatively observed tumor 5-ALA fluorescence. They were 2 of 8 (25%) patients with World Health Organization (WHO) grade II, 9 of 17 (53%) with grade III, and 31 of 35 (89%) patients with grade IV gliomas. Univariate analysis revealed a statistically significant association between 5-ALA fluorescence and the isocitrate dehydrogenase 1 (IDH1) status, 1p19q loss of heterozygosity (LOH), the MIB-1 labeling index, and the tumor margin, -heterogeneity, and -contrast enhancement on MRI scans ($p < 0.001$, $p = 0.003$, $p = 0.007$, $p = 0.046$, $p = 0.021$, and $p = 0.002$, respectively). Multivariate analysis showed that the IDH1 status was the only independent, statistically significant factor related to 5-ALA fluorescence ($p = 0.009$).

Conclusions. This study identified the IDH1 status as the factor with the most influence on the 5-ALA fluorescence of diffuse gliomas.

Key words: glioma; 5-aminolevulinic acid (5-ALA); IDH1 mutation

Introduction

Although the standard treatment for malignant gliomas is the combination of maximal resection followed by radiation therapy and adjuvant chemotherapy (temozolomide)¹, their prognosis remains unfavorable. Maximal resection is the most important factor for improving the survival rate²⁻⁴,

patients who underwent complete resection benefited more from temozolomide than did patients treated by incomplete resection.⁵

According to the 2016 WHO classification, the genetic profile, *e.g.* the isocitrate dehydrogenase 1 (IDH1) mutation status and 1p19q co-deletion, is the key factor for the diagnosis and treatment of diffuse gliomas. The IDH1 mutation status is more

prognostic for overall survival than are standard histological criteria that differentiate high-grade astrocytomas.^{6,7} Also, the prognosis of IDH1 mutant glioblastoma is considerably better than of IDH1 wild-type anaplastic astrocytoma and glioblastoma^{6,7}, and methylation of the O-6-methylguanine DNA methyltransferase (MGMT) promoter in diffuse gliomas is a predictive epigenetic marker of the responsiveness to alkylating agents such as temozolomide.⁸

A naturally occurring intermediary in the heme synthetic pathway, 5-aminolevulinic acid (5-ALA)⁹, is used for the intraoperative visualization of malignant gliomas. After its administration as a prodrug, it is metabolized at the tissue level to the active compound, protoporphyrin IX (PPIX), which is responsible for *in vivo* photosensitization.⁹ 5-ALA-induced fluorescence guidance facilitates complete tumor removal and may enhance progression-free survival.^{4,10} According to previous studies^{9,11}, no visible fluorescence was reported in 100% of World Health Organization (WHO) grade I, 81% of WHO grade II, and 25% of high-grade (WHO grades III and IV) gliomas. High-grade gliomas lacking contrast enhancement on magnetic resonance imaging (MRI) scans may not display appreciable macroscopic fluorescence.¹²

In contrast, it has been reported that 5-ALA-induced fluorescence is associated with contrast enhancement on preoperative MRI scans¹³, a high-grade WHO classification¹⁴⁻¹⁶, high tumor cellularity¹⁷⁻¹⁹, an increased MIB-1 labeling index^{12,15,19}, and a high tumor burden.¹³ Factors that account for the difference in the level of fluorescence in individual tumors remain to be clearly identified.

The aim of this study was to identify the factor(s), including MRI observations and genetic factors, with the greatest influence on intraoperative 5-ALA-induced fluorescence in patients with diffuse gliomas.

Patients and methods

Patient population

The Research Ethics Committee of the Faculty of Medicine, University of Miyazaki, approved this study; prior informed consent for inclusion in the study was obtained from all patients. They underwent tumor removal at Miyazaki University Hospital during the period from January 2014 to December 2015. We collected 71 consecutive glioma patients. Our inclusion criteria were surgery under 5-ALA-induced fluorescence guidance, a

TABLE 1. Clinical characteristics of 60 patients with diffuse gliomas

Characteristics	No. of Patients (%)
Number of patients	60 (100)
Sex	
Male	35 (58.3)
Female	25 (41.7)
Age (yrs)	
Average ± SD	60.7 ± 15.4
Median	62.5
Range	6 - 80
Tumor grades and subtypes (WHO 2007)	
Grade II	8 (13.3)
Astrocytoma	2 (3.3)
Oligoastrocytoma	3 (5.0)
Oligodendroglioma	3 (5.0)
Grade III	17 (28.3)
Anaplastic astrocytoma	2 (3.3)
Anaplastic oligoastrocytoma	3 (5.0)
Anaplastic oligodendroglioma	12 (20.0)
Grade IV	35 (58.3)
Localization	
Frontal	22 (36.7)
Fronto-temporal	2 (3.3)
Temporal	9 (15.0)
Temporo-parietal	5 (8.3)
Temporal & insular	2 (3.3)
Parietal	4 (6.7)
Parieto-occipital	2 (3.3)
Occipital	0 (0)
Insular	4 (6.7)
Central	8 (13.3)
Cerebellar	2 (3.3)
Tumor Status	
Primary	54 (90.0)
Recurrence	6 (10.0)

preoperative MRI evaluation, and a histological diagnosis of astrocytic or oligodendroglial tumors based on the WHO 2007 classification.²⁰ Excluded were patients with WHO grade I tumors and/or needle biopsy only. In patients who had undergone surgical resection more than once during the period, data from the first resection were used. Of

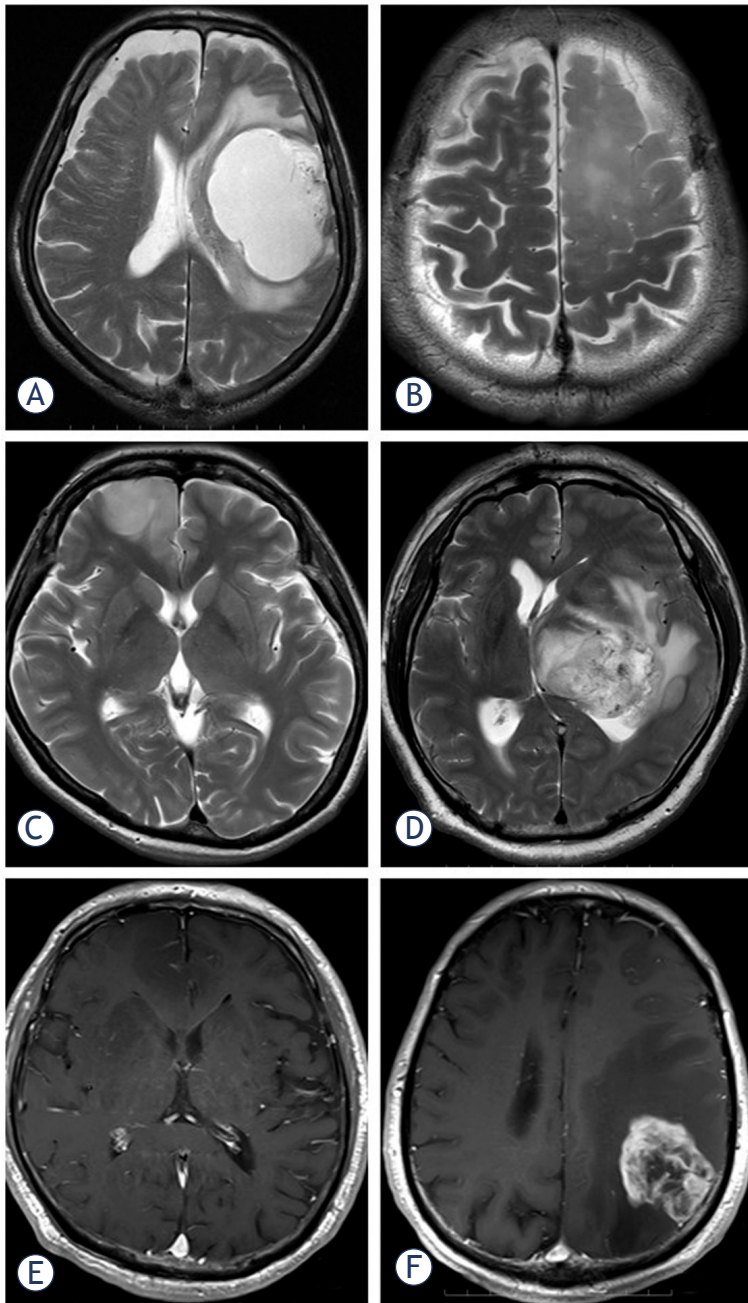


FIGURE 1. Comparison of tumor characteristics on MRI scans. Axial T2W images showing a mass with (A) a smooth and (B) an indistinct tumor border in the left frontal lobe, (C) homogeneous intensity in the right frontal lobe, and (D) heterogeneous intensity in the left thalamus. Axial gadolinium-enhanced T1W images show that (E) the tumor lacks contrast enhancement in the right frontal lobe and is (F) contrast-enhanced in the left parietal lobe.

the 71 patients, 60 (35 men, 25 women; age range 6-80 years, mean age 60.7 years) with astrocytic or oligodendroglial tumors fulfilled our selection criteria; 54 (90.0%) harbored newly diagnosed gliomas. The patient characteristics, histological diag-

nosis, and tumor location are shown in Table 1. Of the included patients, 35 (58.3%) had WHO grade IV, 17 (28.3%) WHO grade III, and 8 (13.3%) had WHO grade II gliomas. The tumor location was the frontal lobe (22 patients, 36.7%), followed by the temporal lobe (9 patients, 15.0%). In 8 patients (13.3%) the tumor was centrally located in the basal ganglion, corpus callosum, and brain stem; none of the tumors were occipital.

Preoperative MRI

All preoperative MRI studies were performed within a week before surgery on a 3 Tesla scanner (Magnetom Verio; Siemens, Erlangen, Germany). T1- and T2-weighted- (T1W, T2W), and contrast-enhanced T1W axial images were used for analysis. The images were assessed consensually by two neuroradiologists blinded to the genotype and the 5-ALA-induced fluorescence of each lesion. They used methods described elsewhere²¹ to qualitatively assess the following findings: a sharp or indistinct tumor border, homogeneous or heterogeneous signal intensity throughout the tumor on T1W and T2W images, and the presence or absence of contrast enhancement on contrast-enhanced T1W images (Figure 1). Identification of the predominant characteristics of individual tumors was based on the readers' judgment of the tumor border and signal heterogeneity.

Surgical procedure

5-ALA (20 mg/kg) was orally administered 3 hours before surgery. For the operation we used an OPMI Pentero instrument (Zeiss, Oberkochen, Germany) equipped with BLUE 400 for visualizing fluorescence and for neuro-navigation. All resections were performed with navigational guidance using contrast-enhanced axial, coronal, and sagittal T1W- or fluid-attenuated inversion recovery (FLAIR) images. The targets for tissue sampling were selected by choosing contrast-enhanced lesions and neuro-navigation, or the tumor center of high-intensity lesions on FLAIR images. Fluorescence was checked repeatedly under our modified neurosurgical microscope by switching between white- and blue-violet excitation light in different areas of the lesion during each procedure. Fluorescence was categorized subjectively by two operating surgeons; a 3rd surgeon confirmed their judgment by reviewing a movie obtained intraoperatively. Fluorescence was categorized as non-visible (negative) and visible (positive).^{19,22} Positive fluorescence included mild



FIGURE 2. Appearance of the tumor cavity under the surgical microscope. (A-B) Violet-blue light excitation yielding visible 5-ALA fluorescence. Note robust (lava-like orange) (A) and mild (pink) brightness (B). (C) No 5-ALA fluorescence is visualized in the tumor cavity.

(pink) and robust brightness (lava-like orange)¹⁸ (Figure 2).

Pathological diagnosis

To diagnose the tumors histopathologically, neuropathologists used the 2007 WHO classification of central nervous system tumors.²⁰ They were blinded to intraoperative 5-ALA fluorescence. Tumor cell proliferation was assessed immunohistochemically using MIB-1 antibody (anti-Ki-67, 1:50; DAKO, Hamburg, Germany). The highest density of Ki-67 immunopositive cells was evaluated in hot spots. The percentage of immunolabeled tumor cell nuclei was expressed as the MIB-1 labeling index.

IDH1 mutation analysis

IDH1 mutation was confirmed by immunohistochemical analysis using R132H antibody²³ or by direct sequencing. Immunostaining was according to the manufacturer's protocol. Briefly, formalin-fixed paraffin-embedded tissue was sliced into 2- μ m sections and dried at 42°C for 3 hours. Deparaffinization was with xylene, rehydration was by submerging the tissue samples in graded series of ethanol (100% to 70%, decreased in 10% steps). Phosphate-buffered saline (PBS) was used for washing. For antigen retrieval, slides were pre-treated by steaming with citric acid buffer (pH 6.0) for 20 min in an autoclave. The sections were then treated with 10% H₂O₂ for 10 min at room temperature to block endogenous peroxidase activity. After washing in 3 changes of PBS for 5 min, the sections were immunostained with monoclonal anti-human IDH1-R132H antibody (1:20 dilution, H09, Dianova, Hamburg, Germany) diluted with PBS, and incubated at 4°C overnight. After being

washed in 3 changes of PBS buffer, the tissues were covered by anti-mouse specific second antibody administered in 1 - 3 drops per slide (Dako EnVision, Hamburg, Germany), and held for 30 min at room temperature. After being washed in 3 changes of PBS buffer, the staining reaction was performed by covering the tissue with a prepared 3, 3'-diaminobenzidine (DAB) chromogen solution (1 drop of DAB chromogen for every 1000 μ l of PBS). This was followed by incubation for approximately 40 sec to allow for proper brown color development. A definite cytoplasmic immunoreaction product was scored as staining cells. Staining was scored on a two-grade scale as negative (no or < 10% staining), and as positive (> 10% positively stained cells).

Direct DNA sequencing was as previously described.^{23,24} IDH1 genomic DNA was isolated from frozen tissue samples with a QIAamp DNA Mini Kit (QIAGEN, Tokyo, Japan). A spanning 90-base pair (bp) fragment was identified with the sense primer IDH1 (forward: 5'-GGCTTGTGAGTGGATGGGTA-3') and the antisense primer IDH (reverse: 5'-GCAAAATCACATTATTGCCAAC-3'). The 25- μ l reaction mixture contained 50 ng of tumor genomic DNA, 1 μ l of each forward and reverse primer (10 μ M), 12.5 μ l of GoTaq Hot Start Green Master Mix (Promega K.K., Tokyo, Japan), and an amount of deionized water to obtain a total volume of 25 μ l. Genomic DNA was subjected to polymerase chain reaction (PCR) amplification, initial denaturation at 95° for 2 min, and 35 cycles of amplification consisting of denaturation at 95° for 30 sec, annealing at 58° for 30 sec, and extension at 72° for 20 sec. Final extension was performed at 72° for 5 min. The 100-bp PCR amplification products were confirmed by 2% agarose gel electrophoresis.

TABLE 2. 5-aminolevulinic acid-induced fluorescence (5-ALA) in 60 diffuse gliomas

5-ALA fluorescence	WHO grade II	WHO grade III	WHO grade IV
Positive	2/8 (25 %)	9/17 (53 %)	31/35 (89%)
Negative	6/8 (75 %)	8/17 (47 %)	4/35 (11%)

The sequence reactions were performed by using a Big Dye Terminator v1.1 Cycle Sequencing Kit (Thermo Fisher Scientific K.K., Yokohama, Japan) in a 20- μ l reaction mixture comprised of 1 μ l of the 100-bp PCR products, 4 μ l of PCR buffer, 2 μ l of the forward primer (5 μ M), 12 μ l of deionized water and 1 μ l of Big Dye Terminator Ready Reaction Mix. Initial denaturation was performed at 96 $^{\circ}$ for 1 min and 25 cycles of amplification (denaturation at 96 $^{\circ}$ for 30 sec, annealing at 50 $^{\circ}$ for 5 sec, and extension at 60 $^{\circ}$ for 4 min). Sequencing products were immediately submitted to direct sequencing on an ABI PRISM 310 Genetic Analyzer (Thermo Fisher Scientific K.K., Yokohama, Japan).

Fluorescence *in situ* hybridization (FISH)

FISH analysis of 1p19q loss of heterozygosity (LOH) was performed on formalin-fixed paraffin-embedded 5- μ m tissues²⁵ prepared for dual-probe hybridization with Vysis LSI FISH Probe according to the manufacturer's instructions (Abbott Japan Co. Ltd.). 1p36/1q25 and 19q13/19p13 dual-color probe sets were used for locus-specific 1p and 19q analysis, respectively, following the manufacturer's instructions (Abbott Japan). Nuclei were counterstained with 4,6-diamidino-2 phenylindole (DAPI).

Analysis of MGMT promoter methylation

Analysis of the methylation status of the MGMT promoter was performed by bisulfite modification and subsequent methylation-specific PCR assay using previously described primers.⁸ The primer sequences for the unmethylated reaction were forward: 5'-TTTGTGTTTGGATGTTTGTAGGTTTTGT-3' and reverse: 5'-AACTCCACACTCTTCCAAAA CAAAACA-3'. Sequences for the methylated reaction were forward: 5'-TTTCGACGTTTCGTAGG TTTTCGC-3' and reverse: 5'-GCACTCTTCCG AAAACGAAACG-3'. The PCR conditions were 35 cycles of 30 sec each at 95 $^{\circ}$, and 60 $^{\circ}$, and 60 sec at 72 $^{\circ}$; the PCR products were electrophoresed on 15% polyacrylamide gels as previously described.²⁶

Statistical analysis

All numeric data were reported as the mean \pm standard deviation. The positive predictive value (PPV) of 5-ALA fluorescence for high-grade gliomas was calculated as the number of 5-ALA fluorescence-positive high grade gliomas / number of all 5-ALA fluorescence-positive tumors. Its negative predictive value (NPV) was calculated as the number of 5-ALA fluorescence-negative low-grade gliomas (WHO grade II) / number of all 5-ALA fluorescence-negative tumors. The diagnostic accuracy of 5-ALA fluorescence for high-grade gliomas was calculated as the number of 5-ALA fluorescence-positive high-grade gliomas plus the number of 5-ALA fluorescence-negative low grade gliomas / the number of all tumors.

Univariate and multivariate logistic regression analyses were used to identify clinical characteristics and genetic- and imaging features associated with the 5-ALA-induced fluorescence of the lesions. Univariate analysis was with the χ^2 -, the Fisher exact-, or the Student *t*-test. Variables with $p < 0.05$ by univariate analysis were used for multivariate analysis. In multivariate logistic regression analysis we computed the odds ratio (OR) and the accompanying 95% confidence interval (CI) using samples with non-visible fluorescence for reference. *P* values < 0.05 were considered statistically significant. All statistical analyses were performed with SPSS software (version 23; IBM SPSS, Chicago IL, USA).

Results

Intraoperative 5-ALA fluorescence

Among the 60 tumors, 42 (70%) were 5-ALA fluorescence-positive; the others were negative. Of the 8 WHO grade II gliomas, 2 were positive, as were 9 of 17 (53%) WHO grade III and 31 (89%) of 35 grade IV gliomas (Table 2). For high-grade gliomas, the PPV of 5-ALA fluorescence was 95.2%; the NPV was 33.3%, and diagnostic accuracy was 76.7%.

As shown in Table 3, among the 60 diffuse gliomas, 13 (22%) harbored IDH1 mutations. These were more often seen in grade II (4/8, 50%) and grade III gliomas (7/17, 41%) than in glioblastomas (2/35, 6%). Of the 13 tumors with IDH1 mutations, 2 (15%) manifested visible fluorescence, the other 11 did not.

Univariate analysis revealed a statistically significant association between 5-ALA fluorescence and the IDH1 status (mutated, non-mutated),

1p19q LOH, MIB-1, and the margin, heterogeneity, and contrast enhancement of the tumors ($p < 0.001$, $p = 0.003$, $p = 0.007$, $p = 0.046$, $p = 0.021$, and $p = 0.002$, respectively); neither the patient age nor the MGMT methylation status was significantly associated. Multivariate analysis showed that the IDH1 status was the only independent, statistically significant factor related to 5-ALA fluorescence ($p = 0.009$) (Table 4). Using tissue samples with non-visible fluorescence as the reference, we found that the OR (95% CI) for IDH1 wild type was 19.238 (1.39, 175.39). No other factors had a significant effect on 5-ALA fluorescence.

Discussion

In this study, we analyzed factors that influence the intraoperative visualization of gliomas by their 5-ALA-induced fluorescence. Our results demonstrate that the IDH1 status was the only independent, statistically significant factor related to 5-ALA fluorescence.

As in an earlier study¹⁵, significantly more high- than low-grade gliomas exhibited 5-ALA fluorescence. Others^{12,15,18,27} reported that MIB-1, an indicator of proliferation activity, and 5-ALA fluorescence were positively correlated. Widhalm *et al.*²⁷ who documented a significantly higher proliferation rate in the tumor area with- than without 5-ALA fluorescence found that visible 5-ALA fluorescence was correlated with a MIB-1 $\geq 10\%$. On the other hand, according to Lau *et al.*¹⁸ 5-ALA intensity is a strong predictor of the degree of tumor cellularity in the most highly fluorescent areas but less predictive in areas with lower 5-ALA intensities. A significant difference in the contrast enhancement of fluorescing and nonfluorescing tissue on T1W MRI scans has been reported.¹³ Our multivariate analysis showed that the IDH1 status was the only independent, significant factor affecting 5-ALA fluorescence.

Yang *et al.*²⁸ showed that in tumor cells the IDH1 mutation may lead to the accumulation of tricarboxylic acid (TCA) cycle metabolites. This results in the activation of the heme biosynthesis pathway that works to remove TCA metabolites. Inactivation of the TCA cycle by fumarate hydratase deficiency involves the biosynthesis and degradation of heme; this facilitates the use of accumulated TCA cycle metabolites and partial mitochondrial nicotinamide adenine dinucleotide (NADH) production.²⁹ A comparison of wild-type- and IDH1-mutant U87MG cell lines showed that mutated

TABLE 3. Relationship between 5-aminolevulinic acid-induced fluorescence (5-ALA) status and clinical-pathologic features

Clinical-pathologic features	Patients with visible fluorescence (n=42)	Patients with no visible fluorescence (n=18)	P value	χ^2 , Fisher, or Student t test
Age (years)				
Average \pm SD	62.4 \pm 16.4	56.7 \pm 12.5	0.16	-
IDH1 mutation			<0.001	23.57
Positive	2	11		
Negative	40	7		
1p19q LOH			0.003	10.22
Positive	5	9		
Negative	37	9		
MGMT methylation			0.05	4.35
Positive	18	13		
Negative	24	5		
MIB1 LI (%)				
Average \pm SD	38.5 \pm 20.7	20.2 \pm 22.8	0.007	-
Tumor margin			0.046	4.88
Irregular	27	6		
Smooth	15	12		
T2 Heterogeneity			0.021	6.48
Homo	2	5		
Hetero	40	13		
Contrast enhancement			0.002	11.71
Positive	41	12		
Negative	1	6		

TABLE 4. Multivariate analysis of significant factors from univariate analysis

Factor	P Value	Odds ratio	95% confidence interval
IDH1 wild type	0.009	19.238	1.39, 175.39
1p19q LOH	0.198	0.301	0.05, 1.87
MIB-1 labeling index	0.157	1.033	0.99, 1.08
Tumor margin	0.743	0.720	0.10, 5.15
T2 heterogeneity	0.470	2.763	0.18, 43.44
Contrast enhancement	0.345	4.107	0.22, 77.32

states of IDH1 are linked to enhance 5-ALA fluorescence.²⁴ Paradoxically, glioma tissue harboring IDH1 mutations accumulated high levels of 2-hydroxyglutarate (2HG) while the level of other TCA cycle metabolites, including alpha-ketoglutarate, malate, fumarate, succinate, and isocitrate, was not significantly altered.³⁰ These observations suggest

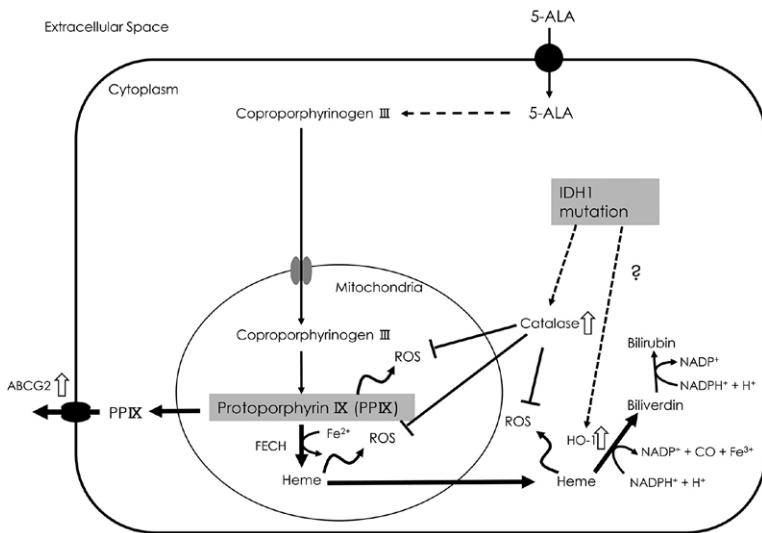


FIGURE 3. Schematic illustration of the relationship between heme synthesis and the IDH1 mutation. Thick arrows indicate metabolism activation, white arrows the activated enzymes or plasma membrane structures involved in porphyrin metabolism. ABCG2 transports porphyrins from the cytoplasm to the extracellular space. NADP⁺ levels increase during metabolization to bilirubin by heme. The IDH1 mutation may promote a defense system against ROS by activating catalase, HO-1, etc. The intracellular PPIX level is downregulated. (ABCG2 = ATP-binding cassette transporter G2; CO = carbon monoxide; FECH = ferrochelatase; HO-1 = heme oxygenase-1; PP = protoporphyrin; ROS = reactive oxygen species).

that IDH1 mutant gliomas do not involve the activation of heme biosynthesis via activation of the TCA cycle.

The increased production of reactive oxygen species (ROS) was suggested to be implicated in human glioma tumorigenesis.³¹ However, in embryonic brain cells from IDH1-mutant mice, intracellular ROS levels were dramatically reduced and the NADP⁺/NADPH ratio and catalase activity were increased.³² We hypothesize that the acquisition of IDH1 mutations by low-grade gliomas upgrades their cell protection from oxidative injury. For example, heme oxygenase-1 (HO-1), one of the most important molecules affording protection against oxidative stress³³, is a microsomal and mitochondrial enzyme.³⁴ HO-1 catalyzes the oxidation of heme to biologically harmless products, *i.e.* carbon monoxide (CO), biliverdin (rapidly reduced to bilirubin), and ferrous iron. The treatment of melanoma cells with ALA during photodynamic therapy increased the accumulation of PPIX and concomitantly enhanced HO-1 expression.³⁵ Hagiya *et al.*³⁶ reported that the messenger RNA level of HO-1 and of ATP-binding cassette transporter G2 (ABCG2), a transporter of porphyrins from the cytoplasm to the extracellular space

across the plasma membrane, was markedly increased when HepG2 cells were exposed to PPIX and visible light. These observations lead us to suspect that the difficulty in inducing fluorescence in IDH1-mutated gliomas is attributable to the establishment of a defense system against oxidative stress (Figure 3).

Although our study population was small, 22% of our 60 patients manifested IDH1 mutations. As in earlier studies^{7,37,38}, the incidence of the IDH1 mutation was highest in patients with WHO grade II gliomas. While there might be a difference in the frequency of IDH1 mutations between the Japanese and other populations, of our 8 WHO grade II gliomas, 75% were 5-ALA fluorescence-negative, a finding similar to that reported by others.^{11,19} Interestingly, in both patients with 5-ALA fluorescence-positive grade II gliomas, IDH1 was wild-type. One of the patients died as a result of malignant transformation 24 months after the operation. Ballester *et al.*³⁹ L. Y. </author><author>Olar, A. </author><author>Roy-Chowdhuri, S. </author></authors></contributors><auth-address>Department of Pathology and Genomic Medicine, Houston Methodist Hospital, Houston, Texas (L.Y.B. proposed that IDH1/2 wild-type gliomas be classified as molecular glioblastomas because, although the pathological diagnosis is low-grade glioma, the prognosis of patients with IDH1/2 wild-type gliomas is unfavorable. They also stated that the molecular subclassification of brain tumors identified important glioma subgroups whose prognosis is favorable and that mutations in IDH1/2, TP53, ATRX, and a 1p19q co-deletion suffice for the accurate molecular classification of diffuse gliomas. Even when the intraoperative pathological diagnosis is low-grade glioma, 5-ALA fluorescence positivity alerts to biological malignancy.¹⁴

The PPV value of fluorescence as an indicator of high-grade gliomas was very high although the NPV was only 33%. Therefore, the possibility of high-grade glioma in the absence of intraoperative 5-ALA fluorescence cannot be excluded.

The IDH1 mutation status of diffuse gliomas is important as the mutation played a strong role in the intraoperative absence of 5-ALA fluorescence. The ability to identify the IDH1 status intraoperatively based on the presence or absence of fluorescence of tumor tissue may be useful for determining the appropriate degree of resection.

Our study has some limitations. First, as our study population was relatively small, our findings warrant validation studies in larger cohorts. Second, fluorescence was evaluated qualitatively

and subjectively by experienced surgeons and quantitative assessment may yield more objective results.

Conclusions

Our study identified the IDH1 status as the only independent, statistically significant factor related to 5-ALA fluorescence. Further studies in a large population are required to clarify the association between the genetic status and the intraoperative 5-ALA-induced fluorescence of diffuse gliomas.

Acknowledgments

We thank Ayumi Nagatomo for technical assistance.

References

- Stupp R, Mason WP, van den Bent MJ, Weller M, Fisher B, Taphoorn MJ, et al. Radiotherapy plus concomitant and adjuvant temozolomide for glioblastoma. *N Engl J Med* 2005; **352**: 987-96. doi: 10.1056/NEJMoa043330
- Lacroix M, Abi-Said D, Fourney DR, Gokaslan ZL, Shi W, DeMonte F, et al. A multivariate analysis of 416 patients with glioblastoma multiforme: prognosis, extent of resection, and survival. *J Neurosurg* 2001; **95**: 190-8. doi: 10.3171/jns.2001.95.2.0190
- Sanai N, Polley MY, McDermott MW, Parsa AT, Berger MS. An extent of resection threshold for newly diagnosed glioblastomas. *J Neurosurg* 2011; **115**: 3-8. doi: 10.3171/2011.2.JNS10998
- Stummer W, van den Bent MJ, Westphal M. Cytoreductive surgery of glioblastoma as the key to successful adjuvant therapies: new arguments in an old discussion. *Acta Neurochir (Wien)* 2011; **153**: 1211-8. doi: 10.1007/s00701-011-1001-x
- Almenawer SA, Badhiwala JH, Alhazzani W, Greenspoon J, Farrokhyar F, Yarascavitch B, et al. Biopsy versus partial versus gross total resection in older patients with high-grade glioma: a systematic review and meta-analysis. *Neuro Oncol* 2015; **17**: 868-81. doi: 10.1093/neuonc/nou349
- Hartmann C, Hentschel B, Wick W, Capper D, Felsberg J, Simon M, et al. Patients with IDH1 wild type anaplastic astrocytomas exhibit worse prognosis than IDH1-mutated glioblastomas, and IDH1 mutation status accounts for the unfavorable prognostic effect of higher age: implications for classification of gliomas. *Acta Neuropathol* 2010; **120**: 707-18. doi: 10.1007/s00401-010-0781-z
- Yan H, Parsons DW, Jin G, McLendon R, Rasheed BA, Yuan W, et al. IDH1 and IDH2 mutations in gliomas. *N Engl J Med* 2009; **360**: 765-73. doi: 10.1056/NEJMoa0808710
- Esteller M, Garcia-Foncillas J, Andion E, Goodman SN, Hidalgo OF, Vanaclocha V, et al. Inactivation of the DNA-repair gene MGMT and the clinical response of gliomas to alkylating agents. *N Engl J Med* 2000; **343**: 1350-4. doi: 10.1056/NEJM200011093431901
- Regula J, MacRobert AJ, Gorchein A, Buonaccorsi GA, Thorpe SM, Spencer GM, et al. Photosensitisation and photodynamic therapy of oesophageal, duodenal, and colorectal tumours using 5 aminolevulinic acid induced protoporphyrin IX - a pilot study. *Gut* 1995; **36**: 67-75.
- Stummer W, Pichlmeier U, Meinel T, Wiestler OD, Zanella F, Reulen HJ, et al. Fluorescence-guided surgery with 5-aminolevulinic acid for resection of malignant glioma: a randomised controlled multicentre phase III trial. *Lancet Oncol* 2006; **7**: 392-401. doi: 10.1016/S1470-2045(06)70665-9
- Valdes PA, Jacobs V, Harris BT, Wilson BC, Leblond F, Paulsen KD, et al. Quantitative fluorescence using 5-aminolevulinic acid-induced protoporphyrin IX biomarker as a surgical adjunct in low-grade glioma surgery. *J Neurosurg* 2015; **123**: 771-80. doi: 10.3171/2014.12.JNS14391
- Ishihara R, Katayama Y, Watanabe T, Yoshino A, Fukushima T, Sakatani K. Quantitative spectroscopic analysis of 5-aminolevulinic acid-induced protoporphyrin IX fluorescence intensity in diffusely infiltrating astrocytomas. *Neurol Med Chir (Tokyo)* 2007; **47**: 53-7; discussion 57.
- Roberts DW, Valdes PA, Harris BT, Fontaine KM, Hartov A, Fan X, et al. Coregistered fluorescence-enhanced tumor resection of malignant glioma: relationships between delta-aminolevulinic acid-induced protoporphyrin IX fluorescence, magnetic resonance imaging enhancement, and neuropathological parameters. Clinical article. *J Neurosurg* 2011; **114**: 595-603. doi: 10.3171/2010.2.JNS091322
- Valdes PA, Kim A, Brantsch M, Niu C, Moses ZB, Tosteson TD, et al. δ -aminolevulinic acid-induced protoporphyrin IX concentration correlates with histopathologic markers of malignancy in human gliomas: the need for quantitative fluorescence-guided resection to identify regions of increasing malignancy. *Neuro Oncol* 2011; **13**: 846-56. doi: 10.1093/neuonc/nor086
- Jaber M, Wolfer J, Ewelt C, Holling M, Hasselblatt M, Niederstadt T, et al. The Value of 5-Aminolevulinic acid in low-grade gliomas and high-grade gliomas lacking glioblastoma imaging features: an analysis based on fluorescence, magnetic resonance imaging, 18F-fluoroethyl tyrosine positron emission tomography, and tumor molecular factors. *Neurosurgery* 2016; **78**: 401-11; discussion 411. doi: 10.1227/NEU.0000000000001020
- Johansson A, Palte G, Schnell O, Tonn JC, Herms J, Stepp H. 5-Aminolevulinic acid-induced protoporphyrin IX levels in tissue of human malignant brain tumors. *Photochem Photobiol* 2010; **86**: 1373-8. doi: 10.1111/j.1751-1097.2010.00799.x
- Arita H, Kinoshita M, Kagawa N, Fujimoto Y, Kishima H, Hashimoto N, et al. (1)(1)C-methionine uptake and intraoperative 5-aminolevulinic acid-induced fluorescence as separate index markers of cell density in glioma: a stereotactic image-histological analysis. *Cancer* 2012; **118**: 1619-27. doi: 10.1002/cncr.26445
- Lau D, Hervey-Jumper SL, Chang S, Molinaro AM, McDermott MW, Phillips JJ, et al. A prospective Phase II clinical trial of 5-aminolevulinic acid to assess the correlation of intraoperative fluorescence intensity and degree of histologic cellularity during resection of high-grade gliomas. *J Neurosurg* 2016; **124**: 1300-9. doi: 10.3171/2015.5.JNS1577
- Widhalm G, Kiesel B, Woehrer A, Traub-Weidinger T, Preusser M, Marosi C, et al. 5-Aminolevulinic acid induced fluorescence is a powerful intraoperative marker for precise histopathological grading of gliomas with non-significant contrast-enhancement. *PLoS One* 2013; **8**: e76988. doi: 10.1371/journal.pone.0076988
- Louis DN, Ohgaki H, Wiestler OD, Cavenee WK, Burger PC, Jouvet A, et al. The 2007 WHO classification of tumours of the central nervous system. *Acta Neuropathol* 2007; **114**: 97-109. doi: 10.1007/s00401-007-0243-4
- Jenkinson MD, du Plessis DG, Smith TS, Joyce KA, Warnke PC, Walker C. Histological growth patterns and genotype in oligodendroglial tumours: correlation with MRI features. *Brain* 2006; **129**: 1884-91. doi: 10.1093/brain/awl108
- Colditz MJ, Jeffree RL. Aminolevulinic acid (ALA)-protoporphyrin IX fluorescence guided tumour resection. Part 1: Clinical, radiological and pathological studies. *J Clin Neurosci* 2012; **19**: 1471-4. doi: 10.1016/j.jocn.2012.03.009
- Agarwal S, Sharma MC, Jha P, Pathak P, Suri V, Sarkar C, et al. Comparative study of IDH1 mutations in gliomas by immunohistochemistry and DNA sequencing. *Neuro Oncol* 2013; **15**: 718-26. doi: 10.1093/neuonc/not015
- Kim JE, Cho HR, Xu WJ, Kim JY, Kim SK, Kim SK, et al. Mechanism for enhanced 5-aminolevulinic acid fluorescence in isocitrate dehydrogenase 1 mutant malignant gliomas. *Oncotarget* 2015; **6**: 20266-77. doi: 10.18632/oncotarget.4060
- Lass U, Hartmann C, Capper D, Herold-Mende C, von Deimling A, Meiboom M, et al. Chromogenic in situ hybridization is a reliable alternative to fluorescence in situ hybridization for diagnostic testing of 1p and 19q loss in paraffin-embedded gliomas. *Brain Pathol* 2013; **23**: 311-8. doi: 10.1111/bpa.12003
- Araki Y, Mizoguchi M, Yoshimoto K, Shono T, Amano T, Nakamizo A, et al. Quantitative digital assessment of MGMT immunohistochemical expression in glioblastoma tissue. *Brain Tumor Pathol* 2011; **28**: 25-31. doi: 10.1007/s10014-010-0004-2

27. Widhalm G, Wolfsberger S, Minchev G, Woehrer A, Krssak M, Czech T, et al. 5-Aminolevulinic acid is a promising marker for detection of anaplastic foci in diffusely infiltrating gliomas with nonsignificant contrast enhancement. *Cancer* 2010; **116**: 1545-52. doi: 10.1002/cncr.24903
28. Yang X, Palasuberniam P, Kraus D, Chen B. Aminolevulinic acid-based tumor detection and therapy: molecular mechanisms and strategies for enhancement. *Int J Mol Sci* 2015; **16**: 25865-80. doi: 10.3390/ijms161025865
29. Frezza C, Zheng L, Folger O, Rajagopalan KN, MacKenzie ED, Jerby L, et al. Haem oxygenase is synthetically lethal with the tumour suppressor fumarate hydratase. *Nature* 2011; **477**: 225-8. doi: 10.1038/nature10363
30. Dang L, White DW, Gross S, Bennett BD, Bittinger MA, Driggers EM, et al. Cancer-associated IDH1 mutations produce 2-hydroxyglutarate. *Nature* 2009; **462**: 739-44. doi: 10.1038/nature08617
31. Yu MO, Song NH, Park KJ, Park DH, Kim SH, Chae YS, et al. Romo1 is associated with ROS production and cellular growth in human gliomas. *J Neurooncol* 2015; **121**: 73-81. doi: 10.1007/s11060-014-1608-x
32. Sasaki M, Knobbe CB, Itsumi M, Elia AJ, Harris IS, Chio, II, et al. D-2-hydroxyglutarate produced by mutant IDH1 perturbs collagen maturation and basement membrane function. *Genes Dev* 2012; **26**: 2038-49. doi: 10.1101/gad.198200.112
33. Liu Y, Liang Y, Zheng T, Yang G, Zhang X, Sun Z, et al. Inhibition of heme oxygenase-1 enhances anti-cancer effects of arsenic trioxide on glioma cells. *J Neurooncol* 2011; **104**: 449-58. doi: 10.1007/s11060-010-0513-1
34. Belcher JD, Beckman JD, Balla G, Balla J, Vercellotti G. Heme degradation and vascular injury. *Antioxid Redox Signal* 2010; **12**: 233-48. doi: 10.1089/ars.2009.2822
35. Na HK, Surh YJ. Oncogenic potential of Nrf2 and its principal target protein heme oxygenase-1. *Free Radic Biol Med* 2014; **67**: 353-65. doi: 10.1016/j.freeradbiomed.2013.10.819
36. Hagiya Y, Adachi T, Ogura S, An R, Tamura A, Nakagawa H, et al. Nrf2-dependent induction of human ABC transporter ABCG2 and heme oxygenase-1 in HepG2 cells by photoactivation of porphyrins: biochemical implications for cancer cell response to photodynamic therapy. *J Exp Ther Oncol* 2008; **7**: 153-67.
37. Mukasa A, Takayanagi S, Saito K, Shibahara J, Tabei Y, Furuya K, et al. Significance of IDH mutations varies with tumor histology, grade, and genetics in Japanese glioma patients. *Cancer Sci* 2012; **103**: 587-92. doi: 10.1111/j.1349-7006.2011.02175.x
38. Wang HY, Tang K, Liang TY, Zhang WZ, Li JY, Wang W, et al. The comparison of clinical and biological characteristics between IDH1 and IDH2 mutations in gliomas. *J Exp Clin Cancer Res* 2016; **35**: 86. doi: 10.1186/s13046-016-0362-7
39. Ballester LY, Olar A, Roy-Chowdhuri S. Next-generation sequencing of central nervous systems tumors: the future of personalized patient management. *Neuro Oncol* 2016; **18**: 308-10. doi: 10.1093/neuonc/nov329

Single nucleotide polymorphisms in genes *MACC1*, *RAD18*, *MMP7* and *SDF-1a* as prognostic factors in resectable colorectal cancer

Matej Horvat¹, Uros Potocnik^{2,3}, Katja Repnik^{2,3}, Rajko Kavalari⁴, Vesna Zadnik⁵, Stojan Potrc⁶, Borut Stabuc⁷

¹ Department of Oncology, University Medical Centre Maribor, Slovenia

² Centre for Human Molecular Genetics and Pharmacogenomics, Faculty of Medicine, University of Maribor, Slovenia

³ Laboratory for Biochemistry, Molecular Biology and Genomics, Faculty for Chemistry and Chemical Engineering, University of Maribor, Slovenia

⁴ Department of Pathology, University Medical Centre Maribor, Slovenia

⁵ Epidemiology and Cancer Registry, Institute of Oncology Ljubljana, Slovenia

⁶ Department of General and Abdominal Surgery, University Medical Centre Maribor, Slovenia

⁷ Department of Gastroenterology, University Medical Centre Ljubljana, Slovenia

Radiol Oncol 2017; 51(2): 151-159.

Received 5 February 2016

Accepted 27 May 2016

Correspondence to: Prof. Borut Štabuc, Ph.D., M.D., Department of Gastroenterology, University Medical Centre Ljubljana, Slovenia.
E-mail: borut.stabuc@kclj.si

Disclosure: No potential conflicts of interest were disclosed.

Background. Colorectal cancer (CRC) represents one of the most common malignancies worldwide. Research has indicated that functional gene changes such as single nucleotide polymorphism (SNP) influence carcinogenesis and metastasis and might have an influence on disease relapse. The aim of our study was to evaluate the role of SNPs in selected genes as prognostic markers in resectable CRC.

Patients and methods. In total, 163 consecutive patients treated surgically for CRC of stages I, II and III at the University Medical Centre in Maribor in 2007 and 2008 were investigated. DNA was isolated from formalin-fixed paraffin-embedded CRC tissue from the Department of Pathology and SNPs in genes *SDF-1a*, *MMP7*, *RAD18* and *MACC1* were genotyped using polymerase chain reaction followed by high resolution melting curve analysis or restriction fragment length polymorphism.

Results. We found worse disease-free survival (DFS) for patients with TT genotype of SNP rs1990172 in gene *MACC1* ($p = 0.029$). Next, we found worse DFS for patients with GG genotype for SNP rs373572 in gene *RAD18* ($p = 0.020$). Higher frequency of genotype GG of *MMP7* SNP rs11568818 was found in patients with T3/T4 stage ($p = 0.014$), N1/N2 stage ($p = 0.041$) and with lymphovascular invasion ($p = 0.018$). For *MACC1* rs1990172 SNP we found higher frequency of genotype TT in patients with T3/T4 staging ($p = 0.024$). Higher frequency of genotype GG of *RAD18* rs373572 was also found in patients with T1/T2 stage with disease relapse ($p = 0.041$).

Conclusions. Our results indicate the role of SNPs as prognostic factors in resectable CRC.

Key words: single nucleotide polymorphism; colorectal cancer; *MACC1*; *RAD18*; *MMP7*; *SDF-1a*

Introduction

Colorectal cancer (CRC) represents the third most common malignancy worldwide in men and sec-

ond most common malignancy in women, accounting for approximately 10% of all tumour types worldwide and 8% of cancer related mortality.¹ In Slovenia according to Cancer registry of

Slovenia yearly reports, CRC is the second most common cancer in men and women. The incidence was steadily increasing in the last decades. From 2001 to 2011 it has risen by 35%, from 1110 in 2001 to 1709 in 2010 when it reached its peak. The incidence is now declining with 1530 in 2012. There is also a relative proximal shift of tumour location with the incidence of colon cancer increasing faster than the incidence of rectal cancer.²⁻⁵

The survival of CRC is improving as a consequence of screening programs, new chemotherapy regimens and targeted treatments as well as improved surgical treatment of metastatic disease. According to Surveillance, Epidemiology, and End Results (SEER) register and a worldwide CONCORD-2 study, the 5-year CRC survival in developed countries is more than 60%.^{6,7}

CRC is a heterogeneous disease and its carcinogenesis a multistep process. CRC develops in 75% sporadically because of mutations acquired during a person's lifetime and in 25% as a combination of hereditary syndromes, a higher risk because of CRC familial burden without criteria for a hereditary syndrome or as a consequence of inflammatory bowel syndrome.⁸ It evolves through distinct genetic pathways: chromosomal instability, microsatellite instability (MSI-H) and the CpG island methylator phenotype (CIMP). Next to »classical adenoma-carcinoma« sequence proposed by Fearon and Voglestein there is also a newly recognized »serrated neoplasia pathway«, where CRC evolves through different precancerous lesions, as for instance serrated adenoma.⁹ The carcinogenesis might also differ in regard to CRC arising either in right or left hemicolon.¹⁰

The current treatment for resectable CRC of stage I, II and III is surgical resection. For patients of stage I, surgical resection is the only recommended treatment without adjuvant chemotherapy. For patients of stage III adjuvant chemotherapy is recommended in all patients. In contrast for patients of stage II adjuvant chemotherapy is not recommended for unselected patients, but for those with clinical or pathological risk factors.¹¹⁻¹³

Potential clinical and pathological risk factors for recurrence of stage II CRC have been investigated and incorporated in different guidelines, but a definite consensus has not yet been reached. According to European and American guidelines (The European Society for Medical Oncology (ESMO), The American Society of Clinical Oncology (ASCO) and The National Comprehensive Cancer Network (NCCN)), negative prognostic risk factors according to all three sets of guidelines are: T4

tumours, bowel perforation, extension of surgical lymphadenectomy, inadequate pathological sampling of lymph nodes and poor tumour differentiation grade. Further negative prognostic markers included in one or two sets of guidelines are: bowel obstruction, lymphovascular invasion and/or perineural invasion and indeterminate or positive margins. Consensus on them has not been reached yet. There is no clear message regarding adjuvant chemotherapy patient selection in stage II CRC.¹¹⁻¹³

Although stage I and early stage II CRC are prognostically very favourable, with a small burden of disease, a proportion of these tumours have certain characteristics, making them clinically more malignant and therefore predisposing them to disease recurrence or metachronous colon cancer.⁹ Up to 30% of patients with stage I and up to 50% of patients with stage II of CRC are going to relapse.^{14,15} Considering these facts it is clear that classical TNM staging system has its limitations, so it is necessary to determine molecular or immunological prognostic and predictive markers to implement in routine clinical practice.^{16,17}

Single nucleotide polymorphisms (SNPs) are molecular factors that might be useful as prognostic markers in CRC. Preliminary genome wide association (GWA) study in non-caucasian population has indicated a role of SNPs in resectable CRC.¹⁸ We hypothesized that SNPs participating in genetic risk for CRC and metastasis might prove as a prognostic factor in resectable CRC. In our study, we have selected SNPs with higher frequency in patients with either local lymph node involvement or systemic dissemination in genes participating in CRC carcinogenesis and disease dissemination: *SDF-1 α* (stromal derived factor 1 alpha) located on chromosome 10, *MMP7* located on chromosome 11, *RAD18* located on chromosome 3, and *MACC1* (metastasis associated in colorectal cancer 1) located on chromosome 7.¹⁹⁻²² The aim of our study was to evaluate the role of SNPs in selected genes as prognostic markers in resectable CRC.

Patients and methods

We have conducted a study, regarding the role of selected SNPs in resectable CRC. In total, 163 consecutive patients treated surgically at University Medical Centre in Maribor in years 2007 and 2008 have been investigated. The inclusion criterion was colorectal adenocarcinoma of stages I, II or III. The exclusion criteria were: history of inflammatory bowel disease, preoperative chemoradiotherapy/

radiotherapy, perioperative mortality within 30 days and confirmed familial CRC (FAP, HNPCC or other familial syndromes). Mean age of the patients at diagnosis was 67 years +/- 11.4 years (range 26–88 years). Clinical and pathohistological characteristics examined were: age, gender, TNM stage, differentiation grade, perineural invasion and lymphovascular invasion. Time to progression was defined as time from diagnosis to progression. Patients were followed-up on average for 69 months. Data regarding their vital status was acquired from Cancer registry of Slovenia. Clinical and pathohistological characteristics of patients and tumours are summarized in Table 1.

DNA isolation and SNP genotyping

DNA was extracted from the formalin-fixed paraffin-embedded (FFPE) CRC tissues of 163 patients from the Department of Pathology, University Medical Centre in Maribor. FFPE tissues were prepared as follow: at macroscopic examination of resected specimen, the pathologist sampled representative tissue samples (2 x 2 x 0.4 cm) from tumour, bowel wall outside the tumour and all lymph nodes from the resected pericolic or mesorectal fat. For determination of resection margin status, the representative tissue samples were taken also from the proximal and distal intestinal resection margin, from circumferential resection margin and dyed with the indian-ink. All representative tissue samples and all obtained lymph nodes were put into labeled histo-cassettes and standardly processed in automated histoprocessors (dehydrated and paraffined). Paraffined tissue samples were embedded in paraffin blocks. For the extraction of DNA, 12µm thick tissue slices were cut with microtome from tumour tissue blocks.

DNA was isolated from FFPE tissues using BiOstic FFPE Tissue DNA Isolation Kit ®(MO BIO Laboratories, Inc.) according to manufacturer recommendations. SNPs of genes *SDF-1α* (rs1801157), *MMP7* (rs11568818), *RAD18* (rs373572) in *MACC1* (rs1990172) were genotyped using polymerase chain reaction (PCR) followed by high resolution melting (HRM) or restriction fragment length polymorphism (RFLP) techniques. Forward and reverse primer sequences, size of product after PCR, primer concentrations, annealing temperatures and genotyping method are shown in Table 2. HRM genotyping was performed using real time PCR LC480 instrument (Roche, Germany). PCR-HRM was carried out using LC480 HRM Master Mix (Roche, Germany). Conditions were as follow:

TABLE 1. Clinical and pathohistological characteristics of patients included in study

Clinical and histopathological characteristics	CRC patients (N = 163)
Sex	
Male/female, N (%)	92/71 (56.4/43.6)
Age at diagnosis	
Mean +/- SD	67.28 +/- 11.44
Stage of disease, N (%)	
I	29 (17.8)
II	81 (49.7)
III	53 (32.5)
TNM staging	
Tumour, N (%)	
T1	8 (4.9)
T2	24 (14.7)
T3	120 (73.6)
T4	11 (6.7)
Lymph nodes, N (%)	
N0	110 (67.5)
N1	38 (23.3)
N2	15 (9.2)
Vital status (5.10.2015), N (%)	
dead	65 (39.9) (42 due to CRC progression, 23 other cause)
alive	98 (60.1)
Disease progression, N (%)	
yes	46 (28.2) (42 dead, 4 alive)
no	117 (71.8)
Disease progression according to stage, N (%)	
stage I	5 (17.2)
stage II	18 (22.2)
stage III	23 (43.4)
Clinical characteristics, N (%)	
more than 12 lymph nodes resected	70 (42.9)
adjuvant therapy	41 (25.2)
Differentiation grade, N (%)	
I	66 (40.5)
II	74 (45.4)
III	21 (12.9)
no data	2 (1.2)
Perineural invasion, N (%)	
yes	13 (8.0)
no	150 (92.0)
Lymphovascular invasion, N (%)	
yes	27 (16.6)
no	136 (83.4)

N = number of patients

initial denaturation at 95°C for 10 min, followed by 45 cycles of 95°C for 10 s, 57 or 60°C (primer pair dependent) for 15 s and 72°C for 10 s, followed by HRM step of 95°C for 1 min, 40°C for 1 min and 60 – 90°C at 0.02°C/s. PCR-RFLP conditions were as follow: initial denaturation at 95°C for 5 min, followed by 35 cycles of 95°C for 30 s, 60 or 63°C (primer pair dependent) for 30 s and 72°C for 30 s. After PCR, products were incubated with restriction enzymes shown in Table 2 at 37°C overnight. Digested products were resolved in 2% agarose gel.

Our study was approved by the National Ethics committee of Slovenia (clinical trial registration number: 65/02/13) and is listed at University

TABLE 2. Primer sequences used in PCR reaction, expected sizes of products, annealing temperatures, primer concentrations and genotyping method of selected SNPs; restriction enzymes and sizes of fragments after restriction for genotyping of SNPs rs1801157 (*CXCL12*) and rs1990172 (*MACC1*)

Gene	SNP ID	Forward and reverse primer	Product size [bp]	Annealing temperature [°C]	Primer concentration [nM]	Genotyping method
<i>CXCL12</i>	rs1801157 A/G	GTGGGATGGGATGGTGGAG CCTCAGCTCAGGGTAGCC	109	60	650	RFLP
<i>MACC1</i>	rs1990172 G/T	CAGGGAAAGAAATGGTATTGCA GGAAAAGGAGGGAAGCATGTG	115	63	300	RFLP
<i>MMP7</i>	rs11568818 A/G	TGGAGTCAATTATGCAGCAG CGAGGAAGTATTACATCGTATTGG	93	57	250	HRM
<i>RAD18</i>	rs373572 A/G	TGTGATTAACCTAGTGGTATTTTCTT GCATCCTAGTCTTCTATATTTTCG	85	60	300	HRM
Gene	SNP ID	Restriction enzyme	Size of fragments after restriction [bp]			
<i>CXCL12</i>	rs1801157	MspI	AA: 109, AG: 109+62+47, GG: 62+47			
<i>MACC1</i>	rs1990172	BseGI	GG: 80+35, GT: 105+80+35, TT: 105			

Medical Centre Maribor as research project: IRP-2014/01-21.

Statistical analysis

The clinical endpoint of our trial was evaluating the role of selected SNPs as prognostic factors by determining disease-free survival from the date of the surgery. Kaplan-Meier survival curves were constructed and compared using the log-rank test. Multivariate analysis was carried out using a Cox proportional hazard model. Group distribution for each clinicopathological characteristic was compared using two-tailed Fischer exact test. Data are expressed as the mean +/- standard deviation. Statistical significance was defined as $p < 0.05$. All analyses were performed using SPSS.

Results

Over an average follow-up period of 69 months, 65 deaths were recorded (39.9%). Out of those 65 patients, 42 died because of disease progression and 23 patients died of another cause.

Selected SNPs were genotyped in 163 CRC patients with well-defined clinical and histopathological characteristics. Genotype and allele frequencies were calculated for all patients and are shown in Table 3. When comparing selected SNPs with clinical and pathohistological characteristics of patients, higher frequency of genotype GG of *MMP7* rs11568818 SNP was found in patients with T3/T4

staging (29.6%) compared to patients with T1/T2 staging (7.1%, $p = 0.014$), in patients with N1/N2 staging (36.2%) compared to N0 staging (19.8%, $p = 0.041$) and in patients with lymphovascular invasion (45.8%) compared to patients without lymphovascular invasion (21.0%, $p = 0.018$). For *MACC1* rs1990172 SNP, we found higher frequency of genotype TT in patients with T3/T4 staging (62.5%) compared to patients with T1/T2 staging (36.0%, $p = 0.024$). All correlations between selected SNPs and clinical and histopathological characteristics are presented in Table 3.

We have further evaluated the correlation of genotype frequencies in patients with progression compared to patients without disease progression. We found association between tumour TNM staging and SNP rs373572 in gene *RAD18*. Higher frequency of genotype GG was found in patients with T1/T2 staging with disease progression (60.0%) compared to patients with T1/T2 staging without disease progression (12.0%, $p = 0.041$). No statistically significant differences were discovered in rs1990172 in gene *MACC1*, rs1801157 in gene *SDF-1 α* or rs11568818 in gene *MMP7*.

The results of survival analysis showed association with SNP rs1990172 in gene *MACC1* and with SNP rs373572 in gene *RAD18*. We found worse disease-free survival (DFS) for patients with TT genotype of SNP rs1990172 in gene *MACC1* compared to patients with GT or GG genotype ($p = 0.029$, Figure 1). One year, 3 years and 5 years DFS were in patients with TT genotype 94.8%, 67.3% and 62.9%, respectively compared to patients with

TABLE 3. Associations between selected SNPs and clinico-histopathological characteristics of patients

Gene/ SNP ID	Frequency	TNM staging				Grade of differentiation		Perineural invasion		Lymphovascular invasion					
		T1+T2	T3+T4	N0	N1+N2	1+2	3	No	Yes	No	Yes				
CXCL12 rs1801157	AA	4.76	0.0	5.9	7.3	0.0	4.8	5.3	5.2	0.0	5.8	0.0			
	AG	29.25	31.0	28.8	26.0	35.3	27.8	42.1	29.9	23.1	27.3	38.5			
	GG	65.99	69.0	65.3	66.7	64.7	67.5	52.6	64.9	76.9	66.9	61.5			
	Statistical analysis			0.346		0.096		1.000		1.000		0.354		p-value	
				1.261		1.573		0.900		1.102		1.228		OR	
				1.159–1.373		1.388–1.783		0.102–7.916		1.045–1.162		1.135–1.329		95% CI	
				0.828		1.000		0.303		0.543		0.656		p-value	
	Statistical analysis			0.814		0.960		0.556		1.860		0.820		OR	
				0.340–1.948		0.471–1.958		0.210–1.471		0.488–7.089		0.342–1.967		95% CI	
			GG	5.84	12.0	4.5	7.8	2.1	5.2	5.3	5.6	7.7	7.1	0.0	
		GT	36.50	52.0	33.0	37.8	34.0	37.9	26.3	38.7	15.4	35.4	41.7		
MACC1 rs1990172	TT	57.66	36.0	62.5	54.4	63.8	56.9	68.4	55.6	76.9	57.5	58.3			
	Statistical analysis			0.024			0.363		1.000		0.560		0.350	p-value	
					2.963		1.477		0.982		0.718		1.229	OR	
				1.202–7.301		0.715–3.050		0.112–8.641		0.081–6.338		1.131–1.334		95% CI	
				0.263		0.160		0.453		0.237		1.000		p-value	
	Statistical analysis			3.880		2.918		1.641		2.657		1.034		OR	
				0.463–32.516		0.649–13.119		0.583–4.620		0.697–10.127		0.523–2.525		95% CI	
			AA	27.27	28.6	27.0	28.1	25.5	27.9	26.3	26.7	33.3	27.7	25.0	
			AG	47.55	64.3	43.5	52.1	38.3	47.5	52.6	48.9	33.3	51.3	29.2	
	MMP7 rs11568818	GG	25.17	7.1	29.6	19.8	36.2	24.6	21.1	24.4	33.3	21.0	45.8		
Statistical analysis				1.000		0.843		1.000		0.736		1.000		p-value	
				1.084		1.141		1.082		0.729		1.151		OR	
				0.433–2.713		0.517–2.521		0.362–3.234		0.207–2.573		0.420–3.152		95% CI	
				0.014		0.041		1.000		0.497		0.018		p-value	
Statistical analysis				5.457		2.296		0.818		1.547		3.182		OR	
				1.226–24.284		1.054–5.002		0.252–2.654		0.437–5.479		1.273–7.952		95% CI	
			AA	51.59	46.7	52.8	48.6	58.0	50.4	55.0	50.7	61.5	51.9	50.0	
			AG	38.22	33.3	39.4	41.1	32.0	39.3	35.0	39.6	23.1	38.2	38.5	
RAD18 rs373572		GG	10.19	20.0	7.9	10.3	10.0	10.4	10.0	9.7	15.4	9.9	11.5		
	Statistical analysis			0.685		0.306		0.812		0.567		1.000		p-value	
				0.784		0.685		0.830		0.643		1.079		OR	
				0.353–1.739		0.348–1.348		0.323–2.133		0.201–2.058		0.465–2.504		95% CI	
				0.085		1.000		1.000		0.624		0.731		p-value	
	Statistical analysis			0.342		0.970		0.960		1.688		1.184		OR	
				0.113–1.030		0.318–2.957		0.201–4.580		0.339–8.399		0.312–4.488		95% CI	
			AA	51.59	46.7	52.8	48.6	58.0	50.4	55.0	50.7	61.5	51.9	50.0	
			AG	38.22	33.3	39.4	41.1	32.0	39.3	35.0	39.6	23.1	38.2	38.5	

GT/GG genotype, where 1 year, 3 years and 5 years DFS were 91.1%, 85.7% and 78.3%, respectively. Next, we found worse survival for patients with GG genotype compared to patients with AG or AA genotype for SNP rs373572 in gene *RAD18* ($p = 0.020$, Figure 2). One year, 3 years and 5 years DFS were in patients with GG genotype 86.7%, 53.3% and 45.7%, respectively, compared to patients with AG/AA genotype, where 1 year, 3 years and 5 years DFS were 94.9%, 78.9% and 74.2%, respectively. The survival analysis for SNP rs11568818 in gene *MMP7* and rs1801157 in gene *SDF-1a* did not show statistically significant differences.

Discussion

Our study is the first report of the association between SNP rs373572 in *RAD18* gene and SNP rs1990172 in *MACC1* gene with DFS in resectable CRC. We also identified the association of SNP rs373572 in *RAD18* gene in patients with stage I CRC and disease relapse.

Association between SNP rs373572 in *RAD18* gene and DFS has been found, where 5-year DFS was significantly shorter for patients with GG genotype compared to patients with AA or AG genotype. Multivariate analysis showed that GG

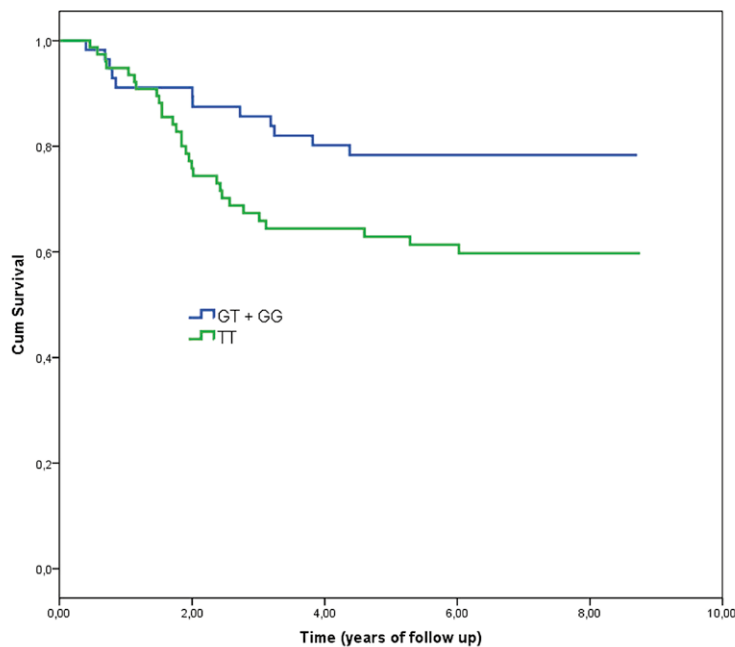


FIGURE 1. Survival analysis curves for different genotype groups of CRC patients according to SNP rs1990172 in gene *MACC1*.

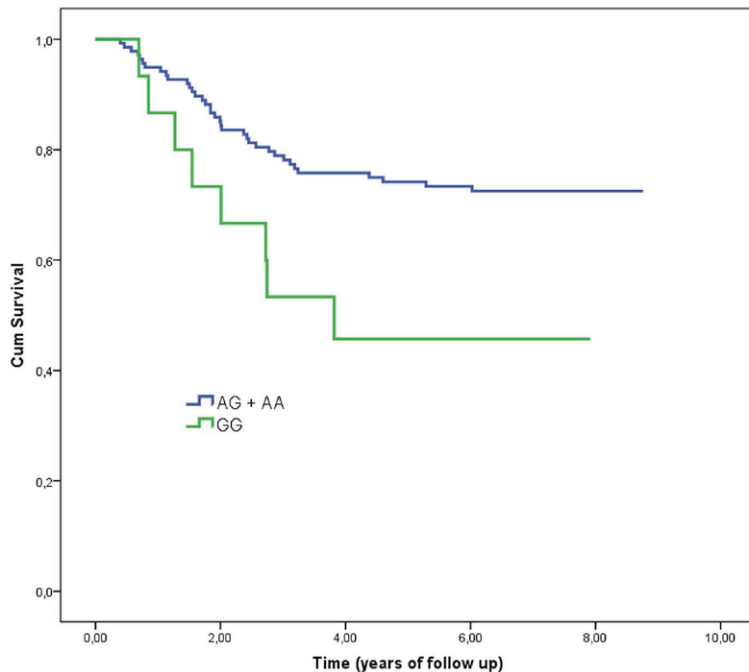


FIGURE 2. Survival analysis curves for different genotype groups of CRC patients according to SNP rs373572 in gene *RAD18*.

genotype could be independent negative prognostic factor, however association was at a borderline of statistical significance. In patients with stage I CRC, the GG genotype was more frequent in patients who relapsed, making it a potential negative

prognostic factor for early stage CRC. *RAD18* gene combines two distinct pathways maintaining genome stability.²³ So far, association between SNP rs373572 and increased risk for CRC has been confirmed and significant association between SNP and clinicopathological features, specifically in differentiated grade and lymph node metastasis has been found in Japanese population.²¹ Association between rs373572 and CRC (colon and rectum cancer) has been also found in Han Chinese and it was shown that SNP is significantly related with increased risk of metastasis in CRC.²⁴ Interestingly, this study showed in contrary better prognosis for patients with GG genotype. Further, statistically significant association has been found between *MACC1* intron rs1990172 SNP genotype GT or TT and higher T stage of TNM. Patients with GT or GG genotype also had higher 5-years DFS compared to patients with TT genotype. Multivariate analysis showed that TT genotype was an independent negative prognostic factor. This may partially explain the poorer prognosis of patients with TT genotype. *MACC1* is a regulator of the HGF/Met signaling pathway which plays a key role in regulating many biological processes including cellular proliferation, cell metastasis, cell invasiveness, angiogenesis, epithelial mesenchymal transition, inducing increased invasiveness, tumorigenesis and also chemoresistance.²⁵ The expression levels of *MACC1* in colon cancer without distant metastases was significantly higher in primary tumours that later developed distant metastases, compared to those that did not metastasize within a 10-year-follow-up period.²⁶ Several SNPs have been discovered in human *MACC1* gene and Lang *et al.*²⁷ conducted a trial researching six SNPs in *MACC1* gene and they report a positive association of the *MACC1* tagging SNP rs1990172 with reduced overall survival in patients with CRC. The study showed, in contrary to our results, better prognosis for patients with TT genotype. There are some differences in the design and clinical endpoint comparing both studies. Lang *et al.* also included patients with metastatic disease making the patient population more heterogenous. Their clinical endpoint was also overall survival (OS) not DFS. The authors concluded that rs1990172 was significantly associated with an increased risk for any death, not just CRC related. As we see in our study, out of 65 patients who died in course of follow up, 42 died of CRC recurrence and in 23 patients' cause of death was different. Considering this, DFS is more reliable to evaluate the role of a prognostic factor in adjuvant setting than OS.

Association between *MACC1* rs1990172 SNP and other cancers has been found. For example, in patients with HER2-positive breast cancer, increased risk for progression or death for carriers of the G allele of SNP rs1990172 has been found.²⁸

In our study we also found association between genotype GG of *MMP7* gene promoter SNP rs11568818 and higher tumour (T) TNM stage, with regional lymph node dissemination and lymphovascular invasion. Our results suggest, that GG genotype of *MMP7* rs11568818 SNP is negative prognostic biomarker for CRC. Consistent with our results, genotype GG of SNP rs11568818 in *MMP7* has been recently associated with patients with CRC and aggressive course of the disease and with higher regional lymph node involvement.²⁹ In this study relationship between GG genotype of *MMP7* rs11568818 SNP and advanced tumour infiltration has also been reported. Higher prevalence of *MMP7* rs11568818 GG genotype was also found among bladder cancer patients compared to controls, however, SNP was not associated with the tumour grade or stage.³⁰ In meta-analysis of *MMP2*, *MMP7* and *MMP9* promoter polymorphisms, AG and GG genotype carriers of *MMP7* rs11568818 SNP had an increased gastric cancer risk, suggesting it may play allele-specific role in cancer development.³¹ In breast cancer, statistically significant association with disease-free survival (DFS) was found for *MMP7* rs11568818 SNP, where patients homozygous for G allele had significantly worse prognosis.³² In our study, statistically significant association with 5-year DFS for *MMP7* rs11568818 SNP has not been found. Altogether, *MMP7* seems very promising candidate for predicting tumour progression and metastasis also in CRC patients, particularly since it was also found, that the overexpression of *MMP7* has considerable metastatic potential and correlates with unfavourable clinicopathological characteristics.³³

We also investigated SNP rs1801157 in *CXCL12* (*SDF-1 α*) gene. The *CXCL12/CXCR4* axis promotes metastasis in numerous cancers. *CXCL12* is being produced and released from tissues as liver or lung and trigger the migration of tumour cells expressing with *CXCR4* receptor thereby promoting invasion, proliferation and survival under suboptimal condition.³⁴ SNPs in *CXCL12* gene have also been studied as a factor of increased likelihood developing cancer and increased likelihood of dissemination.^{35,36} In a clinical trial conducted by Chang *et al.*³⁷, GA/AA genotype of SNP rs1801157 was significantly higher in patients with lymph node metastasis among T3 tumours. In addition, an in-

vestigation of the relationship between *CXCL12* genotypes and different clinico-pathological prognostic factors revealed a positive association between the GA/AA genotype and lympho-vascular invasion. Both of these results indicate a predisposition to worse prognosis. In our study we haven't confirmed statistically significant association for SNP rs1801157 *CXCL12* gene in 5-year DFS nor correlation between genotype distribution and clinicopathological characteristics. However, the distribution of genotypes was in our study similar compared to other studies.³⁷ They however discovered higher AA genotype frequency in patients with T3 CRC in regional lymph node dissemination and lymphovascular invasion. Survival analysis showed worse DFS for the AA genotype in patients with lymph metastases.³⁷

Stage III CRC patients are those who benefit from adjuvant chemotherapy resulting in increased DFS and OS at 6 and 10 years of follow up.^{38,39} Patients with stage II disease with negative prognostic factors also benefit from adjuvant chemotherapy. There is however some controversy regarding unselected patients of stage II and also to some extent of stage I, because it is not always objectively possible to make a clear conclusion regarding negative regional lymph node status and the absence of negative pathohistological prognostic factors.⁴⁰

TNM staging has in proportion of patients low prognostic value. Resection of appropriate number of lymph nodes is frequently impossible. In only about 50% of patients the required resection of 12 lymph nodes is achieved.^{16,41,42} Next to that, light microscopy has its limitations regarding sensitivity regarding detection of malignant cells in regional lymph nodes.⁴³ Also only a proportion of a pathological specimen can be examined and this can lead to false negative reports regarding pathological risk factors.¹⁷ Inadequate resection of appropriate number of lymph nodes and limitations of light microscopy may lead to false downward stage migration. Lymphovascular and perineural invasion are negative prognostic factors, but they can also be underreported.^{44,45} Considering these facts we see, that a substantial proportion of patients is undertreated.

A proportion of patients can have a more malignant phenotype irrespective of the TNM stage and known pathohistological prognostic factors, predisposing them to a more aggressive course of the disease. An intrinsic molecular characteristic, like nucleotide polymorphism, might prove extremely helpful in this regard. Polymorphisms of genes participating in carcinogenesis and disease

dissemination thereby represent a potential new prognostic marker.

We have investigated patients from north-eastern part of Slovenia almost exclusively of Slovenian origin. Our results regarding genotype distribution and connection with pathohistological characteristics are most consistent with study conducted by Dziki *et al.*²⁹ on Polish population, which is as Slovenian also of Slavic origin. Our results compared to other studies are less consistent, but other studies were mainly performed in east Asia and Austria. The differences may be attributable to population genetic differences.

There is however also a question of appropriate study design, especially clinical endpoint. OS is of course the most important endpoint in oncology research, but it may be influenced by many treatment related factors beyond the point of disease relapse. DFS is therefore more appropriate clinical endpoint in resectable disease in research of prognostic markers. Although our results indicate the role of polymorphisms, further research is needed to validate our findings.

Screening of polymorphisms in selected genes of CRC patients in our study suggested that they may have a role as a prognostic factors in resectable CRC. In conclusion, the goal is to identify patients who are going to derive most clinical benefit, without facing unnecessary side effects.

Acknowledgement

The research was funded by University Medical Centre Maribor as an internal research project IRP-2014/01-21.

References

- International Agency for Research on Cancer. *World cancer report 2014*. Stewart B, Wild CP, editors, World Health Organization; 2014.
- Primič-Žakelj M, Zadnik V, Žagar T, Zakotnik B. Survival of cancer patients, diagnosed in 1991-2005 in Slovenia. Ljubljana: Institute of Oncology Ljubljana, Cancer Registry of Republic of Slovenia; 2009.
- Cancer incidence in Slovenia 2001. Ljubljana: Institute of Oncology Ljubljana, Cancer Registry of Republic of Slovenia; 2004.
- Cancer in Slovenia 2010. Ljubljana: Institute of Oncology Ljubljana, Epidemiology and Cancer Registry, Cancer Registry of Republic of Slovenia; 2013.
- Cancer in Slovenia 2012. Ljubljana: Institute of Oncology Ljubljana, Epidemiology and Cancer Registry, Cancer Registry of Republic of Slovenia; 2015.
- Allemani C, Weir HK, Carreira H, Harewood R, Spika D, Wang XS, et al. Global surveillance of cancer survival 1995-2009: analysis of individual data for 25,676,887 patients from 279 population-based registries in 67 countries (CONCORD-2). *Lancet* 2015; **385**: 977-1010.
- Ries LAG, Melbert D, Krapcho M, Stinchcomb DG, Howlander N, Horner MJ, et al. SEER cancer statistics review, 1975-2005. Bethesda: National Cancer Institute.
- Weitz J, Koch M, Debus J, Höhler T, Galle PR, Büchler MW. Colorectal cancer. *Lancet* 2005; **365**: 153-65.
- Kanthan R, Senger JL, Kanthan SC. Molecular events in primary and metastatic colorectal carcinoma: a review. *Patholog Res Int* 2012; **2012**: 597497.
- Iacopetta B. Are there two sides to colorectal cancer? *Int J Cancer* 2002; **101**: 403-8.
- Benson AB, Schrag D, Somerfield MR, Cohen AM, Figueredo AT, Flynn PJ, et al. American Society of Clinical Oncology recommendations on adjuvant chemotherapy for stage II colon cancer. *J Clin Oncol* 2004; **22**: 3408-19.
- Engstrom PF, Arnoletti JP, Benson AB, Chen YJ, Choti MA, Cooper HS, et al. NCCN Clinical Practice Guidelines in Oncology: colon cancer. *J Natl Compr Canc Netw* 2009; **7**: 778-831.
- Labianca R, Nordlinger B, Beretta GD, Brouquet A, Cervantes A, Group EGW. Primary colon cancer: ESMO Clinical Practice Guidelines for diagnosis, adjuvant treatment and follow-up. *Ann Oncol* 2010; **21**(Suppl 5): v70-7.
- Freeman HJ. Early stage colon cancer. *World J Gastroenterol* 2013; **19**: 8468-73.
- Nicastrì DG, Doucette JT, Godfrey TE, Hughes SJ. Is occult lymph node disease in colorectal cancer patients clinically significant? A review of the relevant literature. *J Mol Diagn* 2007; **9**: 563-71.
- Mitchell PJ, Ravi S, Griffiths B, Reid F, Speake D, Midgley C, et al. Multicentre review of lymph node harvest in colorectal cancer: are we understaging colorectal cancer patients? *Int J Colorectal Dis* 2009; **24**: 915-21.
- Mejia A, Schulz S, Hyslop T, Weinberg DS, Waldman SA. Molecular staging individualizing cancer management. *J Surg Oncol* 2012; **105**: 468-74.
- Kang BW, Jeon HS, Chae YS, Lee SJ, Park JY, Choi JE, et al. Association between GWAS-identified genetic variations and disease prognosis for patients with colorectal cancer. *PLoS One* 2015; **10**: e0119649.
- Kollmar O, Rupertus K, Scheuer C, Junker B, Tilton B, Schilling MK, et al. Stromal cell-derived factor-1 promotes cell migration and tumor growth of colorectal metastasis. *Neoplasia* 2007; **9**: 862-70.
- Koskensalo S, Louhimo J, Nordling S, Hagström J, Haglund C. MMP-7 as a prognostic marker in colorectal cancer. *Tumour Biol* 2011; **32**: 259-64.
- Kanzaki H, Ouchida M, Hanafusa H, Sakai A, Yamamoto H, Suzuki H, et al. Single nucleotide polymorphism in the RAD18 gene and risk of colorectal cancer in the Japanese population. *Oncol Rep* 2007; **18**: 1171-5.
- Stein U, Walther W, Arlt F, Schwabe H, Smith J, Fichtner I, et al. MACC1, a newly identified key regulator of HGF-MET signalling, predicts colon cancer metastasis. *Nat Med* 2009; **15**: 59-67.
- Ting L, Jun H, Junjie C. RAD18 lives a double life: Its implication in DNA double-strand break repair. *DNA Repair (Amst)* 2010; **9**: 1241-8.
- Pan J, Chi P, Lu X, Xu Z. Genetic polymorphisms in translesion synthesis genes are associated with colorectal cancer risk and metastasis in Han Chinese. *Gene* 2012; **504**: 151-5.
- Cañadas I, Taus A, González I, Villanueva X, Gimeno J, Pijuan L, et al. High circulating hepatocyte growth factor levels associate with epithelial to mesenchymal transition and poor outcome in small cell lung cancer patients. *Oncotarget* 2014; **5**: 5246-56.
- Arlt F, Stein U. Colon cancer metastasis: MACC1 and Met as metastatic pacemakers. *Int J Biochem Cell Biol* 2009; **41**: 2356-9.
- Lang AH, Geller-Rhomberg S, Winder T, Stark N, Gasser K, Hartmann B, et al. A common variant of the MACC1 gene is significantly associated with overall survival in colorectal cancer patients. *BMC Cancer* 2012; **12**: 20.
- Muendlein A, Hubalek M, Geller-Rhomberg S, Gasser K, Winder T, Drexel H, et al. Significant survival impact of MACC1 polymorphisms in HER2 positive breast cancer patients. *Eur J Cancer* 2014; **50**: 2134-41.
- Dziki L, Przybyłowska K, Majsterek I, Trzcíński R, Mik M, Sygut A. A/G polymorphism of the MMP-7 gene promoter region in colorectal cancer. *Pol Przegl Chir* 2011; **83**: 622-6.
- Wieczorek E, Reszka E, Wasowicz W, Grzegorzczak A, Konecki T, Sosnowski M, et al. MMP7 and MMP8 genetic polymorphisms in bladder cancer patients. *Cent European J Urol* 2014; **66**: 405-10.

31. Peng B, Cao L, Ma X, Wang W, Wang D, Yu L. Meta-analysis of association between matrix metalloproteinases 2, 7 and 9 promoter polymorphisms and cancer risk. *Mutagenesis* 2010; **25**: 371-9.
32. Beeghly-Fadiel A, Shu XO, Long J, Li C, Cai Q, Cai H, et al. Genetic polymorphisms in the MMP-7 gene and breast cancer survival. *Int J Cancer* 2009; **124**: 208-14.
33. Chernov AV, Sounni NE, Remacle AG, Strongin AY. Epigenetic control of the invasion-promoting MT1-MMP/MMP-2/TIMP-2 axis in cancer cells. *J Biol Chem* 2009; **284**: 12727-34.
34. Matsusue R, Kubo H, Hisamori S, Okoshi K, Takagi H, Hida K, et al. Hepatic stellate cells promote liver metastasis of colon cancer cells by the action of SDF-1/CXCR4 axis. *Ann Surg Oncol* 2009; **16**: 2645-53.
35. Coelho A, Calçada C, Catarino R, Pinto D, Fonseca G, Medeiros R. CXCL12-3' A polymorphism and lung cancer metastases protection: new perspectives in immunotherapy? *Cancer Immunol Immunother* 2006; **55**: 639-43.
36. Dommenge F, Cartron G, Espanel C, Gallay N, Domenech J, Benboubker L, et al. CXCL12 polymorphism and malignant cell dissemination/tissue infiltration in acute myeloid leukemia. *FASEB J* 2006; **20**: 1913-5.
37. Chang SC, Lin PC, Yang SH, Wang HS, Li AF, Lin JK. SDF-1alpha G801A polymorphism predicts lymph node metastasis in stage T3 colorectal cancer. *Ann Surg Oncol* 2009; **16**: 2323-30.
38. Schmol HJ, Tabernero J, Maroun J, de Braud F, Price T, Van Cutsem E, et al. Capecitabine plus oxaliplatin compared with fluorouracil/folinic acid as adjuvant therapy for stage III colon cancer: final results of the NO16968 randomized controlled phase III trial. *J Clin Oncol* 2015; **33**: 3733-40.
39. André T, de Gramont A, Vernerey D, Chibaudel B, Bonnetain F, Tijeras-Raballand A, et al. Adjuvant fluorouracil, leucovorin, and oxaliplatin in stage II to III colon cancer: updated 10-year survival and outcomes according to BRAF mutation and mismatch repair status of the MOSAIC study. *J Clin Oncol* 2015; **33**: 4176-87.
40. Gray R, Barnwell J, McConkey C, Hills RK, Williams NS, Kerr DJ, et al. Adjuvant chemotherapy versus observation in patients with colorectal cancer: a randomised study. *Lancet* 2007; **370**: 2020-9.
41. Inese D, Ilze S, Andrejs V, Janis G. Frequency of morphologic prognostic factors in surgically treated colorectal cancer. *Acta Chirurgica Latvensis* 2014; **14**: 3-8.
42. Zhang B, Lv M, Chen T, Wei Q, Wang G, Tian J, et al. The association between lymph node resection and postoperative survival in patients with colorectal cancer. *Hepatogastroenterology* 2013; **60**: 1922-6.
43. Ratto C, Sofo L, Ippoliti M, Merico M, Bossola M, Vecchio FM, et al. Accurate lymph-node detection in colorectal specimens resected for cancer is of prognostic significance. *Dis Colon Rectum* 1999; **42**: 143-54; Discussion 154-48.
44. Liebig C, Ayala G, Wilks J, Verstovsek G, Liu H, Agarwal N, et al. Perineural invasion is an independent predictor of outcome in colorectal cancer. *J Clin Oncol* 2009; **27**: 5131-7.
45. Betge J, Pollheimer MJ, Lindtner RA, Kornprat P, Schlemmer A, Rehak P, et al. Intramural and extramural vascular invasion in colorectal cancer: prognostic significance and quality of pathology reporting. *Cancer* 2012; **118**: 628-38.

MRI reduces variation of contouring for boost clinical target volume in breast cancer patients without surgical clips in the tumour bed

Noora Al-Hammadi, Palmira Caparrotti, Saju Divakar, Mohamed Riyas, Suparna Halsnad Chandramouli, Rabih Hammoud, Jillian Hayes, Maeve Mc Garry, Satheesh Prasad Paloor, Primož Petric

Department of Radiation Oncology, National Center for Cancer Care and Research, Hamad Medical Corporation, Doha, Qatar

Radiol Oncol 2017; 51(2): 160-168.

Received 5 December 2016

Accepted 19 February 2017

Correspondence to: Primož Petrič, M.D., M.Sc., Department of Radiation Oncology, National Center for Cancer Care and Research, Hamad Medical Corporation, P.O. Box 3050, Doha, Qatar. E-mail: ppetric@hamad.qa

Disclosure: No potential conflicts of interest were disclosed.

Background. Omitting the placement of clips inside tumour bed during breast cancer surgery poses a challenge for delineation of lumpectomy cavity clinical target volume (CTV_{LC}). We aimed to quantify inter-observer variation and accuracy for CT- and MRI-based segmentation of CTV_{LC} in patients without clips.

Patients and methods. CT- and MRI-simulator images of 12 breast cancer patients, treated by breast conserving surgery and radiotherapy, were included in this study. Five radiation oncologists recorded the cavity visualization score (CVS) and delineated CTV_{LC} on both modalities. Expert-consensus (EC) contours were delineated by a senior radiation oncologist, respecting opinions of all observers. Inter-observer volumetric variation and generalized conformity index (CI_{gen}) were calculated. Deviations from EC contour were quantified by the accuracy index (AI) and inter-delineation distances (IDD).

Results. Mean CVS was 3.88 +/- 0.99 and 3.05 +/- 1.07 for MRI and CT, respectively (p = 0.001). Mean volumes of CTV_{LC} were similar: 154 +/- 26 cm³ on CT and 152 +/- 19 cm³ on MRI. Mean CI_{gen} and AI were superior for MRI when compared with CT (CI_{gen}: 0.74 +/- 0.07 vs. 0.67 +/- 0.12, p = 0.007; AI: 0.81 +/- 0.04 vs. 0.76 +/- 0.07; p = 0.004). CI_{gen} and AI increased with increasing CVS. Mean IDD was 3 mm +/- 1.5 mm and 3.6 mm +/- 2.3 mm for MRI and CT, respectively (p = 0.017).

Conclusions. When compared with CT, MRI improved visualization of post-lumpectomy changes, reduced inter-observer variation and improved the accuracy of CTV_{LC} contouring in patients without clips in the tumour bed. Further studies with bigger sample sizes are needed to confirm our findings.

Key words: breast cancer; contouring; contouring variation; MRI; CT

Introduction

There are two clinical scenarios in which delineation of the lumpectomy cavity (LC) is required during breast cancer radiotherapy: boost after whole breast irradiation (WBI) and accelerated partial breast irradiation (APBI). WBI after organ-sparing surgery reduces the risk of breast cancer recurrence and mortality.^{1,2} Delivery of boost dose to the LC clinical target volume (CTV_{LC}) is an important component of this treatment. It has been

shown to improve local control at an increased risk of moderate to severe fibrosis.³ APBI is becoming increasingly utilized in selected groups of patients. Shorter overall treatment time, reduced radiation exposure of the organs at risk and comparable disease control make it a good alternative to WBI for early stage disease.⁴⁻⁶ High accuracy of contouring and precision of treatment delivery are needed to optimize the delicate therapeutic ratio between treatment benefit and side effects. This is especially important in the setting of highly conformal dose

delivery to a small volume, such as boost after WBI and becomes critical during APBI where the entire dose is delivered to the CTV_{LC}. Inter-observer variation (IOV) in contouring is one of the main contributors to the cumulative budget of uncertainties in radiotherapy.⁷ It may undermine the gain of high-precision technologies, blur the dose-effect relations and compromise treatment comparisons. For the individual patient, geographical miss of the target volume leads to increased chance of relapse, while unnecessary irradiation of normal tissues increases the probability of side effects. Respecting the common contouring guidelines accompanied by adequate training and high quality imaging are the most important strategies to reduce contouring variation.⁷⁻¹¹

Currently, CT is the standard imaging modality for CTV_{LC} contouring. Due to its poor ability for soft tissue depiction, placement of surgical clips or markers at the edges of LC is recommended to improve tumour bed delineation.¹²⁻¹⁶ But reliability of inserted markers as a surrogate for tumour bed is a matter of debate^{9,16-18} and omission of their placement in some patients poses a special challenge to the radiation oncologist during CTV_{LC} delineation.¹⁹ The role of MRI for contouring in breast cancer radiotherapy is controversial^{11,20-23} and the evidence to support its use in patients without markers in the tumour bed is scarce.^{24,25} In our present study, we aimed to (1) quantify the IOV and (2) assess the accuracy of CT- and MRI-based CTV_{LC} contouring in patients without clips in the LC. Our null hypothesis was that there is no statistically significant difference between MRI- and CT- based contouring in this subgroup of patients.

Patients and methods

Patients and images

Anonymized image data sets of patients with pathology-proven unilateral invasive ductal carcinoma of the breast, treated by breast conserving surgery and adjuvant radiotherapy in 2013 were considered for this study. Cases without surgical clips in the LC and available CT- and MRI-simulator data sets were eligible for inclusion. Adjuvant radiotherapy had to consist of WBI followed by CTV_{LC} boost. Patients who underwent oncologic surgery were excluded. All radiotherapy was completed before initiation of the study and the presented work did not interfere with routine management of our patients. The study protocol was reviewed and given ethical approval by the

Institutional Medical Research Centre which governs our Institutional Review Board (Trial registration number: 15329/15).

Acquisition of CT and MRI simulator images

During simulation and treatment, patients were placed in comfortable and reproducible supine position with arms abducted over the head. For CT simulation patients were placed on breast board and wires were used to identify the surgical scars and drainage sites. Non-contrast volumetric CT study with contiguous slices of 5 mm thickness was obtained from the level of the body of the mandible to at least 5 cm below the inframammary fold (Siemens Somatom Sensation ® 16-slice scanner, 120 kVp, approximately 90 mAs, voxel size of 1.26 × 1.26 × 5 mm, matrix size of 512 × 512). MR images were obtained on a dedicated wide-bore 1.5T 450w MRI simulator (General Electrics Optima ®) equipped with radiotherapy applications. The MRI in this study was a simulation procedure and was acquired supine as per CT planning with efforts made to replicate the positioning as much as achievable. The arms were elevated and cradled, and external alignment lasers used to align the tattoos, albeit the incline was not applied due to limitations of the MRI bore diameter. The supine positioning achieved a more similar deformation of the breast tissue to the planning CT than a prone diagnostic arrangement. General purpose Flex coils were used. Our breast MRI protocol included T2 weighted FSE propellor, proton density with fat saturation, Dixon type LAVA-Flex and balanced steady state gradient echo FIESTA imaging sequences. All sequences were acquired axially with matrix size of 288 × 288, approximately 42 cm field of view and slice thickness of 5 mm. For the T2 FSE sequence, mean system related geometric distortions after the application of the vendor-provided correction algorithms were 0.5, 0.9 and 1.9 mm for radial distances of 100, 200, and 250 mm respectively. Anonymized non-registered CT and MRI data-sets were imported to the ECLIPSE workstation (Varian, Medical Systems ®) for contouring.

Cavity visualization score and contouring

Cavity visualization score (CVS) was recorded by each observer for all cases and both modalities, using the standardized numeric scale ranging from 1 (cavity not visualized) to 5 (all cavity margins

clearly visualized).²⁶ CTV_{LC} was contoured separately on CT and MRI by five experienced radiation oncologists (observers), who were blinded for each other's delineations. The observers had access to clinical and imaging findings at time of diagnosis and to surgical and pathology reports. They were asked to respect the following instructions during delineation:

1. Adjust window level to optimize visualization of the region of interest.
2. Contour on axial images.
3. When contouring on the MRI, use the T2 weighted FSE images as primary data set and take the information from other sequences into account.
4. Allow for a minimum interval of 2-weeks between CT- and MRI-based contouring to minimize bias resulting from familiarity with the cases.
5. Create CTV_{LC} according to our departmental guidelines:
 - A. First, delineate the lumpectomy cavity (LC) as intra-mammary post-lumpectomy changes. During delineation, compare findings with contralateral anatomy to identify differences in geometry, tissue architecture, formation of seroma, hematoma or scar tissue, fat replacement on CT and decreased signal intensity on MRI. While contouring, take all available information into account to identify the LC (tumour location on preoperative imaging, pathology reports, lumpectomy scar on the skin, etc.).
 - B. To define CTV_{LC} , add a 15 mm uniform margin around the LC and edit it to exclude the chest wall and skin.

Finally, the expert consensus (EC) contours of CTV_{LC} were delineated on CT and MRI for all cases. EC contouring was led by the senior radiation oncologist, taking the opinions of all five observers into account.

Analysis of contouring uncertainties

Contouring uncertainties on CT and MRI were analysed from two perspectives, reflecting our study objectives: (1) to quantify the IOV, global variability between delineations was assessed and (2) to quantify contouring accuracy, deviations of observers from the EC contours were analysed. Contour analysis tool 1 (CAT 1) software and related methodology^{27,28} was used for volumetric and distance-based computations.

Inter-observer variation: Mean volumes and standard deviations (SD) of CTV_{LC} were calculated for each study case on CT- and MRI-based approach. Inter-observer coefficients of variance (CoV – ratio between SD and mean value) and ratios between the smallest and largest volume were determined for each case and modality. Inter-observer conformity index was calculated based on the generalized formalism (CI_{gen}), which is independent of the number of the analysed volumes.²⁹ It equals the sum of intersections of all possible volume-pairs divided by the sum of their unions.

Contouring accuracy: We used the EC as a surrogate for the “ground truth” contour. Deviations from EC were measured on CT and MRI for all cases and observers. Accuracy index (AI) was determined according to paired CI formalism.²⁹ AI was calculated as the ratio between common and encompassing volume for each pair of EC and observer's contour. Further, mean absolute distances between contours of individual observers and EC were calculated in contouring plane. This method has been used before and is described in detail.^{27,28,30} Briefly, the inter-delineation distances (IDD) were calculated between each voxel of observer's contour and nearest voxel of the EC contour in 72 angular steps of 5 degrees for all slices.^{27,28,30}

Statistical analysis

Statistical design of the study did not entail calculation of the sample size and the number of observers. Instead, all evaluable cases satisfying the inclusion criteria to the point of study initiation and all available observers from our department were included to maximize the statistical power. Continuous variables were presented as mean values with standard deviations. Paired sample t-test was used to compare mean values of analysed variables between CT and MRI. P-value of < 0.05 was considered as the limit for statistical significance. SPSS for windows (©SPSS Inc., 1989–2015, Chicago, Illinois) was used for data analysis.

Results

Cavity visualization score

The use of MRI improved the cavity visualization in 11 out of 12 (92%) cases (Figure 1). In the remaining one case, mean CVS was equal (3.0) on both modalities. Mean CVS was 3.88 +/- 0.99 and 3.05 +/- 1.07 for MRI and CT, respectively (p = 0.001). Correlation of CI_{gen} and AI with CVS is shown in

Figure 1. CI_{gen} and AI improved with increasing CVS for both contouring approaches. Example of contouring variation for two selected cases with a high and low CVS is presented in Figure 2.

Inter-observer variation

The results of IOV analysis are presented in Table 1 and Figure 1A. Mean CI_{gen} for MRI was significantly superior to CI_{gen} for CT (0.74 +/- 0.07 vs. 0.67 +/- 0.12, $p = 0.007$). CI_{gen} for MRI was higher than for CT in 10 (83 %) cases. In case number 9, CT-based CI_{gen} was superior to MRI (0.77 vs. 0.71) and in case number 6 they were identical (0.76). Mean volumes of CTV_{LC} were 154 +/- 26 cm^3 on CT and 152 +/- 19 cm^3 on MRI (non-significant difference). Mean volumetric CoV was non-significantly lower for MRI when compared with CT (12% vs. 18 %; $p = 0.1$). Similarly, average ratio between the smallest and largest delineated volume was non-significantly higher for MRI when compared with CT (0.8 +/- 0.1 vs. 0.7 +/- 0.1; $p = 0.1$).

Contouring accuracy

Results of analysis of deviations from EC contours are shown in Table 2 and Figure 1B. Observers placed all contours in the correct breast quadrant. Mean AI was higher for MRI when compared with CT (0.81 +/- 0.04 vs. 0.76 +/- 0.07; $p = 0.004$). MRI-based mean AI was superior to CT in 10 (83 %) cases. In case number 9, CT-based AI was slightly superior to MRI (0.81 +/- 0.04 vs. 0.8 +/- 0.05) and in case number 1, AI was the same for both modalities (0.88 +/- 0.1) (Table 2, Figure 1B). There was small but significant difference in mean IDD between CT and MRI (3.6 mm +/- 2.3 mm vs. 3 mm +/- 1.5 mm; $p = 0.017$). Corresponding mean CoV for CT was higher than for MRI (61 % vs. 49 %; $p = 0.003$). The mean value of maximal IDD was 13 +/- 6 mm for CT and 10 +/- 4 mm for MRI ($p = 0.06$).

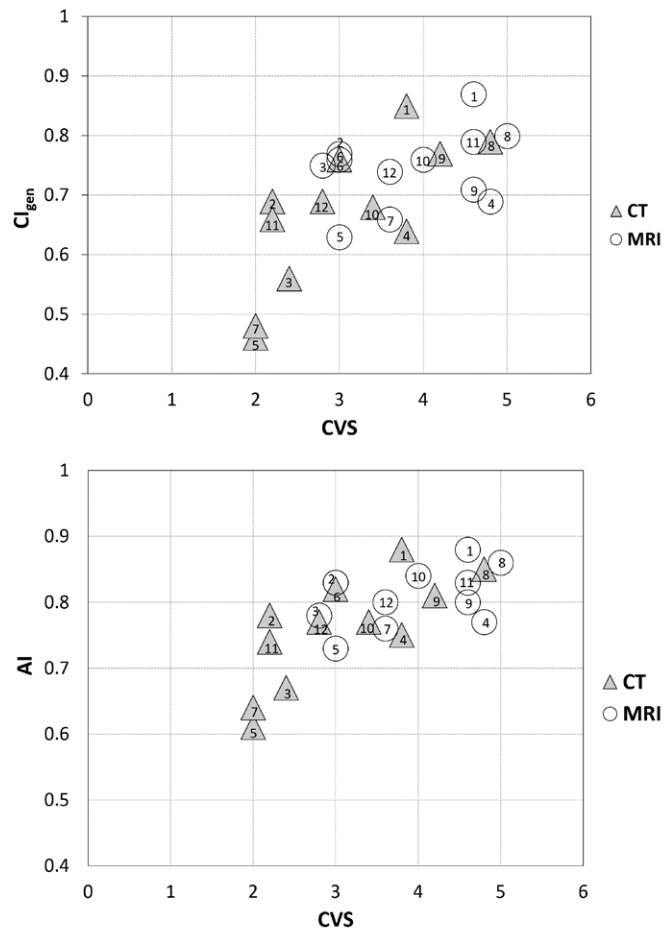


FIGURE 1. (A) Generalized conformity index (CI_{gen}) and **(B)** accuracy index (AI) as a function of the cavity visualization score (CVS) for CT and MRI based contouring of lumpectomy cavity clinical target volume. None of the patients had surgical clips inserted in the tumor bed. Case numbers are indicated for each modality.

FIGURE 2. CT and MRI based contouring in two examples with high and low cavity visualization scores (CVS). Observers' delineations are white and expert consensus (EC) contours black. **(A)** Case with a CVS of 4.8 on CT and 5 on MRI: mean generalized conformity index (CI_{gen}), accuracy index (AI) and inter-delineation distance (IDD) were 0.79, 0.85 and 2.4 mm on CT and 0.80, 0.86 and 2.2 mm on MRI. **(B)** Case with a CVS of 2 on CT and 3 on MRI: mean CI_{gen} , AI and IDD were 0.46, 0.61 and 6 mm for CT and 0.63, 0.73 and 4.5 mm for MRI.

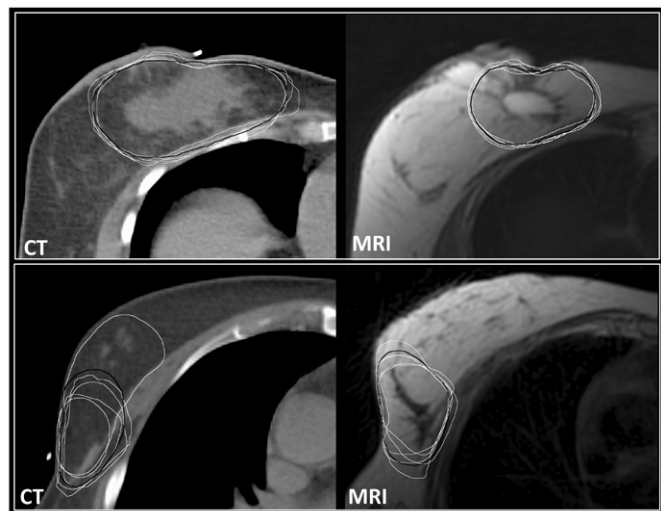


TABLE 1. Results for inter-observer variation in contouring. The difference in mean generalized conformity index (CI_{gen}) between the CT and MRI based contouring was statistically significant ($p = 0.007$)

Case	CT			MRI		
	Mean V [cm ³] (SD)	CoV [%]	CI_{gen}	Mean V [cm ³] (SD)	CoV [%]	CI_{gen}
1	198 (10)	5	0.85	106 (4)	4	0.87
2	241 (37.5)	16	0.69	256 (28)	11	0.77
3	108 (20.7)	19	0.56	125 (10)	8	0.75
4	75 (18.1)	24	0.64	92 (12)	13	0.69
5	175 (47.9)	27	0.46	217 (68)	31	0.63
6	140 (10.1)	7	0.76	125 (14)	11	0.76
7	103(39.7)	39	0.48	64 (2)	4	0.66
8	180 (22.5)	12	0.79	158 (14)	9	0.8
9	135 (19.8)	15	0.77	126 (20)	16	0.71
10	204 (44.3)	22	0.68	215 (19)	9	0.76
11	99 (14.4)	15	0.66	135 (11)	8	0.79
12	195 (27.3)	14	0.69	210 (29)	14	0.74
MEAN (SD)	154 (26)	18	0.67 (0.12)	152 (19)	12	0.74 (0.07)

CoV = Coefficient of Variance; CTV_{LC} = Clinical Target Volume of Lumpectomy Cavity; SD = Standard Deviation

Discussion

Results of the present study rejected our null hypothesis: MRI, when compared with CT, led to (1) reduced IOV and (2) improved accuracy for CTV_{LC} contouring in patients without markers in the tumour bed. Keeping in mind the cost and complexity of utilizing MRI for radiotherapy planning, our findings justify its use in selected cases.

CT-based delineation of the LC is prone to IOV, even among experienced radiation oncologists.^{7,10,11,31-34} In various tumour sites, MRI has been shown to reduce contouring uncertainties when compared with CT.³⁵⁻⁴¹ Based on these findings, MRI is becoming increasingly implemented for contouring and is the recommended gold standard in some malignancies.⁴² However, there are many studies that failed to demonstrate improved contouring with the use of MRI for various tumour sites.⁴³⁻⁴⁷ As far as breast cancer is concerned, several authors investigated the impact of adding MRI to CT for delineation of lumpectomy cavity with negative or inconclusive outcome.^{11,16,20-23} Den Hartogh *et al.* found that addition of postoperative MRI to CT guided delineation marginally increased the target volumes and failed to reduce the IOV.²² Similarly, Kirby *et al.* reported that addition of MRI to CT resulted in tumour bed volumes that were discordant with those based on CT and

TABLE 2. Accuracy index (AI) and inter-delineation distances (IDD), based on the expert consensus (EC) delineation as the reference. The differences in AI and IDD between CT and MRI were statistically significant ($p < 0.05$)

Case	CT						MRI					
	IDD [mm]			AI			IDD [mm]			AI		
	Mean	SD	CoV [%]	Mean	SD	CoV [%]	Mean	(SD)	CoV [%]	Mean	SD	CoV [%]
1	2.1	0.8	38	0.88	0.02	3	1.8	0.58	32	0.88	0.01	2
2	3.6	1.9	53	0.78	0.1	12	3.2	1.9	59	0.83	0.02	3
3	3.9	2.6	67	0.67	0.07	10	3.2	1.8	56	0.78	0.02	2
4	2.3	1	43	0.75	0.06	8	2.3	0.9	39	0.77	0.05	6
5	6	4	67	0.61	0.15	24	4.5	2.1	47	0.73	0.14	20
6	2.6	1.1	42	0.82	0.02	2	2.6	1	38	0.83	0.02	2
7	6	4.1	68	0.64	0.09	14	3.6	1.8	50	0.76	0.05	7
8	2.4	1.2	50	0.85	0.02	2	2.2	1	45	0.86	0.04	4
9	3	2.9	97	0.81	0.04	5	2.9	1.8	62	0.80	0.05	6
10	4.5	3.5	78	0.77	0.07	9	3.3	2	61	0.84	0.02	2
11	3.3	2	61	0.74	0.09	12	2.5	1.3	52	0.83	0.02	3
12	3.4	2.3	68	0.77	0.06	8	3.6	1.7	47	0.80	0.02	2
MEAN	3.6	2.3	61	0.76	0.07	9	3	1.5	49	0.81	0.04	5

CoV = Coefficient of Variance; CTV_{LC} = Clinical Target Volume of Lumpectomy Cavity; SD = Standard Deviation

clips alone. With the use of MRI, the tumour bed volume increased in 28 out of 30 cases included, resulting in a median CTV increase of 10.3% (-33.6%–80.9%).²⁰ Mast *et al.* compared CT- and MRI-based delineations of breast and LC by four observers in 10 patients. The mean CI for the LC was 0.52 for CT and 0.48 for CT combined with MRI ($p = 0.33$).²³ In another similar study, the inter-observer agreement was even lower. While MRI and CT enabled similar visualization of the LC, MRI resulted in lower generalized CI (0.32 +/- 0.25) when compared with CT (0.52 +/- 0.21).²¹

The rationale to use MRI in our study was to improve contouring consistency for cases without surgical clips in the tumour bed. Mean CVS on MRI (3.88 +/- 0.99) was significantly superior to CVS on CT (3.05 +/- 1.07) ($p = 0.001$). CVS was improved in 92% and was accompanied by an increase of CI_{gen} and AI in 83% cases. For both modalities, we found an increase of CI_{gen} and AI with increasing CVS (Figure 2). Therefore, inter-observer concordance depended directly on the ability to visualize lumpectomy cavity, which was superior on MRI. Of note, in all of the reports which failed to show benefit of MRI, clips were placed at the edges of LC.^{11,16,20-23} In a study by Giezen *et al.*, four observers (2 radiologists and 2 radiation oncologists) obtained a mean CVS of 2.8 +/- 1.7 for MRI and 2.9 +/- 1.7 for CT. In contrast to our findings, Giezen *et al.* demonstrated superiority of CT over MRI for contouring, especially at low CVS.²¹ With increasing CVS values, both modalities performed better and the CI_{gen} from MRI approached that from CT. The lack of added value of MRI in this and other published studies²⁰⁻²³ could be attributed to better visibility of the clips on CT, introducing a bias in its favour, as acknowledged by the authors.²¹ This effect becomes especially important at low CVS values. Our positive findings could be attributed also to the fact that MRI was performed as simulation procedure, replicating the CT planning supine position as much as achievable.

To our knowledge, there are only two publications in addition to our present study which demonstrated added value of MRI for delineation of post-lumpectomy tumour bed.^{24,25} In the study by Jolicoeur *et al.*, there were no surgical clips implanted at time of lumpectomy. Three observers delineated the post-lumpectomy tumour bed in 70 patients. Highly significant IOV was demonstrated for CT based contouring of the tumour bed ($p < 0.0001$), while agreement was high for the MRI-based approach. The volumes of MRI based contours were 30–40% smaller than the CT-derived

volumes. In another study with three observers and 36 cases, mean CVS for the LC was 3.3 and 4.3 for CT and T2 MRI, respectively ($p < 0.0001$). Better CVS was reflected in superior inter-observer consistency and volumetric agreement of contours. The authors stated that surgical clips were occasionally, but not routinely placed by the referring surgeons.²⁴

Based on our results, addition of MRI to CT could be justified as a good alternative to CT alone for selected patients in whom the placement of surgical clips in the tumour bed was omitted. But despite concerns regarding their reliability as a surrogate for tumour bed^{17,18,48}, placement of clips followed by CT-based contouring of LC should be currently considered as the gold standard.¹⁶ This approach has been shown to improve the accuracy of LC contouring, reduce the overall boost volume and help prevent geographical miss and underdosage of the LC.^{13-16,49-52} But the technique of placement and the number of inserted markers differs between institutions and surgeons and is even omitted in some cases. Kirwan *et al.* recently reported on a retrospective study of 196 cases, assessing the compliance with recommendations for clip insertion. Although recommended by the clinical guidelines, the clip insertion was omitted in 56% of cases while additional 7% of patients had only two or fewer clips inserted. Ten of 31 referring surgeons routinely omitted clips and the omission rate was significantly higher for centres with low (≤ 1 patient) when compared with high (≥ 14 patients) rate of recruitment to IMRT clinical trials (67% vs. 27%, respectively; $p < 0.001$).¹⁹ These results emphasize the need for good collaboration between radiation oncologists and surgeons and standardization of clip placement.⁹ Auditing of clip insertion has been suggested as one of the key performance indicators for quality control of breast cancer surgery.¹⁹

Based on their study which demonstrated reduction of IOV when adding MRI to CT, Jolicoeur *et al.* proposed that the use of CT-MRI fusion may obviate the need for surgical clips altogether.²⁵ However, while reduction of IOV indicates increased contouring agreement, it doesn't necessarily imply improved accuracy. To assess the accuracy, individual delineations would in theory need to be compared with the ground truth or correct delineation. In the absence of the histopathological proof, the ground truth is an elusive concept. Different approaches, including simultaneous truth and performance level estimation (STAPLE), expert consensus (EC) or their combination have been used as surrogates for correct delineation.^{27,53}

In our current study, the concept of EC delineation was applied. Keeping in mind the limitations of the “ground truth” definition, our results indicate that adding MRI to CT improves contouring accuracy in cases without surgical clips in the LC cavity.

Comparison of our results with findings of other studies is challenging due to the variable conditions under which contouring was performed and the diversity of methods used for IOV assessment. The impact of variables such as experience and specialty of observers, use of guidelines, type of surgery, etc. should be kept in mind when comparing reports.¹⁶ As far as the methods for IOV assessment are concerned, CI is one of the most commonly used quantifiers. In general, CI is a measure of overlap between analyzed volumes, but there is a diversity of formalisms used in the literature which cannot be directly compared. The generalized CI (CI_{gen}) formalism is independent of the number of delineations, enabling the comparisons between studies with different number of observers.²⁹ Regardless of the CI formalism used, the impact of contouring variation on CI is inversely proportional to the size of the analyzed volume. Therefore, same absolute deviation between analyzed contours will result in lower CI for small volumes (*i.e.* tumour bed) when compared with larger volumes (*i.e.* tumour bed with a margin). The effect of margins on CI is particularly relevant in breast cancer, where the contours are typically cropped to exclude the skin and chest wall, improving the apparent conformity between observers.

In our study, mean CI_{gen} of 0.67 (+/- 0.12) and 0.74 (+/- 0.07) was obtained for CT and MRI-based contouring of CTV_{LC} respectively. Major *et al.* studied the impact of contouring guidelines on consistency of LC and planning target volume (PTV) contouring for multi-catheter partial breast irradiation. When contouring was performed on pre-implant scans by experienced observers and according to the guidelines (similar conditions as in our study), they obtained a CI_{gen} of 0.59 and 0.73 for LC and PTV, respectively. The margins for PTV were similar to our margins for CTV_{LC} making the resulting volume sizes comparable between the two studies. Of note, CI_{gen} for PTV, obtained by CT and clip-based contouring⁵⁴ was similar to our CI_{gen} for CTV_{LC} obtained by MRI in patients without clips. The lower CI_{gen} for LC when compared with PTV⁵⁴ reflects the sensitivity of CI to the volume size, as described above. Majority of other published studies reported on contouring uncertainties for tumour bed, with a CI ranging from 0.32–0.52.^{21–23} Our results compare favourably with the existent literature. This can

be attributed to strict compliance with contouring guidelines, participation of experienced observers and use of high quality imaging.

Low number of observers and cases that were entered in analysis can be considered as the main limitations of our study. Considering the need for specific expertise in breast radiotherapy, experience in interpretation of MRI and relative rarity of cases without clips in LC, higher number of observers and cases is challenging to obtain outside a multi-institutional setting. This challenge is reflected in the limited number of observers and cases in studies, published by several authors before us.^{20–23} Multi-centre collaborative projects may represent the optimal approach to overcome this limitation and shed more light on the subject of contouring uncertainties in general.

Conclusions

In breast cancer patients without clips in the tumour bed after breast conserving surgery, MRI improved the visualization of lumpectomy cavity when compared with CT. Consequently, inter-observer agreement and accuracy of contouring of lumpectomy cavity clinical target volume were improved. Placement of surgical clips, followed by CT-based contouring is the gold standard for contouring of the boost volume for postoperative irradiation in breast cancer. However, in patients without clips, addition of MRI to CT simulator images should be considered to improve delineation accuracy. Further studies with higher number of observers and cases are required to confirm our findings.

Declarations

The study protocol was reviewed and given ethical approval by the Institutional Medical Corporation Medical Research Centre. Datasets generated and analysed during study are not publicly available due to patient confidentiality but are available from corresponding author on reasonable request and after institutional approval. This study was not funded.

Acknowledgements

The authors are grateful to Ms. Sally Adnan Sheim, Mr. Tarraf Torfeh, and Ms. Souha Aouadi,

Department of Radiation Oncology, National Center for Cancer Care and Research, Hamad Medical Corporation for their help in image processing and support during preparation of this manuscript.

References

- Fisher B, Anderson S, Bryant J, Margolese RG, Deutsch M, Fisher ER, et al. Twenty-year follow-up of a randomized trial comparing total mastectomy, lumpectomy, and lumpectomy plus irradiation for the treatment of invasive breast cancer. *N Engl J Med* 2002; **347**: 1233-41. doi: 10.1056/NEJMoa022152
- Early Breast Cancer Trialists' Collaborative Group (EBCTCG). Effect of radiotherapy after breast-conserving surgery on 10-year recurrence and 15-year breast cancer death: meta-analysis of individual patient data for 10,801 women in 17 randomised trials. *Lancet* 2011; **378**: 1707-16. doi: 10.1016/S0140-6736(11)61629-2
- Bartelink H, Maingon P, Poortmans P, Weltens C, Fourquet A, Jager J, et al. Whole-breast irradiation with or without a boost for patients treated with breast-conserving surgery for early breast cancer: 20-year follow-up of a randomised phase 3 trial. *Lancet Oncol* 2015; **16**: 47-56. doi: 10.1016/S1470-2045(14)71156-8
- Strnad V, Ott OJ, Hildebrandt G, Kauer-Dorner D, Knauerhase H, Major T, et al. 5-year results of accelerated partial breast irradiation using sole interstitial multicatheter brachytherapy versus whole-breast irradiation with boost after breast-conserving surgery for low-risk invasive and in-situ carcinoma of the female breast: a randomised, phase 3, non-inferiority trial. *Lancet* 2016; **387**: 229-38. doi: 10.1016/S0140-6736(15)00471-7
- Vaidya JS, Wenz F, Bulsara M, Tobias JS, Joseph DJ, Keshtgar M, et al. Risk-adapted targeted intraoperative radiotherapy versus whole-breast radiotherapy for breast cancer: 5-year results for local control and overall survival from the TARGIT-A randomised trial. *Lancet* 2014; **383**: 603-13. doi: 10.1016/S0140-6736(13)61950-9
- Offersen BV, Overgaard M, Kroman N, Overgaard J. Accelerated partial breast irradiation as part of breast conserving therapy of early breast carcinoma: a systematic review. *Radiother Oncol* 2009; **90**: 1-13. doi: 10.1016/j.radonc.2008.08.005
- Segedin B, Petric P. Uncertainties in target volume delineation in radiotherapy – are they relevant and what can we do about them? *Radiol Oncol* 2016; **50**: 254-62. doi: 10.1515/raon-2016-0023
- Strnad V, Hannoun-Levi JM, Guinot JL, Lössl K, Kauer-Dorner D, Resch A, et al. Recommendations from GEC ESTRO Breast Cancer Working Group (I): Target definition and target delineation for accelerated or boost Partial Breast Irradiation using multicatheter interstitial brachytherapy after breast conserving closed cavity surgery. *Radiother Oncol* 2015; **115**: 342-8. doi: 10.1016/j.radonc.2015.06.010
- Major T, Gutiérrez C, Guix B, van Limbergen E, Strnad V, Polgar C., on behalf of Breast Cancer Working Group of GEC ESTRO. Recommendations from GEC ESTRO Breast Cancer Working Group (II): Target definition and target delineation for accelerated or boost partial breast irradiation using multicatheter interstitial brachytherapy after breast conserving open cavity surgery. *Radiother Oncol* 2016; **118**: 199-204. doi: 10.1016/j.radonc.2015.12.006
- Boersma LJ, Janssen T, Elkhuizen PHM, Poortmans P, van der Sangen M, Scholten AN, et al. Reducing interobserver variation of boost-CTV delineation in breast conserving radiation therapy using a pre-operative CT and delineation guidelines. *Radiother Oncol* 2012; **103**: 178-82. doi: 10.1016/j.radonc.2011.12.021
- Vinod SK, Min M, Holloway LC. A review of interventions to reduce interobserver variability in volume delineation in radiation oncology. *J Med Imaging Radiat Oncol* 2016; **60**: 393-406. doi: 10.1111/1754-9485.12462
- Park CK, Pritz J, Zhang GG, Forster KM, Harris EE. Validating fiducial markers for image-guided radiation therapy for accelerated partial breast irradiation in early-stage breast cancer. *Int J Radiat Oncol Biol Phys* 2012; **82**: 425-31. doi: 10.1016/j.ijrobp.2011.07.027
- Shaikh T, Chen T, Khan A, Yue NJ, Kearney T, Cohler A, et al. Improvement in interobserver accuracy in delineation of the lumpectomy cavity using fiducial markers. *Int J Radiat Oncol Biol Phys* 2010; **78**: 1127-34. doi: 10.1016/j.ijrobp.2009.09.025
- Coles CE, Wilson CB, Cumming J, Benson JR, Forouhi P, Wilkinson JS, et al. Titanium clip placement to allow accurate tumour bed localisation following breast conserving surgery: audit on behalf of the IMPORT Trial Management Group. *Eur J Surg Oncol* 2009; **35**: 578-82. doi: 10.1016/j.ejso.2008.09.005
- Weed DW, Yan D, Martinez AA, Vicini FA, Wilkinson TJ, Wong J. The validity of surgical clips as a radiographic surrogate for the lumpectomy cavity in image-guided accelerated partial breast irradiation. *Int J Radiat Oncol Biol Phys* 2004; **60**: 484-92. doi: 10.1016/j.ijrobp.2004.03.012
- Yang JT, Tao R, Elkhuizen PHM, van Vliet Vroegedewij C, Li G, Powell SN. Tumor bed delineation for external beam accelerated partial breast irradiation: A systematic review. *Radiother Oncol* 2013; **108**: 181-9. doi: 10.1016/j.radonc.2013.05.028
- Yang Z, Chen J, Hu W, Pan Z, Cai G, Yu X, et al. Planning the breast boost: how accurately do surgical clips represent the CT seroma? *Radiother Oncol* 2010; **97**: 530-4. doi: 10.1016/j.radonc.2010.09.007
- Goldberg H, Prosnitz RG, Olson JA, Marks LB. Definition of postlumpectomy tumor bed for radiotherapy boost field planning: CT versus surgical clips. *Int J Radiat Oncol Biol Phys* 2005; **63**: 209-13. doi: 10.1016/j.ijrobp.2005.01.044
- Kirwan CC, Al Sarakbi W, Lancaster J, Chan HY, Thompson Am, Wishart GC. Tumour bed clip localisation for targeted breast radiotherapy: compliance is proportional to trial-related research activity: tumour bed clip localisation in breast radiotherapy. *Eur J Surg Oncol* 2014; **40**: 158-62. doi: 10.1016/j.ejso.2013.11.016
- Kirby AM, Yarnold JR, Evans PM, Morgan VA, Schmidt MA, Scurr ED, et al. Tumor bed delineation for partial breast and breast boost radiotherapy planned in the prone position: what does MRI add to X-ray CT localization of titanium clips placed in the excision cavity wall? *Int J Radiat Oncol Biol Phys* 2009; **74**: 1276-82. doi: 10.1016/j.ijrobp.2009.02.028
- Giezen M, Kouwenhoven E, Scholten AN, Coerkam EG, Heijnen M, Jansen WPA, et al. MRI- versus CT-based volume delineation of lumpectomy cavity in supine position in breast-conserving therapy: an exploratory study. *Int J Radiat Oncol Biol Phys* 2012; **82**: 1332-40. doi: 10.1016/j.ijrobp.2011.05.008
- Den Hartogh MD, Phillipens MEP, van Dam IE, Kleynen CE, Terstege RJ, Kotte ANTI, et al. Post-lumpectomy CT-guided tumor bed delineation for breast boost and partial breast irradiation: Can additional pre- and postoperative imaging reduce interobserver variability? *Oncol Lett* 2015; **10**: 2795-801. doi: 10.3892/ol.2015.3697
- Mast M, Coerkamp E, Heijnen M, Scholten A, Jansen W, Kouwenhoven E, et al. Target volume delineation in breast conserving radiotherapy: are co-registered CT and MR images of added value? *Radiat Oncol* 2014; **9**: 65. doi: 10.1186/1748-717X-9-65
- Jacobson G, Zamba G, Betts V, Muruganandham M, Buechler-Price J. Image-based treatment planning of the post-lumpectomy breast utilizing CT and 3TMRI. *Int J Breast Cancer* 2011; **2011**: 1-5. doi: 10.4061/2011/246265
- Jolicoeur M, Racine ML, Trop I, Hathout L, Nguyen D, Derashodian T, et al. Localization of the surgical bed using supine magnetic resonance and computed tomography scan fusion for planification of breast interstitial brachytherapy. *Radiother Oncol* 2011; **100**: 480-4. doi: 10.1016/j.radonc.2011.08.024
- Petersen RP, Truong PT, Kader HA, Berthelet E, Lee JC, Hilts ML, et al. Target volume delineation for partial breast radiotherapy planning: clinical characteristics associated with low interobserver concordance. *Int J Radiat Oncol Biol Phys* 2007; **69**: 41-8. doi: 10.1016/j.ijrobp.2007.01.070
- Petrić P, Hudej R, Rogelj P, Blas M, Tanderup K, Fidarova E, et al. Uncertainties of target volume delineation in MRI guided adaptive brachytherapy of cervix cancer: A multi-institutional study. *Radiother Oncol* 2013; **107**: 6-12. doi: 10.1016/j.radonc.2013.01.014
- Rogelj P, Hudej R, Petrić P. Distance deviation measure of contouring variability. *Radiol Oncol* 2013; **47**(1): 86-96. doi: 10.2478/raon-2013-0005.
- Kouwenhoven E, Giezen M, Struikmans H. Measuring the similarity of target volume delineations independent of the number of observers. *Phys Med Biol* 2009; **54**: 2863-73. doi: 10.1088/0031-9155/54/9/018

30. Petric P, Hudej R, Rogelj P, Blas M, Segedin B, Logar HB, Dimopoulos JC. Comparison of 3D MRI with high sampling efficiency and 2D multiplanar MRI for contouring in cervix cancer brachytherapy. *Radiol Oncol* 2012; **46**: 242-51. doi: 10.2478/v10019-012-0023-1
31. Landis DM, Luo W, Song J, Bellon JR, Punglia RS, Wong JS, et al. Variability among breast radiation oncologists in delineation of the postsurgical lumpectomy cavity. *Int J Radiat Oncol Biol Phys* 2007; **67**: 1299-308. doi: 10.1016/j.ijrobp.2006.11.026
32. Van Mourik AM, Elkhuizen PH, Minkema D, Duppen JC; Dutch Young Boost Study Group, van-Vliet-Vroegindeweij C. Multiinstitutional study on target volume delineation variation in breast radiotherapy in the presence of guidelines. *Radiother Oncol* 2010; **94**: 286-91. doi: 10.1016/j.radonc.2010.01.009
33. Struikmans H, Warlam-Rodenhuis C, Stam T, Stapper G, Tersteeg RJ, Bol GH, Raaijmakers CP. Interobserver variability of clinical target volume delineation of glandular breast tissue and of boost volume in tangential breast irradiation. *Radiother Oncol* 2005; **76**: 293-9. doi: 10.1016/j.radonc.2005.03.029
34. Hurkmans CW, Admiraal M, van der Slangen M, Dijkmans I. Significance of breast boost volume changes during radiotherapy in relation to current clinical interobserver variations. *Radiother Oncol* 2009; **90**: 60-5. doi: 10.1016/j.radonc.2007.12.001
35. Rasch CRN, Steenbakkers RJHM, Fitton I, Duppen JC, Nowak PJ, Pameijer FA, et al. Decreased 3D observer variation with matched CT-MRI for target delineation in Nasopharynx cancer. *Radiat Oncol* 2010; **5**: 21. doi: 10.1186/1748-717X-5-21
36. Viswanathan AN, Dimopoulos JCA, Kirisits C, Berger D, Pötter R. CT versus MRI-based contouring in cervical cancer brachytherapy: results of a prospective trial and preliminary guidelines for standardized Contours. *Int J Radiat Oncol Biol Phys* 2007; **68**: 491-8. doi: 10.1016/j.ijrobp.2006.12.021
37. De Brabandere M, Hoskin P, Haustermans K, Van den Heuvel F, Siebert FA. Prostate post-implant dosimetry: interobserver variability in seed localisation, contouring and fusion. *Radiother Oncol* 2012; **104**: 192-8. doi: 10.1016/j.radonc.2012.06.014
38. Villeirs GM, Van Vaerenbergh K, Vakaet L, Bral S, Claus F, De Neve WJ, et al. Interobserver delineation variation using CT versus combined CT + MRI in intensity-modulated radiotherapy for prostate cancer. *Strahlenther Onkol* 2005; **181**: 424-30. doi: 10.1007/s00066-005-1383-x
39. Cattaneo GM, Reni M, Rizzo G, Castellone P, Ceresoli GL, Cozzarini C, et al. Target delineation in post-operative radiotherapy of brain gliomas: interobserver variability and impact of image registration of MR(pre-operative) images on treatment planning CT scans. *Radiother Oncol* 2005; **75**: 217-23. doi: 10.1016/j.radonc.2005.03.012
40. Weiss E, Hess CF. Comment by E. Weiss and C. F. Hess on G. M. Villeirs et al. "Interobserver delineation variation using CT versus combined CT + MRI in intensity-modulated radiotherapy for prostate cancer" in: *Strahlenther Onkol* 2005; **181**:424-30 (No. 7). *Strahlenther Onkol* 2005; **181**: 743-4. doi: 10.1007/s00066-005-9383-4
41. Hegazy N, Pötter R, Kirisits C, Berger D, Federico M, Sturdza A, Nesvacil N. High-risk clinical target volume delineation in CT-guided cervical cancer brachytherapy: impact of information from FIGO stage with or without systematic inclusion of 3D documentation of clinical gynecological examination. *Acta Oncol* 2013; **52**: 1345-52. doi: 10.3109/0284186X.2013.813068
42. Haie-Meder C, Pötter R, Van Limbergen E, Briot E, De Brabandere M, Dimopoulos J, et al. Recommendations from Gynaecological (GYN) GEC-ESTRO Working Group (I): concepts and terms in 3D image based 3D treatment planning in cervix cancer brachytherapy with emphasis on MRI assessment of GTV and CTV. *Radiother Oncol* 2005; **74**: 235-45. doi: 10.1016/j.radonc.2004.12.015
43. Barkati M, Simard D, Taussky D, Delouya G. Magnetic resonance imaging for prostate bed radiotherapy planning: An inter- and intra-observer variability study. *J Med Imaging Radiat Oncol* 2016; **60**: 255-9. doi: 10.1111/1754-9485.12416
44. Weltens C, Menten J, Feron M, Bellon E, Demaerel P, et al. Interobserver variations in gross tumor volume delineation of brain tumors on computed tomography and impact of magnetic resonance imaging. *Radiother Oncol* 2001; **60**: 49-59.
45. Buijsen J, van den Bogaard J, van der Heide H, Engelsman S, van Stiphout R, Janssen M, et al. FDG-PET-CT reduces the interobserver variability in rectal tumor delineation. *Radiother Oncol* 2012; **12**: 371-6. doi: 10.1016/j.radonc.2011.12.016
46. Daisne JF, Duprez T, Weynand B, Lonneux M, Hamoir M, Reyckler H, Grégoire V. Tumor volume in pharyngolaryngeal squamous cell carcinoma: comparison at CT, MR imaging, and FDG PET and validation with surgical specimen. *Radiology* 2004; **233**: 93-100. doi: 10.1148/radiol.2331030660
47. Khoo V, Adams EJ, Saran F, Bedford JL, Perks JR, et al. A comparison of clinical target volumes determined by CT and MRI for the radiotherapy planning of base of skull meningiomas. *Int J Radiat Oncol Biol Phys* 2000; **46**: 1309-17.
48. Kass R, Kumar G, Klimberg VS, Kass L, Henry-Tillman R, Johnson A, et al. Clip migration in stereotactic biopsy. *Am J Surg* 2002; **184**: 325-31.
49. Benda RK, Yasuda G, Sethi A, Gabram SG, Hinerman RW, Mendenhall NP. Breast boost: are we missing a target? *Cancer* 2003; **97**: 905-9. doi: 10.1002/cncr.11142
50. Dzagshvili M, Pichenot C, Dunant A, Balleyquier C, Delalage S, Mathieu MC, et al. Surgical clips assist in the visualization of the lumpectomy cavity in three-dimensional conformal accelerated partial-breast irradiation. *Int J Radiat Oncol Biol Phys* 2010; **76**: 1320-4. doi: 10.1016/j.ijrobp.2009.04.089
51. Kovner F, Agay R, Merimsky O, Stadler J, Klausner J, Inbar M. Clips and scar as the guidelines for breast radiation boost after lumpectomy. *Eur J Surg Oncol* 1999; **25**: 483-6. doi: 10.1053/ejso.1999.0683
52. Krawczyk JJ, Engel B. The importance of surgical clips for adequate tangential beam planning in breast conserving surgery and irradiation. *Int J Radiat Oncol Biol Phys* 1999; **43**: 347-50.
53. Warfield SK, Zou KH, Wells WM. Simultaneous truth and performance level estimation (STAPLE): an algorithm for the validation of image segmentation. *IEEE Trans Med Imaging* 2004; **23**: 903-21. doi: 10.1109/TMI.2004.828354
54. Major T, Gutierrez C, Guix B, Eموke Moza, Hannoun-Levi JM, Lössl K, et al. Interobserver variations of target volume delineation in multicatheter partial breast radiotherapy after open cavity surgery. *Brachytherapy* 2015; **14**: 925-32. doi: 10.1016/j.brachy.2015.06.008

The influence of the distal resection margin length on local recurrence and long-term survival in patients with rectal cancer after chemoradiotherapy and sphincter-preserving rectal resection

Jan Grosek¹, Vaneja Velenik², Ibrahim Edhemovic³, Mirko Omejc^{1,4}

¹ Department of Abdominal Surgery, University Medical Centre Ljubljana, Ljubljana, Slovenia

² Department of Radiotherapy, Institute of Oncology Ljubljana, Ljubljana, Slovenia

³ Department of Surgery, Institute of Oncology Ljubljana, Ljubljana, Slovenia

⁴ Faculty of Medicine, University of Ljubljana, Ljubljana, Slovenia

Radiol Oncol 2017; 51(2): 169-177.

Received 20 February 2016

Accepted 10 April 2016

Correspondence to: Prof. Mirko Omejc, M.D., Ph.D., Department of Abdominal Surgery, University Medical Centre Ljubljana, Zaloška cesta 7, SI-1000 Ljubljana, Slovenia. E mail: mirko.omejc@kclj.si

Disclosure: No potential conflicts of interest were disclosed.

Background. Low recurrence rates and long term survival are the main therapeutic goals of rectal cancer surgery. Complete, margin-negative resection confers the greatest chance for a cure. The aim of our study was to determine whether the length of the distal resection margin was associated with local recurrence rate and long-term survival.

Patients and methods. One hundred and nine patients, who underwent sphincter-preserving resection for locally advanced rectal cancer after preoperative chemoradiotherapy between 2006 and 2010 in two tertiary referral centres were included in the study. Distal resection margin lengths were measured on formalin-fixed, pinned specimens. Characteristics of patients with distal resection margin < 8 mm (Group I, n = 27), 8–20 mm (Group II, n = 31) and > 20 mm (Group III, n = 51) were retrospectively analysed and compared. Median (range) follow-up time in Group I was 89 (51–111), in Group II 83 (57–111) and in Group III 80 (45–116) months (p = 0.326), respectively.

Results. Univariate survival analysis showed that distal resection margin length was not statistically significantly associated with overall survival or local recurrence rate (p > 0.05). In a multiple Cox regression analysis, after adjusting for pathologic T and N stage (yT, yN), distal resection margin length was still not statistically significantly associated with overall survival.

Conclusions. Our study shows that close distal resection margins can be accepted as oncologically safe for sphincter-preserving rectal resections after preoperative chemoradiotherapy.

Key words: rectal cancer; distal resection margin; chemoradiotherapy; local recurrence; survival

Introduction

Rectal carcinoma is one of the commonest forms of cancer in both men and women in the Western world and the second most common cause of death. Even when disease is still localised and surgical resection is considered curative, survival is approxi-

mately 60% at 5 years and approximately 50% at 10 years.¹ Although disseminated disease is the most common cause of death, local recurrence causes severe disabling symptoms, is difficult to treat and is often fatal.^{2,3} Local control (*i.e.* low recurrence rates) and long term survival are the main therapeutic goals of rectal cancer surgery. Secondary

therapeutic goals are anal sphincter preservation and preservation of voiding and sexual functions, thus improving the quality of life. Complete, margin-negative resection confers the greatest chance for a cure.⁴ Hence, all the resection margins (proximal, distal, and circumferential) must have no microscopic cancer cell residua. Negative distal resection margin (DRM) is defined as a distance from the distal border of the gross tumour (or scar tissue in patients showing clinically complete response after chemoradiation) and the edge of the distal resection margin, in which no cancer cells are found with microscopic examination.

Historically, the standard guidelines recommended DRM of at least 4–5 cm, which meant that sphincter-preserving rectal resection for low lying rectal cancers was practically non-existent. In 1982, Heald published his monumental work in which he recommended the removal of the entire mesorectum with sharp dissection under direct vision, a technique that became known as total mesorectal excision (TME). This ingenious technique, when done properly (*i.e.* along the embryologic avascular areolar plane, between the mesorectal fascia propria and the fascia of the pelvic sidewall), is advantageous because in addition to including removal of the mesorectum containing the rectal draining lymph nodes, it also facilitates autonomic nerve preservation. TME optimises the oncological outcome by reducing the local recurrence rate and also preserves the quality of life.⁵

Thus, the previously applicable 5 cm rule was gradually modified to 2 cm and later with advances in surgical techniques to 1 cm rule or even less.^{6,7} Preoperative long course chemoradiotherapy (CRT) using 5-fluorouracil (5-FU) regimen has since emerged as the standard of care for patients with locally advanced lower and middle rectal cancer (LARC).^{8,9} To date, the refinements in management have led to a decrease in local recurrence rates from 25–40% to less than 6%. Seventy-five percent of local recurrences are detected within two years of diagnosing the primary tumour. Around 20% to 50% of patients with local recurrences have isolated recurrent disease without distant metastases.^{10,11}

Several reports have shown that in approximately one fourth of cases (6.5–58%) there is a substantial, microscopical distal intramural spread of tumour cells (DIS). Whenever DIS is present, it is limited to within 2 cm in 95% of all patients. Rarely does it extend for more than 2 cm in nonirradiated tumours. When it does, it is associated with advanced disease and poor long-term prognosis even when all resection margins are free of disease.^{12,13}

Similarly, not often does DIS extend more than 1 cm from the distal edge of the gross tumour in rectal cancer patients treated with preoperative CRT. When it does, the clinical course of such patients is usually worse, because they rapidly develop distant metastases or/ and locally recurrent disease, regardless of DRM length.¹⁴ This finding suggests that tumour biology as opposed to resection margin determines the ultimate outcome.¹⁵

A positive or close circumferential resection margin is strongly associated with local and metastatic recurrence despite CRT and TME.^{16,17} By contrast, the association of close DRM and its influence on recurrence and long term survival is less clear, with somewhat conflicting reports.¹⁸ Many centres around the world, including our own two Tertiary Referral Centres (University Medical Centre Ljubljana, Institute of Oncology Ljubljana) have accepted close (1 cm or even less) DRMs as oncologically safe in an effort to maximize the eligibility of patients for sphincter-preserving rectal resection.

The aim of our study was to find out whether the length of the distal resection margin (DRM) has any influence on local recurrence rate and long-term survival among patients with locally advanced rectal cancer treated with preoperative chemoradiotherapy and sphincter-preserving rectal resection.

Patients and methods

Patients

Between January 2006 and December 2010, 109 patients who had undergone preoperative CRT and sphincter-preserving rectal resection at two Slovene Tertiary Referral centres (University Medical Centre Ljubljana and Institute of Oncology Ljubljana) were included in our study. We included patients with histologically confirmed rectal adenocarcinoma, confined to the lower and middle third of the rectum without distant disease (M0). Patients had to have had a stage II or stage III disease, confirmed with magnetic resonance imaging (MRI) of the pelvis. Patients enrolled in the study were not supposed to have previously received radiotherapy, chemotherapy or any targeted therapy for rectal cancer. We excluded patients who had other co-existing malignancies or a malignancy within the last 5 years prior to the enrolment other than non-melanoma skin cancer or *in situ* carcinoma of the cervix, as well as patients with non-radical operation (either R1 microscopic residua in

any of the resection margins or R2 macroscopically seen, gross tumour residua).

Pre-treatment work-up consisted of a complete history, physical examination, complete blood count and serum biochemistry, carcinoembryonic antigen (CEA), chest radiography and ultrasonography or computed tomography (CT) scan of the entire abdomen. MRI was done for primary tumour and nodal staging. After discharge, follow-up visits were scheduled every 3 months for the first 2 years, every 6 months during the 2–5. year, and yearly thereafter. Physical examination, CEA determination, colonoscopy, chest radiography and ultrasonography or/ and CT scan of the whole abdomen were performed. Recurrences were confirmed pathologically and/ or by sequential imaging with positron emission tomography or MRI.¹⁹

Patient data and histological tumour characteristics were prospectively collected. The study itself was retrospective and was approved by the National Ethics Committee (#61/09/14).

Surgery

Surgery was performed 6–8 weeks after completion of preoperative CRT. All operations were performed by qualified, experienced colorectal surgeons who performed total mesorectal excision with autonomic nerve preservation as the standard procedure. The option for a temporary ileostomy or colostomy was left to the surgeon's discretion. The anastomoses were performed using circular stapling devices.

Chemoradiotherapy

Patients received preoperative capecitabine-based CRT. They received a total irradiation dose (TD) of 45 Gy to the pelvis plus 5.4 Gy as a boost to the primary tumour in 1.8 Gy daily fractions over 5.5 weeks. Radiotherapy (RT) was delivered using 15 MV photon beams and four-field box technique, once daily, 5 days per week. All fields were treated daily. Patients were irradiated in a prone position with a full bladder and using a belly board to minimise the exposure of the small bowel.

Chemotherapy was administered concomitantly with RT, started on the first day of RT and finished on the last day of RT. Chemotherapy was continuous throughout the RT period and it consisted of oral capecitabine at a daily dose of 1650 mg/m², divided into two equal doses given 12 hours apart. One dose was taken 1 hour prior to RT. All patients received adjuvant chemotherapy with capecitabine

1250 mg/m² orally twice daily on days 1–14 every 3 weeks; 4 cycles were recommended, beginning 6–8 weeks after surgery.

Pathology

Distal bowel margins were measured in formalin-fixed, pinned specimens. The distal resection margin length was defined as the closest distance between the distal border of the gross tumour (or scar tissue in patients showing clinically complete response after chemoradiation) and the edge of the distal resection. The cutting edges of doughnuts were not included in these measurements, but were also assessed microscopically.

Statistical analysis

Differences in categorical variables between study groups were analysed using Chi-square test or likelihood ratio test as appropriate. Differences in numeric variables between groups were investigated using Kruskal-Wallis test. Cox's proportional hazards model was used to test the association between each of the risk factors and local recurrence or overall survival. For overall survival, both univariate and multiple Cox regression models were used, but because of the low number of events, the multiple analysis was restricted to include two possible confounders. Proportional hazard assumption was tested graphically by a log-log plot. Time intervals were calculated from the date of the surgery. The p-values < 0.05 were considered statistically significant. Statistical analysis was performed using the SPSS software program (Version 23.0).

Results

The study included 109 rectal cancer patients. There were 75 male and 34 female patients with an average age of 63 years (range, 34–83). Average length of hospitalization was 9 days (range, 3–52). Altogether, we registered 8 major complications that required surgical re-intervention. There was no postoperative 30 day mortality. Characteristics of patients with distal resection margin (DRM) < 8 mm (Group I, n = 27), 8–20 mm (Group II, n = 31) and > 20 (Group III, n = 51) mm are shown in Table 1. Groups were comparable regarding all characteristics, except for the stage of the illness. Group III consisted of a higher share (29.4%) of patients with N stage of 2 compared with Group II

TABLE 1. Clinicopathological features of patients according to distal resection margin (DRM)

	Group I (n = 27)	Group II (n = 31)	Group III (n = 51)	All (n = 109)	p
Male gender	21 (77.8)	21 (67.7)	33 (64.7)	75 (68.8)	0.490
Age (years)	60 (44–83)	64 (37–76)	66 (34–82)	63 (34–83)	0.453
Length of hospitalisation (days)	10 (7–52)	9 (5–31)	9 (3–36)	9 (3–52)	0.189
Median distance from anal verge to tumor (cm)	5	6	8	8	0.002
DRM (mm) ^a	5 (1–8)	15 (9–20)	40 (25–80)	20 (1–80)	< 0.001
CRM (mm) ^b	10 (1–25)	10 (4–30)	10 (2–40)	10 (1–40)	0.284
Ileostomy / Transversostomy	22 (81.5)	21 (67.7)	35 (68.6)	78 (71.6)	0.509
Surgical complications	2 (7.4)	5 (16.1)	1 (2)	8 (7.3)	0.058
T					0.103
1	0 (0)	0 (0)	1 (2)	1 (0.9)	
2	1 (3.7)	4 (12.9)	1 (2)	6 (5.5)	
3	26 (96.3)	26 (83.9)	42 (82.4)	94 (86.2)	
4	0 (0)	1 (3.2)	5 (9.8)	6 (5.5)	
Missing data	0 (0)	0 (0)	2 (3.9)	2 (1.8)	
N					0.047
0	14 (51.9)	12 (38.7)	9 (17.6)	35 (32.1)	
1	8 (29.6)	15 (48.4)	24 (47.1)	47 (43.1)	
2	4 (14.8)	4 (12.9)	15 (29.4)	22 (20.2)	
Missing data	1 (3.7)	0 (0)	3 (5.9)	4 (3.7)	
yT ^c					0.039
0	3 (11.1)	4 (12.9)	3 (5.9)	10 (9.2)	
1	5 (18.5)	7 (22.6)	2 (3.9)	14 (12.8)	
2	7 (25.9)	10 (32.3)	13 (25.5)	30 (27.5)	
3	12 (44.4)	9 (29)	33 (64.7)	54 (49.5)	
4	0 (0)	1 (3.2)	0 (0)	1 (0.9)	
yN ^c					0.004
0	22 (81.5)	27 (87.1)	26 (51)	75 (68.8)	
1	3 (11.1)	3 (9.7)	17 (33.3)	23 (21.1)	
2	2 (7.4)	1 (3.2)	8 (15.7)	11 (10.1)	
Regression level					0.003
1	0 (0)	4 (20)	14 (35.9)	18 (23.7)	
2	8 (47.1)	5 (25)	18 (46.2)	31 (40.8)	
3	6 (35.3)	6 (30)	4 (10.3)	16 (21.1)	
4	3 (17.6)	5 (25)	3 (7.7)	11 (14.5)	
Vascular invasion	1 (8.3)	4 (21.1)	4 (10.3)	9 (12.9)	0.477
Perineural invasion	0 (0)	1 (5.6)	4 (10)	5 (7.2)	0.342
Positive lymph nodes	5 (18.5)	4 (12.9)	25 (49)	34 (31.2)	0.001

^a DRM = distal resection margin; Group I, DRM < 8mm; Group II, 8 ≤ DRM ≤ 20 mm; Group III, DRM > 20 mm

^b CRM = circumferential resection margin.

^c yT, yN = stage as assessed by pathologic examination of the surgical specimen (after CRT and resection)

Values are shown as median (range) for ordinal and numeric variables and as frequency (percentage) for nominal variable

TABLE 2. Risk factors for time to local recurrence or death using univariate Cox regression analysis

Variable (reference group)	Local recurrence-free survival		Overall survival	
	Hazard Ratio (95 % CI)	P-value	Hazard Ratio (95 % CI)	P-value
Female gender (male)	2.3 (0.3; 16.2)	0.411	0.6 (0.2; 1.6)	0.279
Age (years)	1.1 (0.9; 1.2)	0.395	1 (1; 1.1)	0.125
Length of hospitalisation (days)	1.0 (0.8; 1.2)	0.762	1 (1; 1.1)	0.812
DRM (mm) ^a	1 (1; 1.1)	0.218	1 (1; 1)	0.838
DRM Group III (Group I + Group II) ^a	3.5 (0.4; 33.8)	0.276	1.4 (0.6; 3.3)	0.402
DRM ^a				0.667
DRM Group II (Group I) ^a	-	-	1.3 (0.4; 4.5)	0.714
DRM Group III (Group I)	-	-	1.6 (0.5; 5.1)	0.392
CRM (mm) ^b	1 (0.9; 1.2)	0.524	1 (0.9; 1)	0.343
N 2 - 3 (0 - 1)	3.6 (0.5; 25.6)	0.199	1.7 (0.6; 4.4)	0.293
yT 0 - 1 (2 - 4) ^c	3.1 (0.3; 29.4)	0.333	1.2 (0.4; 3.7)	0.699
yT ^c	-	-		0.017
1 (0)	-	-	0.2 (0; 1.8)	0.15
2 (0)	-	-	0.4 (0.1; 1.7)	0.215
3 (0)	-	-	0.7 (0.2; 2.3)	0.517
4 (0)	-	-	19.5 (1.6; 234.6)	0.019
yN 0 (1-2) ^c	7 (0.7; 67.2)	0.092	2.4 (1.1; 5.6)	0.040
yN ^c	-	-		0.020
1 (0)	-	-	1.6 (0.6; 4.6)	0.382
2 (0)	-	-	4.1 (1.5; 11.2)	0.005
Vascular invasion	2.4 (0.3; 23.4)	0.441	0.9 (0.2; 4)	0.892
Perineural invasion	6.5 (0.7; 62.8)	0.105	0.9 (0.1; 6.9)	0.920

DRM = distal resection margin; Group I, DRM < 8 mm; Group II, 8 ≤ DRM ≤ 20 mm; Group III, DRM > 20 mm

^b CRM = circumferential resection margin.

^c yT, yN = stage as assessed by pathologic examination of the surgical specimen (after CRT and resection)

Values are shown as median (range) for ordinal and numeric variables and as frequency (percentage) for nominal variables

(12.9%) and Group I (14.8%) ($p = 0.020$). After the surgery, a higher share of patients in Group III had a more advanced stage of tumours (yT, $p = 0.039$; yN, $p = 0.004$) and a lower share had regression levels of 3 and 4 ($p = 0.003$).

Median (range) follow-up time in Group I was 89 (51–111), in Group II 83 (57–111) and in Group III 80 (45–116) months ($p = 0.326$), respectively. There were 4 (14.8%) deaths due to rectal cancer in Group I, 6 (19.4%) in Group II and 12 (23.5%) in Group III. There were no local recurrences in Group I, 1 in Group II and 3 in Group III. Univariate survival analysis showed DRM length was not statistically

significantly associated with overall survival or local recurrence rate ($p > 0.05$; Table 2, Figure 1).

Overall survival was statistically significantly associated with tumour stage after surgery (yT, $p = 0.017$; yN, $p = 0.02$). Patients with pathologic T stage 4 (yT4) after the surgery had 19.5 (95% CI, 1.6–234.6) times higher risk of death than patients with pathologic T stage 1 (yT1). Patients with pathologic N stage 2 after the surgery (yN2) had 4.1 (95% CI, 1.5–5.6) times higher risk of death than patients with N stage 0 (yN0). None of the other risk factors was statistically significantly associated with overall survival. No association between

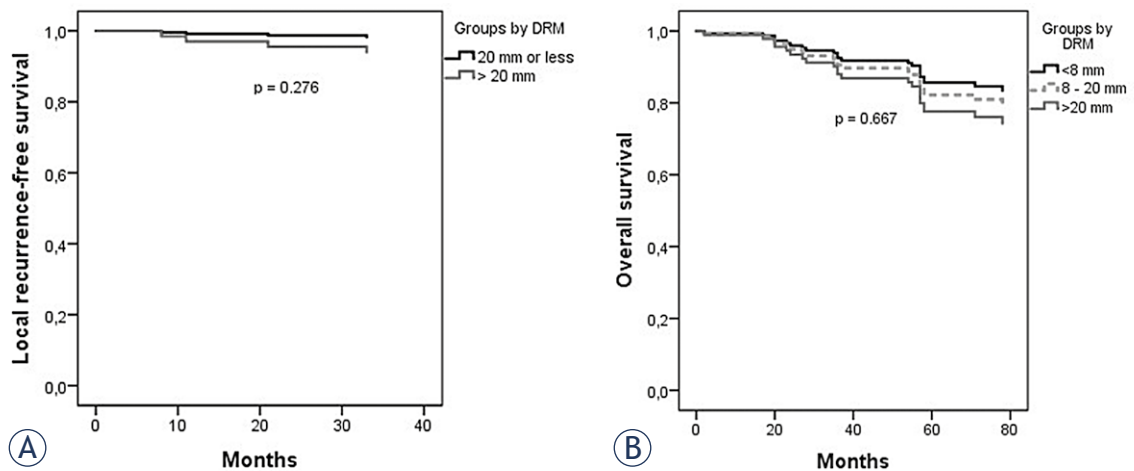


FIGURE 1. Univariate analysis of survival rate: (A) local recurrence-free survival, (B) overall survival rate.

examined risk factors and recurrence-free survival could be found (Table 2, Figure 1).

After adjusting for pathologic stage T and N after surgery (yT, yN), DRM length was still not statistically significantly associated with overall survival. Factors deemed statistically significant in univariate model were also statistically significantly associated with overall survival in multiple survival regression model (Table 3; Figure 2).

Discussion

The management of locally advanced rectal cancer (T3, T4, and/or N+) is multimodal and is based on preoperative CRT followed by surgery with TME. The latter can be done either as sphincter-preserv-

ing low rectal resection or abdominoperineal excision (APE). Preoperative CRT results in downsizing and down-staging of rectal cancer, which often facilitates or even makes possible radical, *i.e.* R0 resection and thus improves local control. Moreover, the tumour regression can be substantial, in 15-27% of cases even complete (pathologic complete response) and in such cases sphincter-preserving resections can be done even in cases where primarily APE would be indicated.^{20,21} However, often, regardless of tumour regression and with or without intersphincteric resection a close DRM must be accepted, in order to preserve the anal sphincter.²²

The present study shows that in patients with rectal cancer after CRT and sphincter-preserving rectal resection, the length of DRM has no statistically significant influence on local recurrence and long-term survival, as long as all the resection margins (proximal, distal, circumferential) have no microscopic cancer cell residua.

Patients in our study were divided into three groups based on the length of the distal resection margins (DRM < 8, 8–20 and > 20 mm, respectively). The cut of values for the subgroups were set theoretically, based on previously published reports.²³⁻²⁸ We observed 4 (14.8%) deaths due to rectal cancer in Group I, 6 (19.4%) in Group II and 12 (23.5%) in Group III. There were no local recurrences in Group I, one in Group II and three in Group III. Univariate survival analysis showed DRM length was not statistically significantly associated with overall survival or local recurrence rate ($p > 0.05$; Table 2, Figure 1,2). After adjusting for pathologic stages T and N after surgery (yT, yN), the DRM length was still not statistically significantly associated with overall survival (Table 3;

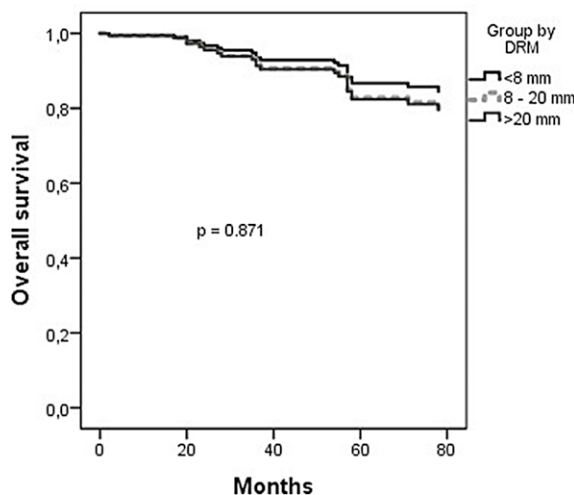


FIGURE 2. Multiple analysis of overall survival rate in the three patient groups.

Figure 3). However, the multiple Cox regression analysis could not be done to the second endpoint of the study (*i.e.* local recurrence free survival), because there were too few local recurrences.

Our results are supported with several recent reports in the literature. Hong *et al.* enrolled 218 rectal cancer patients in their study. Patients were classified into three groups according to the length of the DRM (< 1 cm, 1–2 cm, > 2 cm). There were no statistically significant differences in survival or local recurrence rate among the groups. A limitation of this study was that histopathologic examination was not conducted properly on the circumferential resection margins in more than half of the enrolled patients. Not all the patients received preoperative CRT and some received postoperative chemoradiotherapy.²⁹ This is in contrast to our study, which was a very homogeneous one, as all the enrolled patients uniformly received the same 5-FU based CRT regime. All the specimens were histopathologically tested for all the resection margins, including the circumferential resection margin; if any of the margins were positive, patients were excluded from the study (R1 resection). One of the most comprehensive systematic reviews of the literature was published by Bujko *et al.*²³ In this review authors identified 17 studies showing results in relation to margins < 1 cm versus > 1 cm, five studies in relation to a margin \leq 5 mm versus \geq 5 mm and five studies showing results in a margin of \leq 2 mm. Their meta-analysis showed, that in a selected group of patients, DRM < 1 cm does not jeopardize oncological safety and, furthermore, that even margins shorter than 5 mm may be acceptable. However, Bujko *et al.* emphasized, that patient and tumor selection is very important for such an approach. Nevertheless, they could give no precise rules nor specific criteria for such a selection. Apart from this systematic review, there are several other similar reports in literature, either meta-analysis or reports showing results from individual institutions.^{24–28} These reports are more or less heterogeneous with patients being treated with surgery alone or in combination with pre- or postoperative CRT and in these studies there are very different numbers of enrolled patients with different median times of follow-up. In these studies the DRM is analysed either as a continuous variable or as a variable defining cut-off points of different DRM lengths. However, putting the heterogeneity and biases of these reports aside, they generally show no statistically significant differences among different lengths of the DRM on local recurrence rate or on long term survival.

TABLE 3. Risk factors for time to death using multiple Cox regression analysis

Variable (reference group)	Overall survival	
	Hazard Ratio (95% CI)	P-value
yT ^a		0.014
1 (0)	0.2 (0; 2.3)	0.212
2 (0)	0.3 (0.1; 1.5)	0.158
3 (0)	0.5 (0.1; 1.9)	0.309
4 (0)	23.1 (1.8; 302.3)	0.017
yN ^a		0.034
1 (0)	1.5 (0.4; 5.4)	0.489
2 (0)	4.2 (1.4; 12.6)	0.011
DRM ^b		0.871
DRM Group II (Group I)	1.3 (0.3; 5.1)	0.690
DRM Group III (Group I)	1.4 (0.4; 4.4)	0.609

^ayT, yN = stage as assessed by pathologic examination of the surgical specimen (after CRT and resection)

^bDRM = distal resection margin; Group I, DRM < 8mm; Group II, 8 \leq DRM \leq 20 mm; Group III, DRM > 20 mm

Values are shown as median (range) for ordinal and numeric variables and as frequency (percentage) for nominal variables

By contrast, Vernava *et al.* reported that DRM \leq 8 mm statistically significantly worsens both local control and long term survival.³⁰ The interpretation of this study was, however, complicated by the fact, that the patients between 1977 and 1985 were treated before the adoption of the TME.³¹ We believe that strict adherence to TME principles is critical and this is why we believe our group of patients with DRM < 8 mm did not have statistically significantly worse local recurrence rate or overall survival. None of the 27 patients in group I have had recurrent disease to date (median follow-up 89 months), although there were also minimally negative DRMs in this group of patients (median DRM length 5 mm; 1–8 mm). Moreover, univariate analysis of overall survival rate and local recurrence-free survival as well as a multivariate analysis of overall survival rate in the three patient groups, adjusted for yT and yN stage, showed a slight but still statistically nonsignificant tendency, that patients from group I (DRM < 8 mm) (Figure 1,2) may have had even lower recurrence rates and better long-term survival. Possible explanation for this is that the operating surgeon, due to his experience in rectal cancer, performed APE rather than sphincter-preserving surgery in selected cases with bulky, fixed or otherwise more unfavourable tumours, because he believed that this was the only way to achieve margin negative resection. This hypothesis is supported with our results (Table 1) which show that

the three groups of DRM lengths (DRM < 8 mm; Group II, $8 \leq \text{DRM} \leq 20$ mm; Group III, DRM > 20 mm) are comparable in all characteristics, except for the stage of the illness. Group of patients with DRM > 20 mm had a higher share of patients with more advanced tumours (yT, $p = 0,039$; yN, $p = 0,003$) and a lower share of patients with regression levels of 3 and 4 ($p = 0,003$). This can represent a bias in our study, but one that cannot be avoided when the best interest of patients is in question.

Another possible limitation of our study is that the lengths of DRMs were measured on fixed pinned specimens, whereas the 1 cm rule refers to margins measured by surgeons under fresh anatomically restored *ex vivo* conditions.³² There is no consensus on whether the margins should be measured in fresh or formalin-fixed specimens. Prospective measurements of DRMs with 5 different methods showed that margins were significantly smaller in unpinned than pinned specimens. Although no significant differences were observed in pinned specimens before or after fixation, there was a significant shrinkage after fixation in unpinned specimens.³³ To avoid this and for consistency, we measured all of the DRM lengths in pinned and then fixed specimens.

Finally, although it is a well-established fact, that sphincter-preserving rectal resection improves quality of life, such improvement of functional results must be objectively measured, preferably through reliable, validated and sensitive instruments (*i. e.* questionnaires).³⁴ Such quality of life assessment was not systematically done for our patients, hence this important end-point of rectal surgery could not be properly investigated in our study.

In summary, our study shows that in patients with rectal cancer after CRT and sphincter-preserving rectal resection, the length of the distal resection margin has no statistically significant influence on local recurrence and long-term survival, as long as all the resection margins (proximal, distal, circumferential) have no microscopic cancer cell residua. Based on our results, taken in context with current reports in literature, we believe it is reasonable to accept short (1 cm or even less) lengths of DRM in order to perform sphincter-preserving rectal resections after CRT, as long as the TME principles are strictly followed.

Acknowledgements

We wish to thank Ms. Vanja Erculj, statistician who performed all necessary statistical calculations.

References

- van Gijn W, Marinjnen CA, Nagtegaal ID, Kranenbarg EM, Putter H, Wiggers T, et al. Preoperative radiotherapy combined with total mesorectal excision for resectable rectal cancer: 12- year follow- up of the multicentre, randomised controlled TME trial. *Lancet Oncol* 2011; **12**: 575-82.
- Arredondo A, Baixauli J, Beorlegui C, Arbea L, Rodriguez J, Solla JJ, et al. Prognosis factors for recurrence in patients with locally advanced rectal cancer preoperatively treated with chemoradiotherapy and adjuvant chemotherapy. *Dis Colon Rectum* 2013; **56**: 416-21.
- Trakarnsanga A, Ithimakin S, Weiser MR. Treatment of locally advanced rectal cancer: Controversies and questions. *World J Gastroenterol* 2012; **18**: 5521-32.
- Zorcolo L, Rosman S, Restivo A, Pisano M, Nigri GR, Fancellu A, Melis MI. Complete pathologic response after combined modality treatment for rectal cancer and long term survival: A meta- analysis. *Ann Surg Oncol* 2012; **19**: 2822-32.
- Heald RJ, Husband EM, Ryall RD. The mesorectum in rectal cancer surgery: The clue to pelvic recurrence? *Br J Surg* 1982; **69**: 613-6.
- Williams NS, Dixon MF, Johnston D. Reappraisal of the 5 centimetre rule of distal excision for carcinoma of the rectum: a study of distal intramural spread and of patients survival. *Br J Surg* 1983; **70**: 150-4.
- Moore HG, Riedel E, Minsk BD, Saltz L, Paty P, Wong D, et al. Adequacy of 1 cm distal margin after restorative rectal cancer resection with sharp mesorectal excision and preoperative combined- modality therapy. *Ann Surg Oncol* 2003; **10**: 80-5.
- Velenik V, Oblak I, Anderluh F. Long term results from a randomized phase II trial of neoadjuvant combined- modality therapy for locally advanced rectal cancer. *Radiat Oncol* 2010; **5**: 88-95.
- Velenik V, Ocvirk J, Music M, Bracko M, Anderluh F, Oblak I, et al. Neoadjuvant capecitabine, radiotherapy and bevacizumab (CRAB) in locally advanced rectal cancer: results of an open- label phase II study. *Radiat Oncol* 2011; **6**: 105-12.
- Lim KY, Law WL, Liu R, Poon JT, Fan JF, Lo OS. Impact of neoadjuvant treatment on total mesorectal excision for ultra- low rectal cancers. *World J Surg* 2010; **8**: 23-9.
- Velenik V. Locally recurrent rectal disease: treatment options. *Radiol Oncol* 2009; **43**: 144-51.
- Williams NS, Dixon MF, Johnston D. Reappraisal of the 5 cm rule of distal excision for carcinoma of the rectum: a study of distal intramural spread and of patients' survival. *Br J Surg* 1983; **70**: 150-4.
- Nakagoe T, Yamaguchi E, Tanaka K, Sawai T, Tsuji T, Shibasaki S, et al. Distal intramural spread is an independent prognostic factor for distant metastasis and poor outcome in patients with rectal cancer: A multivariate analysis. *Ann Surg Oncol* 2003; **10**: 163-70.
- Mezhir JJ, Smith KD, Fichera A, Hart J, Posner MC, Hurst RD. Presence of distal intramural spread after preoperative combined- modality therapy for adenocarcinoma of the rectum: What is now the appropriate distal resection margin? *Surgery* 2005; **138**: 658-64.
- Park IJ, Kim JC. Adequate length of the distal resection margin in rectal cancer: From the oncological point of view. *J Gastrointest Surg* 2010; **14**: 1331-7.
- Wibe B, Rendedal PR, Svensson E, Norstein J, Eide TJ, Myrvold HE, et al. Prognostic significance of the circumferential resection margin following total mesorectal excision for rectal cancer. *Br J Surg* 2002; **89**: 327-34.
- Trakarnsanga A, Gonen M, Shia J, Goodman KA, Nash GM, Temple LK, et al. What is the significance of the circumferential margin in locally advanced rectal cancer after neoadjuvant chemoradiotherapy? *Ann Surg Oncol* 2013; **20**: 1179-84.
- Nash GM, Weiss A, Dasgupta R, Gonen M, Guillem JG, Wong WS. Close distal margin and rectal cancer recurrence after sphincter- preserving rectal resection. *Dis Colon Rectum* 2010; **53**: 1365-73.
- Velenik V. Post- treatment surveillance in colorectal cancer. *Radiol Oncol* 2010; **44**: 135-41.
- Maas M, Nelemans PJ, Valentini V, Das P, Roedel C, Kuo LJ, et al. Long- term outcome in patients with a pathological complete response after chemoradiation with a pathological complete response after chemoradiation for rectal cancer: a pooled analysis of individual patient data. *Lancet Oncol* 2010; **11**: 835-44.

21. Kim NK, Kim MS, Al-Asari SF. Update and debate issues in surgical treatment of middle and low rectal cancer. *J Korean Soc Coloproctol* 2012; **28**: 230-40.
22. Ludwig K, Kosinski L. How low is low? Evolving approaches to sphincter-sparing resection techniques. *Semin Radiat Oncol* 2011; **21**: 185-95.
23. Bujko J, Rutkowski A, Chang GJ, Michalski W, Chmielik E, Kusnierz J. Is the 1-cm rule of distal bowel resection margin in rectal cancer based on clinical evidence? A systematic review. *Indian J Surg Oncol* 2012; **3**: 139-46.
24. Kuvshinoff B, Magfoor I, Miedema B, Bryer M, Westgate S, Wilkes J, et al. Distal margin requirements after preoperative chemoradiotherapy for distal rectal carcinomas: are < or = 1 cm distal margins sufficient? *Ann Surg Oncol* 2001; **8**: 163-9.
25. Fitzgerald TL, Brinkley J, Zervos EE. Pushing the envelope beyond a centimeter in rectal cancer: Oncological implications of close, but negative margins. *J Am Coll Surg* 2011; **213**: 589-95.
26. Rutkowski A, Nowacki MP, Chwalinski M, Oledzki J, Liszka-D P, Gornicki A, et al. Acceptance of a 5-mm distal bowel resection margin for rectal cancer: is it safe? *Colorectal Dis* 2011; **14**: 71-8.
27. Komori K, Kanemitsu, Y, Ishiguro S, Shimizu Y, Sano T, Ito S, et al. Adequate length of the surgical distal resection margin in rectal cancer: from the viewpoint of pathological findings. *Am J Surg* 2012; **204**: 474-80.
28. Pahlman L, Bujko K, Rutkowski, Michalski W. Altering the therapeutic paradigm towards a distal bowel margin of < 1 cm in patients with low-lying rectal cancer: a systematic review and commentary. *Colorectal Dis* 2013; **15**: 166-74.
29. Hong KS, Monn N, Chung SS, Lee R, Kim KH. Oncological outcomes in rectal cancer with close distal resection margins: a retrospective analysis. *Ann Surg Treat Res* 2015; **89**: 23-9.
30. Vernava AM, Moran M, Rothenberger DA, Wong WD. A prospective evaluation of distal margins in carcinoma of the rectum. *Surg Gynecol Obstet* 1992; **175**: 333-6.
31. Kwak JY, Kim CW, Lim SB, Yu CS, Kim TW, Kim JH, et al. Oncologically safe distal resection margins in rectal cancer patients treated with chemoradiotherapy. *J Gastrointest Surg* 2012; **16**: 1947-54.
32. Nelson H, Pettreli N, Carlin A, Couture J, Fleshman J, Guillem J, et al. Guidelines 2000 for colon and rectal surgery. *J Natl Cancer Inst* 2001; **93**: 583-96.
33. Sondena K, Kjellevoid KH. A prospective study of the length of the distal margin after low anterior resection for rectal cancer. *Int J Colorectal Dis* 1990; **5**: 103-5.
34. Fazio VW, Zutshi M, Remzi FH, Parc Y, Ruppert R, Furst A, et al. A randomized multicenter trial to compare long-term functional outcome, quality of life, and complications of surgical procedures for low rectal cancers. *Ann Surg* 2007; **246**: 481-90.

Clinical outcomes of 130 patients with primary and secondary lung tumors treated with Cyberknife robotic stereotactic body radiotherapy

Zsolt Levente Janvary¹, Nicolas Jansen², Veronique Baart², Magali Devillers², David Dechambre², Eric Lenaerts², Laurence Seidel³, Nicole Barthelemy², Patrick Berkovic², Akos Gulyban², Ferenc Lakosi², Zsolt Horvath¹, Philippe A. Coucke²

¹ Division of Radiotherapy, Department of Clinical Oncology, Faculty of Medicine, University of Debrecen, Debrecen, Hungary

² Department of Radiation Oncology, Liege University Hospital, Liege, Belgium

³ Department of Biostatistics, Liege University Hospital, Liege, Belgium

Radiol Oncol 2017; 51(2): 178-186.

Received 15 December 2016

Accepted 27 February 2017

Correspondence to: Zsolt Levente Janvary, M.D., Division of Radiotherapy, Department of Clinical Oncology, Faculty of Medicine, University of Debrecen, Nagyerdei krt. 98, 4032 Debrecen, Hungary. Phone: +36 20 506 20 52; Fax: +36 52 255 585; E-mail: janvary.levente@med.unideb.hu, janvarylevente@yahoo.com

Disclosure: No potential conflicts of interest were disclosed.

Background. Authors report clinical outcomes of patients treated with robotic stereotactic body radiotherapy (SBRT) for primary, recurrent and metastatic lung lesions.

Patients and methods. 130 patients with 160 lesions were treated with Cyberknife SBRT, including T1-3 primary lung cancers (54%), recurrent tumors (22%) and pulmonary metastases (24%). The mean biologically equivalent dose (BED_{10Gy}) was 151 Gy (72–180 Gy). Median prescribed dose for peripheral and central lesions was 3x20 Gy and 3x15 Gy, respectively. Local control (LC), overall survival (OS), and cause-specific survival (CSS) rates, early and late toxicities are reported. Statistical analysis was performed to identify factors influencing local tumor control.

Results. Median follow-up time was 21 months. In univariate analysis, higher dose was associated with better LC and a cut-off value was detected at BED_{10Gy} ≤ 112.5 Gy, resulting in 1-, 2-, and 3-year actuarial LC rates of 93%, vs 73%, 80% vs 61%, and 63% vs 54%, for the high and low dose groups, respectively (p = 0.0061, HR = 0.384). In multivariate analysis, metastatic origin, histological confirmation and larger Planning Target Volume (PTV) were associated with higher risk of local failure. Actuarial OS and CSS rates at 1, 2, and 3 years were 85%, 74% and 62%, and 93%, 89% and 80%, respectively. Acute and late toxicities ≥ Gr 3 were observed in 3 (2%) and 6 patients (5%), respectively.

Conclusions. Our favorable LC and survival rates after robotic SBRT, with low rates of severe toxicities, are coherent with the literature data in this mixed, non-selected study population.

Key words: Cyberknife; stereotactic body radiotherapy; non-small cell lung cancer; lung metastasis

Introduction

Although surgical resection is considered as the standard of care in patients with early-stage non-small cell lung cancer (NSCLC), a significant percentage of mostly elderly patients are not eligible

for this treatment. Stereotactic body radiotherapy (SBRT) is considered to be an effective and well tolerated, non-invasive treatment option for this population.^{1,2} Efforts have already been made to directly compare the effectiveness and toxicity of SBRT to surgery for operable patients in rand-

omized trials, but unfortunately, these trials did not reach their accrual target and were prematurely closed because of low recruitment.²

However data from prospective trials show consistently high levels of local control rates with stereotactic irradiation of early stage NSCLC.³⁻⁶ Although SBRT literature is more extensive for early stage primary lung cancer, publications concerning recurrent lung tumors and lung metastases also show high local control rates.⁷⁻⁹ On the basis of the published clinical experience stereotactic radiotherapy of the lung became one of the most established indications of SBRT.¹⁰⁻¹¹ A clear dose-effect relationship has been shown by several SBRT studies, and a BED_{10Gy} ≥ 100 Gy (Biologically Effective Dose with an α/β of 10 Gy) was found to be associated with better results.¹² Nevertheless, the delivered dose and fraction number should be tailored to the anatomical situation and size of the lesion, as the proximity of critical organs can lead to higher probability of toxicity.

Although there have been attempts for single fraction treatments¹³⁻¹⁴, generally lung SBRT is delivered in 3 to 8 fractions. Treatment-related severe toxicities are uncommon using “risk-adapted” fractionation schemes with lower dose per fraction for central tumors.¹⁵

The purpose of this study is to evaluate and report the clinical outcomes of the first 130 consecutively treated patients presented with primary, recurrent primary or secondary lung tumors. The primary objective was to analyse local therapeutic efficacy of robotic SBRT and factors influencing local control. The secondary objectives were to evaluate early and late toxicities and survival results.

Patients and methods

Patients

Cyberknife® (Accuray Inc. Sunnyvale, USA) robotic SBRT treatments were started at the Liege University Hospital in April 2010. Ordinary indications for SBRT treatment include T1-T2 primary NSCLC, recurrent primary lung tumors, and solitary-, or oligometastases. However, more rarely this treatment is applied on T3 tumors or solitary lymph node metastases.¹⁶⁻¹⁹ The majority of primary and recurrent lung tumors in our cohort were considered ineligible for surgical resection because of poor lung functions or severe comorbidities. For metastatic lesions medical inoperability; > 1 lesions in different lobes or lungs; prior lobectomy and patient preference were the major causes leading

to the choice of SBRT. Based on individual medical consideration and absence of realistic therapeutic alternatives a small number of unusual indications were also included, like patients harboring T3N0 or T1N1 disease. In the present study 130 consecutive patients treated with BED_{10Gy} ≥ 72 Gy were evaluated. Central or large tumors were not excluded, but the dose and number of fractions were adapted. Central lesions were defined as lesions located within 2 cm from the pulmonary hilum, heart, great vessels, or trachea. Indications for each individual patient were discussed and approved in multi-disciplinary tumor boards. Especially for primary tumors, pathological confirmation was requested either by bronchofiberscopy or transthoracic biopsy. For patients considered not eligible for histological confirmation (due to technical or medical reasons), the indication was based on strong clinical suspicion supported by positron emission tomography (PET).

One hundred and thirty patients, with a total of 160 lung lesions were treated between April 2010 and June 2012. Patient and tumor characteristics are listed in Table 1.

TABLE 1. Patient, tumor and treatment characteristics

Characteristic	n (%)
Total number of patients/lesions	130 (100%)/160 (100%)
Mean age in years	71 (range: 40–92)
Male/female ratio	77 (59%) / 53 (41%)
No. with COPD	45 (35%)
Mean FEV1 (%)	65 (range: 24–139)
Mean FEV1 (L)	2 (range: 0.53–3.65)
Histological confirmation	79 (61%)
Primary cancer patients/lesions	81 (62%) / 86 (54%)
T1N0	53
T2N0	19
T3N0	5
T1N1	4
Recurrent tumor patients /lesions (n)	23 (18%) / 35 (22%)
Lung metastasis patients /lesions (n)	26 (20%) / 39 (24%)
Mean GTV volume (ml)	11.5 (range: 0.6–86.5)
Mean PTV volume (ml)	33.2 (range: 5.8–118.1)
Location of lesions: peripheral/central	113 (71%) /47 (29%)
Mean total dose (Gy)/Mean no. of fractions	60/3 fx (range: 40–60 / 3–5 fx)
Mean/median BED _{10Gy} (Gy)	151/180 Gy

BED = mean biologically equivalent dose; COPD = chronic obstructive pulmonary disease; FEV1 = forced expiratory volume in 1 second; fx = fractions; GTV = gross tumour volume; PTV = planning target volume

Median age of patients at treatment was 71 years (range 40–93), and 59% (n = 77) were males. Distribution of lesions were: 53% (n = 86) primary, 22% (n = 35) recurrent tumor/intrapulmonary metastasis of a lung tumor and 25% (n = 39) metastases from other cancer. Cancer of origin for metastatic lesions were: colorectal (49%; n = 19), salivary gland (13%; n = 5), breast (10%; n = 4), melanoma (5%; n = 2), kidney (5%; n = 2), neuroendocrinal (3%; n = 1), multiple primary (13%; n = 5), unknown (2%; n = 1). Distribution of histological types for the patient group with pathologically confirmed primary lung cancer was: 47% adenocarcinoma (n = 29), 33% squamous cell carcinoma (n = 21), 15% NSCLC (n = 9), 5% undifferentiated (n = 3). The maximal number of lesions treated by SBRT in the same patient was four. Four patients were presented with stage T1N1 disease. For these patients the affected lymph node(s) were also treated with SBRT. Positivity of these lymph nodes were based on high SUVmax value on PET CT, without cytological confirmation, but usually the histology of the belonging primary tumors were known.

One patient was categorized as T3 for tumor size, the other four T3 patients had mediastinal pleura invasion or separate nodule in the same lobe.

Distribution of the 113 peripheral lesions was: n = 66 primary, n = 21 recurrent, n = 26 metastasis. The group of 47 central lesions was composed of 17 primary tumors plus 3 synchronous N1 lymph nodes, 14 recurrent cancers and 13 metastases.

Treatment preparation

Technical characteristics and tracking options of the Cyberknife robotic SBRT system have been exhaustively detailed elsewhere.¹⁶⁻¹⁷ For thoracic tumors there are three different tracking types, which can be appropriately selected according to each clinical case. Synchrony[®] is a real-time tumor tracking algorithm which requires fiducial markers to be previously inserted inside or near to the target. The fiducials are detected by orthogonal X-rays at the treatment room. The system includes an infrared camera that monitors the movement of the chest. During treatment, spatial information on the location of the fiducials and data of the respiratory cycle are connected to redirect the robot, and realize real-time tracking. Fiducial insertion can be contraindicated for some patients because of the inherent risk of pneumothorax. For selected cases, when tumor silhouette is sharply identified on both orthogonal X-ray detector panels, the algorithm of

Xsight Lung[®] can be used for tracking the target, without the need for implanted markers. When none of these two previously mentioned tracking algorithm is feasible, tracking is performed on the vertebra (XsightSpine[®]).

Planning CT images were obtained with a slice thickness of 1 mm. Patients were immobilised using an individual vacuum bag "in supine position, with arms next to the body. Four-dimensional (4D) CT simulation was not introduced for Cyberknife treatment, thus expiration and moderate inspiration CT scans were acquired to estimate magnitude of respiratory related tumor movement. In case of fiducial-, or direct tumor tracking, only expiration CTs were used for delineation. For patients with fiducial markers, CT simulation was delayed with a minimum of 10 days after implantation to minimise uncertainty linked to the potential marker migration.

The vast majority of patients (n = 125; 96%) had PET CT scans in treatment position using the same individual vacuum bag used at the CT simulation, to optimize target volume definition.

For patients with real-time tumor tracking generally a margin of 3 mm was applied around the gross tumor volume (GTV) to achieve clinical target volume (CTV). CTV contours were then, corrected manually when overlapping with ribs or mediastinal structures. An additional 2 mm was added to create planning target volume (PTV).

When real time tumor tracking was not feasible, we used an internal target volume of GTV, large enough to cover all possible tumor positions during the respiratory cycle. After that, the method and the margins for creating CTV-internal target volume (ITV) and PTV was similar to real time tracked patients.

SBRT procedure

Treatment plans were implemented with Multiplan treatment planning system (TPS) version 5.1 (Accuray Inc. Sunnyvale, USA), using Ray Tracing calculation algorithm. Prescription doses varied between 40 to 60 Gy in 3 to 5 fractions, depending on proximity to organs at risk (OAR) and on tumor size. Dose was typically prescribed to the 80% isodose line (75–82%) encompassing the PTV. Dose constraints to OARs were applied according to a class solution (Table 2) which was based on published data of Timmerman and AAPM Taskgroup 101 guidelines.¹⁸⁻¹⁹

SBRT treatments were performed by Cyberknife Robotic Radiosurgery treatment unit (Accuray Inc.

Sunnyvale, USA). Treatment consisted of typically 100–200 non-coplanar beams using Iris® various aperture collimator in a range between 15 to 60 mm with a dose rate of 600 MU/min.

Follow up and toxicity evaluation

Patients were followed up by the treating radiation oncologist and/or by referring pulmonologist or oncologist. In addition to regular CT-scans, metabolic follow up of treatment effect by PET CT was performed in 118 patients (91%) to make distinction between local disease progression and localized pulmonary fibrosis.^{20,21} Acute and late toxicities were evaluated using the Common Terminology Criteria for Adverse Events (CTCAE v4.0). Toxicity was classified as acute up to 3 months after SBRT.

The patient follow up time was defined as the period between the first day of Cyberknife treatment to the date of last visit or death.

Statistical analysis

Patient and lesion characteristics and toxicities were described in terms of means or medians (range) or in terms of numbers (%). A descriptive analysis was used to present patient and treatment characteristics and toxicity data. Local control (LC), overall survival (OS) and cause-specific survival (CSS) rates were estimated by the Kaplan-Meier method. The prognostic value of patient and tumor characteristics on LC was determined using uni- and multivariate Cox regression models. Results were considered to be statistically significant at p-values ≤ 0.05. Statistical analysis was performed with the SAS version 9.3 software (SAS Institute, Cary, NC, USA).

Ethical considerations

This retrospective cohort study was approved by institutional review board.

Results

The mean and median follow up time (FUP) was 21 months (range 2–39) with only 8 cases (6.2%) with a follow-up of less than 6 months. Total dose and number of fractions was determined with consideration of tumor location and size. In some cases the initially planned dose was reduced and/or the fraction number was increased in order to better meet OAR constraints. The applied dose and fractionation schemes are described in Table 3.

TABLE 2. Dose constraints for organs at risk

Organ	Type of constraint	Dose (Gy) for 3 fractions SBRT	Dose (Gy) for 5 fractions SBRT
Spinal cord	D _{max}	22 (7.33 Gy/fx)	30 (6 Gy/fx)
Esophagus	D _{max}	27 (9 Gy/fx)	35 (7 Gy/fx)
Trachea and main bronchi	D _{max}	30 (10 Gy/fx)	32 (6.4 Gy/fx)
Heart	D _{max}	30 (10 Gy/fx)	38 (7.6 Gy/fx)
Plexus brachialis	D _{max}	24 (8 Gy/fx)	32 (6.4 Gy/fx)
Ribs	D _{max}	37 (12.3/fx)	43 (8.6/fx)
Skin	D _{max}	32 (10.6/fx)	24 (4.8/fx)
Lung (both lungs)	Volumetric	V _{10.5Gy} < 1500 cc V _{11.4Gy} < 1000 cc	V _{12.5Gy} < 1500 cc V _{13.5Gy} < 1000 cc
Liver	Volumetric	V _{17.1Gy} < 700 cc	V _{21Gy} < 700 cc

Delivered dose varied from BED_{10Gy} = 72 Gy (40 Gy in 5 fractions) to BED_{10Gy} = 180 Gy (60 Gy in 3 fractions). The median dose for peripheral lesions was 3x 20Gy, whereas for central lesions the median was 3x 15Gy. Mean/median BED_{10Gy} for peripheral and central lesions were 170/180Gy and 102/112.5 Gy, respectively. Real-time tumor tracking was performed in 42% of treatments (n = 66) either using gold fiducial based (Synchrony) or direct fluoroscopic (Xsight Lung) methods.

Local control

For the whole cohort the actuarial 1-, 2-, and 3-year LC rates were 86%, 75%, and 62%, respectively.

In univariate Cox regression model, a higher BED_{10Gy} was associated with better LC (p = 0.008). Analysis of the different dose levels found a cut-off value between BED 112.5 Gy and 132 Gy. Treatments using doses higher than 112.5 Gy

TABLE 3. Dose-fractionation schemes

Radiotherapy scheme	BED _{10Gy} (Gy)	n (%)
3x20 Gy	180	96 (60%)
3x18 Gy	151.2	7 (4%)
3x17 Gy	137.7	4 (2.5%)
5x12 Gy	132	1 (0.6%)
3x15 Gy	112.5	24 (15%)
5x10 Gy	100	4 (2.5%)
5x9 Gy	85.5	11 (7%)
5x8 Gy	72	13 (8%)

BED = mean biologically equivalent dose

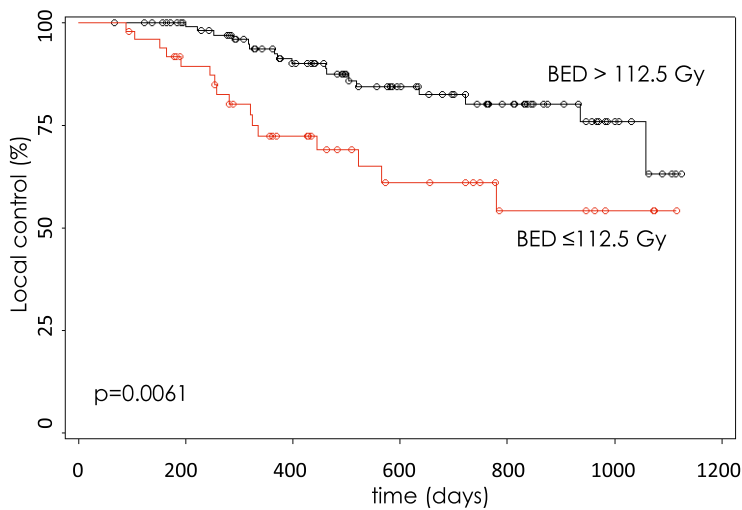


FIGURE 1. Probability of local control according to dose (BED \leq 112.5 Gy vs. higher).

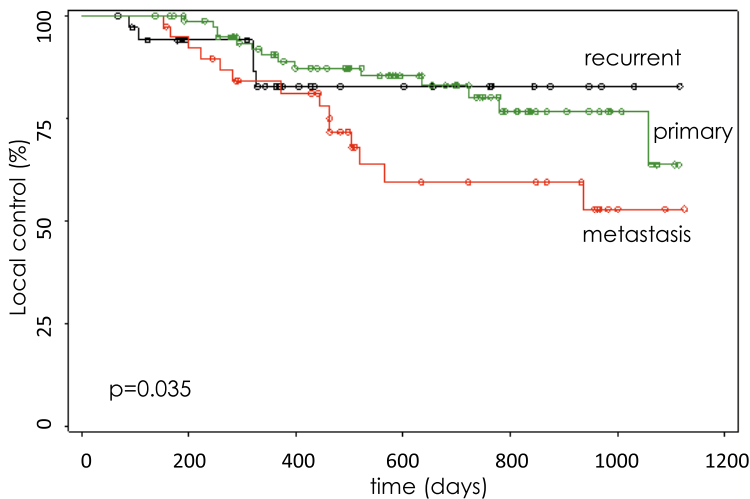


FIGURE 2. Probability of local control for primary (n = 86), recurrent (n = 35) and metastatic (n = 39) lesions.

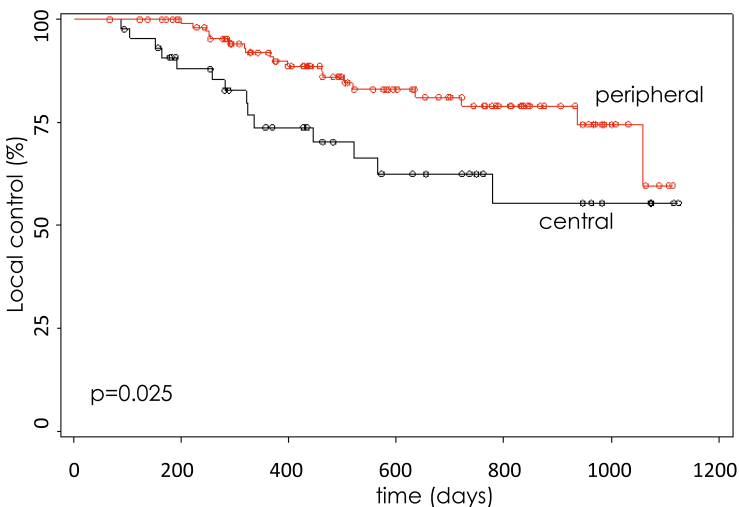


FIGURE 3. Probability of local control for peripheral (n = 113) and central (n = 47) lesions.

showed a significant advantage in terms of LC, resulting 1-, 2-, and 3-year actuarial LC rates of 93% vs 73%, 80% vs 61%, and 63% vs 54%, respectively ($p = 0.0061$, HR = 0.384; Figure 1).

In univariate analysis there were no significant differences between primary (P), recurrent (R) and metastatic (M) lesions in terms of actuarial LC ($p = 0.091$). However in pairwise comparison primary tumors provided improved results compared to metastases: 1-, 2-, and 3-year LC rates were 89% vs 84%, 80% vs 59%, and 64% vs 53%, respectively ($p = 0.035$; Figure 2). Other factors such as tumor tracking (inclusive tracking modality), and histological confirmation of malignancy had no significant effect on LC.

During separate analysis of the primary tumor group there was no significant difference in LC according to T-stage. However, there was a non-significant trend favoring LC in T1 compared to T2 ($p = 0.063$).

Local control was significantly higher for peripheral lesions, compared to central lesions ($p = 0.025$), resulting in 1-, 2-, and 3-year LC rates of 91% vs 74%, 79% vs 63%, and 60% vs 56%, respectively (Figure 3).

In univariate Cox regression model, larger GTV and PTV volumes were associated with a higher risk of local relapse ($p = 0.0034$ and $p = 0.0013$, respectively).

The variables tested in multivariate analysis were tumor type (primary/recurrent/metastasis), tracking (yes/no), confirmed histology (yes/no), location of lesions (central/peripheral), BED_{10Gy}, GTV, PTV, and PTV coverage. These variables were selected in order to determine treatment and tumor factors influencing LC. In multivariate analysis the metastatic origin of lesions (HR = 7.3; $p < 0.0001$), the histological confirmation of malignancy (HR = 4.1; $p = 0.0052$) and larger PTV (HR = 1.03; $p < 0.0001$) were associated with significantly lower LC rate.

Overall survival and cause-specific survival

One-, two-, and three-year actuarial rates of OS were 85%, 74% and 62%, respectively, whereas the respective rates of CSS were 93%, 90%, and 80%.

Early and late toxicities

Treatment related Grade (G) 3 or higher acute and late toxicities were observed at 3 (2%) and 6 patients (5%), respectively. Acute toxicities included 2 cases (1.5%) of G3 pneumonitis and a single case (0.8%) of

TABLE 4. Comparative table of relevant published data and own results

Study	Technic	Histological confirmation %	No. of pts/ lesions	dose (Gy)/fx	BED _{10Gy} (Gray)	Median FUP (month)	Local Control	Overall Survival
PRIMARY								
Chen VJ (26)	CK	100	40	median 48 (42-60)/3 fx	124.8	44	91%@3y	75%@3y
van der Voort van Zyp (27)	CK	51	70	60/3fx (Peripheral) 45/3fx (Central)	180 (Peripheral) 112.5 (Central)	15	96%@2y for 60 Gy 78%@2y for 45 Gy	62%@2y
Factor (28)	CK	95	78	60/3 fx (Peripheral) 48/4 fx (Central)	75-180	14.4	87%@2y	68%@2y
Bahig (4)	CK	84	150	median 60/3 fx 40- 60/3-5 fx	72-180 (Peripheral) 106-180 (Central)	22	96%@2y	87%@2y
Shen (29)	CK	84	50	57 (48-60)/3fx	104-150	35	crude 96%@2y	86%@1y 74%@2y
Davis, RSS REGISTRY (5)	CK, LINAC	100	723/741	median 54 (10-80)/3 fx	151.2	12	88%@1y 76%@2y	T1: 85/63%@1/2y T2: 76/52@1y/2y
Fakiris (30)	LINAC	100	70	60-66/3fx	180-211.2	50.2	88.1%@3y	42.7%@3y
METASTASES								
Nuytens (7)	CK	12	30/57	30/1 fx; 60/3-5 fx; 56/7 fx		36	79%@1y	63%@2y 38%@4y
Inoue (8)	LINAC		87/189	48/3fx; 50/5 fx; 52-60/10 fx;	30-168		80%@2y 80%@3y	47%@2y 32%@3y
MIXED: PRIMARY+METASTASES								
Guckenberger (31)	LINAC	19	124/159	26/1 fx; 37.5/3; 48/8 fx		14	83%@3y	37%@3y (Primary) 16%@3y (Met)
Ernst-Stecken (9)	LINAC	100	21/39	35-40/5 fx	59.5-72	6.3	crude: 87%	crude: 86%
Duncker-Rohr (32)	LINAC	55	39/45	37.5/3 fx; 30/5 fx	84 (Peripheral) 60 (Central)	17	80.5%@2y 95% @2y Prim 59.7%@2y Met	52.7%@2y 45.9% (Primary) 66.7% (Met)
Current study	CK	total 61% primary 77%	130/160	median 60/3 fx (Peripheral) median 45/5 fx (Central)	median 180 (Peripheral) median 112.5 (Central)	21	86%@1y 75%@2y 62%@3y	

BED = mean biologically equivalent dose; CK = Cyberknife; fx = fractions; LINAC = linear accelerator, Met = metastases; Prim = primary tumour; Y = year

G5 pulmonary haemorrhage. This latter elderly (85 years old) patient had a fatal ipsilateral pulmonary haemorrhage 1 month after the completion of his SBRT (45 Gy in 5 fractions) for a right sided central tumor recurrence, and was classified as a possible treatment related adverse event. The patient had already been treated with chemotherapy 4 years earlier for his primary lung tumor, and 1 year earlier by Cyberknife for a contralateral upper lobe relapse without progression until the time of death.

Late toxicities were G3 dyspnea (n = 3; 2.3%, all presenting with chronic obstructive pulmonary disease [COPD] Global Initiative for Chronic Obstructive Lung Disease [GOLD] III prior to SBRT), G3 sick sinus syndrome (n = 1; 0.8%) requiring pacemaker implantation 8 months after SBRT, G3 pain due to a rib fracture requiring major analgesic (n = 1; 0.8%). One patient (0.8%) suffered a fatal haemorrhage (G5) 7 months after SBRT for a centrally located recurrent tumor mass, which invaded vascular structures already at the time of detection, and had shown progression after

Cyberknife treatment (40 Gy in 5 fractions). This case was encoded as a treatment related adverse event, although local tumor progression could not be formally excluded.

Grade 2 late toxicities were also recorded such as asymptomatic or moderately painful rib fractures (n = 5; 3.8%), recurrent laryngeal nerve palsy (n = 1; 0.8%), late radiation pneumonitis (n = 14; 10.8%) and pneumothorax (n = 6; 4.6%) after transthoracic marker placement requiring tube placement for a few days.

Discussion

High (86%, 75%, and 62% at 1, 2, and 3 years) actuarial LC rates were observed at the first 130 consecutive patients treated with lung SBRT in our institution. Our results are comparable with published data from other lung SBRT series (Table 4).^{4-5,7-9, 22-28} Bahig *et al.* reported their results on 150 patients treated with Cyberknife with a median dose of 60

Gy in 3 fractions leading to excellent LC rates of 96% at 2 years. This cohort, including peripheral and central tumors, consisted of purely stage T1-2 primary NSCLC.⁴ In our study favorable LC was observed for primary tumors compared to metastatic lesions. The same finding was reported by Duncken-Rohr³², while Guckenberger *et al.*³¹ n = 41; Stage IA, n = 13; Stage IB, n = 19; T3N0, n = 9 showed comparable 3-year results for primary and metastatic lesions treated with SBRT between the two groups at 3 years. In a comparative study of primary and metastatic lung tumors by Yamamoto *et al.*³³ tumor diameter and metastatic origin were associated with significantly lower LC rates, which is congruent with our findings.

Location of the target in lung SBRT has an important role in defining maximum deliverable doses in function of their proximity to adjacent radiosensitive OARS. In our analysis, LC rates at 1-, 2-, and 3-years are significantly different between central and peripheral lesions. The same observation was reported by van der Voort van Zyp *et al.* with LC of 96% vs. 78% LC at 2 years for peripheral vs. central T1-2 NSCLC lung tumors treated with 60 Gy or 45 Gy in 3 fractions, respectively.²⁷

The question of optimal dose of SBRT for central lesions remains unclear however, careful and appropriate dose-fractionation can lead to high tumor control with low rate of severe toxicities even in this population. In our series the overall mean BED_{10Gy} was 151 Gy with a range between 72–180 Gy. As the total dose and the number of fractions was determined by the location and the size of the target lesion, the same treatment schedules were applied for primary, recurrent and metastatic lesions. Central lesions were treated with a mean / median BED_{10Gy} of 102/112.5 Gy, the corresponding doses for peripheral lesions were 170/180 Gy, respectively. Obviously, the above seen better local control rates for peripheral tumors were linked to higher deliverable dose.

In a recent systematic review of central tumors Senthil *et al.*³⁴ have found that LC rates ≥ 85% can be achieved with low rates of complications when prescribed BED on the tumor is ≥ 100Gy, and at the same time the biologically equivalent normal tissue dose does not exceed 210 Gy. In a recent multicentric analysis of linac based central lung SBRT for NSCLC in German and Austrian institutions, the authors show similar LC rates to ours with 76%, 64% and 52% at 1, 2, and 3 years with a delivered median BED₁₀ of 72 Gy (range 43–180 Gy).³⁵

In series reporting results of purely peripheral, T1-2 NSCLC treated with similar technology and

doses to ours, LC rates as high as 83.8–100% were achieved at 2 years.^{26,29,36-38}

A subgroup analysis of primary lung cancer patients in our cohort yielded actuarial 1-, 2-, and 3-year LC of 89%, 80%, and 64%, respectively. These results are similar to the findings of a recent, large scale publication on data of the RSSearch® Patient Registry of Radiosurgery Society reporting the clinical outcome of 723 patients with early stage, node negative NSCLC treated with various SBRT techniques achieving 88% and 76% LC rates at 1 and 2 years, respectively.⁵

For metastatic and recurrent patient groups we observed 1-, 2-, and 3-year LC rates of 84%, 59%, 53% and 83%, 83%, 83%, respectively. Inoue *et al.*⁸ reported comparable results (3-year LC rate of 80%) in a large cohort study of central and peripheral metastases of 87 pts (189 lesions).

Although the distribution of patient numbers at the different dose-levels was particularly imbalanced in our cohort, analysis was performed on effect of BED_{10Gy} on LC. A clear correlation between the applied dose and the actuarial local control rates were found with a cut-off at BED_{10Gy} of 112.5 Gy, where lower doses were associated with higher rates of local recurrence. Local control rates at 1, 2, and 3 years were 93% vs 73%, 80% vs 61%, and 63% vs 54%, for the higher and lower dose groups, respectively (p = 0.0061, HR = 0.384). These results are coherent with the findings of others, however dose cut-off was found to be somewhat lower in the literature. Onishi *et al.*¹² and Olsen *et al.*³⁹ has shown that SBRT with a BED_{10Gy} ≥ 100 Gy was associated with significantly better LC rates than those with lower doses. In a large cohort study of 505 patients treated for NSCLC BED_{10Gy} < 105 Gy predicted higher local recurrence rates of 15% vs 4% in the low dose and high dose group, respectively.⁴⁰ In contrast, in a cohort of 94 NSCLC Stephens *et al.*⁴¹ did not observe a significant difference in 12 months actuarial LC between fractionation schemes of 5x10 Gy vs 3x20 Gy (BED_{10Gy} = 100 Gy vs 180Gy).

The limitations of our findings concerning the optimal BED_{10Gy} include the imbalanced distribution of patients in different dose-level groups, the possible selection bias and the non-randomized nature of this cohort study.

The incidence of G3 or higher toxicities in our study was coherent with the literature with 2% of acute and 5% of late complications.^{8,38} Two patients out of 130 (1.5%) has died because of pulmonary haemorrhage. Grade 5 toxicities are rare, but existing complications of SBRT, occurring predominant-

ly in centrally located tumors with an incidence of 0–2% in the literature.^{4,35} This low incidence of treatment related deaths can reasonably be considered as acceptable, given the lack of treatment alternatives for this population.

Conclusions

Stereotactic ablative radiotherapy using the CybeKnife system for the treatment of primary, recurrent and metastatic lung lesions seems to be a safe and effective treatment option for medically inoperable patients. A clear dose-response relationship was confirmed with a significantly improved local control with BED_{10Gy} over 112.5 Gy. More firm data from prospective trials are needed to validate findings of this study.

References

- van der Voort van Zyp NC, van der Holt B, van Klaveren RJ, Pattynama P, Maat A, Nuytens JJ. Stereotactic body radiotherapy using real-time tumor tracking in octogenarians with non-small cell lung cancer. *Lung Cancer* 2010; **69**: 296-301. doi: 10.1016/j.lungcan.2009.12.008
- Chang JY, Senan S, Paul MA, Mehran RJ, Louie A V, Groen HJM, et al. Stereotactic ablative radiotherapy versus lobectomy for operable stage I non-small-cell lung cancer: a pooled analysis of two randomised trials. *Lancet Oncol* 2016; **16**: 630-7. doi: 10.1016/S1470-2045(15)70168-3
- Videtic GMM, Stephans K, Reddy C, Gajdos S, Kolar M, Clouser E, et al. Intensity-modulated radiotherapy-based stereotactic body radiotherapy for medically inoperable early-stage lung cancer: excellent local control. *Int J Radiat Oncol Biol Phys* 2010; **77**: 344-9. doi: 10.1016/j.ijrobp.2009.05.004
- Bahig H, Filion E, Vu T, Roberge D, Lambert L, Bouchard M, et al. Excellent cancer outcomes following patient-adapted robotic lung SBRT but a case for caution in idiopathic pulmonary fibrosis. *Technol Cancer Res Treat* 2015; **14**: 667-76. doi: 10.7785/tcr.2012.500445
- Davis JN, Medbery C, Sharma S, Perry D, Pablo J, D'Ambrosio DJ, et al. Stereotactic body radiotherapy for early-stage non-small cell lung cancer: clinical outcomes from a National Patient Registry. *J Radiat Oncol* 2015; **4**: 55-63. doi: 10.1007/s13566-014-0177-0
- Baumann P, Nyman J, Hoyer M, Wennberg B, Gagliardi G, Lax I, et al. Outcome in a prospective phase II trial of medically inoperable stage I non-small-cell lung cancer patients treated with stereotactic body radiotherapy. *J Clin Oncol* 2009; **27**: 3290-6. doi: 10.1200/JCO.2008.21.5681
- Nuytens JJ, van der Voort van Zyp NC, Verhoef C, Maat A, van Klaveren RJ, van der Holt B, et al. Stereotactic body radiation therapy for oligometastases to the lung: a Phase 2 Study. *Int J Radiat Oncol Biol Phys* 2015; **91**: 337-43. doi: 10.1016/j.ijrobp.2014.10.021
- Inoue T, Oh R-J, Shiomi H, Masai N, Miura H. Stereotactic body radiotherapy for pulmonary metastases. Prognostic factors and adverse respiratory events. *Strahlenther Onkol* 2013; **189**: 285-92. doi: 10.1007/s00066-012-0290-1
- Ernst-Stecken A, Lambrecht U, Mueller R, Sauer R, Grabenbauer G. Hypofractionated stereotactic radiotherapy for primary and secondary intrapulmonary tumors: First results of a phase I/II study. *Strahlenther Onkol* 2006; **182**: 696-702. doi: 10.1007/s00066-006-1577-x
- De Ruyscher D, Favier-Finn C, Nestle U, Hurkmans CW, Le Pécoux C, Price A, et al. European Organisation for Research and Treatment of Cancer recommendations for planning and delivery of high-dose, high-precision radiotherapy for lung cancer. *J Clin Oncol* 2010; **28**: 5301-10. doi: 10.1200/JCO.2010.30.3271
- Vansteenkiste J, De Ruyscher D, Eberhardt WEE, Lim E, Senan S, Felip E, et al. Early and locally advanced non-small-cell lung cancer (NSCLC): ESMO Clinical Practice Guidelines for diagnosis, treatment and follow-up. *Ann Oncol* 2013; **24**(Suppl 6): vi89-98. doi: 10.1093/annonc/mdt241
- Onishi H, Shirato H, Nagata Y, Hiraoka M, Fujino M, Gomi K, et al. Hypofractionated stereotactic radiotherapy (HypoFXSRT) for stage I non-small cell lung cancer: updated results of 257 patients in a Japanese multi-institutional study. *J Thorac Oncol* 2007; **2**(7 Suppl 3): S94-100. doi: 10.1097/JTO.0b013e318074de34
- Hof H, Herfarth KK, Münter M, Hoess A, Motsch J, Wannenmacher M, et al. Stereotactic single-dose radiotherapy of stage I non-small-cell lung cancer (NSCLC). *Int J Radiat Oncol Biol Phys* 2003; **56**: 335-41. doi: 10.1016/S0360-3016(02)04504-2
- Hof H, Hoess A, Oetzel D, Debus J, Herfarth K. Stereotactic single-dose radiotherapy of lung metastases. *Strahlenther Onkol* 2007; **183**: 673-8. doi: 10.1007/s00066-007-1724-z
- Senan S, Lagerwaard F. Stereotactic radiotherapy for stage I lung cancer: current results and new developments. *Cancer Radiother* 2010; **14**: 115-8. doi: 10.1016/j.canrad.2009.11.003
- Chen Y, Guo W, Lu Y, Zou B. Dose-individualized stereotactic body radiotherapy for T1-3N0 non-small cell lung cancer: Long-term results and efficacy of adjuvant chemotherapy. *Radiother Oncol* 2008; **88**: 351-8. doi: 10.1016/j.radonc.2008.07.013
- Berriochoa C, Videtic GMM, Woody NM, Djemil T, Zhuang T, Stephans KL. Stereotactic body radiotherapy for T3N0 lung cancer with chest wall invasion. *Clin Lung Cancer* 2016; **17**: 595-601. doi: 10.1016/j.clc.2016.04.007
- Jerezek-Fossa BA, Ronchi S, Orecchia R. Is stereotactic body radiotherapy (SBRT) in lymph node oligometastatic patients feasible and effective? *Rep Pract Oncol Radiother* 2015; **20**: 472-83. doi: 10.1016/j.rpor.2014.10.004
- Meng M, Wang H, Zaorsky NG, Zhao X, Wu Q, Jiang B, et al. Clinical evaluation of stereotactic radiation therapy for recurrent or second primary mediastinal lymph node metastases originating from non-small cell lung cancer. *Oncotarget* 2015; **6**: 15690-703. doi: 10.18632/oncotarget.3704
- Gibbs IC. Frameless image-guided intracranial and extracranial radiosurgery using the Cyberknife robotic system. *Cancer Radiother* 2006; **10**: 283-7. doi: 10.1016/j.canrad.2006.05.013
- Kilby W, Dooley JR, Kuduvali G, Sayeh S, Maurer CR. The CyberKnife robotic radiosurgery system in 2010. *Technol Cancer Res Treat* 2010; **9**: 433-52. doi: 10.1177/153303461000900502
- Timmerman RD. An overview of hypofractionation and introduction to this issue of Seminars in Radiation Oncology. *Semin Radiat Oncol* 2008; **18**: 215-22. doi: 10.1016/j.semdonc.2008.04.001
- Benedict SH, Yenice KM, Followill D, Galvin JM, Hinson W, Kavanagh B, et al. Stereotactic body radiation therapy: the report of AAPM Task Group 101. *Med Phys* 2010; **37**: 4078-101. doi: 10.1118/1.3438081
- Guckenberger M, Heilman K, Wulf J, Mueller G, Beckmann G, Flentje M. Pulmonary injury and tumor response after stereotactic body radiotherapy (SBRT): results of a serial follow-up CT study. *Radiother Oncol* 2007; **85**: 435-42. doi: 10.1016/j.radonc.2007.10.044
- Essler M, Wantke J, Mayer B, Scheidhauer K, Bundschuh RA, Haller B, et al. Positron-emission tomography CT to identify local recurrence in stage I lung cancer patients 1 year after stereotactic body radiation therapy. *Strahlenther Onkol* 2013; **189**: 495-501. doi: 10.1007/s00066-013-0310-9
- Chen VJ, Oermann E, Vahdat S, Rabin J, Suy S, Yu X, et al. CyberKnife with tumor tracking: an effective treatment for high-risk surgical patients with stage I non-small cell lung cancer. *Front Oncol* 2012; **2**: 1-5. doi: 10.3389/fonc.2012.00009
- van der Voort van Zyp NC, Prévost J-B, Hoogeman MS, Praag J, van der Holt B, Levendag PC, et al. Stereotactic radiotherapy with real-time tumor tracking for non-small cell lung cancer: clinical outcome. *Radiother Oncol* 2009; **91**: 296-300. doi: 10.1016/j.radonc.2009.02.011
- Factor OB, Vu CC, Schneider JG, Witten MR, Schubach SL, Gittleman AE, et al. Stereotactic body radiation therapy for stage I non-small cell lung cancer: a small academic hospital experience. *Front Oncol* 2014; **4**: 1-5. doi: 10.3389/fonc.2014.00287
- Shen Z-T, Wu X-H, Li B, Zhu X-X. Clinical outcomes of CyberKnife stereotactic body radiotherapy for peripheral stage I non-small cell lung cancer. *Med Oncol* 2015; **32**: 1-8. doi: 10.1007/s12032-015-0506-1

30. Fakiris AJ, McGarry RC, Yiannoutsos CT, Papiez L, Williams M, Henderson M A, et al. Stereotactic body radiation therapy for early-stage non-small-cell lung carcinoma: four-year results of a prospective phase II Study. *Int J Radiat Oncol Biol Phys* 2009; **75**: 677-82. doi: 10.1016/j.ijrobp.2008.11.042
31. Guckenberger M, Wulf J, Mueller G, Krieger T, Baier K, Gabor M, et al. Dose-response relationship for image-guided stereotactic body radiotherapy of pulmonary tumors: relevance of 4D dose calculation. *Int J Radiat Oncol Biol Phys* 2009; **74**: 47-54. doi: 10.1016/j.ijrobp.2008.06.1939
32. Duncker-Rohr V, Nestle U, Momm F, Prokic V, Heinemann F, Mix M, et al. Stereotactic ablative radiotherapy for small lung tumors with a moderate dose: Favorable results and low toxicity. *Strahlenther Onkol* 2013; **189**: 33-40. doi: 10.1007/s00066-012-0224-y
33. Yamamoto T, Jingu K, Shirata Y, Koto M, Matsushita H, Sugawara T, et al. Outcomes after stereotactic body radiotherapy for lung tumors, with emphasis on comparison of primary lung cancer and metastatic lung tumors. *BMC Cancer* 2014; **14**: 464. doi: 10.1186/1471-2407-14-464
34. Senthil S, Haasbeek CJ a, Slotman BJ, Senan S. Outcomes of stereotactic ablative radiotherapy for central lung tumours: A systematic review. *Radiother Oncol* 2013; **106**: 276-82. doi: 10.1016/j.radonc.2013.01.004
35. Schanne DH, Nestle U, Allgäuer M, Andratschke N, Appold S, Dieckmann U, et al. Stereotactic body radiotherapy for centrally located stage I NSCLC: a multicenter analysis. *Strahlenther Onkol* 2014; **191**: 125-32. doi: 10.1007/s00066-014-0739-5
36. Brown WT, Wu X, Fayad F, Fowler JF, Garcia S, Monterroso MI, et al. Application of robotic stereotactic radiotherapy to peripheral stage I non-small cell lung cancer with curative intent. *Clin Oncol* 2009; **21**: 623-31. doi: 10.1016/j.clon.2009.06.006
37. Collins BT, Vahdat S, Erickson K, Collins SP, Suy S, Yu X, et al. Radical cyberknife radiosurgery with tumor tracking: an effective treatment for inoperable small peripheral stage I non-small cell lung cancer. *J Hematol Oncol* 2009; **2**: 1. doi: 10.1186/1756-8722-2-1
38. Vahdat S, Oermann EK, Collins SP, Yu X, Abedalthagafi M, Debrito P, et al. CyberKnife radiosurgery for inoperable stage IA non-small cell lung cancer: 18F-fluorodeoxyglucose positron emission tomography/computed tomography serial tumor response assessment. *J Hematol Oncol* 2010; **3**: 6. doi: 10.1186/1756-8722-3-6
39. Olsen JR, Robinson CG, El Naqa I, Creach KM, Drzymala RE, Bloch C, et al. Dose-response for stereotactic body radiotherapy in early-stage non-small-cell lung cancer. *Int J Radiat Oncol Biol Phys* 2011; **81**: 299-303. doi: 10.1016/j.ijrobp.2011.01.038
40. Grills IS, Hope AJ, Guckenberger M, Kestin LL, Werner-Wasik M, Yan D, et al. A collaborative analysis of stereotactic lung radiotherapy outcomes for early-stage non-small-cell lung cancer using daily online cone-beam computed tomography image-guided radiotherapy. *J Thorac Oncol* 2012; **7**: 1382-93. doi: 10.1097/JTO.0b013e318260e00d
41. Stephans KL, Djemil T, Reddy CA, Gajdos SM, Kolar M, Mason D, et al. A comparison of two stereotactic body radiation fractionation schedules for medically inoperable stage I non-small cell lung cancer: the Cleveland Clinic experience. *J Thorac Oncol* 2009; **4**: 976-82. doi: 10.1097/JTO.0b013e3181adf509

Genetic counselling, BRCA1/2 status and clinico-pathologic characteristics of patients with ovarian cancer before 50 years of age

Mirjam Cvelbar, Marko Hocevar, Srdjan Novakovic, Vida Stegel, Andraz Perhavec, Mateja Krajc

Institute of Oncology Ljubljana, Ljubljana, Slovenia

Radiol Oncol 2017; 51(2): 187-194.

Received 1 November 2016

Accepted 13 January 2017

Correspondence to: Assist. Prof. Mateja Krajc, M.D., Ph.D., Cancer Genetic Clinic, Institute of Oncology Ljubljana, Zaloska c. 2, SI-1000 Ljubljana, Slovenia. E-mail: mkrajc@onko-i.si

Disclosure: No potential conflicts of interest were disclosed.

Background. In Slovenia like in other countries, till recently, personal history of epithelial ovarian cancer (EOC) has not been included among indications for genetic counselling. Recent studies reported up to 17% rate of germinal BRCA1/2 mutation (gBRCA1/2m) within the age group under 50 years at diagnosis. The original aim of this study was to invite to the genetic counselling still living patients with EOC under 45 years, to offer gBRCA1/2m testing and to perform analysis of gBRCA1/2m rate and of clinico-pathologic characteristics. Later, we added also the data of previously genetically tested patients with EOC aged 45 to 49 years.

Patients and methods. All clinical data have to be interpreted in the light of many changes happened in the field of EOC just in the last few years: new hystology stage classification (FIGO), new hystology types and differentiation grades classification, new therapeutic possibilities (PARP inhibitors available, also in Slovenia) and new guidelines for genetic counselling of EOC patients (National Comprehensive Cancer Network, NCCN), together with next-generation sequencing possibilities.

Results. Compliance rate at the invitation was 43.1%. In the group of 27 invited or previously tested patients with EOC diagnosed before the age of 45 years, five gBRCA1/2 mutations were found. The gBRCA1/2m detection rate within the group was 18.5%. There were 4 gBRCA1 and 1 gBRCA2 mutations detected. In the extended group of 42 tested patients with EOC diagnosed before the age of 50 years, 14 gBRCA1/2 mutations were found. The gBRCA1/2m detection rate within this extended, partially selected group was 33.3%. There were 11 gBRCA1 and 3 gBRCA2 mutations detected.

Conclusions. The rate of gBRCA1/2 mutation in tested unselected EOC patients under the age of 50 years was higher than 10%, namely 18.5%. Considering also a direct therapeutic benefit of PARP inhibitors for BRCA positive patients, there is a double reason to offer genetic testing to all EOC patients younger than 50 years. Regarding clinical data, it is important to perform their re-interpretation in everyday clinical practice, because this may influence therapeutic possibilities to be offered.

Key words: ovarian cancer; BRCA1/2 gene; genetic counselling

Introduction

The frequency of germinal BRCA1/2 mutations in unselected patients with epithelial ovarian cancer (EOC) was found to be higher than 10%, according to recent studies.¹⁻⁵ Within the age group under 50

years at diagnosis, the reported frequency is even higher and it amounts up to 17%, and within a subgroup of patients aged 40–49 years the frequency amounts up to 24%.^{4,6}

It is of utmost importance for optimal healthcare sistem in every country to have its own epidemio-

logical data on frequency of germinal mutations of different hereditary cancers. Substantial research on BRCA1/2 germinal mutations in Slovenian population has been already done.⁷⁻¹² However, we haven't performed yet an analysis on the frequencies of BRCA1/2 mutations in ovarian cancer patients before the age of 50 years. In Slovenia like in other countries, till recently, personal history of epithelial ovarian cancer (EOC) has not been included among the indications for genetic counselling.

The original aim of this study was to include into the process of genetic counselling all living patients with epithelial ovarian cancer (EOC) diagnosed in the period 1999–2008 according to the data of the Slovenian National Cancer Registry who were younger than 45 years at the time of diagnosis and were treated at the Institute of Oncology Ljubljana. The process of genetic counselling included the possibility of genetic BRCA1/2 testing, with all possible clinical implications offered afterwards.

Our hypothesis was that the frequency of BRCA1/2 mutations in the tested patients would be higher than 10%. Original study started in 2012. Later, we added also the data of previously genetically tested patients with EOC aged 45 to 49 years at the time of diagnoses who were diagnosed in the period 1999–2010.

All germinal BRCA1/2 mutation (gBRCA1/2m) positive patients were offered inclusion into the screening and prophylactic program for the high-risk group for breast cancer. In addition, since in the meantime the first PARP inhibitor was registered in European Union for therapy of BRCA positive serous ovarian cancers, in case of relapses mutation carriers were offered this treatment. Following new guidelines of SGO and National Comprehensive Cancer Network (NCCN), genetic counselling is offered now to all EOC patients in Slovenia. However, genetic testing is still restricted to EOC patients that were diagnosed with high-grade-serous EOC.

Patients and methods

Ethical approval

The study was approved by the National Medical Ethics Committee (201/02/1011).

Patients accrual

Data from 87 patients diagnosed with ovarian cancer (code C56 according to ICD-10) before the age

of 45 years, in the period 1999–2008 and treated at the Institute of Oncology Ljubljana, were analyzed using the National Cancer Registry of Republic of Slovenia database. Patients with EOC and still alive were included. Two patients with borderline tumors and one patient with mixed ovarian cancer (carcinosarcoma) were included as well. Patients with germinal, stromal and some other rare non-epithelial ovarian cancers like primary ovarian lymphoma were excluded from the study.

With these inclusion and exclusion criteria, 57 patients were eligible to participate in the study. Since five of them have already undergone genetic counselling and BRCA testing, their anonymous data were included in the study with an extra approval of the National Medical Ethics Committee. The other 52 patients were invited by the letter to participate in the study. The invitation letter included patient information leaflet with all the data about the genetic counselling and testing and an invitation for genetic counselling at the Cancer Genetic Clinic of the Institute of Oncology Ljubljana. In patients under acute stress of an ongoing diagnostics or treatment, the invitation was postponed until the conclusion of such a process.

Genetic testing (mutation screening, BRCA analysis)

The DNA was isolated from peripheral blood using the DNA isolation kit (Quiagen, Hilden, Germany). Mutation screening was performed at the Institute of Oncology Ljubljana, Slovenia, and, for two samples, still at the Vrije University Brussels, Belgium. Complete screening of all BRCA1/2 exons was performed, using method of multiplex ligation-dependent probe amplification analysis (MLPA; MRC Holland, Amsterdam, the Netherlands) for detection of large genomic deletions and insertions, and using high-resolution melting, denaturing gradient gel electrophoresis and direct sequencing methods already reported, for small mutations.^{8,9,11,12,13}

Clinico-pathologic data of tested patients were collected from medical records following prepared study protocol. These included: family history of cancer including age at diagnosis in 1st and 2nd degree relatives, number of deliveries, histologic type of ovarian cancer, tumor grade and disease stage. The old FIGO staging classification and histologic type and grade classification were used for all patients since data accrual dated back to 1999.

Due to 46.8% compliance rate and the small number of tested patients during the study, a de-

TABLE 1. BRCA1/2 molecular diagnostics at patients with epithelial ovarian cancer under 50 years of age

Patient code	BRCA1 HGVS c.DNA*	BRCA1 HGVS protein*	Type	BRCA2 HGVS c.DNA*	BRCA2 HGVS protein*	Type
1A01	c.5377A>T	p.(Lys1793*)	Nonsense			
2A01	c.68_69delAG	p.(Glu23Valfs*17)	Frameshift	c.7195A>G	p.(Thr2399Ala)	Missense(UV)
	c.1067A>G	p.(Gln356Arg)	Missense(UV)			
2A02				c.9117G>A	p.(Pro3039Pro)	Synonimus and splicing
2A03	c.3018_3021delTTCA	p.(His1006Glnfs*17)	Frameshift			
2A04	c.181T>G	p.(Cys61Gly)	Missense			
3A01				c.3265C>T	p.(Gln1089*)	Nonsense
3A02	c.181T>G	p.(Cys61Gly)	Missense			
3A03	c.844_850dupTCATTAC	p.(Gln284Leufs*5)	Frameshift			
3A04	c.191G>A	p.(Cys64Tyr)	Missense			
4A01	c.1687C>T	p.(Gln563*)	Nonsense			
4A02	c.3718C>T	p.(Gln1240*)	Nonsense			
4A03	c.1687C>T	p.(Gln563*)	Nonsense			
4A04				c.5101C>T	p.(Gln1701*)	Nonsense
4A05	c.5266dupC	p.(Gln1756Profs*74)	Frameshift			

cision was reached of changing inclusion criteria to include also data of previously tested patients with ovarian cancer aged 45 to 49 years diagnosed in the period 1999–2008 and previously tested patients with ovarian cancer at age up to 49 years diagnosed during 2009–2010. The final number of patients included in the analysis of genetic and clinico-pathologic data was 42 patients, with 43 ovarian cancers (one patient had synchronously two different ovarian cancers).

Statistical analysis

Descriptive and bivariate statistics were used for analysis of the data. Due to small study group, exact tests (hi2 and t) were used. Statistical tests were performed with SPSS v.22 statistical software program.

Results

Compliance

Of the 52 invited patients, in one case patient’s husband answered that the patient had recently died. Of the other 51 patients there were 22 (43.1%) who decided for genetic counselling and were first counselled in 2012 and 2013. They all gave informed consent also for BRCA genetic testing. All tested patients received second-session genetic

TABLE 2. Family history of BRCA tested patients with EOC before age 45, diagnosed 1999–2008

		gBRCAm + N = 5	gBRCAm – N = 22	p (Fisher’s exact test)
Family history(of any cancer at 1 st or 2 nd degree)	Positive	5	14	p = 0.280
	Negative	0	8	
Family history of 1 st -degree breast cancer	Positive	1	1	p = 0.342
	Negative	4	21	
Family history of 1 st -degree ovarian cancer	Positive	2	0	P = 0.028
	Negative	3	22	

counselling afterwards when the result of genetic testing was known. There was no response from 17 patients; three patients postponed genetic counselling for several times and it became clear they are not sure about wanting it, therefore they were not included into the study. In four cases, the letter came back because the address was changed and patients were unretrievable. Five patients answered explicitly they did not want to participate.

BRCA1/2 status analysis (mutation detection rate)

In the group of 27 invited or previously tested patients with ovarian cancer diagnosed before the age of 45 years, 5 mutations were found. Mutation detection rate within the group therefore was 18.5%.

TABLE 3. Clinicopathologic characteristics at BRCA tested patients with EOC at age under 50 years

		BRCA+ Ovarian cancers N = 15	BRCA- Ovarian cancers N = 28	p
Age at 1 st cancer	mean	40.8	36.9	0.149 (t test)
Age at the ovarian cancer	mean	42.8	37.1	0.036 (t test)
Sequence of the ovarian cancer	first	11	23	0.037 (exact χ^2)
	second	3	0	
Stage of the ovarian cancer (FIGO)	parallel to 1 st	1	5	0.055 (exact χ^2)
	I	4 (26.7%)	17 (60.7%)	
	II	4 (26.7%)	2 (7.1%)	
	III	5 (33.3%)	7 (25.0%)	
	IV	2 (13.3%)	2 (7.1%)	
Hystology Type of the Ovarian cancer	serous	6 (40%)	13 (46.4%)	0.451 (exact χ^2)
	mucinous	0	3 (10.7%)	
	endometrioid	7 (46.7%)	7 (25.0%)	
	clearcell	0	2 (7.1%)	
	mixed Ca	2 (13.3%)	1 (3.6%)	
	mixed Ca+Sa	0	1 (3.6%)	
	unknown	0	1 (3.6%)	
Grade of the Ovarian cancer	borderline	1 (6.7%)	1 (3.6%)	0.008 (exact χ^2)
	first	1 (6.7%)	11 (39.3%)	
	second	3 (20.0%)	9 (32.1%)	
	third	10 (66.7%)	6 (21.4%)	
	unidentifiable	0	1 (3.6%)	

TABLE 4. Other cancers characteristics in BRCA tested patients with EOC at age under 50 years

		BRCA+ N = 14	BRCA- N=28	p
Previous invasive breast cancer	Yes	2	0	P = 0.106 (exact χ^2)
	No	12	28	
Later invasive breast cancer	Yes	3	0	P = 0.032 (exact χ^2)
	No	11	28	
Occurrence of DCIS breast cancer	Yes	0	2	P = 0.545 (exact χ^2)
	No	14	26	
Concurrent Endometrial Cancer (with ovarian one)	Yes	0	5	P = 0.151 (exact χ^2)
	No	14	23	

There were four BRCA1 and one BRCA2 mutations (Table 1).

In the extended group of 42 tested patients with ovarian cancer diagnosed before the age of 50 years (during the period 1999–2010), 14 mutations were found. Mutation detection rate within this extended, partially selected group was 33.3%.

There were 11 BRCA1 and three BRCA2 mutations (Table 1).

Clinicopathologic results

Family history of a presence of any cancer in 1st or 2nd degree relative didn't show significant difference in the rate between gBRCA1/2m positive and negative group. As well, a family history of 1st degree breast cancer was of similar rate between the groups. There was significantly higher rate of 1st degree ovarian cancer in family history of gBRCA1/2m positive patients (Table 2).

Mean age at the ovarian cancer diagnosis was significantly higher at gBRCA1/2m positive patients (42.8 years *vs.* 37.1 years; $p = 0.036$). There was no statistically significant difference in mean age at the diagnosis of first cancer (Table 3).

Analysis of the *sequence* of cancers showed that the rate of ovarian cancer as the second cancer was significantly higher in gBRCA1/2m positive group.

Regarding *stage* of ovarian cancer, there was a trend of higher rate of the first stage in gBRCA1/2m negative group (60.7% *vs.* 26.7% in gBRCA1/2m positive; $p = 0.055$).

In ovarian cancer *hystology type* there was no statistically significant difference and the rate of serous type was nearly the same (40% in gBRCA1/2m positive patients *vs.* 46% in negative ones). There was no mucinous type in gBRCA1/2m positive group. Clear-cell type was present only in one case

of mixed carcinoma. Carcinosarcoma case did not make part of gBRCA1/2m positive group.

In ovarian cancer grade there was significantly higher rate of high-grade (G2 and G3) cancers in gBRCA1/2m positive group (66.7% vs. 21.4% in negative group; $p = 0.008$). There was also a case of *borderline* ovarian cancer in gBRCA1/2m positive group. This *borderline* ovarian cancer of stage I was concomitant with contralateral grade I and stage I ovarian cancer. Therefore, there were 43 cancers diagnosed in 42 patients (Table 3).

Tubal contralateral serous malignant changes defined as synchronous contralateral tubal cancer stage III were found in one patient. They were defined as second primary cancer because ovarian cancer was endocystical (endophitic growth in serous cystadenoma). Patient was gBRCA1/2m positive.

Analysis of *the other cancers* diagnosed in the same patients showed that there was at least a trend (considering No of patients, and significant difference considering No of ovarian cancers) of higher rate of previous invasive breast cancer in gBRCA1/2m positive group. As well, there was significantly higher rate of later invasive breast cancer in gBRCA1/2m positive group. The rate of DCIS of the breast showed no statistical difference between the groups (Table 4).

Concurrent endometrial cancer was found in 5 out of 28 gBRCA1/2m negative patients and in 0 out of 14 positive patients, but the difference was not statistically significant ($p = 0.151$).

Discussion

Genetic counselling and testing

Compliance of the OC patients invited to genetic counselling was similar to our previous study.¹⁰ It would've been probably higher if there had been a direct therapeutic benefit of testing already present. At the time when our study started, PARP inhibitors have not been yet registered and used in standard therapy of OC patients. Therefore direct benefit of testing consisted in surveillance for eventual second primary breast cancer or in its prevention in gBRCA1/2 positive OC patients. Indirect benefit was present for patients' relatives.

Pal *et al.*¹ reported a higher compliance than ours: 64% vs. 43.1%, respectively. Both studies were performed in a period before olaparib therapy was approved. We may speculate that the reason for the difference might have been the way of inviting the patients, which is not described in their paper. Namely, one can suppose that the invitation

coming from medical doctor directly involved in therapy process is more efficient than the invitation coming from Cancer Genetic Clinic team. Indeed, our latest data from October 2014 show much higher compliance rate of 82.5%, since genetic counselling and testing was performed for therapeutic reasons and patients were referred to Cancer Genetic Clinics by their medical oncologists.¹⁴

Mutation rate of 18.5% (5/27) within the group of unselected EOC patients under 50 years of age is in accordance with studies already mentioned and with our hypothesis. In accordance are also results of Australian Ovarian Cancer Study Group, published after the beginning of our study, which found gBRCA1/2m rate of 22.2% in EOC patients diagnosed before the age of 50 years.¹⁵ As someone could expect it is higher than the rate found in most of population-based studies with EOC patients unselected for the age.¹⁶

We are aware of limitations of our small study group as a consequence of several factors, above all of low incidence of EOC under the age of 50 years and of small population of our country. Therefore, it was not possible to perform a subanalysis of mutation rate of the EOC patients aged 40–49 years and compare results to recently published large Canadian population-based study which found mutation rate of 24.0%.⁶ Nevertheless it is noteworthy that one of gBRCA1/2m positive patients in our study was only 24 years old at EOC diagnosis. In the European multicentric study of Lakhani *et al.* there was no such case of gBRCA1/2 positive EOC patient under 30 years age found. Therefore, it is rare, but not impossible.

The gBRCA1/2 mutation rate of 33.3% for our larger, combined and partly selected EOC group under the age of 50 years is not representative for the entire population of EOC patients under the age of 50 years in Slovenia, because 20 out of 42 patients were tested on the basis of BRCAPRO calculation and not on the basis of EOC diagnosis under the age of 50 years.

Regarding the type of mutations no new slovenian mutations and also no founder mutations were found. All mutations found have already been described.¹¹

Clinicopathologic features

Family history of gBRCA1/2m positive patients not surprisingly had higher 1st degree ovarian cancer rate. With larger sample we would expect also higher 1st degree breast cancer history rate, according to published data.^{1,3,4}

The mean age of gBRCA1/2m positive patients (42.8 years) was higher than that of negative ones (37.1 years). Eleven out of fourteen positive patients were 40–49 years old. This surprising result is however in accordance with Canadian study in which the prevalence of mutations was particularly high among women in their forties.⁶ Contrary, Danish study found the highest gBRCA1/2 mutation rate (23%) in EOC patients under the age of 40 years.⁴ The large European multicentric study of 207 gBRCA1/2m positive EOC patients found not a single case at the age below 30 years, while there were 13 gBRCA1/2m negative EOC patients in this very young age group. In age groups of 30–39 and 40–49 years old there were more patients with, than without gBRCA1/2 mutation (20 *vs.* 16 and 68 *vs.* 49). In patients older than 50 years sporadic cases prevailed.¹⁷ Interestingly the youngest patient with gBRCA1/2m in our study was only 24 years old at the time of OC diagnosis.

EOC was significantly more often a second primary cancer, after the breast cancer which had developed earlier, in the group of gBRCA1/2m positive in comparison to gBRCA1/2m negative patients (2/12 compared to 0/28). This is in accordance with published data on double primary breast and ovarian cancer.^{10,18,19} In a large international pathology study of CIMBA consortium published in 2012 it was found that 415 of 1129 (36.8%) gBRCA1/2m positive EOC patients had developed breast cancer before developing ovarian cancer.²⁰

Higher grade of EOC in patients with gBRCA1/2m mutation observed in our study is in accordance with most of the published data.^{17,20}

In accordance with published data is also a higher stage trend in gBRCA1/2m positive group observed in our study.^{15,21}

The most unexpected finding of our study is high rate of endometrioid type of EOC in gBRCA1/2m positive group (46.7%). This seems in contrast with current concepts of tubal origin and of high-grade serous type of »ovarian« cancer in gBRCA1/2m positive patients.²² It is also in contrast with our previous results of a pilot study (10) where 8/12 (66.7%) gBRCA1/2m positive ovarian cancers were serous and only 2/12 (16.7%) were endometrioid ones. But interestingly, high rate of endometrioid type was noted in unselected OC patients in Slovenia also in the past.^{23,24} It was argued that this could be attributed to different histopathological criteria and interpretation.

Internationally, the problem of histopathological interpretation was specifically addressed in a large European study published in 2004.¹⁷ Aware of the

problem of interobserver variation and of particular difficulty when a lesion is high grade, they attempted to minimise the effects of interobserver variability. In so doing, they found that even if the frequency of serous EOC was higher among gBRCA1m carriers compared with controls, it accounted for only 40% of EOC, and consecutively the frequencies of other (but mucinous) histology types were higher than in previous reports, with endometrioid type accounting for 33% in gBRCA1m carriers, 29% in gBRCA2m carriers and 33% in gBRCAm negative EOC patients. Also clear cell EOC frequencies were similar in carriers than in controls.

In the light of these data, the rates of various histologic types found in our study are more correspondent to international data of that period.

Further decisive highlights on relationship between serous and endometrioid type of EOC are coming from a series of studies with molecular approach, making research in gene expression profiling; the results show that high-grade serous type EOC and high-grade endometrioid EOC are molecularly similar.^{25,26} Therefore, it emerges that morphological similarity has its basis in molecular similarity of these two, only apparently different histologic subtypes of EOC. Indeed, Alsop *et al.* report that increasingly, high-grade endometrioid EOC are being reclassified as high-grade serous EOC.¹⁵

In our study, four out of seven endometrioid gBRCA1/2m positive EOC were high-grade (G3) and therefore morphologically and molecularly similar to serous high-grade type. Other three endometrioid gBRCA1/2m positive EOC were borderline, low-grade (G1) and medium grade (G2). Therefore, even if high-grade and also medium-grade endometrioid EOC case would've been reclassified today in high-grade serous EOC, there remains a case of gBRCA1/2m positive patient with borderline and low-grade endometrioid EOC which can not be reclassified.

It's known that in general, 15–20% of endometrioid EOC is associated with carcinoma of the endometrium.²² In our study there was no such case found in gBRCA1/2m positive EOC patients, but there were 5 cases in gBRCA1/2m negative patients. We found no specific data in the literature with regard to gBRCA1/2 mutation in patients with concurrent (synchronous) endometrial and ovarian cancer. However, a case of germline mutation in another tumor suppressor gene RAD51D was recently described in such a patient.²⁷

Concurrent primary contralateral invasive tubal cancer was found in one gBRCA1/2m positive EOC

patient. STIC (serous tubal intraepithelial carcinoma) as a precursor of serous »ovarian« cancer was not addressed in present study, because a change of concepts and of histologic practice occurred only a few years ago and therefore STIC has not yet been a part of standardised histopathologic report in EOC patients in the period analysed.

Conclusions

The rate of gBRCA1/2 mutation in tested EOC patients under the age of 50 years is higher than 10% (18.5%). Considering also a direct therapeutic benefit of PARP inhibitors for BRCA positive patients, there is a double reason to offer genetic testing to all EOC patients younger than 50 years.

Positive patients for gBRCA1/2m can be younger than 30 years so even very young patients can not be excluded from gBRCA1/2m testing.

Almost half of the gBRCA1/2m positive patients has been diagnosed as having endometrioid histologic type of EOC. It is important to consider for individual patient how far ago the histologic diagnosis was made, since high-grade endometrioid type, on the basis of recent molecular studies, is more and more often reclassified to high-grade serous type.

However, among our gBRCA1/2m positive patients, there was also a case of concurrent low-grade endometrioid ovarian tumor and contralateral borderline endometrioid EOC, so endometrioid EOC in positive patients is not only a question of overlapping of high-grade endometrioid and high-grade serous EOC. Therefore we must consider for gBRCA1/2 testing all patients with EOC younger than 50 years and not only serous-type EOC patients.

Acknowledgement

This work was supported by the grant P3 0352 from the Ministry of Education, Science and Sport of the Republic Slovenia.

References

1. Pal T, Permuth-Wey J, Betts JA, Krischer JP, Fiorica J, Arango H, et al. BRCA1 and BRCA2 mutations account for a large proportion of ovarian carcinoma cases. *Cancer* 2005; **104**: 2807-16. doi: 10.1038/bjc.2012.483
2. Brozek I, Ochman K, Debniak J, Morzuch L, Ratajska M, Stepnowska M, et al. High frequency of BRCA1/2 germline mutations in consecutive ovarian cancer patients in Poland. *Gynecol Oncol* 2008; **108**: 433-7. doi: 10.1016/j.ygyno.2007.09.035
3. Ramus SJ, Gayther SA. The contribution of BRCA1 and BRCA2 to ovarian cancer. *Mol Oncol* 2009; **3**: 138-50. doi: 10.1016/j.molonc.2009.02.001
4. Soegaard M, Kruger Kjaer S, Cox M, Wozniak E, Høgdall E, Høgdall C, et al. BRCA1 and BRCA2 mutation prevalence and clinical characteristics of a population-based series of ovarian cancer cases from Denmark. *Clin Cancer Res* 2008; **14**: 3761-7. doi: 10.1158/1078-0432
5. Trainer AH, Meiser B, Watts K, Mitchell G, Tucker K, Friedlander M. Moving toward personalized medicine: treatment-focused genetic testing of women newly diagnosed with ovarian cancer. *Int J Gynecol Cancer* 2010; **20**: 704-16. doi: 10.1111/IGC.0b013e3181dbd1a5
6. Zhang S, Royer R, Li S, McLaughlin JR, Rosen B, Risch HA, et al. Frequencies of BRCA1 and BRCA2 mutations among 1342 unselected patients with invasive ovarian cancer. *Gynecol Oncol* 2011; **121**: 353-7. doi: 10.1016/j.ygyno.2011.01.020
7. Krajc M, De Greve J, Goelen G, Teugels E. BRCA2 founder mutation in Slovenian breast cancer families. *Eur J Hum Genet* 2002; **10**: 879-82. doi: 10.1038/sj.ejhg.5200886
8. Krajc M, Teugels E, Žgajnar J, Goelen G, Bešič N, Novaković S, et al. Five recurrent BRCA1/2 mutations are responsible for cancer predisposition in the majority of Slovenian breast cancer families. *BMC Med Genet* 2008; **9**: 83. doi: 10.1186/1471-2350-9-83
9. Stegel V, Krajc M, Žgajnar J, Teugels E, De Greve J, Hočevar M, et al. The occurrence of germline BRCA1 and BRCA2 sequence alterations in Slovenian population. *BMC Med Genet* 2011; **12**: 9. doi: 10.1186/1471-2350-12-9
10. Cvelbar M, Hočevar M, Vidmar G, Teugels E. BRCA1/2 status and clinicopathologic characteristics of patients with double primary breast and ovarian cancer. *Neoplasma* 2011; **58**: 198-204. doi: 10.4149/neo_2011_03_198
11. Novaković S, Milatović M, Cerkovnik P, Stegel V, Krajc M, Hočevar M, et al. Novel BRCA1 and BRCA2 pathogenic mutations in Slovene hereditary breast and ovarian cancer families. *Int J Oncol* 2012; **41**: 1619-27. doi: 10.3892/ijo.2012.1595
12. Krajc M, Zadnik V, Novaković S, Stegel V, Teugels E, Bešič N, et al. Geographical distribution of Slovenian BRCA1/2 families according to family origin: implications for genetic screening. *Clin Genet* 2014; **85**: 59-63. doi: 10.1111/cge.12119
13. Bešič N, Černivc B, de Grève J, Lokar K, Krajc M, Novaković S, et al. BRCA2 gene mutations in Slovenian male breast cancer patients. *Genet Test* 2008; **12**: 203-9. doi: 10.1089/gte.2007.0071
14. Krajc M, Blatnik A, Stegel V, Cerkovnik P, Škof E, Novaković S. BRCA status in ovarian cancer patients predicts therapeutic approach – first results. In: Writzl K, Teran N, Maver A, editors. *6th symposium of the Slovenian Association of Medical Genetics. Gene editing technology: applications and societal implications*. Book of abstracts; 2016 Apr 22; Ljubljana, Slovenia. Ljubljana: Slovenian Association of Medical Genetics, Slovenian Medical Association; 2016. p. 19.
15. Alsop K, Fereday S, Meldrum C, deFazio A, Emmanuel C, George J, et al. BRCA mutation frequency and patterns of treatment response in BRCA mutation-positive women with ovarian cancer: a report from the Australian Ovarian Cancer Study Group. *J Clin Oncol* 2012; **30**: 2654-63. doi: 10.1200/JCO.2011.39.8545
16. Girolimetti G., Perrone AM, Santini D, Barbieri E, Guerra F, Ferrari S, et al. BRCA-associated ovarian cancer: From molecular genetics to risk management. *Biomed Res Int* 2014; **2014**: 787143. doi: 10.1155/2014/787143
17. Lakhani SR, Manek S, Penault-Lorca F, Flanagan A, Arnout L, Merrett S, et al. Pathology of ovarian cancers in BRCA1 and BRCA2 carriers. *Clin Cancer Res* 2004; **10**: 2473-81. doi: 10.1158/1078-0432.CCR-1029-3
18. Fishman A, Dekel E, Chetrit A, Lerner-Geva L, Bar-Am, Deck D, et al. Patients with double-primary tumors in the breast and ovary – clinical characteristics and BRCA1-2 mutations status. *Gynecol Oncol* 2000; **79**: 74-8. doi: 10.1006/gy.2000.5895
19. Schorge JO, Mahoney NM, Miller DS, Coleman RL, Muller CY, Euhus DM, et al. Germline BRCA1-2 mutations in Non-Ashkenazi families with double primary breast and ovarian cancer. *Gynecol Oncol* 2001; **83**: 383-7. doi: 10.1006/gy.2001.6431
20. Mavaddat N, Barrowdale D, Andrulis IL, Domchek SM, Eccles D, Nevanlinna H, et al. Pathology of breast and ovarian cancers among BRCA1 and BRCA2 mutation carriers: Results from the Consortium of Investigators of Modifiers of BRCA1/2 (CIMBA). *Cancer Epidemiol Biomarkers Prev* 2012; **21**: 134-47. doi: 10.1158/1055-9965.EPI-11-0775

21. Boyd J, Sonoda Y, Federici MG, Bogomolny F, Rhei E, Maresco DL, et al. Clinicopathologic features of BRCA-linked and sporadic ovarian cancer. *JAMA* 2000; **283**: 2260-5.
22. Prat J. Ovarian carcinomas: five distinct diseases with different origins, genetic alterations, and clinicopathologic features. *Virchows Arch* 2012; **460**: 237-49. doi: 10.1007/s00428-012-1203-5
23. Rakar S, Štolfa A, Kovačič J. Ovarijski karcinom: današnje stanje in perspektive. *Zdrav Vestn* 1994; **63**: 569-71.
24. Cvelbar M, Kralj B. Zgodnje odkrivanje epitelnega karcinoma jajčnika. *Zdrav Vestn* 2001; 81-4.
25. Schwartz DR, Kardia SLR, Shedden KA, Kuick R, Michailidis G, Taylor JMG, et al. Gene expression in ovarian cancer reflects both morphology and biological behavior, distinguishing clear cell from other poor-prognosis ovarian carcinomas. *Cancer Res* 2002; **62**: 4722-9.
26. Tothill RW, Tinker AV, George J, Brown R, Fox SB, Lade S, et al. Novel molecular subtypes of serous and endometrioid ovarian cancer linked to clinical outcome. *Clin Cancer Res* 2008; **14**: 5198-208. doi: 10.1158/1078-0432
27. Wickramanayake A, Bernier G, Pennil C, Casadei S, Agnew KJ, Stray SM, et al. Loss of function germline mutations in RAD51D in women with ovarian carcinoma. *Gynecol Oncol* 2012; **127**: 552-5. doi: 10.1016/j.ygyno.2012.09.009

Insulin-like growth factor 1 receptor expression in advanced non-small-cell lung cancer and its impact on overall survival

Mojca Humar¹, Izidor Kern², Gregor Vlacic², Vedran Hadzic³, Tanja Cufer²

¹ General hospital of Nova Gorica, Šempeter Pri Gorici, Slovenia

² University Clinic Golnik, Golnik, Slovenia

³ Faculty of Sport, University of Ljubljana, Slovenia, Ljubljana, Slovenia

Radiol Oncol 2017; 51(2): 195-202.

Received 16 October 2016

Accepted 8 November 2016

Correspondence to: Mojca Humar, M.D., General Hospital of Nova Gorica, Ulica padlih borcev 13a, 5290 Šempeter pri Gorici, Slovenia. Phone: +386 5 330 1000; Fax: +386 5 330 1057; Email: moj.humar@gmail.com

Disclosure: No potential conflicts of interest were disclosed.

Background. The insulin-like growth factor 1 receptor (IGF1R) expression has been addressed as a potential prognostic marker in non-small-cell lung cancer (NSCLC) in various studies; however, the associations between IGF1R expression and prognosis of advanced NSCLC patients is still controversial. The aim of our observational, cohort study was to evaluate the expression of IGF1R in advanced NSCLC and its prognostic role. A subgroup analysis was performed to address the influence of pre-existing type 2 diabetes mellitus (T2DM) status on IGF1R expression and overall survival (OS).

Patients and methods. IGF1R expression was evaluated in 167 consecutive advanced NSCLC patients (stage IIIb and IV), diagnosed and treated at one university institution, between 2005 and 2010. All patients received at least one line of standard cytotoxic therapy and 18 of them had pre-existing T2DM. IGF1R expression was determined by immunohistochemical (IHC) staining, with score $\geq 1+$ considered as positive. Information on baseline characteristics, as well as patients' follow-up data, were obtained from the hospital registry. Associations of IGF1R expression with clinical characteristics and overall survival were compared.

Results. IGF1R expression was positive in 79.6% of patients, significantly more often in squamous-cell carcinoma (SCC) compared to non-squamous-cell (NSCC) histology (88.7% vs. 74.3%; $P = 0.03$). IGF1R positivity did not correlate with T2DM status or with other clinical features (sex, smoking status, performance status). Median OS was similar between IGF1R positive and IGF1R negative group (10.2 vs. 8.5 months, $P = 0.168$) and between patients with or without T2DM (8.7 vs. 9.8 months, $P = 0.575$). Neither IGF1R expression nor T2DM were significant predictors of OS.

Conclusions. IGF1R or T2DM status were not significantly prognostic in described above collective of advanced NSCLC treated with at least one line of chemotherapy. In addition, no association between T2DM status and IGF1R expression was found. Further studies on IGF1R expression and its prognostic as well as therapeutic consequences in a larger collective of advanced NSCLC patients, with or without T2DM, are needed.

Key words: insulin-like growth factor 1 receptor; type 2 diabetes mellitus; advanced non-small-cell lung cancer; overall survival

Introduction

Lung cancer is the most common cancer diagnosed worldwide, and approximately 85% of cases represent non-small-cell lung cancer (NSCLC).¹ Since

lung cancer in the early stages is generally asymptomatic, almost two-thirds of patients are diagnosed in advanced stages.^{2,3} While patients with localized or locally advanced lung cancer have approximately 50% and 30% chance of five-year

survival⁴, advanced lung cancer is still incurable. Despite the rise in survival rates lately, five-year relative survival of patients with advanced lung carcinoma remains poor.⁴

Advances in recent survival rates are attributable to the discovery of potential targets such as mutations in the epidermal growth factor receptor (EGFR) or rearrangements in the anaplastic lymphoma kinase (ALK) gene and consecutive development of targeted therapies with monoclonal antibodies (mAb) and tyrosine kinase inhibitors (TKI).^{5,6} However, although targeted therapies offer high objective response rates and improved progression-free survival (PFS), eventually acquired resistance develops, leading to disease progression.⁷ To overcome the resistance mechanisms new molecular alterations in different other co-activated pathways are extensively sought.

The insulin-like growth factor 1 receptor (IGF1R) signalling pathway has been shown to promote oncogenic transformation and cancer cell growth and survival^{8,9} and has been associated with resistance to specific oncologic therapies in various human cancers¹⁰⁻¹², including EGFR-TKI^{13,14} and ALK-TKI¹⁵ in NSCLC. With various lines of evidence supporting IGF1R signalling pathway as a potential target for cancer therapy, different anti-IGF1R mAbs and small-molecule TKIs were developed and entered clinical trials. However, despite the encouraging preclinical data, all the trials performed so far failed to confirm a meaningful clinical response in NSCLC patients treated with IGF1R inhibitors, although such results can be attributed to unselected patients, lack of predictive biomarkers and compensatory signalling through other growth factor pathways.¹⁶

IGF1R is a transmembrane heterotetrameric protein with tyrosine kinase activity. Binding of IGF1 and IGF2 activates the IGF1R, triggering a series of reactions via the PI3K-AKT and RAS/RAF/mitogen-activated protein kinase signalling pathways, enhancing cancer cell growth, survival and metastasizing.

IGF1R and its signalling pathway were extensively studied in various human cancers. In hormone-receptor positive breast cancer (luminal A, luminal B) positive IGF1R expression is associated with better prognosis^{17,18}, while in triple negative breast cancer it negatively affects survival.^{17,19} Similarly, IGF1R overexpression in laryngeal²⁰, cervical²¹, pancreatic²², gastric²³, renal²⁴ and urothelial carcinoma²⁵ is linked to worse survival rates, whereas the influence of IGF1R overexpression on

survival in colorectal and endometrial carcinoma remains unconfirmed.²⁶⁻²⁹

IGF1R expression was also addressed as a potential prognostic marker in NSCLC in various studies.^{14,30-47} Most of the studies involved patients with resected lung cancer and only four among them were performed in advanced NSCLC.^{12,32,42,44} Cappuzzo *et al.* found that gefitinib-treated patients with high IGF1R overexpression had longer median survival⁴⁴, while Yeo *et al.* reported a shorter progression-free survival in response to EGFR-TKI in EGFR mutated patients¹⁴, while Kim *et al.* found no significant connection between IGF1R overexpression and survival of advanced NSCLC patients.⁴⁶ Similar results were obtained in surgically treated NSCLC patients.^{30-33,35-42,45,47} In 2014 a meta-analysis including 17 studies evaluating IGF1R expression and its impact on survival in NSCLC patients was published, that confirmed the association between positive IGF1R expression and worse disease-free survival, but not OS.⁴⁸ However, only three studies evaluated IGF1R expression in advanced NSCLC^{34,44,46}, and a subgroup analysis of two of them^{44,46}, including 77 and 68 patients respectively, showed a significant correlation between IGF1R expression and better OS.

Moreover, optimal evaluation of IGF1R expression remains unconfirmed. In most of the published studies in NSCLC IGF1R protein expression was measured by immunohistochemistry, while some also evaluated *IGF1R gene* expression using quantitative reverse transcription polymerase chain reaction (qRT-PCR) and *IGF1R gene* copy number by in situ hybridization. In summary, scarce and conflicting information exist concerning IGF1R expression impact on survival in advanced NSCLC.

There are epidemiological data supporting the biological link between cancer and type 2 diabetes mellitus (T2DM) and the well-known fact that patients with T2DM have an increased risk of cancer and cancer-related mortality.⁴⁹ In a recently published study, a higher IGF1R expression - according to the previously mentioned meta-analysis a detrimental prognostic factor in operable NSCLC - was found in early stage NSCLC patients with pre-existing T2DM, suggesting a possible role of IGF1R signalling pathway in the development and growth of NSCLC.⁵⁰ Type 2 diabetes mellitus is characterized by insulin resistance and resultant chronic hyperinsulinemia, which enhances growth hormone receptor expression in the liver, increases IGF1 production and availability, thus leading to the IGF1R signalling pathway activation.^{51,52} Several meta-

analyses and studies have been published in the recent years, confirming diabetes mellitus as a negative prognostic factor for breast, colorectal, gastric, pancreatic, liver, prostate, renal and cervical cancer survival.⁵³⁻⁶⁰ Studies addressing the prognostic role of T2DM in NSCLC patients have been contradictory.⁶¹⁻⁶³ However, the recently published meta-analysis confirmed a significant association between T2DM and worse prognosis in NSCLC patients, especially in surgically treated patients.⁶⁴ There are also data showing that the use of metformin, one of the most commonly prescribed drugs for diabetes mellitus, improves the generally bad prognosis of cancer patients with concomitant T2DM. In a large meta-analysis, the use of metformin was associated with a significant improvement in overall survival and cancer-specific survival of cancer patients.⁶⁵

The purpose of this study was to evaluate IGF1R expression in advanced NSCLC and its impact on OS. Furthermore, we evaluated the influence of T2DM on OS and IGF1R expression in advanced NSCLC.

Patients and methods

Our study was performed following the Recommendations for Tumour Marker Prognostic Studies (REMARK).⁶⁶

Patient selection

In the present study 167 consecutive patients, with pathohistologically confirmed advanced NSCLC stage IIIB (20 patients) and IV (147 patients), treated with at least one line of cytotoxic therapy at the University Clinic Golnik, Slovenia, between 2005 and 2010, and with available tissue for immunohistochemical analysis, were included. All patients were treated and followed according to the standard clinical practices at the time. All patients received at least one systemic treatment, that comprised of platinum doublets in a vast majority of them (165/167 patients; 98.8%), only two patients (1.2%) received gemcitabine monotherapy. The median follow-up time was 9.79 months (range 0.20–72.34 months).

Information on baseline demographics and clinicopathological characteristics of the patients were obtained from our hospital registry system, whilst date of death was obtained from the National Cancer Registry.

The study was reviewed and approved by the National Ethics Committee (No. 135/07/09).

Tissue preparation and immunohistochemical analysis

Formalin-fixed, paraffin-embedded tissue sections containing preserved tumour tissue from primary tumour obtained at diagnosis were used for immunohistochemical analysis.

Tissue sections 4- μ m thick were deparaffinized in xylene and rehydrated in a graded series ethanol. After standard antigen retrieval with Cell Conditioning 1 (CC1) buffer solution (Ventana Medical Systems, Tucson, Arizona, USA), staining with pre-diluted rabbit monoclonal antibody against human IGFR-1 (Ventana G11; CONFIRM, Ventana Medical Systems, Tucson, Arizona, USA; ready-to-use concentration 1.7 μ g/mL) was performed on Ventana BenchMark XT autostainer with a 16 minutes primary antibody incubation time at 37°C. Binding detection of the primary antibody was performed utilizing the *ultraView* Universal DAB Detection Kit (Ventana Medical Systems, Tucson, Arizona, USA), and subsequently, the slides were counterstained with Hematoxylin II (Ventana Medical Systems, Tucson, Arizona, USA), according to the manufacturers' recommendations. The omission of the primary antibody was used as a negative control. IGF1R expression in adjoining normal-appearing bronchial epithelium within each tissue section was used as an internal positive control.

Immunohistochemical (IHC) staining of the invasive cancer components was independently evaluated on at least 2 x 2 mm cores per patient by two observers (MH, GV), blinded to all patient data. Discrepant cases were reviewed by a third observer (IK). Cell membrane and cytoplasm staining was scored on a scale of 0 (no staining), 1+ (weak staining), 2+ (moderate staining), and 3+ (strongly positive staining). Since there are no validated and standardized cut-off values for IGF1R-IHC positivity, membrane staining equal or above 1+ in at least 1% of tumour cells was considered positive.

Statistical analysis

Associations of IGF1R expression with patient clinical characteristics were compared by chi-square test. OS (time in months from diagnosis date to patient death) was evaluated using Kaplan-Meier method and hazard ratio was calculated by using the Cox proportional hazards regression model. OS for the subgroups was compared using the log-rank test.

Statistical analysis was performed using IBM SPSS ver. 19.0 (SPSS Inc., Chicago, IL, USA). A

TABLE 1. Patient and tumour characteristics

Variable	No (%)
All patients	167 (100%)
Histology	
NSCC	105 (62.9%)
SCC	62 (37.1%)
Sex	
Male	119 (71.3%)
Female	48 (28.7%)
Smoking status	
Current/former smoker	145 (86.8%)
Never smoker	22 (13.2%)
ECOG-PS	
0–1	152 (91.0%)
≥ 2	15 (9.0%)
Diabetes mellitus type 2	
No	149 (89.2%)
Yes	18 (10.8%)
IGF1R expression	
Positive	133 (79.6%)
Negative	34 (20.4%)

ECOG-PS = Eastern Cooperative Oncology Group performance status; IGF1R = insulin-like growth factor-1 receptor; NSCC = non-squamous cell carcinoma; SCC = squamous cell carcinoma

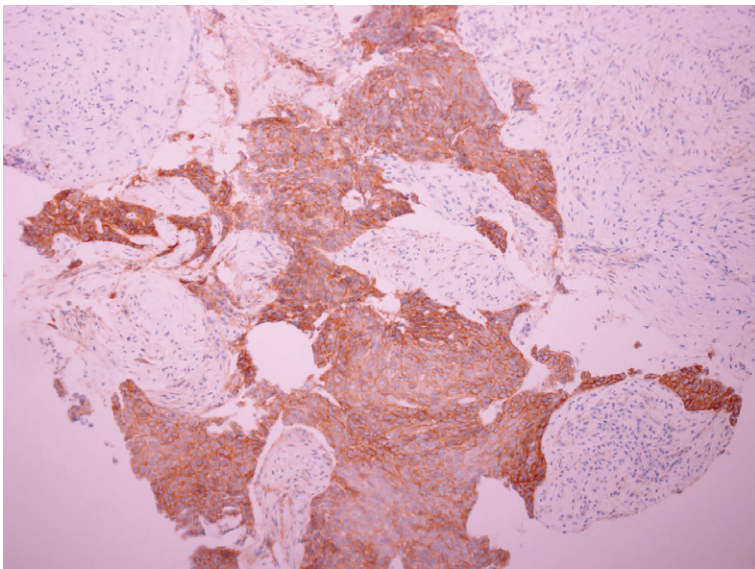


FIGURE 1. Representative immunohistochemical staining of insulin-like growth factor 1 receptor in a squamous-cell carcinoma sample.

P-value less than 0.05 was determined as statistically significant. All reported *P*-values are two-tailed.

Results

Patient and tumour characteristics

A total of 167 patients were included in this study. Baseline demographics and clinicopathological characteristics are summarized in Table 1. At the time of diagnosis, median age was 63 years (range 40–82 years), 37.1% of cases were squamous-cell carcinoma (SCC; 62/167 patients) and 62.9% were non-squamous-cell (NSCC; 105/167 patients) histology. The majority of patients were males (119/167; 71.3%), smokers or former smokers (145/167; 86.8%) and had an estimated Eastern Cooperative Oncology Group (ECOG) performance status of 0–1 (152/167; 91.0%). Pre-existing T2DM was present in 18 (10.8%) of patients; 8 out of 18 were receiving metformin, while the rest of them were treated with other oral antidiabetic medications or insulin.

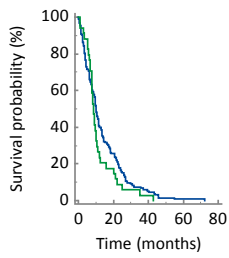
IGF1R expression

IGF1R expression was found in 133/167 (79.6%) of tumour samples. IGF1R positivity was significantly more frequent in SCC (88.7%) compared to NSCC (74.3%) ($P = 0.03$) (Figure 1). However, there was no significant association between IGF1R positivity rate and sex, smoking status, performance status or T2DM (Table 2). The IGF1R positivity rate was quite similar in patients with or without T2DM; 77.8% and 79.9%, respectively.

Survival analysis

Median OS was similar between IGF1R positive and IGF1R negative group (10.2 versus 8.5 months, $P = 0.168$) (Figure 2) and also between patients with or without T2DM (8.7 versus 9.8 months, $P = 0.575$) (Figure 3).

Neither IGF1R expression nor T2DM were significant predictors of overall survival in the univariate and multivariate analysis. Regarding the other characteristics included in the analysis, no significant differences in survival were observed based on histology, whereas sex, smoking status and performance status were borderline significant in the univariate analysis, but in multivariate analysis only performance status remained borderline significant ($P = 0.057$) (Table 3).

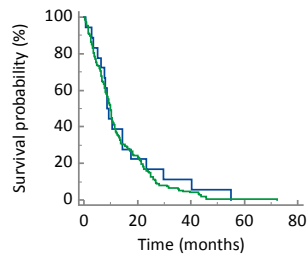


Number at risk

Group: IGF1R IHC POSITIVE	133	34	7	1	0
Group: IGF1R IHC NEGATIVE	34	6	1	0	0

Legend: IGF1R IHC POSITIVE (blue line), IGF1R IHC NEGATIVE (green line)

FIGURE 2. Median overall survival based on insulin-like growth factor 1 receptor (IGF1R) expression.



Number at risk

Group: T2DM YES	18	4	2	0	0
Group: T2DM NO	149	36	6	1	0

Legend: T2DM YES (blue line), T2DM NO (green line)

FIGURE 3. Median overall survival based on type 2 diabetes mellitus (T2DM) status.

TABLE 2. IHC IGF1R expression by histological/clinical characteristics and diabetes mellitus

Variable	IGF1R positive No (%)	IGF1R negative No (%)	P value
All patients	133 (79.6%)	34 (20.4%)	
Histology			0.03
NSCC	78 (74.3%)	27 (25.7%)	
SCC	55 (88.7%)	7 (11.3%)	
Sex			0.17
Male	98 (82.4%)	21 (17.6%)	
Female	35 (72.9%)	13 (27.1%)	
Smoking status			0.77
Current/former smoker	116 (80.0%)	29 (20.0%)	
Never smoker	17 (77.3%)	5 (22.7%)	
ECOG PS			0.97
0-1	121 (79.6%)	31 (20.4%)	
≥ 2	12 (80.0%)	3 (20.0%)	
Diabetes mellitus type 2			0.84
No	119 (79.9%)	30 (20.1%)	
Yes	14 (77.8%)	4 (22.2%)	

ECOG-PS = Eastern Cooperative Oncology Group performance status; IGF1R = insulin-like growth factor-1 receptor; NSCC = non-squamous cell carcinoma; SCC = squamous cell carcinoma

Discussion

In the present study, we aimed to assess the prognostic impact of IGF1R expression in 167 advanced NSCLC patients treated with at least one line of chemotherapy, and to evaluate the impact of T2DM on IGF1R expression, as well as its prognostic role. Neither IGF1R expression nor T2DM status were found to be independent predictors of OS in advanced NSCLC in the multivariate analysis of survival. In addition, no association between T2DM status and IGF1R expression was found. However,

a significantly higher expression of IGF1R in SCC compared to NSCC histology was observed.

Interestingly, a significant association between positive IGF1R expression and SCC histology was

TABLE 3. Univariate and multivariate analysis of overall survival

Variable	Univariate Analysis			Multivariate Analysis		
	HR	95%CI	P value	HR	95%CI	P value
Histology						
SCC vs NSCC	1.097	0.798-1.509	0.569	1.249	0.885-1.763	0.206
Sex						
Male vs female	1.396	0.994-1.961	0.054	1.390	0.939-2.057	0.100
Smoking status						
Current/former smoker vs. non-smoker	1.692	1.064-2.689	0.026	1.509	0.908-2.510	0.113
ECOG-PS						
0-1 vs ≥ 2	0.600	0.351-1.025	0.061	0.589	0.341-1.015	0.057
Diabetes mellitus type 2						
Yes vs No	0.869	0.531-1.423	0.576	0.828	0.498-1.378	0.468
IGF1R						
Positive vs negative	0.766	0.523-1.121	0.170	0.776	0.518-1.162	0.219

ECOG-PS = Eastern Cooperative Oncology Group performance status; IGF1R = insulin-like growth factor-1 receptor; NSCC = non-squamous cell carcinoma; SCC = squamous cell carcinoma

observed in our study ($P = 0.03$), that is in line with the data from the meta-analysis of Zhao *et al.*, where a trend towards an increased IGF1R expression in SCC histology was noted.⁴⁸ However, only 10 out of 17 included studies (46% of included patients) had sufficient data to assess the relationship between IGF1R expression and histology. In addition, in advanced NSCLC Kim *et al.* found a significantly higher IGF1R expression in the SCC subgroup.⁴⁶ Although the molecular basis of IGF1R overexpression in SCC remains unknown, these data suggest IGF1R expression might reflect an important role of the IGF1R signalling pathway in SCC development and spread.

No significant associations were noted between IGF1R expression and sex, smoking status and performance status in our study. Similarly, other published studies in advanced NSCLC did not report an association between IGF1R expression and the aforementioned prognostic factors^{14,34,44}, with the exception of the study by Kim *et al.*, where IGF1R expression was associated with smoking status⁴⁶, in accordance to the meta-analysis.⁴⁸ Whether this is a consequence of an underlying molecular mechanism, or the result of the majority of NSCLC patients being smokers, remains to be elucidated.

Although the OS of IGF1R positive patients with advanced NSCLC was longer than OS to IGF1R negative counterparts (10.2 *vs.* 8.5 months, $P = 0.168$), this difference was not statistically significant. The trend shown in our study is consistent with the subgroup analysis in the meta-analysis, where IGF1R positive expression was associated with significantly better OS in NSCLC stage III and IV patients⁴⁸, proposing that aberrant signalling pathways, other than IGF1R, take over the major role in advanced NSCLC progression.

Despite the increasing evidence that T2DM negatively affects cancer prognosis^{49,53-61,63,64}, we could not prove a significant influence of T2DM on advanced NSCLC survival. Besides a relatively small proportion of patients with T2DM in our study ($N = 18$; 10.8%), another confounding factor might be the fact, that almost half of our patients with T2DM were treated with metformin, known to improve cancer prognosis.⁶⁵ Furthermore, IGF1R was not overexpressed in T2DM patients, compared to non-T2DM patients, opposing findings of Ding *et al.* who found higher IGF1R expression in patients with T2DM, compared to non-T2DM patients.⁵⁰ However, as our T2DM subgroup was underpowered, our results need further confirmation on a larger group of patients with advanced NSCLC and T2DM.

In the present study, IGF1R expression was determined by immunohistochemistry, with an arbitrarily predefined cut-off value of $\geq 1+$. To emphasise, there are no validated scoring systems or cut-off values for IGF1R expression available, and in the published studies different thresholds were used, resulting in great differences in the percentage of positive samples (range 12.7% to 78.0%).^{14,30-45} Moreover, Dziadziuszko *et al.* reported that different anti-IGF1R antibodies on the market have different specificity to IGF1R.³⁰ In summary, methodological issues might have a strong influence on IGF1R expression evaluation and the need for a validated system for IGF1R expression detection is warranted.

The major limitation of our study is the retrospective design and a relatively small number of advanced NSCLC patients included, especially patients with T2DM, affecting statistical power of survival analysis and accuracy of the findings. In addition, no validated scoring system for immunohistochemical IGF1R expression and an arbitrarily defined cut-off value for IGF1R positivity may be another source of bias. Unfortunately, in all of the studies addressing the prognostic role of IGF1R expression in advanced NSCLC the same limitations arise.^{14,34,44,46} Furthermore, tissue samples retrieved in NSCLC are often scanty, with small biopsies failing to show any intra-tumoural biomarker heterogeneity.

In conclusion, we did not confirm a prognostic value of IGF1R overexpression or T2DM in advanced NSCLC patients, treated with at least one line of chemotherapy. In spite of those negative findings in relation to IGF1R overexpression, we have shown a significant association between IGF1R and SCC, indicating a possible oncogenic role of IGF1R in SCC that deserves a further research. Yet, based on a small number of patients in our study, further prospective studies on IGF1R expression and its prognostic as well as therapeutic consequences in a larger collective of advanced NSCLC patients, with or without T2DM, are needed.

Acknowledgements

The authors thank Tončka Urbanc and Mitja Rot for help with tissue sections preparation and immunohistochemistry. This work was funded by Slovenian Research Agency Grant J3-4076.

References

- International Agency for Research on Cancer. World Health Organization. *GLOBOCAN 2012: estimated cancer incidence, mortality and prevalence worldwide in 2012*. Lung cancer fact sheet. [Cited 2016 Jun 15]. Available at http://globocan.iarc.fr/Pages/fact_sheets_cancer.aspx?cancer=lung.
- Morgensztern D, Ng SH, Gao F, Govindan R. Trends in stage distribution for patients with non-small cell lung cancer: A National Cancer Database survey. *J Thorac Oncol* 2010; **5**: 29-33. doi: 10.1097/JTO.0b013e3181c5920c
- Debevec L, Jerič T, Kovač V, Bitenc M, Sok M. Is there any progress in routine management of lung cancer patients? A comparative analysis of an institution in 1996 and 2006. *Radiol Oncol* 2009; **43**: 47-53. doi: 10.2478/v10019-009-0008-x
- Howlander N, Noone AM, Krapcho M, Miller D, Bishop K, Altekruse SF, et al. *SEER cancer statistics review, 1975-2013*. Bethesda: National Cancer Institute. [Cited 2016 Sept 04]. Available at http://seer.cancer.gov/csr/1975_2013/
- Sechler M, Cizmic AD, Avasarala S, Van Scoyk M, Brzezinski C, Kelley N, et al. Non-small-cell lung cancer: molecular targeted therapy and personalized medicine – drug resistance, mechanisms, and strategies. *Pharmgenomics Pers Med* 2013; **6**: 25-36. doi: 10.2147/PGPM.S26058
- Zwitter M, Stanic K, Rajer M, Kern I, Vrankar M, Edelbaher N, Kovac V. Intercalated chemotherapy and erlotinib for advanced NSCLC: high proportion of complete remissions and prolonged progression-free survival among patients with EGFR activating mutations. *Radiol Oncol* 2014; **48**: 361-8. doi: 10.2478/raon-2014-0038
- Wang J, Wang B, Chu H, Yao Y. Intrinsic resistance to EGFR tyrosine kinase inhibitors in advanced non-small-cell lung cancer with activating EGFR mutations. *Onco Targets Ther* 2016; **9**: 3711-26. doi: 10.2147/OTT.S106399
- Ward CW, Garrett TP, McKern NM, Lou M, Cosgrove LJ, Sparrow LG, et al. The three dimensional structure of the type I insulin-like growth factor receptor. *Mol Pathol* 2001; **54**: 125-32.
- Blakesley VA, Stannard BS, Kalebic T, Helman LJ, LeRoith D. Role of the IGF-1 receptor in mutagenesis and tumor promotion. *J Endocrinol* 1997; **152**: 339-44.
- Eckstein N, Servan K, Hildebrandt B, Politz A, von Jonquieres G, Wolf-Kümmeth S, et al. Hyperactivation of the insulin-like growth factor receptor I signalling pathway is an essential event for cisplatin resistance of ovarian cancer cells. *Cancer Res* 2009; **69**: 2996-3003. doi: 10.1158/0008-5472.CCR-08-3153
- Huang F, Xu LA, Khambata-Ford S. Correlation between gene expression of IGF-1R pathway markers and cetuximab benefit in metastatic colorectal cancer. *Clin Cancer Res* 2012; **18**: 1156-66. doi: 10.1158/1078-0432.CCR-11-1135
- Yuen JS, Akkaya E, Wang Y, Takiguchi M, Peak S, Sullivan M, et al. Validation of the type I insulin-like growth factor receptor as a therapeutic target in renal cancer. *Mol Cancer Ther* 2009; **8**: 1448-59. doi: 10.1158/1535-7163.MCT-09-0101
- Suda K, Mizuuchi H, Sato K, Takemoto T, Iwasaki T, Mitsudomi T. The insulin-like growth factor 1 receptor causes acquired resistance to erlotinib in lung cancer cells with the wild-type epidermal growth factor receptor. *Int J Cancer* 2014; **135**: 1002-6. doi: 10.1002/ijc.28737
- Yeo CD, Park KH, Park CK, Lee SH, Kim SJ, Yoon HK, et al. Expression of insulin-like growth factor 1 receptor (IGF-1R) predicts poor responses to epidermal growth factor receptor (EGFR) tyrosine kinase inhibitors in non-small cell lung cancer patients harboring activating EGFR mutations. *Lung Cancer* 2015; **87**: 311-7. doi: 10.1016/j.lungcan.2015.01.004
- Lovly CM, McDonald NT, Chen H, Ortiz-Cuaran S, Heukamp LC, Yan Y, et al. Rationale for co-targeting IGF1R and ALK in ALK fusion-positive lung cancer. *Nat Med* 2014; **20**: 1027-34. doi: 10.1038/nm.3667
- Beckwith H, Yee D. Minireview: Were the IGF signaling inhibitors all bad? *Mol Endocrinol* 2015; **29**: 1549-57. doi: 10.1210/me.2015-1157.
- Yerushalmi R, Gelmon KA, Leung S, Gao D, Cheang M, Pollak M, et al. Insulin-like growth factor receptor (IGF-1R) in breast cancer subtypes. *Breast Cancer Res Treat* 2012; **132**: 131-42. doi: 10.1007/s10549-011-1529-8
- Mountzios G, Aivazi D, Kostopoulos I, Kourea HP, Kouvatseas G, Timotheadou E, et al. Differential expression of the insulin-like growth factor receptor among early breast cancer subtypes. *PLoS One* 2014; **9**: e91407. doi: 10.1371/journal.pone.0091407
- Bahnassy A, Mohanad M, Shaarawy S, Ismail MF, El-Bastawisy A, Ashmawy AM, et al. Transforming growth factor- β , insulin-like growth factor I/insulin-like growth factor I receptor and vascular endothelial growth factor-A: prognostic and predictive markers in triple-negative and non-triple-negative breast cancer. *Mol Med Rep* 2015; **12**: 851-64. doi: 10.3892/mmr.2015.3560
- Mountzios G, Kostopoulos I, Kotoula V, Sfakianaki I, Fountzilas E, Markou K, et al. Insulin-like growth factor 1 receptor (IGF1R) expression and survival in operable squamous-cell laryngeal cancer. *PLoS One* 2013; **8**: e54048. doi: 10.1371/journal.pone.0054048
- Huang Y-F, Shen M-R, Hsu K-F, Cheng Y-M, Chou C-Y. Clinical implications of insulin-like growth factor 1 system in early-stage cervical cancer. *Br J Cancer* 2008; **99**: 1096-102. doi: 10.1038/sj.bjc.6604661
- Hirakawa T, Yashiro M, Murata A, Hirata K, Kimura K, Amano R, et al. IGF-1 receptor and IGF binding protein-3 might predict prognosis of patients with resectable pancreatic cancer. *BMC Cancer*. 2013; **13**: 392. doi: 10.1186/1471-2407-13-392
- Numata K, Oshima T, Sakamaki K, Yoshihara K, Aoyama T, Hayashi T, et al. Clinical significance of IGF1R gene expression in patients with Stage II/III gastric cancer who receive curative surgery and adjuvant chemotherapy with S-1. *J Cancer Res Clin Oncol* 2016; **142**: 415-22. doi: 10.1007/s00432-015-2039-6
- Sichani MM, Yazdi FS, Moghaddam NA, Chehrei A, Kabiri M, Naeimi A, et al. Prognostic value of insulin-like growth factor-I receptor expression in renal cell carcinoma. *Saudi J Kidney Dis Transpl* 2010; **21**: 69-74.
- Gonzalez-Roibon N, Kim JJ, Faraj SF, Chau X, Bezerra SM, Munari E, et al. Insulin-like growth factor-1 receptor overexpression is associated with outcome in invasive urothelial carcinoma of urinary bladder: a retrospective study of patients treated using radical cystectomy. *Urology* 2014; **83**: 1444.e1-6. doi: 10.1016/j.urol.2014.01.028
- Cappuzzo F, Varella-Garcia M, Finocchiaro G, Skokan M, Gajapathy S, Carnaghi C, et al. Primary resistance to cetuximab therapy in EGFR FISH-positive colorectal cancer patients. *Br J Cancer* 2008; **99**: 83-9. doi: 10.1038/sj.bjc.6604439
- Takahari D, Yamada Y, Okita N, T, Honda T, Hirashima Y, Matsubara J, et al. Relationships of insulin-like growth factor-1 receptor and epidermal growth factor receptor expression to clinical outcomes in patients with colorectal cancer. *Oncology* 2009; **76**: 42-8. doi: 10.1159/000178164
- Joehlin-Price AS, Stephens JA, Zhang J, Backes FJ, Cohn DE, Suarez AA. Endometrial cancer insulin-like growth factor 1 receptor (IGF1R) expression increases with body mass index and is associated with pathologic extent and prognosis. *Cancer Epidemiol Biomarkers Prev* 2016; **25**: 438-45. doi: 10.1158/1055-9965.EPI-15-1145
- Peiró G, Lohse P, Mayr D, Diebold J. Insulin-like growth factor-I receptor and PTEN protein expression in endometrial carcinoma. Correlation with bax and bcl-2 expression, microsatellite instability status, and outcome. *Am J Clin Pathol* 2003; **120**: 78-85. doi: 10.1309/C1KA-H1PR-L1UB-W798
- Dzadzadziszko R, Merrick DT, Witta SE, Mendoza AD, Szostakiewicz B, Szymanowska A, et al. Insulin-like growth factor receptor 1 (IGF1R) gene copy number is associated with survival in operable non-small-cell lung cancer: a comparison between IGF1R fluorescent in situ hybridization, protein expression, and mRNA expression. *J Clin Oncol* 2010; **28**: 2174-80. doi: 10.1200/JCO.2009.24.6611
- Lee CY, Jeon JH, Kim HJ, Shin DH, Roh TW, Ahn CM, et al. Clinical significance of insulin-like growth factor-1 receptor expression in stage I non-small-cell lung cancer: immunohistochemical analysis. *Korean J Intern Med* 2008; **23**: 116-20. doi: 10.3904/kjim.2008.23.3.116
- Gong Y, Yao E, Shen R, Goel A, Arcila M, Teruya-Feldstein J, et al. High expression levels of total IGF-1R and sensitivity of NSCLC cells in vitro to an anti-IGF-1R antibody (R1507). *PLoS One* 2009; **4**: e7273. doi: 10.1371/journal.pone.0007273
- Cappuzzo F, Tallini G, Finocchiaro G, Wilson RS, Ligorio C, Giordano L, et al. Insulin-like growth factor receptor 1 (IGF1R) expression and survival in surgically resected non-small-cell lung cancer (NSCLC) patients. *Ann Oncol* 2010; **21**: 562-7. doi: 10.1093/annonc/mdp357

34. Ning XH, Wang YZ, Bai CM, Li J. Clinical significance of insulin-like growth factor-1 receptor in platinum-based chemotherapy for non-small cell lung cancer. [Chinese]. *Zhongguo Yi Xue Ke Xue Yuan Xue Bao* 2010; **32**: 366-70. doi: 10.3881/j.issn.1000-503X.2010.04.002
35. Tsuta K, Mimae T, Nitta H, Yoshida A, Maeshima AM, Asamura H, et al. Insulin-like growth factor-1 receptor protein expression and gene copy number alterations in non-small cell lung carcinomas. *Hum Pathol* 2013; **44**: 975-82. doi: 10.1016/j.humpath.2012.09.002
36. Ludovini V, Flacco A, Bianconi F, Ragusa M, Vannucci J, Bellezza G, et al. Concomitant high gene copy number and protein overexpression of IGF1R and EGFR negatively affect disease-free survival of surgically resected non-small-cell-lung cancer patients. *Cancer Chemother Pharmacol* 2013; **71**: 671-80. doi: 10.1007/s00280-012-2056-y
37. Zhang X, Sun J, Wang H, Lou Y, Zhang Y, Sha H, et al. IGF-1R and Bmi-1 expressions in lung adenocarcinoma and their clinicopathologic and prognostic significance. *Tumour Biol* 2014; **35**: 739-45. doi: 10.1007/s13277-013-1100-9
38. Gately K, Forde L, Cuffe S, Cummins R, Kay EW, Feuerhake F, et al. High coexpression of both EGFR and IGF1R correlates with poor patient prognosis in resected non-small-cell lung cancer. *Clin Lung Cancer* 2014; **15**: 58-66. doi: 10.1016/j.clc.2013.08.005
39. Tran TN, Selinger CI, Yu B, Ng CC, Kohonen-Corish MR, McCaughan B, et al. Alterations of insulin-like growth factor-1 receptor gene copy number and protein expression are common in non-small cell lung cancer. *J Clin Pathol* 2014; **67**: 985-91. doi: 10.1136/jclinpath-2014-202347
40. Nakagawa M, Uramoto H, Shimokawa H, Onitsuka T, Hanagiri T, Tanaka F. Insulin-like growth factor receptor-1 expression predicts postoperative recurrence in adenocarcinoma of the lung. *Exp Ther Med* 2011; **2**: 585-90. doi: 10.3892/etm.2011.258
41. Kim JS, Kim ES, Liu D, Lee JJ, Solis L, Behrens C, et al. Prognostic impact of insulin receptor expression on survival of patients with non small cell lung cancer. *Cancer* 2012; **118**: 2454-65. doi: 10.1002/cncr.26492
42. Yamamoto T, Oshima T, Yoshihara K, Nishi T, Arai H, Inui K, et al. Clinical significance of immunohistochemical expression of insulin-like growth factor-1 receptor and matrix metalloproteinase-7 in resected non-small cell lung cancer. *Exp Ther Med* 2012; **3**: 797-802. doi: 10.3892/etm.2012.493
43. Xu C, Xie D, Yu SC, Yang XJ, He LR, Yang J, et al. β -Catenin/POU5F1/SOX2 transcription factor complex mediates IGF-1 receptor signaling and predicts poor prognosis in lung adenocarcinoma. *Cancer Res* 2013; **73**: 3181-9. doi: 10.1158/0008-5472.CAN-12-4403
44. Cappuzzo F, Toschi L, Tallini G, Ceresoli GL, Domenichini I, Bartolini S, et al. Insulin-like growth factor receptor 1 (IGFR-1) is significantly associated with longer survival in non-small-cell lung cancer patients treated with gefitinib. *Ann Oncol* 2006; **17**: 1120-7. doi: 10.1093/annonc/mdl077
45. Kikuchi R, Sonobe M, Kobayashi M, Ishikawa M, Kitamura J, Nakayama E, et al. Expression of IGF1R is associated with tumor differentiation and survival in patients with lung adenocarcinoma. *Ann Surg Oncol* 2012; **19**(Suppl 3): S412-20. doi: 10.1245/s10434-011-1878-x
46. Kim YH, Sumiyoshi S, Hashimoto S, Masago K, Togashi Y, Sakamori Y, et al. Expressions of insulin-like growth factor receptor-1 and insulin-like growth factor binding protein 3 in advanced non-small-cell lung cancer. *Clin Lung Cancer* 2012; **13**: 385-90. doi: 10.1016/j.clc.2011.11.009
47. Park E, Park SY, Kim H, Sun PL, Jin Y, Cho SK, et al. Membranous Insulin-like Growth Factor-1 Receptor (IGF1R) Expression Is Predictive of Poor Prognosis in Patients with Epidermal Growth Factor Receptor (EGFR)-Mutant Lung Adenocarcinoma. *J Pathol Transl Med* 2015; **49**: 382-8. doi: 10.4132/jptm.2015.07.10
48. Zhao S, Qiu Z, He J, Li L, Li W. Insulin-like growth factor receptor 1 (IGF1R) expression and survival in non-small cell lung cancer patients: a meta-analysis. *Int J Clin Exp Pathol* 2014; **7**: 6694-704.
49. Richardson LC, Pollack LA. Therapy insight: Influence of type 2 diabetes on the development, treatment and outcomes of cancer. *Nat Clin Pract Oncol* 2005; **2**: 48-53. doi: 10.1038/ncponc0062
50. Ding J, Tang J, Chen X, Men HT, Luo WX, Du Y, et al. Expression characteristics of proteins of the insulin-like growth factor axis in non-small cell lung cancer patients with preexisting type 2 diabetes mellitus. *Asian Pac J Cancer Prev* 2013; **14**: 5675-80.
51. LeRoith D, Roberts CT Jr. The insulin-like growth factor system and cancer. *Cancer Lett* 2003; **195**: 127-37.
52. Wang HS, Wang TH. Polycystic ovary syndrome (PCOS), insulin resistance and insulin-like growth factors (IGFs)/IGF-binding proteins (IGFBPs). *Chang Gung Med J* 2003; **26**: 540-53.
53. Zhou Y, Zhang X, Gu C, Xia J. Diabetes mellitus is associated with breast cancer: systematic review, meta-analysis, and in silico reproduction. *Panminerva Med* 2015; **57**: 101-8.
54. Jiang Y, Ben Q, Shen H, Lu W, Zhang Y, Zhu J. Diabetes mellitus and incidence and mortality of colorectal cancer: a systematic review and meta-analysis of cohort studies. *Eur J Epidemiol* 2011; **26**: 863-76. doi: 10.1007/s10654-011-9617-y
55. Tian T, Zhang LQ, Ma XH, Zhou JN, Shen J. Diabetes mellitus and incidence and mortality of gastric cancer: a meta-analysis. *Exp Clin Endocrinol Diabetes* 2012; **120**: 217-23. doi: 10.1055/s-0031-1297969
56. Walter U, Kohlert T, Rahbari NN, Weitz J, Welsch T. Impact of preoperative diabetes on long-term survival after curative resection of pancreatic adenocarcinoma: a systematic review and meta-analysis. *Ann Surg Oncol* 2014; **21**: 1082-9. doi: 10.1245/s10434-013-3415-6
57. Wang YG, Wang P, Wang B, Fu ZJ, Zhao WJ, Yan SL. Diabetes mellitus and poorer prognosis in hepatocellular carcinoma: a systematic review and meta-analysis. *PLoS One*. 2014; **9**: e95485. doi: 10.1371/journal.pone.0095485
58. Cai H, Xu Z, Xu T, Yu B, Zou Q. Diabetes mellitus is associated with elevated risk of mortality amongst patients with prostate cancer: a meta-analysis of 11 cohort studies. *Diabetes Metab Res Rev* 2015; **31**: 336-43. doi: 10.1002/dmrr.2582
59. Chen L, Li H, Gu L, Ma X, Li X, Gao Y, et al. The impact of diabetes mellitus on renal cell carcinoma prognosis: a meta-analysis of cohort studies. *Medicine (Baltimore)* 2015; **94**: e1055. doi: 10.1097/MD.0000000000001055
60. Jiamset I, Hanprasertpong J. Impact of diabetes mellitus on oncological outcomes after radical hysterectomy for early stage cervical cancer. *J Gynecol Oncol* 2016; **27**: e28. doi: 10.3802/jgo.2016.27.e28
61. Inal A, Kaplan MA, Kucukoner M, Urakci Z, Kilinc F, Isikdogan A. Is diabetes mellitus a negative prognostic factor for the treatment of advanced non-small-cell lung cancer? *Rev Port Pneumol* 2014; **20**: 62-8. doi: 10.1016/j.rppneu.2013.09.001
62. Hatlen P, Gronberg BH, Langhammer A, Carlsen SM, Amundsen T. Prolonged survival in patients with lung cancer with diabetes mellitus. *J Thorac Oncol* 2011; **6**: 1810-7. doi: 10.1097/JTO.0b013e31822a75be
63. Imai H, Kaira K, Mori K, Ono A, Akamatsu H, Matsumoto S, et al. Prognostic significance of diabetes mellitus in locally advanced non-small cell lung cancer. *BMC Cancer* 2015; **15**: 989. doi: 10.1186/s12885-015-2012-4
64. Zhu L, Cao H, Zhang T, Shen H, Dong W, Wang L, et al. The effect of diabetes mellitus on lung cancer prognosis: a PRISMA-compliant meta-analysis of cohort studies. *Medicine (Baltimore)* 2016; **95**: e3528. doi: 10.1097/MD.0000000000003528
65. Yin M, Zhou J, Gorak EJ, Quddus F. Metformin is associated with survival benefit in cancer patients with concurrent type 2 diabetes: a systematic review and meta-analysis. *Oncologist* 2013; **18**: 1248-55. doi: 10.1634/theoncologist.2013-0111
66. Altman DG, McShane LM, Sauerbrei W, Taube SE. Reporting recommendations for tumor marker prognostic studies (REMARK): explanation and elaboration. *PLoS Med* 2012; **9**: e1001216. doi: 10.1371/journal.pmed.1001216

Carotid artery stiffness, digital endothelial function, and coronary calcium in patients with essential thrombocytosis, free of overt atherosclerotic disease

Matjaz Vrtovec^{1,2}, Ajda Anzic², Irena Preloznik Zupan^{3,4}, Katja Zaletel^{1,4}, Ales Blinc^{2,4}

¹ Department of Nuclear Medicine, University Medical Centre Ljubljana, Slovenia

² Department of Vascular Diseases, University Medical Centre Ljubljana, Slovenia

³ Department of Haematology, University Medical Centre Ljubljana, Slovenia

⁴ Faculty of Medicine, University of Ljubljana; Slovenia

Radiol Oncol 2017; 51(2): 203-210.

Received 21 September 2016
Accepted 17 December 2016

Correspondence to: Aleš Blinc, Department of Vascular Diseases, University Medical Centre Ljubljana, Zaloška 7, SI-1525 Ljubljana, Slovenia.
E-mail: ales.blinc@kclj.si

Disclosure: No potential conflicts of interest were disclosed.

This work has been supported by the Slovenian Research Agency, Research Program No. P3-0308. The authors are grateful to Dr. Borut Jug for his contribution to initiating the study.

Background. Patients with myeloproliferative neoplasms (MPNs) are at increased risk for atherothrombotic events. Our aim was to determine if patients with essential thrombocytosis (ET), a subtype of MPNs, free of symptomatic atherosclerosis, have greater carotid artery stiffness, worse endothelial function, greater coronary calcium and carotid plaque burden than control subjects.

Patients and methods. 40 ET patients without overt vascular disease, and 42 apparently healthy, age and sex-matched control subjects with comparable classical risk factors for atherosclerosis and Framingham risk of coronary disease were enrolled. All subjects were examined by physical and laboratory testing, carotid echo-tracking ultrasound, digital EndoPat pletysmography and CT coronary calcium scoring.

Results. No significant differences were found between ET patients and controls in carotid plaque score [1 (0-1.25) vs. 0 (0-2), $p=0.30$], β -index of carotid stiffness [7.75 (2.33) vs. 8.44 (2.81), $p=0.23$], pulse wave velocity [6.21 (1.00) vs. 6.45 (1.04) m/s; $p=0.46$], digital reactive hyperemia index [2.10 (0.57) vs. 2.35 (0.62), $p=0.07$], or augmentation index [19 (3-30) vs. 13 (5-22) %, $p=0.38$]. Overall coronary calcium burden did not differ between groups [Agatston score 0.1 (0-16.85) vs. 0 (0-8.55), $p=0.26$]. However, significantly more ET patients had an elevated coronary calcium score of >160 [6/40 vs. 0/42, $p < 0.01$].

Conclusions. No significant differences between groups were found in carotid artery morphology and function, digital endothelial function or overall coronary calcium score. Significantly more ET patients had an elevated coronary calcium score of >160 , indicating high cardiovascular risk, not predicted by the Framingham equation.

Key words: arterial wall; functional properties; morphological properties; calcium score; Framingham risk score; myeloproliferative disease

Introduction

Philadelphia chromosome-negative chronic myeloproliferative neoplasms (MPNs) are clonal haematopoietic stem cell disorders, traditionally

divided into essential thrombocytosis (ET), polycythemia vera (PV), and primary myelofibrosis (PMF). Transitions between these disease entities are common, and may represent a continuum from early disease to the advanced myelofibrosis

stage and finally to leukemic transformation.¹ The Janus kinase JAK2 V617F mutation is detected in more than 95% of patients with PV and in approximately 50% of patients with ET and PMF.² It is not known in detail, how the Janus kinase (JAK) signal pathway dysregulation affects MPNs initiation and evolution, but elevated biomarkers of chronic inflammation have been described in all MPNs entities.³⁻⁹ In addition to thrombotic and haemorrhagic complications and bone marrow failure in the advanced stage, patients with MPNs often suffer atherothrombotic events.⁹⁻¹¹ Thrombosis may involve the veins as well as the arteries, with acute coronary disease being the most prevalent manifestation of the latter.¹⁰ Over a period of 10 years, about 10% of patients with PV and ET suffered myocardial infarction.¹¹

Chronic inflammation plays an important role in the development of atherosclerosis in general population.^{12,13} In MPNs, it seems that chronic inflammation could be a trigger and promoter of the clonal expansion of leukocytes and platelets which release inflammatory cytokines.¹⁴ Since inflammatory cytokines contribute to leukocyte and platelet generation, a positive feedback loop is established¹⁴, contributing to premature atherosclerosis in patients with MPNs.^{8,9,15}

Ultrasonographic measurement of carotid arterial stiffness has been proposed as a sensitive method for detecting early vascular changes.¹⁶⁻¹⁸ Endothelial dysfunction is associated with cardiovascular risk¹⁹, and also a contributor to the progression of atherosclerosis.²⁰ Coronary artery calcium scanning is the most reliable predictor of coronary events in subjects with intermediate cardiovascular risk.²¹ Little is known about functional and morphological properties of the arterial wall and the prevalence of asymptomatic coronary atherosclerosis in patients with JAK2 V617F positive myeloproliferative disease.

Our aim was to test whether patients with JAK2 V617F positive MPNs, without clinically manifest atherosclerosis, have more prevalent asymptomatic carotid plaques, greater carotid artery stiffness, greater coronary calcium burden and worse digital endothelial function than apparently healthy control subjects, matched for classical risk factors for atherosclerosis.

Patients and methods

Patients were recruited from University Medical Centre Ljubljana, Department of Haematology

among JAK2 V617F positive patients with ET, treated between 2011 and 2014. Among 180 ET consecutive patients, 124 were JAK2 positive and 61 did not have a personal history of clinically manifest atherosclerotic vascular disease (angina pectoris, myocardial infarction, transient ischemic attack, ischemic stroke, peripheral arterial disease or known aortic disease). Among those, 40 patients gave their informed consent for participating in the cross-sectional study of functional and morphological properties of the carotid arteries, coronary calcium burden and endothelial function of the digital arteries. The control group was recruited among apparently healthy employees of the University Medical Centre Ljubljana and their relatives, aiming to match the patient group regarding age and sex. After screening 57 volunteers, 42 apparently healthy subjects were selected matching the ET patients for age, sex distribution and classical risk factors for atherosclerosis.

All participating subjects had to be at least 18 years old, not pregnant, and free of documented or clinically suspected atherosclerotic vascular disease. After giving their informed consent, all subjects were questioned for their medical history according to a structured questionnaire, examined physically and drawn blood for laboratory testing. Subsequently, their extracranial carotid arteries were examined by ultrasound, reactive hyperemia response of the digital arteries was assessed by EndoPat pletysmography, and coronary calcium burden was assessed by CT. Workup of each study participant was done in single visit, between January 2014 and August 2015, strictly on Fridays between 12.00 and 16.00 hours, in the facilities of the Clinical Department for Vascular Diseases and Department of Nuclear Medicine, University Medical Centre Ljubljana. The study was approved by the Committee for Medical Ethics of the Republic of Slovenia with the decision letter 154/05/12.

The 10-year risks of coronary heart disease, myocardial infarction, stroke and overall cardiovascular disease were calculated according to the Framingham risk equations, taking into account the subjects age, sex, smoking status, presence of diabetes, systolic blood pressure total serum cholesterol and HDL-cholesterol.²² Left ventricular hypertrophy as determined by EKG was not taken into account. The Framingham risk calculator in Microsoft Excel was used for the calculations.²³

The extracranial carotid arteries (common, internal and external carotid on both sides) were examined by a single ultrasonographer, using an Aloka

prosound $\alpha 7$ (Hitachi Aloka Medical, Ltd., Japan) machine with a linear vascular probe (working frequency of 5-13 MHz). Testing was performed with subjects comfortably lying supine in a quiet room with the air temperature of 22-24°C.

Asymptomatic carotid atherosclerosis was assessed by identifying carotid plaques, which were defined as focal lesions exceeding the intima-media thickness by at least 50% or reaching an absolute thickness of at least 1.5 mm in two orthogonal projections. Scoring of atherosclerotic plaques was performed by a modification of the methodology used in the Rotterdam Study.²⁴ The extracranial carotid arteries were divided into three sectors on each side: the common carotid artery and its bulb, the internal carotid artery, and the external carotid artery. At least one plaque in any sector was scored 1 point, while the absence of plaques was scored as 0. Thus, the carotid plaque score ranged from 0 (absence of plaques) to 6 (plaques in all sectors).²⁴

Echo-tracking of the common carotid arterial wall 2 cm proximal to the bulb was used to the β -stiffness index (β)²⁵ and to estimate pulse wave velocity (PWV)²⁶. The β -stiffness index was calculated as:

$$\beta = \ln(P_{\max} / P_{\min}) / [(D_{\max} - D_{\min}) / D_{\min}]$$

where P_{\max} was the systolic blood pressure, P_{\min} the diastolic pressure; D_{\max} the maximum arterial diameter and D_{\min} the minimal arterial diameter.

The PWV was estimated according to the formula:²¹

$$PWV = \sqrt{((\beta \times P_{\min}) / 2q)}$$

where q was the specific mass of blood ($q = 1050 \text{ kg/m}^3$).

Coronary artery calcium scanning was performed on a Biograph M 128-row PET-CT scanner (Siemens, Erlangen, Germany). We used a non-contrast protocol with sequential, prospective ECG triggering, rotation time 0.33 sec, tube voltage 120 kV, CARE Dose 4D, slice thickness 3 mm, with no slice overlap. Scanning was done in sustained breath hold, from the carina to the base of the heart. Post-processing was done on the Syngo Leonardo workstation. Evaluation of the dataset of every study subject was done three times, and the calculated average value was used for further analysis. The coronary calcium burden was expressed as the Agatston score.²⁷

Endothelial function of the digital arteries was measured by digital pletysmography before and after a 5-min arterial occlusion of the forearm by inflating a cuff to 60 mmHg more than the arterial blood pressure in order to assess the response to reactive hyperemia by the apparatus EndoPAT2000 (Itamar Medical REF, Israel). All subjects were examined in the fasting state and were requested to abstain from drinking coffee or smoking at least 3 hours before the examination, and to abstain from drinking alcohol at least 10 hours before the examination. Testing was performed with subjects comfortably lying supine in a quiet room with the air temperature 22-24°C.

The reactive hyperemia index (RHI) and augmentation index (AI) were determined.²⁸ RHI was calculated by the formula:

$$RHI = (A/B) / (C/D)$$

where A is the post-occlusion pulse wave amplitude (PWA) of the occluded hand, B the baseline PWA of the occluded hand, C the post-occlusion PWA of the contralateral hand, and D the baseline PWA of the contralateral hand.

The AI was determined from the shape of the arterial pulse wave by the EndoPAT 2000 software which distinguished between the primary pulse wave (P1) and the reflected pulse wave (P2) by the formula: $AI = ((P2-P1)/P1) \times 100$.²⁸ The results were normalized to a heart rate of 75/min.

All sets of data were tested for normality of distribution using the normal-quintile plot, calculating the correlation coefficient and checking it for the critical value that would warrant rejection of normal distribution with an α -error probability of 0.05. Normally distributed data are presented as mean and standard deviation, while non-normally distributed data are presented as median and range between the 1st and 3rd quartile. Differences between subjects with ET and control subjects were tested by the chi-square test for discrete variables, for normally distributed continuous variables by the paired Student's t-test for independent samples, and for non-normally distributed continuous variables by the Mann-Whitney test for independent samples.

The Pearson correlation coefficient was calculated between the Framingham prediction of coronary heart disease and the coronary calcium score, and between the coronary calcium score and the carotid plaque score of the two groups. The calculations were done by Microsoft Excel software or by the Social Science Statistics Calculators available at www.socscistatistics.com.

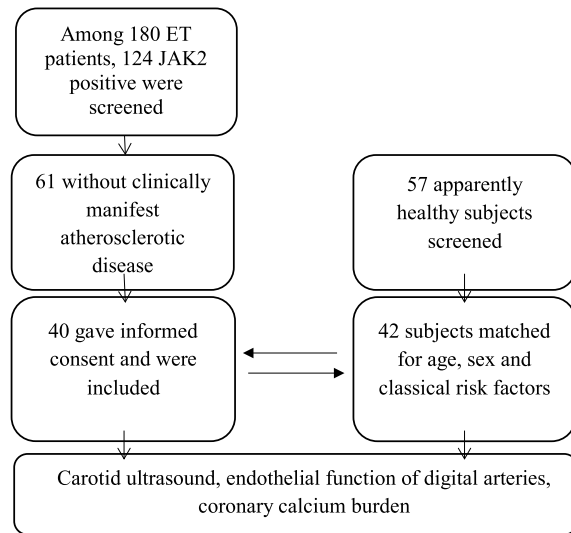


FIGURE 1. Recruitment of essential thrombocytosis (ET) and control subjects for the cross-sectional study of endothelial function and preclinical atherosclerosis.

Results

The flow chart of recruitment is shown in Figure 1

The baseline characteristics of our subjects are shown in Table 1. The groups were matched for age and sex distribution and there were no significant differences in blood pressure, blood lipids, smoking status or diabetes. Thus, there were no differences in the Framingham prediction of cardiovascular risk between the two groups (Table 2).

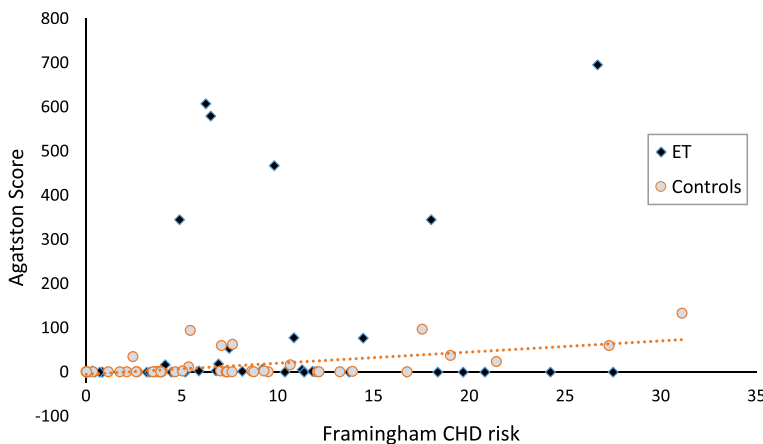


FIGURE 2. Correlation of the Framingham coronary heart disease (CHD) risk and coronary calcification (Agatston score). While a significant Pearson correlation between the Framingham CHD risk and the Agatston score was found for control subjects ($r = 0.577$, $p < 0.001$), no significant correlation was found for the patients with essential thrombocytosis (ET).

The patients with ET differed from the control group in most parameters of blood cell count, most notably the number of platelets (Table 3). No differences were found between the two groups in the carotid plaque score, carotid artery stiffness or the estimated pulse wave velocity (Table 4).

The RHI of the digital arteries showed a trend towards toward better endothelial reactivity in control subjects [2.35 (0.62) vs. 2.10 (0.57)], but the difference did not reach statistical significance ($p = 0.07$). There were also no differences in the AI, an estimate of stiffness of the conductive arteries of the upper limb (Table 5).

The majority of our patients and control subjects had their coronary arteries free of calcification (Figure 2), and the overall Agatston calcium score did not differ between the two groups. However, a significant number of patients with ET had a high calcium score not predicted by the Framingham risk equation for coronary disease (Table 6, Figure 2). While a significant correlation between the Framingham CHD risk and the Agatston was found for control subjects ($r = 0.577$, $p < 0.001$), no significant correlation was found for the patients with ET ($r = 0.197$, $p = 0.223$).

A weak correlation between the carotid plaque score and the Agatston coronary artery calcium score was found in patients with ET ($r = 0.418$, $p < 0.01$), but there was no correlation in the control group ($r = 0.063$, $p = 0.69$).

Discussion

This cross-sectional study of patients with JAK2 V617F positive ET did not find differences in carotid artery plaque score, carotid artery stiffness, endothelial function or overall coronary calcium score in comparison to control subjects, but there were more patients with a high coronary calcium score among the patients. The Framingham coronary disease risk prediction correlated with the coronary calcium score in control subjects, but not in patients with ET, indicating that Philadelphia chromosome-negative MPNs, specifically ET, represent a non-classical risk factor for coronary atherosclerosis.

Why was high calcium scoring the only parameter that differed between patients with ET and apparently healthy control subjects, whereas arterial stiffness and endothelial function did not show any significant difference?

Coronary calcium scanning is the most reliable predictor of coronary events in asymptomatic individuals with an intermediate risk according to

TABLE 1. Baseline characteristics. Numbers of subjects are given for discrete data. Mean and standard deviation are shown for normally distributed continuous data; median and interquartile range are given for non-normally distributed continuous data. Comparisons between groups were tested by χ -square¹, Student's t-test², or Mann-Whitney test³

Variable	ET patients (n= 40)	Control group (n= 42)	Comparison between groups (p)
² Age (years)	57.1 (14.1)	58.2 (13.1)	0.71
¹ Sex (M/F)	14/26	16/26	0.77
² BMI (kg/m ²)	25.4 (3.5)	27.0 (4.5)	0.07
² Waist circumference (cm)			
M	95.4 (10.4)	101.1(10.2)	0.14
F	89.7 (8.8)	89.4 (13.6)	0.92
³ Systolic blood pressure (mmHg)	139 (129-148)	136 (130-143)	0.33
³ Diastolic blood pressure (mmHg)	80 (73-89)	80 (74-87)	0.92
² Total cholesterol (mmol/l)	5.01 (1.07)	5.23 (0.83)	0.30
² LDL-cholesterol (mmol/l)	2.73 (0.77)	2.86 (0.69)	0.42
² HDL-cholesterol (mmol/l)	1.44 (0.48)	1.63 (0.48)	0.07
² Triglycerides (mmol/l)	1.82 (0.79)	1.65 (0.82)	0.33
¹ Current smoking (yes/no)	5/35	3/39	0.41
¹ Ever smoking (yes/no)	16/24	11/31	0.12
¹ Diabetes (yes/no)	3/37	0/42	0.07
³ Serum glucose (mmol/l)	5.4 (4.7-6.1)	5.1 (4.8-5.6)	0.64
Kidney disease (yes/no)	0/40	0/42	-
² Serum creatinine (μ mol/l)	75.7 (15.0)	75.7 (14.1)	0.99
Family history of premature CVD (yes/no)	0/40	0/42	-
¹ Family history of CVD (yes/no)	16/24	16/26	0.86

BMI = body mass index; CVD = cardiovascular disease; ET = essential thrombocytosis; F = female; HDL = high density lipoprotein; LDL = low density lipoprotein; M = male

TABLE 2. Cardiovascular 10-year risk estimation by the Framingham risk equations. Median and interquartile range are shown. Comparisons between groups were tested by the Mann-Whitney test

Framingham 10-year risk calculation (%)	ET patients (n= 40)	Control group (n= 42)	Comparison between groups (p)
CHD	7.80 (3.98-13.73)	7.20 (3.57-11.37)	0.52
MI	2.87 (1.25-6.72)	2.17 (0.77-4.73)	0.47
Stroke	2.93 (1.19-5.37)	2.59 (1.49-4.09)	0.73
CVD	14.56 (7.16 – 23.68)	12.99 (6.43-19.52)	0.84

CHD = coronary heart disease; CVD = overall cardiovascular disease; ET = essential thrombocytosis; MI = myocardial infarction; Stroke = ischemic stroke

the Framingham score.²¹ Many studies have demonstrated its prognostic superiority over risk-factor based predictions, and the radiation exposure is no greater than that of mammography.²¹ Individuals with an Agatston score of >160 have a significantly increased risk for a major adverse cardiac event²⁹, and our cross-sectional study identified 6 such patients among the 40 patients with ET, but

none among the 42 control subjects. Since there was no correlation between the Framingham risk prediction and the coronary calcium score among patients with ET, this speaks for JAK2 positive ET being a non-classical risk factor for coronary atherosclerosis. With the increasing availability of coronary artery calcium scanning and its decreasing radiation exposure it might be desirable to test

TABLE 3. Blood cell count and C-reactive protein (CRP). Mixed cells denote a composite reading for monocytes, eosinophils and basophils. When CRP was reported as < 5 mg/L, a value of 2.5 mg/L was ascribed to the subject, therefore the CRP values are only an approximation. Mean and standard deviation are shown for normally distributed data; median and interquartile range are given for non-normally distributed data. The comparisons between groups were tested by Student's t-test¹, or by Mann-Whitney test²

Variable	ET patients (n= 40)	Control group (n= 42)	Comparison between groups (p)
¹ Red blood cells [10 ¹² /L]	4.37 (0.67)	4.76 (0.41)	<0.01
¹ Platelets [10 ⁹ /L]	509 (182)	243 (53)	<0.001
¹ Leukocytes [10 ⁹ /L]	7.60 (3.00)	7.02 (1.63)	0.28
¹ Lymphocytes [10 ⁹ /L]	1.67 (0.80)	2.23 (0.75)	<0.01
¹ Neutrophils [10 ⁹ /L]	5.15 (2.48)	4.15 (1.20)	0.02
² Mixed cells [10 ⁹ /L]	0.6 (0.4-0.9)	0.6 (0.5-0.7)	0.76
² CRP [mg/L]	5.0 (2.5-8.4)	5.4 (2.5-6.1)	0.27

ET = essential thrombocytosis

TABLE 4. Asymptomatic carotid plaques, carotid β -stiffness index and estimated pulse wave velocity. Mean and standard deviation are given for normally distributed continuous data, median and interquartile range are given for non-normally distributed continuous data and the number of subjects with a carotid plaque score of ≥ 2 is given. Comparisons between groups were tested by: χ -square¹, Student's t-test², or the Mann-Whitney test³

	ET patients (n= 40)	Control group (n= 42)	Comparison between groups (p)
³ Carotid plaque score	1 (0-1.25)	0 (0-2)	0.30
¹ Carotid plaque score ≥ 2 (yes/no)	10/30	14/28	0.41
² β -stiffness index	7.75 (2.34)	8.44 (2.81)	0.23
² pulse wave velocity (m/s)	6.21 (1.00)	6.45 (1.04)	0.46

ET = essential thrombocytosis

TABLE 5. Endothelial function of the digital arteries - reactive hyperemia index (RHI) and estimate of vascular stiffness - augmentation index (AI). Means and standard deviations are given for the normally distributed RHI, medians and interquartile range are given for non-normally distributed AI. Comparisons between groups were tested by the Student's t-test¹, or the Mann-Whitney test²

	ET patients (n= 40)	Control group (n= 42)	Comparison between groups (p)
¹ RHI	2.10 (0.57)	2.35 (0.62)	0.07
² AI [%]	19 (3-30)	13 (5-22)	0.38

ET = essential thrombocytosis

TABLE 6. Coronary calcium burden. Median and interquartile range are given for the Agatston score of coronary calcification, and the number of subjects with an Agatston score of > 160 is given. The comparison between groups were tested by χ -square¹- or Mann-Whitney test²

Coronary calcium burden	ET patients (n= 40)	Control group (n= 42)	Comparison between groups (p)
² Agatston score	0.1 (0-16.85)	0 (0-8.55)	0.26
¹ Agatston score > 160 (yes/no)	6/34	0/42	<0.01

ET = essential thrombocytosis

all middle aged patients with JAK2 positive MPNs for coronary calcium regardless of their perceived Framingham risk.

Carotid plaque score and the Agatston coronary artery calcium score, two markers of advanced atherosclerosis, were weakly correlated in patients with ET ($r = 0.418$, $p < 0.01$), but not at all in the control group.

Functional methods for assessing arterial stiffness and endothelial function are less robust than coronary calcium scanning and morphological carotid ultrasound examination. Although arterial stiffness and endothelial dysfunction strongly correlate with vascular risk factors and atherothrombotic events, there is no universally accepted method of their measurement and their clinical utility is not well established.^{16,19} Since arterial stiffness and endothelial function can be measured in many different ways, each research group has to focus on methods that are available to them and with which they are familiar. We chose the ultrasound based echo-tracking method to determine the local stiffness of the common carotid artery, expressed by the β -stiffness index, which has the advantage of being independent of blood pressure in a wide physiological range.²⁵ Detecting and analyzing carotid wall motion as a function of cardiac cycle by echo-tracking is straightforward, but carotid stiffness tells little about the coronary arteries, which have much greater stiffness than the common carotid arteries.³⁰ Carotid stiffness predicted cardiovascular events in patients with advanced renal disease³¹ and following renal transplantation³², but was not predictive in a broader sample of patients with manifest cardiovascular disease.³³

The most widely used non-invasive method of measuring endothelial function is flow-mediated vasodilatation of the brachial artery, which however is time-consuming and may be operator dependent.¹⁹ We used finger pletysmography/pulse amplitude tonometry with the EndoPat method which has the advantage of being relatively rapid and operator-independent.^{19,34} Endothelial dysfunction, assessed by this method correlated with traditional and metabolic cardiovascular risk factors in the third generation of the Framingham cohort.³⁵ The hyperaemic pulse amplitude response was somewhat blunted by increasing body mass index.³⁵ In our subjects, there was a trend toward lower body mass index in patients with ET in comparison to control subjects [25.4 (SD3.5) vs 27.0 (SD4.5) kg/m², $p = 0.07$]. Nevertheless, we noted a trend towards better reactive hyperaemia index in the control subjects [2.35 (SD 0.62) vs. 2.10 (SD 0.57), $p = 0.07$].

The main limitation of our study is its cross-sectional design. Each participant was examined only once, so we could not estimate the progression of atherosclerotic disease or follow the clinical outcomes. The relatively small number of patients is another important limitation, but we have recruited all actively treated patients with ET registered at our Department of Hematology, and similar studies are expected to face the same problem, since ET has a relatively low prevalence.

Also, due to a limited pool of control subjects, they were not perfectly matched to the ET patients in terms of classical risk factors for atherosclerosis, since there was a trend toward higher prevalence of diabetes, lower HDL-cholesterol and higher prevalence of ever smoking among patients with ET. However, the striking discrepancies between the Framingham risk prediction and high coronary calcium score strongly argue against classical risk factors being predominantly responsible for the advanced coronary atherosclerosis in patients with ET.

Sensitive markers of inflammation were not measured and could therefore not be correlated with endothelial function, arterial stiffness and preclinical atherosclerosis. However, the association of JAK2 positive status and markers of inflammation has been firmly established^{2,4-7,9} and all our patients with ET were JAK2 positive.

The assessment of arterial stiffness and endothelial function was limited by our methods of measurement (see above). Although all subjects were examined at the same time of day under standardized conditions, the examination period ranged for more than a year and a half, so there might have been some effects of seasonal variability on endothelial function and arterial stiffness. However, this would have affected both groups equally, since the patients and the control subjects were examined in an interspersed fashion. Also, in clinical practice patients are seen year-round and it is mandatory to use tests that are robust enough not to be dependent on many confounders.

Conclusions

In our cross-sectional study, we did not find significant differences in asymptomatic carotid plaque score, carotid stiffness, digital endothelial function or overall coronary calcium score between patients with JAK2 positive ET and control subjects. However, significantly more patients with JAK2 positive ET than control subjects had a coronary

calcium Agatston score of > 160, indicating high cardiovascular risk that was not predicted by the Framingham equation. CT calcium score is a robust, widely available and simple test which might prove useful in identifying ET patients at high risk for coronary events.

References

- Campbell PJ, Green AR. The myeloproliferative disorders. *N Engl J Med* 2006; **355**: 2452-66. doi:10.1056/NEJMra063728
- Hasselbalch HC. Perspectives on chronic inflammation in essential thrombocythemia, polycythemia vera, and myelofibrosis: is chronic inflammation a trigger and driver of clonal evolution and development of accelerated atherosclerosis and second cancer? *Blood* 2012; **119**: 3219-25. doi:10.1182/blood-2011-11-394775
- Hasselbalch H. Idiopathic myelofibrosis: a clinical study of 80 patients. *Am J Hematol* 1990; **34**: 291-300.
- Kristinsson SY, Landgren O, Samuelsson J, Björkholm M, Goldin LR. Autoimmunity and the risk of myeloproliferative neoplasms. *Haematologica*. 2010; **95**: 1216-20. doi:10.3324/haematol.2009.020412
- Koschmieder S, Mughal TI, Hasselbalch HC, Barosi G, Valent P, Kiladjian JJ, et al. Myeloproliferative neoplasms and inflammation: whether to target the malignant clone or the inflammatory process or both. *Leukemia* 2016; **30**:1018-24. doi:10.1038/leu.2016.12
- Fleischman AG. Inflammation as a Driver of Clonal Evolution in Myeloproliferative Neoplasm. *Mediators Inflamm* 2015; **2015**: 606819. doi:10.1155/2015/606819
- Hermouet S, Bigot-Corbel E, Gardie B. Pathogenesis of Myeloproliferative Neoplasms: Role and Mechanisms of Chronic Inflammation. *Mediators Inflamm* 2015; **2015**:145293. doi:10.1155/2015/145293
- Sørensen AL, Hasselbalch HC. Antecedent cardiovascular disease and autoimmunity in Philadelphia-negative chronic myeloproliferative neoplasms. *Leuk Res* 2016; **41**:27-35. doi:10.1016/j.leukres.2015.11.017
- Hasselbalch HC, Bjørn ME. MPNs as inflammatory diseases: the evidence, consequences, and perspectives. *Mediators Inflamm* 2015; **2015**: 102476. doi:10.1155/2015/102476
- Saif MW, Khan U, Greenberg BR. Cardiovascular manifestations of myeloproliferative disorders: a review of the literature. *Hosp Physician* 1999; **35**: 43-54.
- Rossi C, Randi L, Zerbinati P, Rinaldi V, Girolami A. Acute coronary disease in essential thrombocythemia and polycythemia vera. *J Intern Med* 1998; **244**: 49-53.
- Ross R. Atherosclerosis. An inflammatory disease. *N Engl J Med* 1999; **340**: 115-26. doi:10.1056/NEJM199901143400207
- Hansson GK, Hermansson A. The immune system in atherosclerosis. *Nat Immunol* 2011; **12**: 204-12. doi:10.1038/ni.2001
- Landolfi R, Di Gennaro L. Pathophysiology of thrombosis in myeloproliferative neoplasms. *Haematologica* 2011; **96**: 183-6. doi:10.3324/haematol.2010.038299
- Fleischman AG, Aichberger KJ, Luty SB, Bumm TG, Petersen CL, Doratotaj S, et al. Tumor necrosis factor-alpha facilitates clonal expansion of JAK2V617F positive cells in myeloproliferative neoplasms. *Blood* 2011; **118**: 6392-98. doi:10.1182/blood-2011-04-348144
- Laurent S, Cockcroft J, Van Bortel L, Boutouyrie P, Giannattasio C, Hayoz D, et al. European Network for Non-invasive Investigation of Large Arteries. Expert consensus document on arterial stiffness: methodological issues and clinical applications. *Eur Heart J* 2006; **27**:2588-605. doi:10.1093/eurheartj/ehl254
- Núñez F, Martínez-Costa C, Sanchez-Zahonero J, Morata J, Chorro FJ, Brines J. Carotid artery stiffness as an early marker of vascular lesions in children and adolescents with cardiovascular risk factors. *Rev Esp Cardiol* 2010; **63**:1253-60.
- Cote AT, Phillips AA, Harris KC, Sandor GGS, Panagiotopoulos C, Devlin AM. Obesity and arterial stiffness in children. Systematic review and meta-analysis. *Arterioscler Thromb Vasc Biol* 2015; **35**:1038-44. doi:10.1161/ATVBAHA.114.305062
- Flammer AJ, Anderson T, Celermajer DS, Creager MA, Deanfield J, Ganz P, et al. The assessment of endothelial function - from research into clinical practice. *Circulation* 2012; **126**: 753-67. doi:10.1161/CIRCULATIONAHA.112.093245
- Halcox JP, Donald AE, Ellins E, Witte DR, Shipley MJ, Brunner EJ, et al. Endothelial function predicts progression of carotid intima-media thickness. *Circulation* 2009; **119**:1005-12. doi:10.1161/CIRCULATIONAHA.108.765701
- Hecht HS. Coronary artery calcium scanning - past, present and future. *JACC Cardiovasc Img* 2015; **8**: 579-96. doi:10.1016/j.jcmg.2015.02.006
- D'Agostino RB, Vasan RS, Pencina MJ, Wolf PA, Cobain M, Massaro JM et al. General cardiovascular risk profile for use in primary care - the Framingham Heart Study. *Circulation* 2008; **117**: 743-52. doi:10.1161/CIRCULATIONAHA.107.699579
- Available at: <http://cvrisk.mvm.ed.ac.uk/calculator/riskcalculator.xls>. Accessed: Sep 7, 2016.
- Hollander M, Bots ML, Iglesias del Sol A, Koudstaal PJ, Witteman JCM, Grobbee DE, et al. Carotid plaques increase the risk of stroke and subtypes of cerebral infarction in asymptomatic elderly - the Rotterdam Study. *Circulation* 2002; **105**: 2872-7.
- Hayashi K, Handa H, Nagasawa S, Okumura A, Moritake K. Stiffness and elastic behavior of human intracranial and extracranial arteries. *J Biomech* 1980; **13**:175-184.
- Aloka, ultrasound diagnostic instrument, prosound $\alpha 7$, instruction manual, how to use (volume 2/2) MN 1 - 5369 rev. 9: 140-9.
- Agatston AS, Janowitz WR, Hילander FJ, Zusmer RN, Viamonte M, Detrow R. Quantification of coronary artery calcium using ultrafast computed tomography. *J Am Coll Cardiol* 1990; **15**: 827-32.
- Axtell AL, Gomari FA, Cooke JP. Assessing endothelial vasodilator function with the Endo-PAT 2000. *J Vis Exp* 2010; **44**: e2167. doi:10.3791/2167
- Arad Y, Spadaro LA, Goodman K, Newstein D, Guerci AD. Prediction of coronary events with electron beam computed tomography. *J Am Coll Cardiol* 2000; **36**: 1253-60.
- Hayashi K, Yamamoto T, Takahara A, Shirai K. Clinical assessment of arterial stiffness with cardio-ankle vascular index: theory and application. *J Hypertens* 2015; **33**: 1742-57. doi:10.1097/HJH.0000000000000651
- Blacher J, Pannier B, Guerin A, Marchais SJ, Safar ME, London GM. Carotid arterial stiffness as a predictor of cardiovascular and all-cause mortality in end-stage renal disease. *Hypertension* 1998; **32**: 570-574.
- Barenbrock M, Kosch M, Joster E, Kisters K, Rahn K, Hausberg M. Reduced arterial distensibility is a predictor of cardiovascular disease in patients after renal transplantation. *J Hypertens* 2002; **20**:79-84.
- Dijk JM, Algra A, van der Graaf Y, Grobbee DE, Bots ML, SMART study group. Carotid stiffness and the risk of new vascular events in patients with manifest cardiovascular disease. The SMART study. *Eur Heart J* 2005; **26**:1213-1220. doi:10.1093/eurheartj/ehi254
- Celermajer DS. Reliable endothelial function testing : at our fingertips? *Circulation* 2008, **117**: 2428-30. doi:10.1161/CIRCULATIONAHA.108.775155
- Hamburg NM, Keyes MJ, Larson MG, Vasan RS, Schnabel R, Pryde MM, et al. Cross-sectional relations of digital vascular function to cardiovascular risk factors in the Framingham Heart Study. *Circulation* 2008; **117**: 2467-74. doi:10.1161/CIRCULATIONAHA.107.748574

Perioperative increase in neutrophil CD64 expression is an indicator for intra-abdominal infection after colorectal cancer surgery

Milena Kerin Povsic¹, Bojana Beovic², Alojz Ihan³

¹ Institute of Oncology Ljubljana, Ljubljana, Slovenia

² Clinic for Infectious Diseases and Febrile Illnesses, University Medical Centre Ljubljana, Ljubljana, Slovenia

³ Institute of Microbiology and Immunology, Faculty of Medicine, University of Ljubljana, Ljubljana, Slovenia

Radiol Oncol 2017; 51(2): 211-220.

Received 15 January 2016

Accepted 30 January 2016

Correspondence to: Prof. Dr. Alojz Ihan, M.D., Ph.D., Institute of Microbiology and Immunology, Faculty of Medicine, University of Ljubljana, Zaloška cesta 4, SI-1000 Ljubljana, Slovenia. Phone: +386 1 543 74 00; Fax: +386 1 543 74 01; E-mail: Alojz.Ihan@mf.uni-lj.si

Disclosure: No potential conflicts of interest were disclosed.

Background. Colorectal surgery is associated with a high incidence of postoperative infections. Early clinical signs are difficult to distinguish from the systemic inflammatory response related to surgical trauma. Timely diagnosis may significantly improve the outcome. The objective of this study was to compare a new biomarker index CD64 for neutrophils (iCD64n) with standard biomarkers, white blood cell (WBC) count, neutrophil/lymphocyte ratio (NLR), C-reactive protein (CRP) and procalcitonin (PCT) for the early detection of postoperative infection.

Methods. The prospective study included 200 consecutive patients with elective colorectal cancer surgery. Postoperative values of biomarkers from the postoperative day (POD) 1 to POD5 were analysed by the receiver operating characteristic (ROC) analysis to predict infection. The Cox regression model and the Kaplan-Meier method were used to assess prognostic factors and survival.

Results. The increase of index CD64n (iCD64n) after surgery, expressed as the ratio iCD64n after/before surgery was a better predictor of infection than its absolute value. The best 30-day predictors of all infections were CRP on POD4 (AUC 0.72, 99% CI 0.61–0.83) and NLR on POD5 (AUC 0.69, 99% CI 0.57–0.80). The best 15-day predictors of organ/space surgical site infection (SSI) were the ratio iCD64n on POD1 (AUC 0.72, 99% CI 0.58–0.86), POD3 (AUC 0.73, 99% CI 0.59–0.87) and CRP on POD3 (AUC 0.72, 99% CI 0.57–0.86), POD4 (AUC 0.79, 99% CI 0.64–0.93). In a multivariate analysis independent risk factors for infections were duration of surgery and perioperative transfusion while the infection itself was identified as a risk factor for a worse long-term survival.

Conclusions. The ratio iCD64n on POD1 is the best early predictor of intra-abdominal infection after colorectal cancer surgery. CRP predicts the infection with the same predictive value on POD3.

Key words: colorectal surgery; index CD64n; postoperative infection

Introduction

Colorectal cancer surgery is often followed by postoperative complications. They appear in 24–38%^{1,2}, prolong hospitalization and increase hospital cost. The perioperative mortality rate has been reported to be 3–4%.^{2,3} The most common are infectious complications, especially surgical site infections (SSIs). SSIs are divided into incisional (superficial and deep) wound infections and organ/space infec-

tions, which are mostly the result of anastomotic leak.⁴ Intra-abdominal infection can be manifested as abscess, local or diffuse peritonitis.⁵ The incidence of SSI after elective colorectal resection is 5–30%.^{6,7} Rectal surgery has a higher risk for infection because of longer duration and greater bacterial contamination compared with colon surgery.^{8,9} Postoperative infectious complications, particularly severe infections influence patient outcomes and worsen long-term survival.¹⁰⁻¹² The most common

mechanisms causing this are deregulated host immune response during the infection and extraluminal implantation of malignant cells in anastomotic leakage.¹³

Early clinical signs of postoperative infections are nonspecific and difficult to distinguish from the systemic inflammatory response syndrome (SIRS) triggered by surgical trauma. SIRS is usually self-limiting or may progress to infection, sepsis and septic shock.¹⁴ The median time to diagnosis of infection has been reported to be from POD (postoperative day) 7 to POD9.^{4,7,15-19} Organ/space SSIs have been diagnosed significantly later than incisional SSIs.²⁰ Most causes of infection, such as anastomotic leak, can appear much earlier.⁵ Early identification of patients with a high probability of infections is necessary so that clinicians may focus on additional diagnostic investigations. Pre-emptive antibiotic therapy decreases the incidence and severity of postoperative infections and significantly improves the outcome.²¹

The most commonly used laboratory test during the postoperative period, namely white blood cell (WBC) count is neither very sensitive nor specific.^{22,23} Many studies affirmed the predictive value of a non-specific C-reactive protein (CRP) for infection after surgery, but it is more reliable if analysed together with the clinical assessment.²⁴⁻²⁶ The results of procalcitonin (PCT) studies have been contradictory. In some studies PCT proved to be as good as or even better predictor of infections than CRP^{5,23,27,28}, but in others worse than CRP.^{29,30} Neutrophil/lymphocyte ratio (NLR) is a marker of immunosuppression and is increased in SIRS after major surgery, polytrauma, endotoxaemia and sepsis.³¹ In some studies it proved to be a predictor of all complications after abdominal surgery.^{32,33}

A biological marker which could predict infections before the development of clinical signs and symptoms develop is needed. Therefore we studied a new biomarker neutrophil CD64 (CD64n), in laboratory analysis expressed as an index CD64n (iCD64n). CD64 is a high-affinity Fc receptor for IgG1 and IgG3 subclasses of immunoglobulins (FcγRI), expressed on macrophages, monocytes, less on eosinophils and very weakly on non-activated neutrophils.^{34,35} Neutrophil expression of CD64 is down-regulated or lost with cell maturation and strongly up-regulated in response to pro-inflammatory cytokines in SIRS and sepsis.³⁶⁻³⁹ The main functions triggered by FcγRs include phagocytosis, enzyme release and clearance of immune complexes.⁴⁰ The expression of CD64n can be induced by bacteria as well as viruses.^{41,42} Two me-

ta-analyses by Cid *et al.*⁴³ and Li *et al.*⁴⁴ concluded iCD64n could be a promising diagnostic biomarker for bacterial infections. Another meta-analysis reported iCD64n is a helpful marker for early diagnosis of sepsis in critically ill adult patients⁴⁵ and in neonates.⁴⁶⁻⁴⁸ It can differentiate systemic infection from disease flare in patients with inflammatory autoimmune diseases.⁴⁹

A new biomarker iCD64n has up to now been investigated very scarcely after a major surgery.^{34,50-54} The objective of this study was to compare iCD64n with standard predictive markers of infections - WBC count, NLR, CRP and PCT - after colorectal cancer resection. We investigated the risk factors of infection and their impact on survival.

Patients and methods

In this prospective study 200 consecutive patients with elective colorectal carcinoma surgery were included. The study was conducted at the surgery department of the Institute of Oncology Ljubljana from September 2010 to March 2013. The study protocol was approved by the Republic of Slovenia National Medical Ethics Committee. All the patients provided written consent for data collection and publication.

The exclusion criteria were preoperative infection, preoperative ileus and palliative surgical procedure. Neo-adjuvant chemotherapy (CTX) and/or radiotherapy (RT) were carried out in 118 (59%) patients and finished six to eight weeks before surgery. The stage of tumour was evaluated clinically according to the nuclear magnetic resonance (NMR) investigation before the beginning of the treatment. The stage of tumour without neo-adjuvant CTX/RT was diagnosed by histopathological examination. The TNM (Tumour, Node, Metastasis) classification was used for staging colorectal cancer disease.⁵⁵ Each patient was assessed preoperatively according to American Society of Anesthesiologists (ASA) physical status classification which accurately predicts morbidity and mortality.^{56,57} Bioelectric impedance analysis (BIA) measurement was performed on the day before the surgery. Body mass index (BMI) was calculated according to the formula in which body mass (kg) is divided by the square of the body height (cm).

On the day of the surgery blood samples for inflammation markers, albumins and haematocrit analysis were taken in the operating room before intravenous fluid application started. Each patient received systemic antibiotic prophylaxis for Gram

negative and anaerobic bacteria on induction of anaesthesia and prior to skin incision. A standardized protocol for general and epidural anaesthesia was used. During the surgery we recorded the length of the procedure, the blood loss volume and the volume of blood transfusion. The body temperature was measured at the end of the procedure.

Values of WBC count, WBC differential, CRP, PCT and iCD64n were recorded just before surgery and after surgery daily from POD1 to POD5. NLR was calculated by dividing the number of neutrophils by the number of lymphocytes. The ratio iCD64 was calculated by dividing a postoperative value of iCD64n by its preoperative value. SIRS criteria from POD1 to POD5 and postoperative infections up to 30 days after surgery were recorded. SSIs (incisional, organ/space), pneumonia, central venous catheter related bloodstream infections (CRBSIs), urinary tract infections (UTIs) and enterocolitis were recorded. Microbial cultures were used as the gold standard to identify the source of infection. Criteria for SIRS reconsidered in the year 2001 by SCCM/ESICM/ACCP/ATS/SIS International Sepsis Definitions Conference⁵⁸ and criteria for nosocomial infections defined by Centres for Disease Control and Prevention (CDC) were used.⁵⁹ The perioperative transfusion of red blood cells was considered as a risk factor for infection until the infection has developed and as a risk factor for survival 30 days after surgery. The duration of hospitalization was recorded. After discharge each patient was monitored by outpatient clinic examinations 30 days after surgery. The data from medical records and the data of the Cancer Registry of the Republic of Slovenia were used to follow survival.

Biomarkers measurement

WBC count (reference range $4\text{--}10 \times 10^9/\text{L}$), WBC differential (neutrophil count $1.50\text{--}7.40 \times 10^9/\text{L}$, lymphocyte count $1.10\text{--}3.50 \times 10^9/\text{L}$) and haematocrit (reference range 0.390–0.500) were analysed with a haematological blood analyser LH75 (Beckman Coulter). The immunobiochemic analyser Modular Analytics SWE (Roche Diagnostics) was used for serum samples analysis. Serum concentration of CRP (reference range 0–5mg/L) was measured by immunoturbidimetric method, PCT (reference range 0–0.5µg/L) by electrochemiluminescence method and albumins (reference range 35–52g/L) by bromocresol green method.

Neutrophil CD64 was quantified by flow cytometry using the Leuko64 assay (Trillium Diagnostics, LLC, Maine, USA) according to the manufacturer's

instructions. Whole blood EDTA-anticoagulated samples were used for analysis. During working days samples were immediately transported to the laboratory and analysed on the same day. The results were available after a few hours. During weekends samples were stored up to 48 hours in refrigerator at 4°C. 100 µL of the whole blood was incubated for 15 minutes in the dark at room temperature with a mixture of murine monoclonal antibodies. Fluorescence beads were then added and flow cytometer analysis was performed. The iCD64 was derived by the ratio of linearized mean fluorescence intensity (MFI) of the cell population to the fluorescein isothiocyanate (FITC) signal from the beads. An internal negative control was the automatically measured lymphocyte iCD64 (< 1.0) and an internal positive control was the automatically measured monocyte iCD64 (> 3.0). The limit value of iCD64n for probable sepsis was > 1.5.

Bioelectric impedance analysis (BIA)

BIA was performed using a portable bioelectrical impedance analyser BodyStat QuadScan 4000 (Douglas, Great Britain). Phase angle (PA) is a ratio between the reactance (X_c) and resistance (R).⁶⁰ The normal range for men is from 7.90° to 6.19° and for women 7.04° to 5.64°.⁶¹ The illness marker (IM) is the ratio between the impedance measurement at 200kHz and 5kHz. A ratio closer to 1.00 indicates poor cellular health or extreme fluid overload.

Statistical analysis

The t-test was used to compare numeric variables (age, BMI, temperature, PA, IM and albumins) between infected and non-infected patients. Non-normally distributed continuous variables were summarised using medians and interquartile ranges and Mann-Whitney U test was used to compare these variables (infected versus non-infected patients). Categorical variables were analysed with the Pearson's chi-square test and the Fisher's exact test. To counteract the problem of multiple comparisons the Holm-Bonferroni corrected p values were used.⁶²

The predictive values of biomarkers WBC, NLR, CRP, PCT, iCD64 and the ratio iCD64n for postoperative infection were assessed by the receiver operating characteristic (ROC) curve. Each cut-off value was determined by using the maximum value of the Youden index. The Bonferroni correction for AUC confidence intervals was used because multiple statistical tests were performed. The cal-

TABLE 1. Comparison of patient and surgical characteristics between infected and non- infected group

Characteristic		Total N=200	No infection N=132	Infection N=68	p-value	Corrected ^e p-value
Age (years)		62.8 (11.3)	62.2 (11.0)	63.8 (11.9)	0.3787 ^f	1
Gender	male	131 (65.5%)	86 (65.2%)	45 (66.2%)	1 ^g	1
	female	69 (34.5%)	46 (34.8%)	23 (33.8%)		
ASA score	I	14 (7%)	12 (9.1%)	2 (2.9%)	0.0503 ^h	0.8546
	II	105 (52.5%)	74 (56.1%)	31 (45.6%)		
	III	76 (38%)	42 (31.8%)	34 (50%)		
	IV	5 (2.5%)	4 (3%)	1 (1.5%)		
Diabetes mellitus	no	161 (80.5%)	110 (83.3%)	51 (75%)	0.2222 ^g	1
	yes	39 (19.5%)	22 (16.7%)	17 (25%)		
BMI (kg/m ²)		27.2 (4.3)	27.3 (4.1)	27.2 (4.6)	0.8461 ^f	1
Phase angle ^a (°)		5.4 (1.0)	5.5 (1.0)	5.3 (1.1)	0.4632 ^f	1
Illness marker ^a		0.81 (0.04)	0.81 (0.04)	0.81 (0.04)	0.8567 ^f	1
Dry lean body mass ^a (kg)		12.2 (9.8-16.5)	12.8 (9.9-16.5)	11.3 (8.8-16.5)	0.1852 ^f	1
Hematocrit ^b	≥ 38%	100 (50%)	66 (50%)	34 (50%)	1 ^h	1
	30-37%	87 (43.5%)	57 (43.2%)	30 (44.1%)		
	26-29%	12 (6%)	8 (6.0%)	4 (5.9%)		
	21-25%	1 (0.5%)	1 (0.8%)	0 (0%)		
Albumin ^b (g/l)		42.1 (3.6)	42.4 (3.3)	41.6 (4.0)	0.1583 ^f	1
Tumour site	rectum	137 (68.5%)	84 (63.6%)	53 (77.9%)	0.0909 ^h	1
	colon	60 (30%)	46 (34.8%)	14 (20.6%)		
	rectum+ colon	3 (1.5%)	2 (1.5%)	1 (1.5%)		
Stage (TNM)	0	3 (1.5%)	2 (1.5%)	1 (1.5%)	0.0265 ^h	0.477
	I	27 (13.5%)	21 (15.9%)	6 (8.8%)		
	II	42 (21%)	34 (25.8%)	8 (11.8%)		
	III	109 (54.5%)	66 (50%)	43 (63.2%)		
	IV	19 (9.5%)	9 (6.8%)	10 (14.7%)		
Preoperative RT/CTX	no	82 (41%)	62 (47%)	20 (29.4%)	0.0251 ^g	0.477
	yes	118 (59%)	70 (53%)	48 (70.6%)		
Antibiotic prophylaxis	< 24 hours	54 (27%)	35 (26.5%)	19 (27.9%)	0.9404 ^h	1
	24 hours	132 (66%)	87 (65.9%)	45 (66.2%)		
	> 24 hours	14 (7%)	10 (7.6%)	4 (5.9%)		
Surgical procedure						
Rectum resection	LAR	86 (43%)	62 (47%)	24 (35.3%)	0.0034 ^h	0.0749
	Miles + Hartmann	50 (25%)	23 (17.4%)	27 (39.7%)		
Colon resection		64 (32%)	47 (35.6%)	17 (25%)		
Synchronous resection of liver metastases	no	186 (93%)	126 (95.5%)	60 (88.2%)	0.0784 ^h	1
	yes	14 (7%)	6 (4.5%)	8 (11.8%)		
Duration of surgery (min)		170 (130-220)	160 (120-196.2)	200 (150-242.5)	< 0.0001 ^f	0.0004
Loss of blood (ml)		500 (300-800)	400 (200-675)	600 (400-1000)	< 0.0001 ^f	0.0003
Temperature ^c (°C)		35.3 (0.6)	35.3 (0.5)	35.3 (0.7)	0.8719 ^f	1
Perioperative ^d transfusion of PRBC (ml)		0 (0-606.2)	0 (0-326.2)	345 (0-842.5)	< 0.0001 ^f	0.0009
SIRS 1 (POD 1)	no	138 (71.1%)	95 (74.8%)	43 (64.2%)	0.1657 ^g	1
	yes	56 (28.9%)	32 (25.2%)	24 (35.8%)		
SIRS 2 (POD 2)	no	147 (75.4%)	100 (78.7%)	47 (69.1%)	0.1895 ^g	1
	yes	48 (24.6%)	27 (21.3%)	21 (30.9%)		
SIRS 3 (POD 3)	no	161 (82.6%)	107 (84.3%)	54 (79.4%)	0.5151 ^g	1
	yes	34 (17.4%)	20 (15.7%)	14 (20.6%)		
SIRS 4 (POD 4)	no	149 (77.2%)	104 (83.2%)	45 (66.2%)	0.012 ^g	0.2392
	yes	44 (22.8%)	21 (16.8%)	23 (33.8%)		
SIRS 5 (POD 5)	no	144 (80.9%)	99 (87.6%)	45 (69.2%)	0.005 ^g	0.1055
	yes	34 (19.1%)	14 (12.4%)	20 (30.8%)		
Re-operation	no	188 (94%)	132 (100%)	56 (82.4%)	< 0.0001 ^h	< 0.0001
	yes	12 (6%)	0 (0%)	12 (17.6%)		

ASA = American Society of Anesthesiologists; BMI = body mass index; CTX – chemotherapy; Hartmann = proctosigmoidectomy; LAR = low anterior rectum resection; Miles = abdominoperineal rectum resection; POD = postoperative day; PRBC = packed red blood cells; RT = radiotherapy; SIRS = systemic inflammatory response syndrome; TNM = classification of malignant tumors (Tumour, Nodes, Metastasis)

^a measured one day before surgery; ^b in the morning before surgery; ^c at the end of surgery; ^d during the surgery and 30 days after the surgery or until the infection develops; ^e Holm-Bonferroni correction; ^f T-test (mean, standard deviation); ^g Chi-square test; ^h Fisher's exact test; ⁱ Mann-Whitney U test (median, interquartile range)

culated confidence interval (CI) for AUC was 99%, but interpreted as the 95% one.⁶³ Multivariate logistic regression analysis was used to explore the prediction of the probability of infection. Considering survival of the patients, Kaplan-Meier curves between groups of infected and non-infected patients were compared by the log-rank test.⁶⁴ Prognostic factors were investigated by univariate and multivariate Cox proportional hazard model. A p-value ≤ 0.05 was considered statistically significant. All analyses were performed with R statistical software, version 3.2.1.

Results

A total of 200 patients were included in the study, 131 males (65.5%) and 69 females (34.5%). The characteristics of the patients, cancer disease and surgical procedure are shown in Table 1.

Infectious complications

Sixty-eight patients (34%) developed infectious complications, 132 patients did not. Sepsis was diagnosed in 47 patients (23.5%). Two infections were diagnosed in 10 patients. The most frequent postoperative infection was SSI in 61 patients (30.5%). Incisional SSI was diagnosed as the first infection in 28 patients, organ/space SSI in 30 patients, both of them in 3 patients. Most of the incisional SSIs (58%) were diagnosed in patients with abdominoperineal rectum resection and most of organ/space SSIs (52%) in patients with LAR (low anterior rectum resection). Other infections were quite rare (8 UTIs, 5 pneumonias, 1 *Clostridium difficile* enterocolitis). The median number of days until the first infection occurred was seven with interquartile range (IQR) 6–9. The median time to organ/space SSI occurrence was 8 days (IQR 6–12). Antibiotic therapy was applied in 116 patients. In the cases of negative microbiologic results and clinical signs not concordant with infection it was stopped after a few days. Reoperation was necessary in 12 patients (6%), because of infection in 7 and for other reasons in 5 patients.

Risk factors for any perioperative infection as shown by univariate analysis were: duration of surgery (corrected $p = 0.0004$), loss of blood (corrected $p = 0.0003$) and perioperative transfusion of red blood cells (corrected $p = 0.0009$). Surgical procedure and SIRS on POD5 were on the threshold of statistical significance for postoperative infections. Albumins before surgery, PA, IM and dry lean body

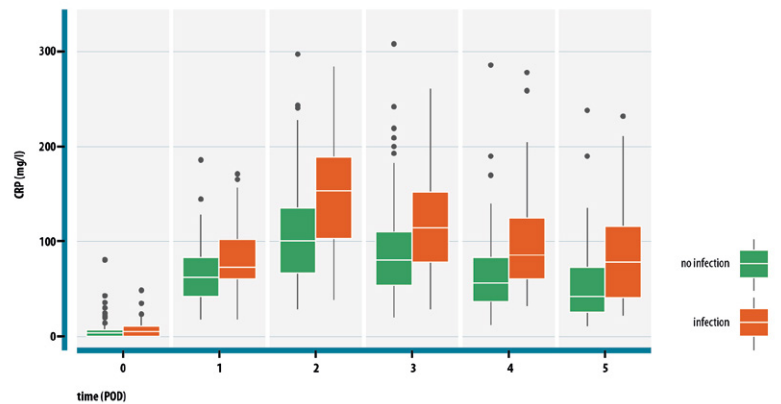


FIGURE 1. The dynamics of CRP shown with median for infected/non-infected group 5 days after colorectal surgery. The width of the box shows the interquartile range. The distal points of vertical line show the highest and the lowest values of CRP.

CRP = C-reactive protein; POD = postoperative day

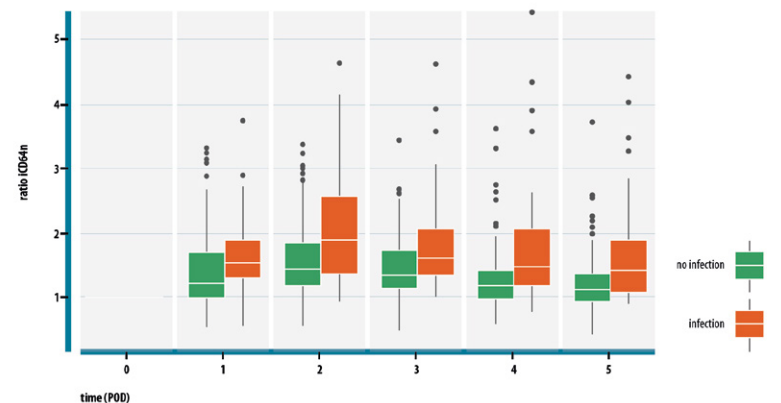


FIGURE 2. The dynamics of the ratio iCD64n shown with median 5 days after colorectal surgery. The width of the box shows the interquartile range. The distal points of vertical line show the highest and the lowest values of the ratio iCD64n.

iCD64n = index CD64n

mass were not found to be risk factors for postoperative infections. A risk factor for organ/space SSI was perioperative transfusion (corrected $p < 0.0001$) while the blood loss was at the border of statistical significance (corrected $p = 0.07$). The hospital stay of 19 days (IQR 14–24) in the infected group was significantly longer as compared to 10 days (IQR 7–12) in the non-infected group ($p < 0.0001$).

Multivariate analysis

The multiple logistic regression analysis was made for prediction of all postoperative infections. It included ASA score, type of surgical procedure, duration of surgery and perioperative transfusion. Independent risk factors for infections were found to be duration of surgery (odds ratio [OR] 1.63, 95%

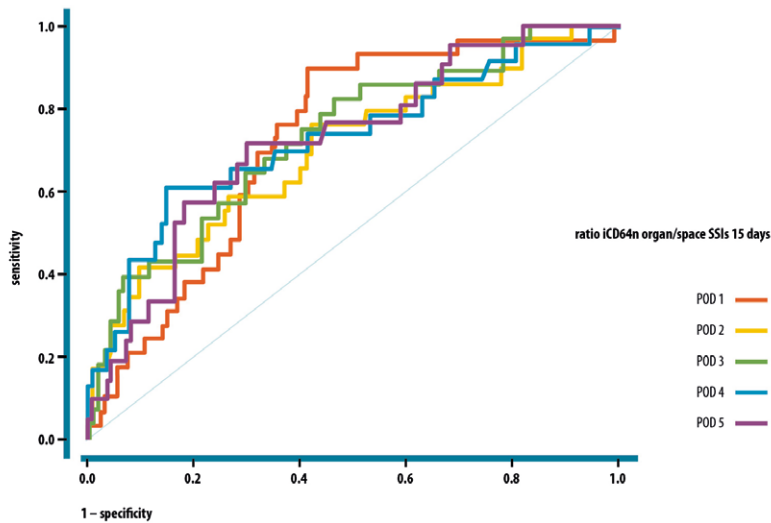


FIGURE 3. ROC curve for the ratio iCD64n POD1-POD5 as a predictor of organ/space SSIs 15 days after colorectal surgery.

iCD64n = index CD64n; POD = postoperative day; ROC = receiver operating characteristic; SSIs = surgical site infections

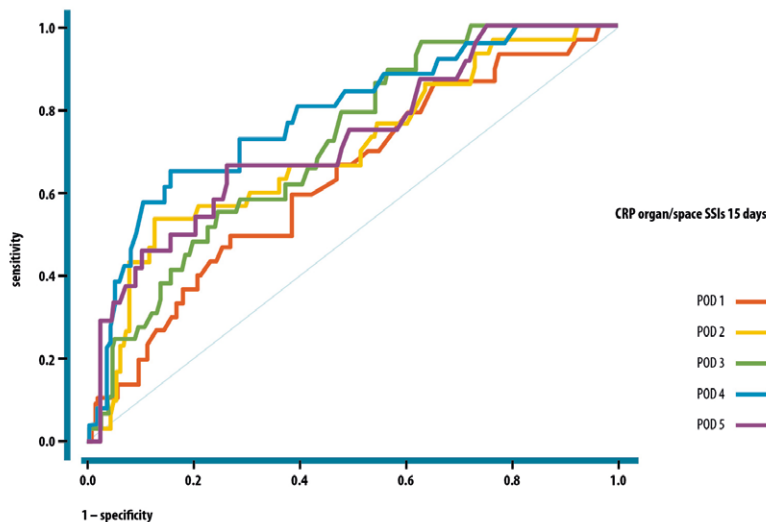


FIGURE 4. ROC curve for CRP POD1-POD5 as a predictor of organ/space SSIs 15 days after colorectal surgery.

CRP = C-reactive protein; POD = postoperative day; ROC = receiver operating characteristic; SSIs = surgical site infections

CI 1.14–2.40, $p = 0.01$) and perioperative transfusion (OR 1.10, 95% CI 1.02–1.19, $p = 0.014$). The expected odds for infection increased with every hour of surgery by 63% (95% CI 14–140%) or with every 100 mL of transfusion by 10% (95% CI 2–19%).

Biomarkers analysis

The values of all biomarkers after surgical procedures were elevated, reaching the peak values on the first day (WBC count, NLR and PCT) or on the

second day (CRP, iCD64n, ratio iCD64n) and later slowly decreasing. The increase of biomarkers was greater in the infection group than in the non-infection group (Figure 1,2).

The ROC analysis was used to compare biomarkers WBC count, NLR, CRP, PCT, iCD64n and the ratio iCD64n from POD1 to POD5 as early predictors of postoperative infections. Predictions for all infections in 15 and 30 days and for organ/space SSIs in 15 days were made. The 15-day prediction was made because the great majority (97%) of the first infections had been diagnosed up to and including this day. The highest diagnostic accuracy for 30-day prediction of all infections was for CRP observed on POD4 (AUC 0.72, 99% CI 0.61–0.83), POD2 (AUC 0.70, 99% CI 0.59–0.80) and POD3 (AUC 0.69, 99% CI 0.58–0.80). The cut-off value for CRP POD4 was 69 mg/L. Two other, rather good predictors were NLR on POD4 (AUC 0.65, 99% CI 0.54–0.77), POD5 (AUC 0.69, 99% CI 0.57–0.80) and the ratio iCD64n on POD2 (AUC 0.67, 99% CI 0.56–0.78) with the cut-off value 1.74. The results of ROC analysis for 15-day prediction of all infections were similar.

In the 15-day prediction of organ/space infections the diagnostic accuracies of CRP and the ratio iCD64n were better than in the two previously mentioned analyses for all infections. The ratio iCD64n was a better predictor on POD3 (AUC 0.73, 99% CI 0.59–0.87) and POD1 (AUC 0.72, 99% CI 0.58–0.86), followed by POD4 (AUC 0.72, 99% CI 0.57–0.88) and POD2 (AUC 0.70, 99% CI 0.55–0.84). The cut-off value for POD1 was 1.37 and POD3 1.40 (Figure 3). The predictive value of CRP was the best on POD4 (AUC 0.79, 99% CI 0.64–0.93) followed by POD5 (AUC 0.73, 99% CI 0.57–0.88), POD3 (AUC 0.72, 99% CI 0.57–0.86) and POD2 (AUC 0.70, 99% CI 0.56–0.85). The cut-off value for CRP on POD4 was 103 mg/L (Figure 4). The prognostic value of PCT for 15-day prediction of organ/space infection was most sensitive on POD4 (AUC 0.72, 99% CI 0.57–0.88) (Figure 5) and for iCD64n on POD5 (AUC 0.69, 99% CI 0.53–0.85).

Survival

The thirty-day mortality was 0% and the ninety-day mortality 0.5%. The Kaplan Meier analysis showed a one-year survival rate in the non-infected group was 97.7% (95% CI 93.1–99.3) and in the infected group 92.6% (95% CI 83.2–96.9). A two-year survival was significantly higher in the non-infected group 92.4% (95% CI 86.4–95.9) as compared to the infected group 80.9% (95% CI 69.4–88.4). P value in log-rank test was 0.0134 (Figure 6). A me-

dian follow-up of patients was 40.9 months (range 32.4–51.5).

Prognostic factors were investigated by univariate and multivariate Cox proportional hazard model. Predictive factors for shorter survival in univariate analysis were: age ($p < 0.0001$), ASA score ($p = 0.0006$), tumour stage ($p = 0.027$), PA ($p = 0.0024$), dry lean body mass ($p = 0.015$), perioperative transfusion ($p = 0.0004$) and postoperative infection ($p = 0.016$). Multivariate analysis showed independent factors associated with shorter survival were: age (hazard ratio [HR] 1.06, 95% CI 1.02–1.10, $p = 0.0044$) and postoperative infection (HR 1.96, 95% CI 1.03–3.73, $p = 0.04$).

Discussion

Colorectal surgery is associated with an intensive release of pro-inflammatory cytokines followed by an anti-inflammatory response and immuno-paralysis. Cellular immunity, crucial for defence against cancer cells in the perioperative period is significantly suppressed.⁶⁵⁻⁶⁷ Postoperative immunosuppression can be further exacerbated by blood transfusion. These immune changes predispose the host to infection, sepsis and even multiple organ dysfunction syndrome (MODS).⁶⁸

In the present study we compared a new biomarker iCD64n and the ratio iCD64n with other biomarkers - WBC count, NLR, CRP and PCT. We found out the best early predictor of organ/space SSIs was the ratio iCD64n. CRP and PCT predicted these infections with the same AUC later, on POD3 and POD4. Other biomarkers as predictive factors for infections after colorectal surgery had already been much studied widely whereas iCD64n had not yet been.

Warschkow *et al.* reported in a diagnostic meta-analysis of 1832 patients the best CRP predictive value for postoperative complications after colorectal surgery was 135 mg/L on POD4 with a negative predictive value (NPV) 89%.⁶⁹ In another retrospective study with 1187 patients Warschkow *et al.* concluded CRP on POD4 with the cut-off 123 mg/L had the highest diagnostic accuracy for the early detection of infections (sensitivity 66%, specificity 77%).²² In a meta-analysis with 2215 patients Gans *et al.* reported infectious complications after major abdominal surgery were very unlikely in patients with CRP below 159 mg/L on POD3 (pooled values: AUC 0.87, sensitivity 77%, specificity 77%, NPV 90%). Maximum predictive values were reached on POD5 (pooled values: AUC 0.83, sen-

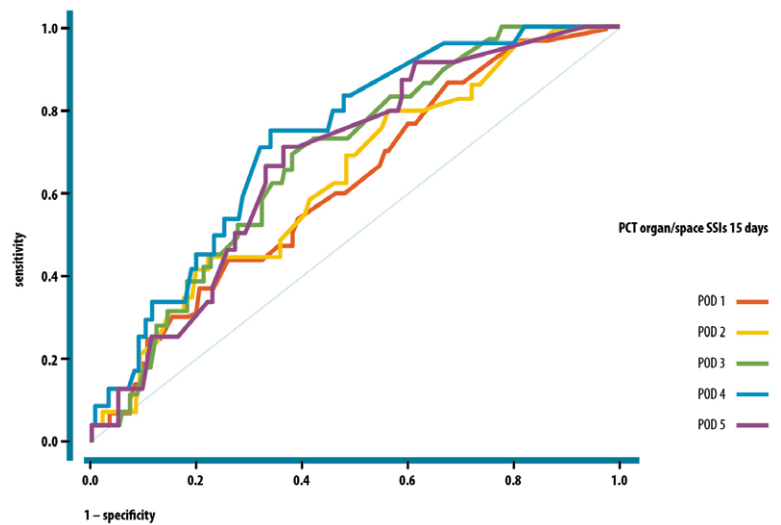


FIGURE 5. ROC curve for PCT POD1-POD5 as a predictor of organ/space SSIs 15 days after colorectal surgery.

POD = postoperative day; PCT = procalcitonin; ROC = receiver operating characteristic; SSIs = surgical site infections

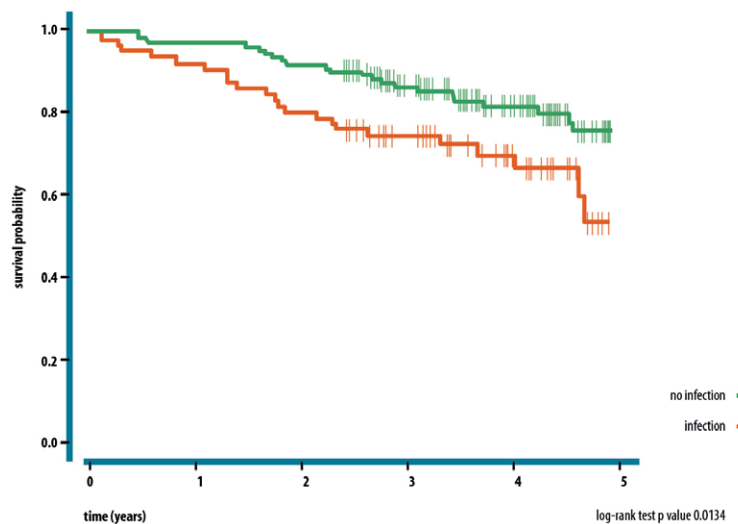


FIGURE 6. Kaplan-Meier survival curve for infected and non-infected group. Patients have been followed up for a minimum of 28 months.

sitivity 86%, specificity 86%, NPV 92%).⁷⁰ The conclusion of the pooled analysis with 1427 patients made by Straatman *et al.* was that CRP on POD3 below 75 mg/L may be a safe discharge criterion after major abdominal surgery with a NPV 97.2%. The probability of major postoperative complications for CRP cut-off 215 mg/L was 20% (95% CI 14.7–25.60%).⁷¹ In our study CRP on POD4 had the best predictive value in the 30-day prediction of all infections and even better on POD4 in the 15-day prediction of organ/space SSIs.

Some recent studies have compared the diagnostic accuracy of PCT and CRP for infection after colorectal surgery. Takakura *et al.* reported in the study which included 114 patients with colorectal resection PCT on POD1 and POD3 (AUC 0.76 and 0.77) was a more relevant predictor for surgical site infection than CRP (AUC 0.71).²⁷ Garcia-Granero *et al.* reported that in 205 patients undergoing surgery for colorectal cancer PCT was better than CRP in the early prediction of major anastomotic leak on POD3, POD4 and POD5. The best AUC values for PCT were 0.87 and for CRP 0.85 on POD5.²³ The results of study, made by Lagoutte *et al.* were different. It included 100 patients and showed PCT is neither earlier nor more accurate than CRP for the detection of anastomotic leakage after colorectal surgery. The best accuracy for CRP and PCT was obtained on POD4 (AUC 0.87 and 0.75).²⁹ Oberhofer *et al.* reported in a study with 79 colorectal surgical patients PCT on POD2 and CRP on POD3 had similar predictive values for infections (AUC 0.75 and 0.75).²⁸ In the present study we found out that PCT on POD4 (AUC 0.64) was a worse predictor than CRP (AUC 0.72) in the 30-day prediction of all infections. In the 15-day prediction of organ/space SSIs PCT on POD4 (AUC 0.72) was worse than CRP (AUC 0.79) again.

As in other studies WBC count proved to be a poor early diagnostic marker of postoperative infections. The best predictive value of NLR was on POD5 (AUC 0.69) in the 30-day prediction of all infections and was as good as for CRP (AUC 0.68).

Only few studies have investigated the dynamics of iCD64n in the postoperative period. The first have been done in cardiovascular and orthopedic surgery. Two studies done by Kolackova *et al.* with 40 cardiac patients³⁴ and Katoh *et al.*⁵⁰ with 41 orthopaedic patients reported the expression of CD64n after surgery was significantly increased with the peak on POD3. Studies by Fjaertoft *et al.*⁵¹ and Gerrits *et al.*⁵² reported that iCD64n was significantly higher in septic patients compared to patients with SIRS after surgery and control group. Unlike clean surgical procedures, the iCD64n in clean-contaminated surgery has only recently been explored. In the study Janež *et al.*⁵³ included 77 patients. They compared postoperative differences in inflammatory and immunological response between opened and laparoscopically assisted colorectal surgery. There was a considerable increase of iCD64n in both groups of patients on POD1 (1.42 in open surgery group versus 1.24 in laparoscopic surgery group). But they did not observe difference in infectious complications in these two

groups. In a very recent study, which included 189 patients with colorectal, 17 with maxillofacial and 23 with open heart surgery, Jukic *et al.*⁵⁴ reported that iCD64n is the best predictor of postoperative infections in the first 48 hours after major surgery compared to WBC count, neutrophils and CRP. The AUC value after 24 hours was 0.89 and after 48 hours 0.82. The most frequent infection was the respiratory tract infection (40%).

In the present study index CD64n was not found to be a good early predictor for any infection including organ/space SSIs. However, we found that the ratio iCD64n was a better predictor of infection than its absolute value. In the 30-day prediction of all infections the ratio iCD64n on POD2 (AUC 0.67) was a worse predictor than CRP (AUC 0.70). However, for the 15-day prediction of organ/space SSI the ratio iCD64n on POD1 (AUC 0.72) was the best early predictor among all studied biomarkers (AUC on POD1 for iCD64n and CRP was 0.63 and for PCT 0.61). Patients with the ratio iCD64n higher than the cut-off value 1.37 on POD1 should be closely monitored and additional diagnostic measures should be taken to confirm or exclude infection. Our study group was homogeneous and it is comprised of patients with clean-contaminated colorectal surgery. SSIs were the most common postoperative infections. We explain this with a high number of rectum surgeries (68%), a high stage of the disease (64% stage III and IV) and a high proportion of patients preoperatively treated with neo-adjuvant CTX and/or RT (59%). Risk factors for infections were analysed. It was shown that duration of surgery and transfusion of red blood cells were independent risk factors for infections. The length of surgery procedure is closely correlated with perioperative immunoparalysis and predisposition to infection.⁷¹

We found out that age, ASA score, tumour stage, PA, dry lean body mass, perioperative transfusion and postoperative infection correlated with the length of survival. Multivariate analysis showed that the only independent factors associated with shorter survival were age and postoperative infection. In our study a perioperative transfusion of red blood cells was not an independent prognostic marker for survival. However, in many other studies postoperative infections and perioperative transfusion were independent risk factors for worse long-term survival.⁷³⁻⁷⁷ Both of them aggravate cytokine response after surgery, suppress cell mediated immunity and can facilitate the growth of tumour cells. Due to the synergistic effect patients with both risk factors represent a group with

a particularly poor prognosis.⁷⁸ The efforts to reduce postoperative infections may have a favourable effect on cancer prognosis.

Conclusions

In the present study we found the ratio iCD64n on POD1 was the earliest predictor of intra-abdominal infection after colorectal cancer surgery. CRP predicts the infection with the same predictive value later, not before POD3. Further research is needed to evaluate the role of neutrophil CD64 expression in infection diagnosis after major surgery. Postoperative infection was found to be an independent predictive factor of shorter long-term survival.

References

- Zoucas E, Lydrup ML. Hospital costs associated with surgical morbidity after elective colorectal procedures: a retrospective observational cohort study in 530 patients. *Patient Saf Surg* 2014; **8**: 2.
- Sjo OH, Larsen S, Lunde OC, Nesbakken A. Short term outcome after emergency and elective surgery for colon cancer. *Colorectal Dis* 2009; **11**: 733-9.
- Alves A, Panis Y, Mathieu P, Mantion G, Kwiatkowski F, Slim K. Postoperative mortality and morbidity in French patients undergoing colorectal surgery: results of a prospective multicenter study. *Arch Surg* 2005; **140**: 278-83.
- Korner H, Nielsen HJ, Soreide JA, Nedrebo BS, Soreide K, Knapp JC. Diagnostic accuracy of C reactive protein for intra-abdominal infections after colorectal resections. *J Gastrointest Surg* 2009; **13**: 1599-606.
- Dominguez-Comesana E, Lopez-Gomez V, Estevez-Fernandez SM, Padin EM, Ballinas-Miranda J, Carrera-Dacosta E, et al. [Procalcitonin and C-reactive protein as early indicators of postoperative intra-abdominal infection after surgery for gastrointestinal cancer]. [Spanish]. *Cir Esp* 2014; **92**: 240-6.
- Tang R, Chen HH, Wang YL, Changchien CR, Chen JS, Hsu KC, et al. Risk factors for surgical site infection after elective resection of the colon and rectum: A single-center prospective study of 2809 consecutive patients. *Ann Surg* 2001; **234**: 181-9.
- Smith RL, Bohl JK, McElearney ST, Friel CM, Barclay MM, Sawyer RG, et al. Wound infection after elective colorectal resection. *Ann Surg* 2004; **239**: 599-607.
- Konishi T, Watanabe T, Kishimoto J, Nagawa H. Elective colon and rectal surgery differ in risk factors for wound infection: results of prospective surveillance. *Ann Surg* 2006; **244**: 758-63.
- Horzic M, Kopljur M. Postoperative infections in colorectal cancer patients. *Hepatogastroenterology* 2005; **52**: 101-4.
- Nespoli A, Gianotti L, Totis M, Bovo G, Nespoli L, Chiodini P, et al: Correlation between postoperative infections and long term survival after colorectal resection for cancer. *Tumori* 2004; **90**: 485-90.
- Khuri SF, Henderson WG, DePalma RG, Mosca C, Healey NA, Kumbhani DJ, et al. Determinants of long-term survival after major surgery and the adverse effect of postoperative complications. *Ann Surg* 2005; **242**: 326-41.
- Artinyan A, Orcutt ST, Anaya DA, Richardson P, Chen GJ, Berger DH. Infectious postoperative complications decrease long-term survival in patients undergoing curative surgery for colorectal cancer. A study of 12075 patients. *Ann Surg* 2015; **261**: 497-505.
- Tsujimoto H, Ueno H, Hashiguchi Y, Ono S, Ichikura T, Hase K. Postoperative infections are associated with adverse outcome after resection with curative intent for colorectal cancer. *Oncol Lett* 2010; **1**: 119-25.
- Mokart D, Merlin M, Sannini A, Brun JP, Tison A, Delperio JL, et al. Procalcitonin, interleukin 6 and systemic inflammatory response syndrome (SIRS): early markers of postoperative sepsis after major surgery. *Br J Anaesth* 2005; **94**: 767-73.
- Pedersen T, Roikjaer O, Jess P. Increased levels of C-reactive protein and leukocyte count are poor predictors of anastomotic leakage following laparoscopic colorectal resection. *Dan Med J* 2012; **59**: A4552.
- Welsch T, Müller SA, Ulrich A, Kischlat A, Hinz U, Kienle P, et al. C reactive protein as early predictor for infectious postoperative complications in rectal surgery. *Int J Colorectal Dis* 2007; **22**: 1499-507.
- den Dulk M, Noter SL, Hendriks ER, Brouwers MAM, van der Vlies CH, Oostenbroek RJ, et al. Improved diagnosis and treatment of anastomotic leakage after colorectal surgery. *Eur J Surg Oncol* 2009; **35**: 420-6.
- Matthiessen P, Henriksson M, Hallböök O, Grunditz E, Noren B, Arbman G. Increase of serum C-reactive protein is an early indicator of subsequent symptomatic leakage after anterior resection. *Colorectal Dis* 2008; **10**: 75-80.
- Ishikawa K, Kusumi T, Kosokawa M, Nishida Y, Sumikawa S, Furukawa H. Incisional surgical site infection after elective open surgery for colorectal cancer. *Int J Surg Oncol* 2014; **2014**: 419712.
- Blumetti J, Luu M, Sarosi G, Hartless K, McFarlin J, Parker B, et al. Surgical site infections after colorectal surgery: Do risk factors vary depending on the type of infection considered? *Surgery* 2007; **142**: 704-11.
- Chromik AM, Endter F, Uhl W, Thiede A, Reith HB, Mittelkötter U. Preemptive antibiotic treatment vs standard treatment in patients with elevated serum procalcitonin levels after elective colorectal surgery: a prospective randomised pilot study. *Langenbecks Arch Surg* 2006; **391**: 187-94.
- Warschko R, Tarantino I, Torzewski M, Näf F, Lange J, Steffen T. Diagnostic accuracy of C-reactive protein and white blood cell counts in the early detection of inflammatory complications after open resection of colorectal cancer: a retrospective study of 1187 patients. *Int J Colorectal Dis* 2011; **26**: 1405-13.
- Garcia-Granero A, Frasson M, Flor-Lorente B, Blanco F, Puga R Carratala A, et al: Procalcitonin and C-reactive protein as early predictors of anastomotic leak in colorectal surgery: a prospective observational study. *Dis Colon Rectum* 2013; **56**: 475-83.
- Nunes BK, Lacerda RA, Jardim JM. Systematic review and meta-analysis of the predictive value of C-reactive protein in postoperative infections. *Rev Esc Enferm USP* 2011; **45**: 1480-5.
- Neumaier M, Scherer MA. C-reactive protein levels for early detection of postoperative infection after fracture surgery in 787 patients. *Acta Orthop* 2008; **79**: 428-32.
- Welsch T, Frommhold K, Hinz U, Weigand M, Kleeff J, Friess H, et al. Persisting elevation of C-reactive protein after pancreatic resections can indicate developing inflammatory complications. *Surgery* 2008; **143**: 20-8.
- Takakura Y, Hinoi T, Egi H, Shimomura M, Adachi T, Saito Y, et al. Procalcitonin as a predictive marker for surgical site infection in elective colorectal cancer surgery. *Langenbecks Arch Surg* 2013; **398**: 833-9.
- Oberhofer D, Juras J, Pavičić AM, Rančić Žurić I, Rumanjak V. Comparison of C-reactive protein and procalcitonin as predictors of postoperative infectious complications after elective colorectal surgery. *Croat Med J* 2012; **53**: 612-9.
- Lagoutte N, Facy O, Ravoire A, Chalumeau C, Jonval L, Rat P, et al. C-reactive protein and procalcitonin for the early detection of anastomotic leakage after elective colorectal surgery: pilot study in 100 patients. *J Visc Surg* 2012; **149**: e345-9.
- Silvestre J, Rebanda J, Lourenco C, Povoia P. Diagnostic accuracy of C-reactive protein and procalcitonin in the early detection of infection after elective colorectal surgery-a pilot study. *BMC Infect Dis* 2014; **14**: 444.
- Zahorec R. Ratio of neutrophil to lymphocyte counts-rapid and simple parameter of systemic inflammation and stress in critically ill. *Bratisl Lek Listy* 2001; **102**: 5-14.
- Cook EJ, Walsh SR, Farooq N, Alberts JC, Justin TA, Keeling NJ. Post-operative neutrophil-lymphocyte ratio predicts complications following colorectal surgery. *Int J Surg* 2007; **5**: 27-30.
- Forget P, Dinant V, De Kock M. Is the neutrophil to lymphocyte ratio more correlated than C-reactive protein with postoperative complications after major abdominal surgery? *PeerJ* 2015; **3**: e713.
- Kolackova M, Kudlova M, Kunes P, Lonsky V, Mandak J, Andrys C, et al. Early expression of FcγRI (CD64) on monocytes of cardiac surgical patients and higher density of monocyte anti-inflammatory scavenger CD163 receptor in on pump patients. *Mediators Inflamm* 2008; **2008**: 235461.
- Radaev S, Sun P. Recognition of immunoglobulins by Fcγ receptors. *Mol Immunol* 2001; **38**: 1073-83.

36. Davis BH, Olsen SH, Ahmad E, Bigelow NC. Neutrophil CD64 is an improved indicator of infection or sepsis in emergency department patients. *Arch Pathol Lab Med* 2006; **130**: 654-61.
37. Repp R, Valerius T, Sendler A, Gramatzki M, Iro H, Kalden R, et al. Neutrophils express the high affinity receptor for IgG (FcγRI, CD64) after in vivo application of recombinant human granulocyte colony-stimulating factor. *Blood* 1991; **78**: 885-9.
38. van der Meer W, Pickkers P, Scott CS, van der Hoeven JG, Gunnewiek JK. Hematological indices, inflammatory markers and neutrophil CD64 expression: comparative trends during experimental human endotoxemia. *J Endotoxin Res* 2007; **13**: 94-100.
39. Qureshi SS, Lewis SM, Gant VA, Treacher D, Davis BH, Brown KA. Increased distribution and expression of CD64 on blood polymorphonuclear cells from patients with the systemic inflammatory response syndrome (SIRS). *Clin Exp Immunol* 2001; **125**: 258-65.
40. Hoffmeyer F, Witte K, Schmidt RE. The high affinity FcγRI on PMN: regulation of expression and signal transduction. *Immunology* 1997; **92**: 544-52.
41. Jalava Karvinen P, Hohenthal U, Laitinen I, Kotilainen P, Rajamäki A, Nikoskelainen J, et al. Simultaneous quantitative analysis of FcγRI (CD64) and CR1 (CD35) on neutrophils in distinguishing between bacterial infections, viral infections and inflammatory diseases. *Clin Immunol* 2009; **133**: 314-23.
42. Mokuda S, Doi O, Takasugi K. Simultaneous quantitative analysis of CD64 and CD35 on neutrophils as markers to differentiate between bacterial and viral infections in patients with rheumatoid arthritis. *Mod Rheumatol* 2012; **22**: 750-7.
43. Cid J, Aguinaco R, Sanchez R, Garcia Pardo G, Llorente A. Neutrophil CD64 expression as marker of bacterial infection: A systematic review and meta-analysis. *J Infect* 2010; **60**: 313-9.
44. Li S, Huang X, Chen Z, Zhong H, Peng Q, Deng Y, et al. Neutrophil CD64 expression as a biomarker in the early diagnosis of bacterial infection: a meta-analysis. *Int J Infect Dis* 2013; **17**: e12-e23.
45. Wang X, Li ZY, Zeng L, Zhang AQ, Pan W, Gu W, et al. Neutrophil CD64 expression as a diagnostic marker for sepsis in adult patients: a meta-analysis. *Crit Care* 2015; **19**: 245.
46. Bhandari V, Wang C, Rinder C, Rinder H. Hematologic profile of sepsis in neonates: neutrophil CD64 as a diagnostic marker. *Pediatrics* 2008; **121**: 129-34.
47. Fang DH, Fan CH, Li J, An Q, Yao H, Ji Q, et al. Ratios of CD64 expressed on neutrophils, monocytes, and lymphocytes may be a novel method for diagnosis of neonatal sepsis. *J Infect Dev Ctries* 2015; **9**: 175-81.
48. Du J, Li L, Dou Y, Li P, Chen R, Liu H. Diagnostic utility of neutrophil CD64 as a marker for early onset sepsis in preterm neonates. *PLoS One* 2014; **9**: e102647.
49. Allen E, Bakke AC, Purtzer MZ, Deodhar A. Neutrophil CD64 expression: distinguishing acute inflammatory autoimmune disease from systemic infections. *Ann Rheum Dis* 2002; **61**: 522-5.
50. Katoh N, Nishino J, Nishimura K, Kawabata C, Hotta Y, Matsui T, et al. Normal sequential changes in neutrophil CD64 expression after total joint arthroplasty. *J Orthop Sci* 2013; **18**: 949-54.
51. Fjaertoft G, Hakansson LD, Pauksens K, Sisask G, Venge P. Neutrophil CD64 (FcγRI) expression is a specific marker of bacterial infection: A study on the kinetics and the impact of major surgery. *Scand J Infect Dis* 2007; **39**: 525-35.
52. Gerrits JH, McLaughlin PMJ, Nienhuis BN, Smit JW, Loef B. Polymorphic mononuclear neutrophils CD64 index for diagnosis of sepsis in postoperative surgical patients and critically ill patients. *Clin Chem Lab Med* 2013; **51**: 897-905.
53. Janež J, Korač T, Rebolj Kodre A, Jelenc F, Ihan A. Laparoscopically assisted colorectal surgery provides better short-term clinical and inflammatory outcomes compared to open colorectal surgery. *Arch Med Sci* 2015; **11**: 1217-26.
54. Jukic T, Ihan A, Stubljar D. Dynamics of inflammation biomarkers C-reactive protein, leukocytes, neutrophils, and CD64 on neutrophils before and after major surgical procedures to recognize potential postoperative infection. *Scand J Clin Lab Invest* 2015; e1-8.
55. International Union Against Cancer (UICC). *TNM classification of malignant tumours*. 7th edition. Sobin LH, Gospodarowicz MK, Wittekind Ch, editors. New York: Wiley; 2009.
56. Fitz-Henry J. The ASA classification and perioperative risk. *Ann R Coll Surg Engl* 2011; **93**: 185-7.
57. Daabis M. American society of anaesthesiologists physical status classification. *Indian J Anaesth* 2011; **55**: 111-5.
58. Levy MM, Fink MP, Marshall JC, Abraham E, Angus D, Cook D, et al. 2001 SCCM/ESICM/ACCP/ATS/SIS international sepsis definitions conference. *Crit Care Med* 2003; **31**: 1250-6.
59. Horan TC, Andrus M, Dudeck MA. CDC/NHSN surveillance definition of health care-associated infection and criteria for specific types of infections in the acute care setting. *Am J Infect Control* 2008; **36**: 309-32.
60. Gupta D, Lis CG, Dahlk SL, King J, Vashi PG, Grutck JF, et al. The relationship between bioelectrical impedance phase angle and subjective global assessment in advanced colorectal cancer. *Nutr J* 2008; **7**: 19.
61. Barbosa-Silva MCG, Barros AJD, Wang J, Heymsfield SB, Pierson RN. Bioelectrical impedance analysis: population reference values for phase angle by age and sex. *Am J Clin Nutr* 2005; **82**: 49-52.
62. Holm S. A simple sequentially rejective multiple test procedure. *Scand J Statist* 1979; **6**: 65-70.
63. Zweig MH, Campbell G. Receiver-Operating Characteristic (ROC) Plots: A fundamental evaluation tool in clinical medicine. *Clin Chem* 1993; **39**: 561-77.
64. Rich JT, Neely JG, Paniello RC, Voelker CJC, Nussenbaum B, Wang EW. A practical guide to understanding Kaplan-Meier curves. *Otolaryngol Head Neck Surg* 2010; **143**: 331-6.
65. Karanika S, Karantanos T, Theodoropoulos GE. Immune response after laparoscopic colectomy for cancer: a review. *Gastroenterol Rep* 2013; **1**: 85-94.
66. Evans C, Galustian C, Kumar D, Hagger R, Melville DM, Bodman-Smith M, et al. Impact of surgery on immunologic function: comparison between minimally invasive techniques and conventional laparotomy for surgical resection of colorectal tumors. *Am J Surg* 2009; **197**: 238-45.
67. Huang C, Huang R, Jiang T, Huang K, Cao J, Qiu Z. Laparoscopic and open resection for colorectal cancer: an evaluation of cellular immunity. *BMC Gastroenterol* 2010; **10**: 127.
68. Choileain NN, Redmond HP. Cell response to surgery. *Arch Surg* 2006; **141**: 1132-40.
69. Warschkow R, Beutner U, Steffen T, Müller SA, Schmied BM, Güller U, et al. Safe and early discharge after colorectal surgery due to C-reactive protein. A diagnostic meta-analysis of 1832 patients. *Ann Surg* 2012; **256**: 245-50.
70. Gans SL, Atema JJ, van Dieren S, Koerkamp BG, Boermeester MA. Diagnostic value of C-reactive protein to rule out infectious complications after major abdominal surgery: a systematic review and meta-analysis. *Int J Colorectal Dis* 2015; **30**: 861-73.
71. Straatman J, Harmsen AMK, Cuesta MA, Berkhof J, Jansma EP, van der Peet DL. Predictive value of C-reactive protein for major complications after major abdominal surgery: A systematic review and pooled-analysis. *PLoS One* 2015; **10**: e0132995.
72. Menges P, Kessler W, Kloecker C, Feuerherd M, Gaubert S, Diedrich S, et al. Surgical trauma and postoperative immune dysfunction. *Eur Surg Res* 2012; **48**: 180-6.
73. Cho JY, Han HS, Yoon YS, Hwang DW, Jung K. Postoperative complications influence prognosis and recurrence patterns in periampullary cancer. *World J Surg* 2013; **37**: 2234-41.
74. Law WL, Choi HK, Lee YM, Ho JWC. The impact of postoperative complications on long-term outcomes following curative resection for colorectal cancer. *Ann Surg Oncol* 2007; **14**: 2559-66.
75. Miki C, Hiro J, Ojima E, Inoue Y, Mohri Y, Kusunoki M. Perioperative allogeneic blood transfusion, the related cytokine response and long-term survival after potentially curative resection of colorectal cancer. *Clin Oncol* 2006; **18**: 60-6.
76. Amato A, Pescatori M. Perioperative blood transfusion and recurrence of colorectal cancer. *Cochrane Database Sys Rev* 2006; **1**. Art. No.: CD005033.
77. Acheson AG, Brookes MJ, Spahn DR. Effects of allogeneic red blood cell transfusions on clinical outcomes in patients undergoing colorectal cancer surgery, a systematic review and meta-analysis. *Ann Surg* 2012; **256**: 235-44.
78. Mynster T, Christensen IJ, Moesgaard F, Nielsen HJ. Effects of the combination of blood transfusion and postoperative infectious complications on prognosis after surgery for colorectal cancer. *Br J Surg* 2000; **87**: 1553-62.

Treatment-related cardiovascular toxicity in long-term survivors of testicular cancer

Jasenka Gugic, Lorna Zadavec Zaletel, Irena Oblak

Department of Radiotherapy, Institute of Oncology Ljubljana, Ljubljana, Slovenia

Radiol Oncol 2017; 51(2): 221-227.

Received 4 February 2016
Accepted 14 February 2016

Correspondence to: Lorna Zadavec Zaletel, M.D., Ph.D., Department of Radiotherapy, Institute of Oncology Ljubljana, Zaloška 2, SI-1000 Ljubljana, Slovenia. Phone: +386 1 5879 500. E-mail: lzaletel@onko-i.si

Disclosure: No potential conflicts of interest were disclosed.

Backgrounds. Testicular cancer is the most common malignancy in young men. Considering increasing incidence, exceptionally high cure rate, as well as long life expectancy, assessment of long term toxicity in testicular cancer survivors is of great importance. In the last decades a major effort has been made in order to reduce toxicity of treatment, while maintaining its high effectiveness.

Conclusions. Actual knowledge on treatment toxicity is based on outdated treatment modalities. Hopefully, modern treatment modalities could reduce toxicity, but, there is no firm confirmation for that at the moment, as data dealing with late sequelae of modern treatment of testicular cancer are not available yet due to the short period of observation. The life-threatening cardiovascular toxicity in testicular cancer survivors is major complication of platinum-based chemotherapy, mediastinal radiotherapy and even subdiaphragmatic radiotherapy.

Key words: testicular cancer; cardiovascular toxicity; long-term survivors

Introduction

Although rare disease, testicular cancer is the most common malignancy in young men aged 20 to 40 years. Considering increasing incidence worldwide¹⁻³, exceptionally high cure rate with 5-year survival rate exceeding 95% for all stages⁴ and life expectancy almost comparable to age-matched healthy male population⁵, evaluation of treatment-related long-term morbidity has become increasingly important. In the past decades efforts have been made in order to optimize treatment with objective to decrease toxicity, while maintaining high cure rates. The introduction of less toxic chemotherapeutic schemes⁶⁻⁸, reduction in radiation doses and volumes⁹⁻¹¹ and preferred use of active surveillance¹², have all led to reduced treatment toxicity. Irrespective of that, some treatment-related sequelae remained unavoidable. Most of the current studies represent complications of treatment modalities administered several years or even decades ago, but are still of a major concern.

With the 25-year risk of approximately 16%, cardiovascular diseases (CVD) are among the most important life-threatening long-term complications in testicular cancer survivors.¹³ Long-term testicular cancer survivors are more likely to develop unfavourable cardiovascular risk profile.¹⁴⁻²¹ In addition, an increased risk of mortality caused by CVD has also been observed.^{5,22-24}

According to the current knowledge, cardiovascular toxicity is mainly due to cisplatin based chemotherapy and mediastinal radiation therapy^{13,19,25}; although subdiaphragmatic radiotherapy is associated with an increased risk of CVD as well.^{14,26}

Treatment-related cardiovascular morbidity

The introduction of cisplatin based chemotherapeutic regimens into treatment of testicular cancer in the early 1970s represents cornerstone in

TABLE 1. Risk for coronary artery disease in testicular cancer survivors regarding to different treatment modalities

Author (year)	N	Period of treatment	Median follow up (range), in years	Age at diagnosis (range)	Age at follow-up (range)	Risk for CAD (CI 95 %)	Treatment Modalities	Note
Meinardi <i>et al.</i> ¹⁷ (2000)	87	Before 1987 ^a	14 (10 to 20)	27 (17-36)	42 (30-50)	SIR=7.1 (1.9 to 18.3)	ChT	Age adjusted results. Older than 50 years at follow-up were excluded.
Huddart <i>et al.</i> ²⁴ (2003)	992	1982-1992	10.2 (0 to 20.3)	31.7 (10-82)	44 (23-78)	RR=1.00 (reference) RR=2.59 (1.15 to 5.84) RR=2.40 (1.04 to 5.45) RR=2.78 (1.09 to 7.07)	Surveillance ChT RT ChT and RT	Age adjusted results. Only 8.3 % of RT treated patients had also med. RT.
Van der Belt-Dusebut <i>et al.</i> ¹¹ (2006)	2339	1965-1995	18.4 (5 to 38.4)	38.3 ^b (n.r.) 28.1 ^c (n.r.)	59.8 ^b (n.r.) 50.4 ^c (n.r.)	SIR=0.94 (0.61 to 1.39) SIR=1.35 (0.97 to 1.83) SIR=1.07 (0.92 to 1.23) SIR=2.48 (1.77 to 3.37) SIR=0.92 (0.77 to 1.08) SIR=2.97 (1.73 to 4.77) SIR=1.83 (1.08 to 2.90)	Surveillance ChT RT RT – med. RT – subdia. RT – med. + ChT RT – subdia. + ChT	Patients with CAD before or within 5 years from diagnosis were excluded.
Haughnes <i>et al.</i> ¹² (2010)	990	1980-1994	19 (13 to 28)	31 (15-53)	51 (31-69)	HR=1.0 (reference) HR=2.0 (0.64 to 6.1) HR=5.7 (1.9 to 17.1) HR=2.1 (0.78 to 5.4) HR=5.3 (1.5 to 18.3)	Surveillance ChT (CVB) ChT (BEP) RT ChT + RT	Age adjusted results. Patients with CAD before or within 2 years from diagnosis were excluded. Only 3 of 420 RT treated patients had also med. RT.

BEP = bleomycin, etoposid, cisplatin; CAD = coronary artery disease; ChT = chemotherapy; CVB = cisplatin, etoposid, bleomycin; HR = hazard ratio; med. = mediastinal; N = number of patients; n.r. = not reported; RT = radiotherapy; RR = relative risk; SIR = standardized incidence ratio; subdia. = subdiaphragmatic;

^a All patients treated with cisplatin based chemotherapy before 1987.

^b Age for seminoma patients.

^c Age for nonseminoma patients.

testicular cancer management. Prior to that, different chemotherapeutic regimens were used, some of them containing even anthracyclines, cytotoxic drugs with well known cardiotoxic effect. Although reports on cisplatin cardiovascular toxicity date back to the 1980s^{20,27-29}, first study systematically reporting the frequency of late cardiac morbidity by Meinardi *et al.* was published in 2000. After a median follow up of 14 years, a major cardiac event was documented in 5 of 87 patients (5.8%) treated with cisplatin based chemotherapy; myocardial infarction in 2 (2.3%) and angina pectoris in the remaining 3 (3.5%) patients. Compared with the general male population, this corresponded to approximately 7-fold increased risk (observed-to-expected ratio [O/E] = 7.1, 95% confidence interval [CI], 1.9 to 18.3-fold). In this study, additional analysis of subclinical cardiac disease was performed as well. Echocardiographic evaluation showed abnormal diastolic function of the left ventricle in 33% of the patients treated with cisplatin based chemotherapy, probably as an early sign of microvasculopathy.¹⁹

Subsequent studies with larger testicular cancer cohorts in following years revealed the magnitude of the problem (Table 1). Huddart *et al.* reported on cardiovascular morbidity in 992 testicular cancer survivors, treated between 1982 and 1992 at the Royal Marsden Health Service Trust. In particular, they reported on cardiac events, comprising

angina pectoris, long-term chest pain, myocardial infarction, surgery for coronary artery disease and others cardiac abnormalities. Approximately two thirds of the patients were treated with chemotherapy; cisplatin-based in two thirds and carboplatin-based in remaining third. After a median follow up of 10.2 years, age-adjusted relative risk (RR) for cardiac events was 2.59 (95% CI, 1.15 to 5.84) with no significant difference between patients treated with cisplatin and those treated with carboplatin. There was no difference in risk for cardiac events between patients treated with bleomycin containing regimens and those, who didn't get bleomycin, indicating that bleomycin did not significantly contribute to cardiac damage. Moreover, in this study, risk for cardiac events was increased in patients treated with radiotherapy (RR = 2.4, 95% CI, 1.04 to 5.45), although a minority of them - only 8.3%, received mediastinal radiotherapy. Patients treated with chemotherapy and radiotherapy were, as expected, at the highest risk, with age-adjusted RR = 2.78 (95% CI, 1.09 to 7.07).²⁶

After a median follow up of 18.4 years, van der Belt-Dusebut *et al.* reported on 694 cardiovascular events in 2 512 5-year testicular cancer survivors. The overall standardized incidence ratio (SIR) for coronary artery disease was significantly elevated (SIR = 1.17, 95% CI, 1.04 to 1.31). They found slightly, but not significantly increased risk for coronary artery disease in chemotherapy treated patients

compared to the general population (SIR = 1.35, 95% CI, 0.97 to 1.83). Chemotherapy with cisplatin, vinblastine, bleomycin (PVB) regimen was associated with 1.9-fold (95% CI, 1.7 to 2.0-fold), significantly increased risk for myocardial infarction, while chemotherapy with bleomycin, etoposide, cisplatin (BEP) was associated with borderline significantly increased risk for CVD (SIR = 1.5, 95% CI, 1.0 to 2.2), but not for myocardial infarction. Analysis of patients treated with radiotherapy revealed 3.7-fold (95% CI, 2.2 to 6.2-fold) increased risk for myocardial infarction after a mediastinal radiotherapy, while there was no increased risk for CVD after subdiaphragmatic radiotherapy. There was a trend towards higher risk for coronary artery disease with younger age at diagnosis and younger age at follow up as well, for the whole study group. In addition, in nonseminoma group of patients there was a significant influence of attained age of patient on the risk for myocardial infarction, with increased risk in 54 years old or younger (SIR = 1.86, 95% CI, 1.20 to 2.74), even higher risk in younger than 45 years (SIR = 2.06, 95% CI, 1.15 to 3.41) and decreased risk in 55 years or older (SIR = 0.53, 95% CI, 0.25 to 0.98).¹³

Haugnes *et al.* recently reported on cardiovascular morbidity in 990 testicular cancer survivors treated between 1980 and 1994. The incidence of two end-points were evaluated: coronary artery disease, including myocardial infarction and angina pectoris and atherosclerotic diseases, including coronary artery disease, cerebrovascular insult, transitory ischemic attack, carotid stenosis and other peripheral atherosclerotic disease. With a median follow up of 19 years, testicular cancer survivors treated with chemotherapy had increased risk for coronary artery disease (hazard ratio [HR] = 2.6, 95% CI, 0.96 to 6.9) and atherosclerotic disease (HR = 2.6, 95% CI, 1.1 to 5.9), compared to surgery only group. Treatment with BEP was associated with a 5.7-fold (95% CI, 1.9 to 17.1-fold), significantly increased risk for coronary artery disease and a 4.7-fold (95% CI, 1.8 to 12.2-fold), significantly increased risk for atherosclerotic disease, while treatment with CVB was associated with nonsignificantly increased risk for CVD, in contrary with the results of van der Belt-Dusebout study. Additional subanalyses, taking into account chemotherapy type, revealed that higher cumulative dose of etoposide was associated with increased risk for coronary artery disease, while higher cumulative doses of etoposide and cisplatin were associated with increased risk for atherosclerotic disease as well. Interestingly, risk for coronary artery disease

and atherosclerotic disease were increased even in patients treated with mostly non-mediastinal radiotherapy (only 3 of 420 irradiated patients received mediastinal radiotherapy), being 2.1-fold (95% CI, 0.78 to 5.4-fold) and 2.3-fold (95% CI, 1.03 to 5.3-fold), respectively. In accordance with results of other studies, treatment with chemotherapy and radiotherapy posed the highest risk, 5.3-fold (95% CI, 1.5 to 18.3-fold) for coronary artery disease and 4.7-fold (95% CI, 1.6 to 14.1-fold) for atherosclerotic disease, respectively.¹⁴

Treatment-related cardiovascular mortality

Hanks *et al.* reported on elevated cardiac mortality after 15-years follow up in 387 testicular cancer survivors treated with radiotherapy in 1973 and 1974. Seventy-nine percent of patients with stage II and 27% of patients with stage I had mediastinal irradiation. A significant, 3.1-fold increase in non-cancer mortality was observed compared to general male population. Further analysis of causes of death revealed a 2.3-fold increase in cardiac deaths. Eight out of ten patients, who died due to cardiac disease, received mediastinal irradiation.²²

In Zagars' study only minority of patients (71 of 477) received mediastinal irradiation. The cardiac mortality rate was significantly elevated only beyond 15 years of follow-up with standardized mortality ratio (SMR) 1.95 (95% CI, 1.24 to 2.94). Cardiac mortality rate was not significantly elevated during the first 15 years of follow up for the whole group of patients, except for the subgroup of patients treated with mediastinal irradiation (SMR = 1.63, 95% CI, 0.44 to 4.17).²³

Fossa *et al.* was the first author reporting on cardiac mortality among testicular cancer survivors treated with combination of radiotherapy and chemotherapy. They found slightly, but significantly increased risk of dying from circulatory disease (SMR = 1.20, 95% CI, 1.0 to 1.5). A comparison according to the diagnostic periods failed to show increase of mortality after the introduction of cisplatin, probably due to other treatment modifications that happened in that period: omission of mediastinal irradiation, confinement of subdiaphragmatic fields and introduction of modern radiotherapy planning and delivery facilities.²⁴

In another large international study by Fossa *et al.*, there was no significant increase in overall mortality from circulatory disease in whole study population of 38 907 patients treated for testicular cancer with only surgery, chemotherapy or ra-

diotherapy or with combination of chemotherapy and radiotherapy. However, a significantly increased mortality due to hypertensive disorder (SMR = 1.39, 95% CI, 1.01 to 1.89) was documented. Mortality caused by all circulatory diseases was significantly higher in testicular cancer survivors treated with chemotherapy (SMR = 1.44, 95% CI, 1.06 to 1.91) compared to group of patients treated with radiotherapy or surgery only. The risk was even higher in testicular cancer survivors treated with radiotherapy and chemotherapy (SMR = 2.06, 95% CI, 1.27 to 3.14). In comparison with the general population, mortality from circulatory disease was significantly increased in patients treated with radiotherapy at the age under 35 years (SMR = 1.7, 95% CI, 1.21 to 2.31), as well as in patients treated with chemotherapy (with or without radiotherapy) at the age under 35 years after 1975 (SMR = 1.58, 95% CI, 1.25 to 2.01). The latter coincides with introduction of cisplatin based chemotherapy.⁵

Pathophysiology of CVD caused by cisplatin based chemotherapy

Although mechanisms that would explain an increased risk of CVD after cisplatin based chemotherapy are not completely clarified, endothelial damage is considered to play a main role in pathogenesis. Microalbuminuria, thought to be an early sign of endothelial damage, was reported by Meinardi *et al.* in 22% of patients treated with cisplatin based chemotherapy.¹⁹ Patients with microalbuminuria had a tendency of higher blood pressure, which could be a consequence of systemic endothelial damage as well.³⁰ Moreover, microalbuminuria was shown to be a predictor of cardiac events.^{31,32} Nuver *et al.* observed microalbuminuria in 12% of patients treated with cisplatin based chemotherapy for testicular cancer after median follow up of 7 years, compared to 0% in surgery only group and 4.6% in a larger group of healthy men from general population.³³

Nuver *et al.* proposed other endothelial and inflammatory markers as potential early indicators of endothelial damage and atherosclerosis, which is essentially an inflammatory process.³³ Namely, they found significantly higher levels of von Willebrandt factor (vWF), tissue plasminogen activator (t-PA), plasminogen activator inhibitor-1 (PAI-1), fibrinogen and high sensitivity C-reactive protein (hs-CRP) in patients treated with chemotherapy compared to healthy men. Elevated levels of endothelial and inflammatory markers were shown to be associated with higher risk for

coronary artery disease.^{34,35} In addition, elevated levels of inflammatory proteins were associated with more pronounced atherosclerosis as well.³⁶ Moreover, according to the available data from the literature, hs-CRP could be a predictive marker for CVD.³⁶⁻³⁹ In the same study by Nuver *et al.* evaluation of vascular structure and function of common carotid artery was performed. Irrespective of high levels of endothelial and inflammatory markers, this evaluation failed to show any significant changes in wall structure or function of blood vessel, except a small, but statistically significant increase in carotid wall stiffness. Explanation for this could be impairment of microvasculature at the early stages, with later impairment of the macrovasculature. The same author in another study also reported on small, but statistically significant increase in carotid intima media thickness in patients treated with cisplatin based chemotherapy, which was shown to be associated with higher myocardial infarction incidence.⁴⁰

Gietema *et al.* showed a presence of circulating platinum in plasma up to 20 years after treatment with cisplatin based chemotherapy in testicular cancer survivors, which, together with the awareness of signs for endothelial damage, led to the theory that cisplatin may chronically stimulate the endothelium, eventually resulting in vasculature impairment.^{41,42} Correlation between cisplatin plasma levels and severity of neurotoxicity was recently shown, indicating that cisplatin level may serve as a putative marker for long-term toxicity, perhaps even for CVD.⁴³

Unfavourable cardiovascular risk profile, metabolic syndrome and hypogonadism in testicular cancer survivors

CVD following cisplatin based chemotherapy could, on the other hand, be caused by a gradual development of unfavourable cardiovascular risk profile. Namely, several studies reported significantly higher prevalence of hypertension in testicular cancer survivors treated with platinum based chemotherapy.^{14,16,19} Another cause of hypertension in testicular cancer survivors could be abdominal radiotherapy. Namely, some studies with patients treated with abdominal radiotherapy for malignant disease in abdomen reported on increased risk of hypertension. Possible explanation for this is development of radiation nephropathy with resulting hypertension, probably through a renovascular mechanism with activation of the renin-angiotensin-aldosterone system.⁴⁴⁻⁴⁶ Furthermore, a

few studies reported on increased risk for hypercholesterolemia, as well as increased prevalence of obesity following cisplatin based chemotherapy in testicular cancer survivors, which was, on the other hand, not confirmed by others.^{14-19,21} Haugnes *et al.* found significantly higher levels of HbA1c in all chemotherapy and radiotherapy treated testicular cancer patients compared to surgery only group, moreover, patients treated with radiotherapy were at a greater risk of being diagnosed with diabetes as well. Namely, the prevalence of diabetes for the whole study group was 7.3%, while it was 10.2% and 15.6% for radiotherapy and radiotherapy/chemotherapy group, respectively. The most likely explanation for this is radiation damage of pancreatic gland tissue, as the large part of the gland is included in subdiaphragmatic radiation field. Insulin resistance in testicular cancer patients treated with chemotherapy could be a consequence of persistent hypomagnesemia, caused by cisplatin-induced damage of proximal renal tubules. In Haugnes' study it was found that the prevalence of other unfavourable risk factors for CVD was the highest in radiotherapy/chemotherapy group as well, suggesting a possibility of synergistic effect.¹⁴

Hypertension, dyslipidaemia, obesity and insulin resistance are all components of the metabolic syndrome. Considering that testicular cancer survivors are at greater risk to have one or more of these components, the metabolic syndrome could be a possible causal link between cytotoxic treatment and CVD.^{47,48} The prevalence rates of metabolic syndrome in testicular cancer survivors range from 8% to 40%, depending on applied criteria for diagnosis of this syndrome. Patients treated with chemotherapy are at higher risk for development of metabolic syndrome, compared to controls and to radiotherapy or surgery only group. This is especially true for patients receiving higher cumulative dose of cisplatin – 850 mg or more. Beside association with cumulative dose of cisplatin, a positive correlation was demonstrated between prevalence of metabolic syndrome and cumulative doses of bleomycin and etoposide as well.⁴⁸ The aetiology of the metabolic syndrome is not entirely clear. Gietema *et al.* were the first authors reporting on the possible association of metabolic syndrome with low serum testosterone levels in patients who received chemotherapy.⁴⁹ Nuver *et al.* proposed that low serum testosterone level and metabolic syndrome could be associated through increased body mass index.⁴⁸

It's well known that hypogonadism increases risk for CVD and correlates with the severity of ath-

erosclerosis, even in a healthy male population. In addition, it was shown that gonadal dysfunction is associated with obesity, dyslipidaemia and insulin resistance, as well as with higher levels of markers of endothelial damage. A middle aged men from general population with free testosterone levels in the lower third of normal range were at a 2.7-fold (95% CI, 2.0 to 3.7-fold) increased risk for metabolic syndrome in age-adjusted analyses. After further adjusting for body mass index, low free testosterone level was associated with 1.7-fold (95% CI, 1.2 to 2.4-fold) increased risk for metabolic syndrome. This correlation was even more pronounced for total testosterone levels and sex-hormone binding globulin levels.⁵⁰ In testicular cancer survivors, gonadal dysfunction may be result of prior treatment with chemotherapy, subdiaphragmatic radiotherapy and with surgery as well.⁵¹

However, it is still ongoing debate, whether metabolic syndrome is a consequence of hypogonadism or intrinsic feature of testicular cancer survivors, as a part of testicular dysgenesis syndrome. If the first assumption is true, the testosterone substitution therapy could have a favourable impact on metabolic syndrome and development of CVD in testicular cancer survivors. To date, there is no evidence for that. According to the literature, substitution therapy with testosterone might be useful in men with significantly reduced testosterone levels, while its benefit is questionable in a case of modest hypogonadism.⁴⁸

Pathophysiology of CVD caused by irradiation

Increased risk for CVD after mediastinal radiotherapy in patients treated for testicular cancer is a consequence of a direct exposure of the heart to irradiation.⁵²⁻⁵⁴ Data from the literature indicate that irradiation of the heart leads to the tissue damage through microvasculopathy and eventually macrovasculopathy. Endothelial damage of small blood vessels is due to radiation induced generation of reactive oxygen species. Typically, irregularities of the endothelial cell membranes, cytoplasmic swelling, thrombosis and rupture of the walls are present in early phase. This eventually results in reduced ratio of capillaries to myocytes by approximately 50%, leading to ischaemia and fibrosis in late phase.⁵⁵

Less is known about pathologic association between subdiaphragmatic radiotherapy and CVD. According to the physical model, in series of Huddart *et al.*, the expected mean dose to the

heart in a case of “dog leg” radiation field, extending upwards to the bottom of tenth thoracic vertebra, was approximately 2.5% of the total dose, which is unlikely to cause any serious damage.²⁶ Possible mechanism of CVD in patients treated with abdominal radiotherapy could be radiation nephropathy, as well as hypogonadism, as mentioned above. A direct endothelial damage, eventually resulting in atherosclerosis, is another possible mechanism, supported by increased levels of hs-CRP in patients treated with radiotherapy.⁵⁶

Up to 1980's, total dose of subdiaphragmatic radiotherapy was 36 to 40 Gy and even more. After that, radiation dose was gradually reduced, being 20 Gy for stage I seminoma, 30 Gy for stage II A and 36 Gy for stage II B. In case of prophylactic mediastinal irradiation, testicular cancer survivors usually received 30 Gy. Fractionation, mainly used in subdiaphragmatic, as well as in mediastinal irradiation, is 2 Gy daily fractions 5 days per week.

Implication for future

Current knowledge about long-term treatment-related toxicity in testicular cancer survivors is based on treatment modalities administered years to decades ago. Optimization of treatment, including omission of mediastinal irradiation, confinement of subdiaphragmatic fields, use of modern radiotherapy planning and delivery techniques, lowering the cumulative doses of cytotoxic drugs and preferential use of active surveillance will probably all reduce risk for cardiac toxicity.⁷⁻¹² However, as data from newer studies are not yet available, we do not have confirmation for this and further research is essential.⁵⁷

Following successful treatment, most of the testicular cancer survivors are under the medical surveillance of their oncologists for subsequent 5 to 10 years. Obviously, these patients need a longer, probably life-long follow-up with special attention to modifiable CVD risk factors. Patients should be treated for hypertension, diabetes, hyperlipidaemia and dyslipidaemia and advised about healthy lifestyle. A smoking cessation is highly recommended, along with regular physical activity and maintaining of optimal body weight. At the moment, no guidelines concerning CVD risk in testicular cancer survivors are available and several study groups proposed their development.²⁵

References

- Znaor A, Lortet-Tieulent J, Jemal A, Bray F. International variations and trends in testicular cancer incidence and mortality. *Eur Urol* 2014; **65**: 1095-106.
- Trabert B, Chen J, Devesa SS, Bray F, McGlynn KA. International patterns and trends in testicular cancer incidence, overall and by histologic subtype, 1973-2007. *Andrology* 2015; **3**: 4-12.
- Kovač V. The cause of testicular cancer. *Radiol Oncol* 1998; **32**: 201-5.
- National Cancer Institute. Surveillance, Epidemiology, and End Results (SEER) Program. [cited 2 Feb 2016]. Available at <https://seer.cancer.gov/statfacts/html/testis.html>
- Fossa SD, Gilbert E, Dores GM, Chen J, McGlynn KA, Schonfeld S, et al. Noncancer causes of death in survivors of testicular cancer. *J Natl Cancer Inst* 2007; **99**: 533-44.
- De Wit R, Roberts JT, Wilkinson PM, de Mulder PHM, Mead GM, Fossa SD, et al. Equivalence of three or four cycles of bleomycin, etoposide, and cisplatin chemotherapy and of a 3- or 5-day schedule in good-prognosis germ cell cancer: a randomized study of the European EORTC-GTCCG and. *J Clin Oncol* 2001; **19**: 1629-40.
- Saxman SB, Finch D, Gonin R, Einhorn LH. Long-term follow up of a phase III study of three versus four cycles of bleomycin, etoposide, and cisplatin in favorable-prognosis germ-cell tumors: The Indiana University experience. *J Clin Oncol* 1998; **16**: 702-6.
- Nichols CR, Williams SD, Loehrer PJ, Greco FA, Crawford ED, Weetlauffer J, et al. Randomized study of cisplatin dose intensity in poor-risk germ cell tumors: A Southeastern Cancer Study Group and Southwest Oncology Group Protocol. *J Clin Oncol* 1991; **9**: 1163-72.
- Fossa SD, Horwich A, Russell JM, Roberts JT, Cullen MH, Hodson NJ, et al. Optimal planning target volume for stage I testicular seminoma: A MRC randomized trial. *J Clin Oncol* 1999; **17**: 1146.
- Jones WG, Fossa SD, Mead GM, Roberts JT, Sokal M, Horwich A, et al. Randomized trial of 30 versus 20 Gy in the adjuvant treatment of stage I seminoma: A report on MRC Trial TE 18, EORTC Trial 30942. *J Clin Oncol* 2005; **23**: 1200-8.
- Kovač V. Prevention of fertility disturbances in oncological male patients. *Radiol Oncol* 1996; **30**: 286-90.
- Horwich A, Alsanjari N, A'Hern R, Nicholls J, Dearnaley DP, Fisher C. Surveillance following orchidectomy for stage I testicular seminoma. *Br J Cancer* 1992; **65**: 775-8.
- Van den Belt-Dusebout AW, Nuver J, de Wit R, Gietema JA, ten Bokkel Huinink WW, Rodrigus PT, et al. Long-term risk of cardiovascular disease in 5-year survivors of testicular cancer. *J Clin Oncol* 2006; **24**: 467-75.
- Haugnes HS, Wethal T, Aass N, Dahl O, Klepp O, Langberg CW, et al. Cardiovascular risk factors and morbidity in long-term survivors of testicular cancer: A 20-year follow-up study. *J Clin Oncol* 2010; **28**: 4649-57.
- Raghavan D, Cox K, Childs A, Grygiel J, Sullivan D. Hypercholesterolemia after chemotherapy for testis cancer. *J Clin Oncol* 1992; **10**: 1386-9.
- Sagstuen H, Aass N, Fossa SD, Dahl O, Klepp O, Wist EA, et al. Blood pressure and body mass index in long-term survivors of testicular cancer. *J Clin Oncol* 2005; **23**: 4980-90.
- Nord C, Fossa SD, Egeland T. Excessive annual BMI increase after chemotherapy among young survivors of testicular cancer. *Br J Cancer* 2003; **88**: 36-41.
- Strumberg D, Brugge S, Korn MW, Koeppen S, Ranft J, Scheiber G, et al. Evaluation of long-term toxicity in patients after cisplatin-based chemotherapy for non-seminomatous testicular cancer. *Ann Oncol* 2002; **13**: 229-36.
- Meinardi MT, Gietema JA, van der Graaf WTA, van Veldhuisen DJ, Runne MA, Sluiter WJ, et al. Cardiovascular morbidity in long-term survivors of metastatic testicular cancer. *J Clin Oncol* 2000; **18**: 1725-32.
- Stoter G, Koopman A, Vendrik CP, Struyvenberg A, Sleyfer DT, Willemsse PH, et al. Ten-year survival and late sequelae in testicular cancer patients treated with cisplatin, vinblastine, and bleomycin. *J Clin Oncol* 1989; **7**: 1099-104.

21. Gietema JA, Sleijfer DT, Willemse PH, Schraffordt HK, van Ittersum E, Verschuren WM, et al. Long-term follow-up of cardiovascular risk factors in patients given chemotherapy for disseminated nonseminomatous testicular cancer. *Ann Intern Med* 1992; **116**: 709-15.
22. Hanks GE, Peters T, Owen J. Seminoma of the testis: long-term beneficial and deleterious results of radiation. *Int J Radiat Oncol Biol Phys* 1992; **24**: 913-19.
23. Zagars GK, Ballo MT, Lee AK, Strom SS. Mortality after cure of testicular seminoma. *J Clin Oncol* 2004; **22**: 640-7.
24. Fossa SD, Aass N, Harvei S, Tretli S. Increased mortality rates in young and middle-aged patients with malignant germ cell tumours. *Br J Cancer* 2004; **90**: 607-12.
25. Van den Belt-Dusebout AW, de Wit R, Gietema JA, Horenblas S, Louwmann MWJ, Ribot JG, et al. Treatment-specific risk of second malignancies and cardiovascular disease in 5-year survivors of testicular cancer. *J Clin Oncol* 2007; **25**: 4370-8.
26. Huddart RA, Norman A, Shahidi M, Horwich A, Coward D, Nicholls J, et al. Cardiovascular disease as a long-term complication of treatment for testicular cancer. *J Clin Oncol* 2003; **21**: 1513-23.
27. Samuels BL, Vogelzang NJ, Kennedy BJ. Severe vascular toxicity associated with vinblastine, bleomycin, and cisplatin chemotherapy. *Cancer Chemother Pharmacol* 1987; **19**: 253-6.
28. Lederman GS, Sheldon TA, Chaffey JT, Herman TS, Gelman RS, Coleman CN. Cardiac disease after mediastinal irradiation for seminoma. *Cancer* 1987; **60**: 772-6.
29. Bokemeyer C, Berger CC, Kuczyk MA, Schmoll HJ. Evaluation of long-term toxicity after chemotherapy for testicular cancer. *J Clin Oncol* 1996; **14**: 2923-32.
30. Pedrinelli R, Giampietro O, Carmassi F, Melillo E, Dell'Omo G, Catapano G, et al. Microalbuminuria and endothelial dysfunction in essential hypertension. *Lancet* 1994; **344**: 14-18.
31. Stehouwer CD, Yudkin JS, Fioletto P, Nosadini R. How heterogeneous is microalbuminuria in diabetes mellitus? The case for „benign“ and „malignant“ microalbuminuria. *Nephrol Dial Transplant* 1998; **13**: 2751-4.
32. Hillege HL, Fidler V, Diercks GF, van Gilst WH, de Zeeuw D, van Veldhuisen DJ, et al. Urinary albumin excretion predicts cardiovascular and noncardiovascular mortality in general population. *Circulation* 2002; **106**: 1777-82.
33. Nuver J, Smit AJ, Sleijfer DT, van Gessel AI, van Roon AM, van der Meer J, et al. Microalbuminuria, decreased fibrinolysis, and inflammation as early signs of atherosclerosis in long-term survivors of disseminated testicular cancer. *Eur J Cancer* 2004; **40**: 701-6.
34. Thogersen AM, Jansson JH, Boman K, Nilsson TK, Weinehall L, Huhtasaari F, et al. High plasminogen activator inhibitor and tissue plasminogen activator levels in plasma precede a first acute myocardial infarction in both men and women: evidence for fibrinolytic system as an independent primary risk factor. *Circulation* 1998; **98**: 2241-7.
35. Juhan-Vague I, Pyke SD, Alessi MC, Jespersen J, Haverkate F, Thompson SG. Fibrinolytic factors and the risk of myocardial infarction or sudden death in patients with angina pectoris. ECAT Study Group. European Concerted Action on Thrombosis and Disabilities. *Circulation* 1996; **94**: 2057-63.
36. Ridker PM, Cushman M, Stampfer MJ, Tracy RP, Hennekens CH. Inflammation, aspirin, and the risk of cardiovascular disease in apparently healthy men. *N Engl J Med* 1997; **336**: 973-9.
37. Danesh J, Wheeler JG, Hirschfield GM, Eda S, Eiriksdottir G, Rumley A, et al. C-reactive protein and other circulating markers of inflammation in the prediction of coronary heart disease. *N Engl J Med* 2004; **350**: 1387-97.
38. Calabro P, Golia E, Yeh ET. CRP and the risk of atherosclerotic events. *Semin Immunopathol* 2009; **31**: 79-94.
39. Sellmayer A, Limmert T, Hoffmann U. High sensitivity C-reactive protein in cardiovascular risk assessment. CRP mania or usefull screening? *Int Angiol* 2003; **22**: 15-23.
40. Nuver J, Smit AJ, van der Meer J, van den Berg MP, van den Graaf WTA, Meinardi MT, et al. Acute chemotherapy-induced cardiovascular changes in patients with testicular cancer. *J Clin Oncol* 2005; **23**: 9130-7.
41. Gietema JA, Meinardi MT, Messerschmidt J, Gelevert T, Alt F, Uges DR, et al. Circulating plasma platinum more than 10 years after cisplatin treatment for testicular cancer. *Lancet* 2000; **355**: 1075-6.
42. Efsthathiou E, Logothetis CJ. Review of late complications of treatment and late relapse in testicular cancer. *J Natl Compr Canc Netw* 2006; **4**: 1059-70.
43. Sprauten M, Darrah TH, Peterson DR, Campbell ME, Hannigan RE, Cvancarova M, et al. Impact of long-term serum platinum concentrations on neuro- and ototoxicity in cisplatin-treated survivors of testicular cancer. *J Clin Oncol* 2012; **30**: 300-7.
44. Verheij M, Dewit LG, Valdes Olmos RA, Arisz L. Evidence for a renovascular component in hypertensive patients with late radiation nephropathy. *Int J Radiat Oncol Biol Phys* 1994; **30**: 677-83.
45. Kim TH, Somerville PJ, Freeman CR. Unilateral radiation nephropathy – the long-term significance. *Int J Radiat Oncol Biol Phys* 1984; **10**: 2053-9.
46. Cassady JR. Clinical radiation nephropathy. *Int J Radiat Oncol Biol Phys* 1995; **31**: 1249-56.
47. Hagnes HS, Aass N, Fossa SD, Dahl O, Klepp O, Wist EA, et al. Components of the metabolic syndrome in long-term survivors of testicular cancer. *Ann Oncol* 2007; **18**: 241-8.
48. Nuver J, Smit AJ, Wolffenbuttel BHR, Sluiter WJ, Hoekstra HJ, Sleijfer DT, et al. The metabolic syndrome and disturbances in hormone levels in long-term survivors of disseminated testicular cancer. *J Clin Oncol* 2005; **23**: 3718-25.
49. Gietema JA, Meinardi MT, van der Graaf WT, Sleijfer DT. Syndrome X in testicular cancer survivors. *Lancet* 2001; **357**: 228-9.
50. Laaksonen DE, Niskanen L, Punnonen K, Nyyssonen K, Tuomainen TP, Salonen R, et al. Sex hormones, inflammation and the metabolic syndrome: a population-based study. *Eur J Endocrinol* 2003; **149**: 601-8.
51. Nord C, Bjoro T, Ellingsen D, Mykletun A, Dahl O, Klepp O, et al. Gonadal hormones in long-term survivors 10 years after treatment for unilateral testicular cancer. *Eur Urol* 2003; **44**: 322-8.
52. Corn BW, Trock BJ, Goodman RL. Irradiation-related ischemic heart disease. *J Clin Oncol* 1990; **8**: 741-50.
53. Martinou M, Gaya A. Cardiac complications after radical radiotherapy. *Semin Oncol* 2013; **40**: 178-85.
54. Vasiliadis I, Kolovou G, Mikhailidis DP. Cardiotoxicity and cancer therapy. *Angiol* 2014; **65**: 369-71.
55. Celik T, Yuksel C, Demirkol S, Iyisoy A, Ulutin C. Coronary artery disease associated with radiation therapy. *Cent Eur J Med* 2010; **5**: 180-3.
56. Wethal T, Kjekshus J, Roislien J, Ueland T, Andreassen AK, Wergeland R, et al. Treatment-related differences in cardiovascular risk factors in long-term survivors of testicular cancer. *J Cancer Surviv* 2007; **1**: 8-16.
57. Hagnes HS, Bosl GJ, Boer H, Gietema JA, Brydoy M, Oldenburg J, et al. Long-term and late effects of germ cell testicular cancer treatment and implications for follow up. *J Clin Oncol* 2012; **30**: 3752-63.

Dosimetric predictors of treatment-related lymphopenia induced by palliative radiotherapy: predictive ability of dose-volume parameters based on body surface contour

Tetsuo Saito, Ryo Toya, Tomohiko Matsuyama, Akiko Semba, Natsuo Oya

Department of Radiation Oncology, Kumamoto University Hospital, 1-1-1 Honjo, Chuo-ku, Kumamoto-shi, Kumamoto, 860-8556, Japan

Radiol Oncol 2017; 51(2): 228-234.

Received 18 July 2016
Accepted 30 August 2016

Correspondence to: Tetsuo Saito, M.D., Department of Radiation Oncology, Kumamoto University Hospital, 1-1-1, Honjo, Chuo-ku, Kumamoto-shi, Kumamoto, 860-8556, Japan. Phone: +81 96 373 5261; Fax: +81 96 373 5342; E-mail: tsaito@kumamoto-u.ac.jp

Disclosure: No potential conflicts of interest were disclosed.

Background. Radiation-related lymphopenia has been associated with poor patient outcome. Our aim was to identify predictors of lymphopenia after palliative radiotherapy, with a focus on dose-volume parameters.

Patients and methods. To retrospectively assess patients with various cancers who had undergone palliative radiotherapy, we delineated three organs at risk: the volume enclosed by the body surface contour (body A), the volume left after excluding air, pleural effusion, ascites, bile, urine, and intestinal content (body B), and the volume of the bone marrow (BM). We then noted the absolute volume of the three organs at risk that had received 5–30 Gy, and assessed the predictive value for post-treatment lymphopenia of grade 3 or higher (LP3+).

Results. Of 54 patients, 23 (43%) developed LP3+. Univariate logistic regression analysis showed that body A V5, body A V10, body B V5, body B V10, the number of fractions, and splenic irradiation were significant predictors of LP3+ ($p < 0.05$). By multivariate analysis, body A V5, body A V10, body B V5, body B V10, and the number of fractions retained significance ($p < 0.05$). BM dose-volume parameters did not predict lymphopenia.

Conclusions. Higher body A and body B dose-volume parameters and a larger number of fractions may be predictors of severe lymphopenia after palliative radiotherapy.

Key words: palliative radiotherapy; radiation-related lymphopenia; dose-volume parameters

Introduction

The important role of lymphocytes in the immune response to cancer¹ is evidenced by the better survival of lung-, colorectal-, and breast cancer-, and glioblastoma patients whose cancer tissues manifest lymphocyte infiltration.²⁻⁵ Survival tends to be poor in cancer- and lymphoma patients with lymphopenia before undergoing treatment⁶⁻¹⁰, and treatment-related lymphopenia is associated with a poor outcome in patients subjected to curative chemoradiotherapy for pancreatic-, lung-, cervical-, and nasopharyngeal cancer and malignant glioma.¹¹⁻¹⁸

The irradiation of circulating peripheral blood may elicit radiation-related lymphopenia.^{19,20} Although studies to evaluate the effect of irradiation on lymphocytes showed that radiation-related lymphopenia was associated with organ-specific (lung¹⁴ and brain²¹) dose-volume parameters, dosimetric predictors applicable at various treatment sites remained to be identified.

Radiation-related lymphopenia has been studied mainly in patients who had received curative treatment¹¹⁻¹⁸; there are few reports on patients subjected to palliative radiotherapy (RT). Because lymphocytes are highly radiosensitive, exposure to even low doses of radiation can lead to a decrease

in the number of peripheral blood lymphocytes.^{22,23} Consequently, even low radiation doses delivered by palliative RT can lead to lymphopenia affecting the immune system and the treatment outcome.

Focusing on dose-volume parameters, we attempted to identify predictors of lymphopenia after palliative RT. We used organs at risk based on body surface contour to evaluate their predictive value.

Patients and methods

Patients

This retrospective study was approved by the institutional review board of Kumamoto University Hospital (No. 1171). The study was carried out according to the Declaration of Helsinki. Our inclusion criteria were as follows: patients treated with palliative RT between October 2010 and June 2013 at the Kumamoto University Hospital; the availability of laboratory data acquired within 2 weeks prior to the start of RT; and of two or more laboratory data obtained within one month after the start of RT, the latest data recorded at least 2 weeks after the start of RT. The exclusion criteria were hematologic tumor; chemotherapy, molecular targeted therapy, interferon treatment, or radiotherapy delivered from one month before to one month after the start of RT; or grade 2 or higher lymphopenia based on the Common Terminology Criteria for Adverse Events (CTCAE) v 4.0 at the start of RT. Patient-, tumor-, and treatment data were obtained from medical charts.

Laboratory data

The study endpoints were (1) the absolute lymphocyte count at nadir, defined as the lowest value recorded within one month after the start of RT, (2) the lymphocyte count ratio, obtained by dividing the nadir absolute lymphocyte count by the pre-RT absolute lymphocyte count, and (3) lymphopenia of grade 3 or higher (LP3+, absolute lymphocyte count $< 500 \times 10^6/L$) determined by CTCAE v 4.0, with the highest grade within one month after the start of RT recorded for analysis.

Dose-volume parameters

All patients underwent CT simulation in the supine position, and three-dimensional treatment planning. For this study, we delineated organs at risk on planning CT images with commercially

available software (Velocity AI, Velocity Medical System, Atlanta, GA, USA). To evaluate the effect of radiation on peripheral blood lymphocytes, one radiation oncologist delineated the volume of two organs at risk where body A is the volume enclosed by the body surface contour, and body B is the volume left after excluding air, pleural effusion, ascites, bile, urine, and intestinal content (Figure 1). For body A, the body surface contour was obtained first by using threshold-based segmentation and then by manual correction. To obtain body B, we excluded volumes whose irradiation would not contribute to the reduction of lymphocytes; lung tissue was included and the trachea and bronchi were excluded. For bone marrow (BM), all bones were delineated by threshold-based segmentation and manual correction (Figure 1); intervertebral disks and costal-, thyroid-, cricoid-, and tracheal cartilage were excluded. The distal half of the femur and humerus were also excluded from BM because they contain little proliferating bone marrow.²⁴ The absolute volumes of the three organs at risk receiving 5-, 10-, 20-, and 30 Gy (V5, V10, V20, and V30) were recorded.

Statistical analysis

Data were summarized by using descriptive statistics (frequency, percentage, median, range). The correlation between the dose-volume parameters and the nadir lymphocyte count was evaluated with the Spearman correlation coefficient. For univariate and multivariate logistic regression analysis, the age, interval from tumor diagnosis, the pre-RT absolute lymphocyte count, total radiation dose, number of fractions, total monitor units, total irradiation time, and all dose-volume parameters were the continuous variables. The categorical variables included the gender, previous RT, previous chemotherapy, concurrent steroid use, bone metastasis, brain metastasis, splenic irradiation, and thymic irradiation. Variables that were significant

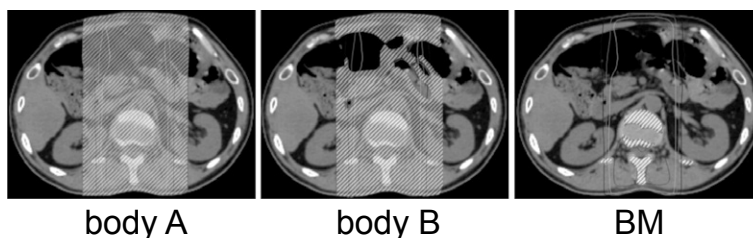


FIGURE 1. Delineation of the three organs at risk. Body A is the volume enclosed by the body surface contour. Body B excludes air, pleural effusion, ascites, bile, urine, and the intestinal content. BM = bone marrow.

TABLE 1. Patient and treatment characteristics (n = 54)

Characteristic	No. of patients	%
Patient characteristics		
Male gender	33	61
Age (years)		
Median	69	
Range	39-86	
Primary tumor		
Lung	14	26
Gastrointestinal	9	17
Skin	4	7
Liver	3	6
Uterus	3	6
Others ^a	21	39
Previous radiotherapy	15	28
Previous chemotherapy	26	48
Concurrent steroid use	23	43
Bone metastasis	27	50
Brain metastasis	11	20
Interval from tumor diagnosis to radiotherapy (months)		
Median	13	
Range	0-168	
Pre-radiotherapy absolute lymphocyte count (x 10 ⁶ /L)		
Median	1356	
Range	844-3468	
Treatment characteristics		
Total radiation dose (Gy)		
Median	30	
Range	16-50	
Number of fractions		
Median	10	
Range	4-25	
Fraction size (Gy)		
Median	3	
Range	2-5	
Total monitor units for all fractions		
Median	4433	
Range	1896-13890	
Total irradiation time for all fractions (minutes)		
Median	7.5	
Range	3.2-37.7	
Treatment site		
Head and neck	14	26
Chest	24	44
Abdomen	10	19
Pelvis	11	20
Limb	1	2
Splenic irradiation ^b	9	17
Thymic irradiation ^c	15	28

^a Others include head and neck (3 patients), breast (3 patients), mediastinal (3 patients), urogenital (8 patients), and soft tissue (4 patients) tumors; ^b Yes, if any part of the spleen was covered by the 5 Gy isodose line; ^c Yes, if any part of the thymus was covered by the 5 Gy isodose line.

in univariate analysis were included in multivariate analysis. The overall survival, calculated from the start of RT, was estimated with the Kaplan-Meier method; differences determined with the log-rank test. Values of $p < 0.05$ were considered statistically significant. All statistical analyses were performed with SPSS software, version 23 (IBM SPSS, Armonk, NY, USA).

Results

Patients

We included 54 patients whose solid tumors were treated with palliative RT. The patient and treatment characteristics are summarized in Table 1. As we excluded patients with lymphopenia of grade 2 or higher (absolute lymphocyte count $< 800 \times 10^6/L$), all included patients had a pre-RT absolute lymphocyte count $\geq 800 \times 10^6/L$. The median follow-up period from the start of RT was 4.5 months (range 0–42.0 months).

Laboratory data

The median pre-RT absolute lymphocyte count was $1356 \times 10^6/L$ (range 844–3468 $\times 10^6/L$), and the median nadir post-RT absolute lymphocyte count was $536 \times 10^6/L$ (range 131–1653 $\times 10^6/L$). The median lymphocyte count ratio, obtained by dividing the nadir- by the pre-RT absolute lymphocyte count, was 0.410 (range 0.108–0.983). Of the 54 patients, 12 (22%), 19 (35%), 20 (37%), and 3 (6%) patients had post-treatment lymphopenia of grade 1, 2, 3, and 4, respectively; a total of 23 (43%) patients developed LP3+.

Dose-volume parameters

The median (range) V5, V10, V20, and V30 for body A were 2.880 (0.399–8.976), 2.519 (0.344–6.596), 1.629 (0.000–4.255), and 0.660 (0.000–3.365) $\times 10^3$ mL, respectively. These values were 2.704 (0.392–8.143), 2.384 (0.341–5.959), 1.597 (0.000–3.919), and 0.645 (0.000–3.326) $\times 10^3$ mL for body B and 0.348 (0.000–0.974), 0.258 (0.000–0.909), 0.174 (0.000–0.737), and 0.076 (0.000–0.724) $\times 10^3$ mL for BM.

Correlation between the dose-volume parameters and the nadir lymphocyte count

There was a negative correlation between body dose-volume parameters (V5, V10, and V30 for

body A and body B) and the nadir lymphocyte count ($p < 0.05$, Table 2). Higher body A and body B dose-volume parameters were correlated with a lower post-RT lymphocyte count. There was no significant correlation between BM dose-volume parameters and the nadir lymphocyte count (Table 2). We observed a strong correlation between body A V5 and body B V5 (Spearman's rho = 0.992, $p < 0.001$), between body A V10 and body B V10 (Spearman's rho = 0.992, $p < 0.001$), between body A V20 and body B V20 (Spearman's rho = 0.997, $p < 0.001$), and between body A V30 and body B V30 (Spearman's rho = 0.999, $p < 0.001$).

Predictors of severe treatment-related lymphopenia

Univariate logistic regression analysis showed that body A V5, body A V10, body B V5, body B V10, the number of fractions, and splenic irradiation were significant predictors of LP3+ ($p < 0.05$, Table 3). For multivariate analysis, we took into account factors with $p < 0.05$ by univariate analysis (number of fractions and splenic irradiation) to test the independent significance of dose-volume parameters (Table 4). We found that body A V5, body A V10, body B V5, body B V10, and the number of fractions retained significance ($p < 0.05$). Higher body A and body B dose-volume parameters and a larger number of fractions were predictive of LP3+.

Relationship between radiation-related lymphopenia and overall survival

The median survival for all patients was 6.3 months (95% confidence interval: 4.1–8.5 months). The overall survival based on the grade of radiation-related lymphopenia is shown in Figure 2. There was no statistically significant difference in the overall survival of patients with LP3+ and the other grades of lymphopenia ($p = 0.79$).

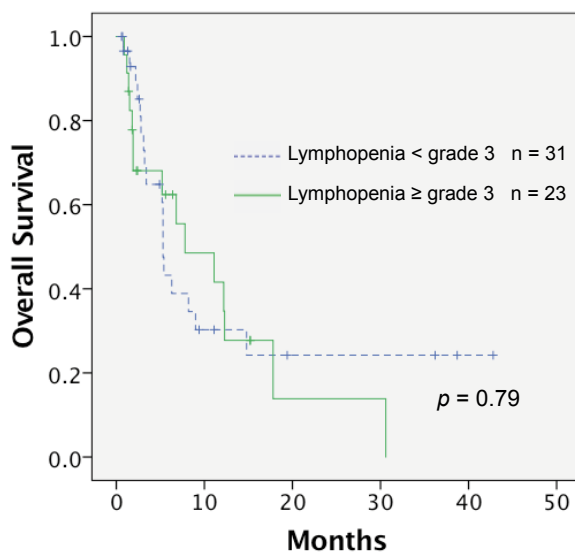
Discussion

We found that body A V5, body A V10, body B V5, body B V10, and the number of fractions were significant predictors of severe radiation-related lymphopenia. Higher body A and body B dose-volume parameters and a larger number of fractions were predictive of LP3+. In contrast, irradiation to lymphoid organs such as the bone marrow, spleen, and thymus were not predictive of radiation-related lymphopenia.

TABLE 2. Spearman correlation coefficients between the dose-volume parameters and the nadir lymphocyte count

Variable	Nadir lymphocyte count			
	Absolute lymphocyte count at nadir		Lymphocyte count ratio ^a	
	Spearman's rho	p-value	Spearman's rho	p-value
Body A V5	-0.265	0.053	-0.350	0.010
Body A V10	-0.283	0.038	-0.367	0.006
Body A V20	-0.231	0.093	-0.255	0.063
Body A V30	-0.305	0.025	-0.281	0.039
Body B V5	-0.274	0.045	-0.347	0.010
Body B V10	-0.280	0.040	-0.352	0.009
Body B V20	-0.236	0.086	-0.260	0.057
Body B V30	-0.302	0.027	-0.280	0.041
BM V5	-0.152	0.27	-0.210	0.13
BM V10	-0.161	0.25	-0.207	0.13
BM V20	-0.135	0.33	-0.161	0.25
BM V30	-0.168	0.23	-0.185	0.18

BM = bone marrow; ^a The lymphocyte count ratio was calculated by dividing the nadir absolute lymphocyte count by the pre-radiotherapy absolute lymphocyte count.



Median survival

Lymphopenia < grade 3 5.3 months (95% CI: 5.1–5.5 months)

Lymphopenia ≥ grade 3 7.8 months (95% CI: 0.5–15.1 months)

FIGURE 2. Overall survival according to the grade of radiation-related lymphopenia.

CI = confidence interval.

TABLE 3. Univariate logistic regression analysis for lymphopenia of grade 3 or higher

Variable	OR	95% CI	p-value
Patient characteristics			
Male vs. female	1.39	0.46–4.22	0.55
Age (per 1 year increase)	0.99	0.94–1.03	0.53
Previous radiotherapy (yes vs. no)	1.02	0.30–3.47	0.98
Previous chemotherapy (yes vs. no)	0.53	0.18–1.58	0.26
Concurrent steroid use (yes vs. no)	1.07	0.36–3.17	0.91
Bone metastasis (yes vs. no)	0.86	0.29–2.53	0.78
Brain metastasis (yes vs. no)	0.72	0.18–2.84	0.64
Interval from tumor diagnosis to radiotherapy (per 1 month increase)	1.00	0.99–1.02	0.81
Pre-radiotherapy absolute lymphocyte count (per increase of $1 \times 10^6/l$)	0.99	0.99–1.00	0.23
Treatment characteristics			
Total radiation dose (per 1-Gy increase)	1.06	0.99–1.14	0.11
Number of fractions (per 1-fraction increase)	1.18	1.01–1.38	0.036
Total monitor units over the entire treatment course (per increase of 100 monitor units)	1.01	0.99–1.03	0.29
Total irradiation time over the entire treatment course (per 1-minute increase)	0.99	0.92–1.08	0.91
Splenic irradiation (yes vs. no) ^a	6.34	1.18–34.24	0.032
Thymic irradiation (yes vs. no) ^b	0.58	0.17–2.03	0.39
Body A V5 (per 1×10^3 mL increase)	1.55	1.06–2.26	0.025
Body A V10 (per 1×10^3 mL increase)	1.60	1.04–2.45	0.032
Body A V20 (per 1×10^3 mL increase)	1.60	0.96–2.68	0.074
Body A V30 (per 1×10^3 mL increase)	1.87	0.95–3.68	0.069
Body B V5 (per 1×10^3 mL increase)	1.58	1.05–2.38	0.027
Body B V10 (per 1×10^3 mL increase)	1.63	1.04–2.56	0.035
Body B V20 (per 1×10^3 mL increase)	1.59	0.94–2.72	0.087
Body B V30 (per 1×10^3 mL increase)	1.84	0.93–3.67	0.082
BM V5 (per 1×10^3 mL increase)	3.62	0.37–35.36	0.27
BM V10 (per 1×10^3 mL increase)	2.88	0.27–31.10	0.38
BM V20 (per 1×10^3 mL increase)	1.78	0.15–20.92	0.65
BM V30 (per 1×10^3 mL increase)	4.73	0.19–115.78	0.34

BM = bone marrow; OR = odds ratio; CI = confidence interval; ^a Yes, if any part of the spleen was covered by the 5 Gy isodose line; ^b Yes, if any part of the thymus was covered by the 5 Gy isodose line.

Others^{19,20} suggested that the irradiation of circulating peripheral blood may lead to the development of radiation-related lymphopenia. This hypothesis is supported by findings that lymphopenia was observed after the delivery of RT to various body parts that did, or did not, include lymphoid organs.^{19,25} The irradiation of extracorporeal blood can lead to long-lasting lymphopenia.²⁶ Tang *et al.*¹⁴ found that in lung cancer patients, higher lung V5

to V10 values were associated with a lower lymphocyte nadir, and Huang *et al.*²¹ reported that in patients with high-grade glioma, higher brain volume receiving 25 Gy was a significant predictor of acute severe lymphopenia during RT and concurrent temozolomide. We document that the body dose-volume parameters we applied are useful predictors of lymphopenia in patients exposed to RT at different sites including the head and neck, the chest, abdomen, and the pelvis.

Our univariate and multivariate logistic regression analysis showed that irradiation to the bone marrow, spleen, and thymus was not a consistently significant predictor. Lymphoid organs such as the thymus, bone marrow, and spleen are central components of the mammalian immune system; lymphocytes are developed in these organs.²⁷ While splenic irradiation was a significant predictor of LP3+ by univariate logistic regression analysis, it lost its significance upon multivariate analysis. Because the 95% confidence interval was wide in our multivariate analysis (Table 4), the predictive value of splenic irradiation should be examined in large patient populations. We detected no significant association between lymphopenia and bone marrow irradiation although Sini *et al.*²⁸ reported that the exposure of bone marrow to radiation played a significant role. They found that higher BM V40 was associated with higher risk of acute Grade3 or late Grade2 lymphopenia in prostate cancer patients treated with whole-pelvis RT. Because information on the role of lymphoid organs in radiation-related lymphopenia is limited, additional studies are warranted.

The number of fractions was a significant predictor of severe radiation-related lymphopenia. This finding agrees with earlier observations.^{20,29} MacLennan *et al.*²⁹ analyzed the consequences of prophylactic cranial irradiation in children with leukemia. In their prospective study, the total radiation dose was constant (24 Gy) and the number of fractions was determined by the participating centers. They found that the level of radiation-related lymphopenia induced by that total dose depended on the number of fractions into which it was divided. The mean lymphocyte count of patients examined 3 months after receiving this dose in 5-, 12-, and 20 fractions was 1.84-, 1.12-, and $0.64 \times 10^9/L$, respectively. Yovino *et al.*²⁰ analyzed a model that calculated the radiation dose received by circulating lymphocytes; they found that as the number of fractions increased, the percentage of blood receiving ≥ 0.5 Gy increased rapidly. We also found that the number of fractions was a significant predictor

of radiation-related lymphopenia, however, in our study the total radiation dose was not a significant predictor. Because lymphocytes are highly radio-sensitive^{22,23}, their number killed by one fraction may not be strongly associated with the dose per fraction. A larger dose per fraction might be relatively less effective in killing lymphocytes than a small dose.

We observed a strong correlation between body A and body B dose-volume parameters when the volume was equal (e.g. body A and body B exposed to 5 Gy). It is easier to obtain the volume of body A than body B because body A is based on the body surface contour that can be acquired by auto-segmentation using commercially available software tools. Body A dose-volume parameters may be a convenient tool for predicting radiation-related lymphopenia.

Our data showed that there was no significant difference in the overall survival of patients with LP3+ and other grades of lymphopenia. Although lymphopenia related to curative chemoradiotherapy has been shown to be associated with poor patient outcomes¹¹⁻¹⁸, its prognostic value for palliative RT remains to be determined.

Our study has some limitations. The study population was small and some useful predictors of lymphopenia may have gone undetected. Also, as our study was retrospective, laboratory data were acquired at different points after the start of RT. Consequently, the true nadir lymphocyte count may not have been evaluated in some patients.

In summary, we identified body A and body B dose-volume parameters were useful new predictors of radiation-related lymphopenia. These body dose-volume parameters were acquired by delineating the body surface and they may be convenient for predicting radiation-related lymphopenia. As the parameters are not organ-specific, they are applicable at various treatment sites. Although their predictive value for radiation-related lymphopenia should be examined in groups of patients with different diseases, our findings may help to elucidate the mechanisms underlying the elicitation of radiation-related lymphopenia in patients treated with palliative RT.

References

- Mellman I, Coukos G, Dranoff G. Cancer immunotherapy comes of age. *Nature* 2011; **480**: 480-9.
- Hiraoka K, Miyamoto M, Cho Y, Suzuoki M, Oshikiri T, Nakakubo Y, et al. Concurrent infiltration by CD8+ T cells and CD4+ T cells is a favourable prognostic factor in non-small-cell lung carcinoma. *Br J Cancer* 2006; **94**: 275-80.

TABLE 4. Multivariate logistic regression analysis for lymphopenia of grade 3 or higher

Variable	OR	95% CI	p-value
Body A V5 (per 1 x 10 ³ mL increase)	1.58	1.03–2.42	0.036
Number of fractions (per 1-fraction increase)	1.26	1.03–1.53	0.027
Splenic irradiation (yes vs. no) ^a	5.12	0.74–35.28	0.098
Body A V10 (per 1 x 10 ³ mL increase)	1.68	1.04–2.70	0.034
Number of fractions (per 1-fraction increase)	1.26	1.03–1.55	0.026
Splenic irradiation (yes vs. no) ^a	5.25	0.77–35.76	0.090
Body B V5 (per 1 x 10 ³ mL increase)	1.63	1.03–2.57	0.038
Number of fractions (per 1-fraction increase)	1.25	1.03–1.53	0.028
Splenic irradiation (yes vs. no) ^a	5.46	0.79–37.53	0.085
Body B V10 (per 1 x 10 ³ mL increase)	1.72	1.04–2.87	0.036
Number of fractions (per 1-fraction increase)	1.26	1.03–1.55	0.027
Splenic irradiation (yes vs. no) ^a	5.59	0.82–37.99	0.078

CI = confidence interval; OR = odds ratio; ^a Yes, if any part of the spleen was covered by the 5 Gy isodose line; Factors with $p < 0.05$ by univariate analysis (number of fractions and splenic irradiation) were taken into account to test the independent significance of the dose-volume parameters.

- Ohtani H. Focus on TILs: prognostic significance of tumor infiltrating lymphocytes in human colorectal cancer. *Cancer Immunol* 2007; **7**: 4.
- Lohr J, Ratliff T, Huppertz A, Ge Y, Dictus C, Ahmadi R, et al. Effector T-cell infiltration positively impacts survival of glioblastoma patients and is impaired by tumor-derived TGF- β . *Clin Cancer Res* 2011; **17**: 4296-308.
- Gu-Trantien C, Loi S, Garaud S, Equeter C, Libin M, de Wind A, et al. CD4+ follicular helper T cell infiltration predicts breast cancer survival. *J Clin Invest* 2013; **123**: 2873-92.
- Le Scodan R, Massard C, Mouret-Fourme E, Guinebretille JM, Cohen-Solal C, De Lalonde B, et al. Brain metastases from breast carcinoma: Validation of the radiation therapy oncology group recursive partitioning analysis classification and proposition of a new prognostic score. *Int J Radiat Oncol Biol Phys* 2007; **69**: 839-45.
- Fumagalli LA, Vinke J, Hoff W, Ypma E, Brivio F, Nespola A. Lymphocyte counts independently predict overall survival in advanced cancer patients: A biomarker for IL-2 immunotherapy. *J Immunother* 2003; **26**: 394-402.
- De Giorgi U, Rihawi K, Aieta M, Lo Re G, Sava T, Masini C, et al. Lymphopenia and clinical outcome of elderly patients treated with sunitinib for metastatic renal cell cancer. *J Geriatr Oncol* 2014; **5**: 156-63.
- Jin Y, Ye X, He C, Zhang B, Zhang Y. Pretreatment neutrophil-to-lymphocyte ratio as predictor of survival for patients with metastatic nasopharyngeal carcinoma. *Head Neck* 2015; **37**: 69-75.
- Feng J, Wang Z, Guo X, Chen Y, Cheng Y, Tang Y. Prognostic significance of absolute lymphocyte count at diagnosis of diffuse large B-cell lymphoma: A meta-analysis. *Int J Hematol* 2012; **95**: 143-8.
- Balmanoukian A, Ye X, Herman J, Laheru D, Grossman SA. The association between treatment-related lymphopenia and survival in newly diagnosed patients with resected adenocarcinoma of the pancreas. *Cancer Invest* 2012; **30**: 571-6.
- Wild AT, Ye X, Ellsworth SG, Smith JA, Narang AK, Garg T, et al. The association between chemoradiation-related lymphopenia and clinical outcomes in patients with locally advanced pancreatic adenocarcinoma. *Am J Clin Oncol* 2015; **38**: 259-65.

13. Wild AT, Herman JM, Dholakia AS, Moningi S, Lu Y, Rosati LM, et al. Lymphocyte-sparing effect of stereotactic body radiation therapy in patients with unresectable pancreatic cancer. *Int J Radiat Oncol Biol Phys* 2016; **94**: 571-9.
14. Tang C, Liao Z, Gomez D, Levy L, Zhuang Y, Gebremichael RA, et al. Lymphopenia association with gross tumor volume and lung V5 and its effects on non-small cell lung cancer patient outcomes. *Int J Radiat Oncol Biol Phys* 2014; **89**: 1084-91.
15. Wu ES, Oduyebo T, Cobb LP, Cholakian D, Kong X, Fader AN, et al. Lymphopenia and its association with survival in patients with locally advanced cervical cancer. *Gynecol Oncol* 2016; **140**: 76-82.
16. Grossman SA, Ye X, Lesser G, Sloan A, Carraway H, Desideri S, et al. Immunosuppression in patients with high-grade gliomas treated with radiation and temozolomide. *Clin Cancer Res* 2011; **17**: 5473-80.
17. Mendez JS, Govindan A, Leong J, Gao F, Huang J, Campian JL. Association between treatment-related lymphopenia and overall survival in elderly patients with newly diagnosed glioblastoma. *J Neurooncol* 2016; **127**: 329-35.
18. Cho O, Oh YT, Chun M, Noh OK, Hoe JS, Kim H. Minimum absolute lymphocyte count during radiotherapy as a new prognostic factor for nasopharyngeal cancer. *Head Neck* 2016; **38 (Suppl 1)**: E1061-7.
19. Raben M, Walach N, Galili U, Schlesinger M. The effect of radiation therapy on lymphocyte subpopulations in cancer patients. *Cancer* 1976; **37**: 1417-21.
20. Yovino S, Kleinberg L, Grossman SA, Narayanan M, Ford E. The etiology of treatment-related lymphopenia in patients with malignant gliomas: Modeling radiation dose to circulating lymphocytes explains clinical observations and suggests methods of modifying the impact of radiation on immune cells. *Cancer Invest* 2013; **31**: 140-4.
21. Huang J, DeWees TA, Badiyan SN, Speirs CK, Mullen DF, Fergus S, et al. Clinical and dosimetric predictors of acute severe lymphopenia during radiation therapy and concurrent temozolomide for high-grade glioma. *Int J Radiat Oncol Biol Phys* 2015; **92**: 1000-7.
22. Trowell OA. The sensitivity of lymphocytes to ionising radiation. *J Pathol Bacteriol* 1952; **64**: 687-704.
23. Nakamura N, Kusunoki Y, Akiyama M. Radiosensitivity of CD4 or CD8 positive human T-lymphocytes by an *in vitro* colony formation assay. *Radiat Res* 1990; **123**: 224-7.
24. Campbell BA, Callahan J, Bressel M, Simoens N, Everitt S, Hofman MS, et al. Distribution atlas of proliferating bone marrow in non-small cell lung cancer patients measured by FLT-PET/CT imaging, with potential applicability in radiation therapy planning. *Int J Radiat Oncol Biol Phys* 2015; **92**: 1035-43.
25. Campbell AC, Hersey P, MacLennan IC, Kay HE, Pike MC. Immunosuppressive consequences of radiotherapy and chemotherapy in patients with acute lymphoblastic leukaemia. *Br Med J* 1973; **2**: 385-8.
26. Weeke E. The development of lymphopenia in uremic patients undergoing extracorporeal irradiation of the blood with portable beta units. *Radiat Res* 1973; **56**: 554-9.
27. Boehm T, Bleul CC. The evolutionary history of lymphoid organs. *Nat Immunol* 2007; **8**: 131-5.
28. Sini C, Fiorino C, Perna L, Noris Chiorda B, Deantoni CL, Bianchi M, et al. Dose-volume effects for pelvic bone marrow in predicting hematological toxicity in prostate cancer radiotherapy with pelvic node irradiation. *Radiother Oncol* 2016; **118**: 79-84.
29. MacLennan IC, Kay HE. Analysis of treatment in childhood leukemia. IV. The critical association between dose fractionation and immunosuppression induced by cranial irradiation. *Cancer* 1978; **41**: 108-11.

Excess of radiation burden for young testicular cancer patients using automatic exposure control and contrast agent on whole-body computed tomography imaging

Hannele Niiniviita^{1,2}, Jarmo Kulmala^{1,3}, Tuukka Pölönen⁴, Heli Määttänen¹, Hannu Järvinen⁵, Eeva Salminen^{3,5}

¹ Department of Medical Physics, Turku University Hospital, Turku, Finland

² Department of Diagnostic Radiology, University of Turku, Turku, Finland

³ Oncology and Radiotherapy, Turku University Hospital, Turku, Finland

⁴ Department of Biostatistics, University of Turku, Turku, Finland

⁵ STUK-Radiation and Nuclear Safety Authority, Helsinki, Finland

Radiol Oncol 2017; 51(2): 235-240.

Received 28 July 2016

Accepted 3 February 2017

Correspondence to: Eeva Salminen, STUK, Radiation and Nuclear Safety Authority, Laippatie 4, FI-00880 Helsinki, Finland.
Phone: +358975988752; E-mail: eevsal@utu.fi

Disclosure: The authors of this manuscript declare no relationships with any companies, whose products or services may be related to the subject matter of the article.

Background. The aim of the study was to assess patient dose from whole-body computed tomography (CT) in association with patient size, automatic exposure control (AEC) and intravenous (IV) contrast agent.

Patients and methods. Sixty-five testicular cancer patients (mean age 28 years) underwent altogether 279 whole-body CT scans from April 2000 to April 2011. The mean number of repeated examinations was 4.3. The GE LightSpeed 16 equipped with AEC and the Siemens Plus 4 CT scanners were used for imaging. Whole-body scans were performed with (216) and without (63) IV contrast. The ImPACT software was used to determine the effective and organ doses.

Results. Patient doses were independent ($p < 0.41$) of patient size when the Plus 4 device (mean 7.4 mSv, SD 1.7 mSv) was used, but with the LightSpeed 16 AEC device, the dose (mean 14 mSv, SD 4.6 mSv) increased significantly ($p < 0.001$) with waist circumference. Imaging with the IV contrast agent caused significantly higher (13% Plus 4, 35% LightSpeed 16) exposure than non-contrast imaging ($p < 0.001$).

Conclusions. Great caution on the use of IV contrast agent and careful set-up of the AEC modulation parameters is recommended to avoid excessive radiation exposure on the whole-body CT imaging of young patients.

Key words: automatic exposure control; computed tomography; contrast agent; radiation exposure; waist circumference

Introduction

The use of computed tomography (CT) as a diagnostic tool has increased in the past decades and nowadays CT imaging contributes most to the increase in radiation exposure of all medical radiation applications.¹ Increased CT use has resulted in growing rates of repeat or multiple imaging in various patient populations and risks from cumu-

lative radiation exposure have recently received more attention.^{2,3} Some patients may go through many CT studies during the treatment and follow-up and they may have a long life expectancy so the associated risk from imaging should be kept as low as reasonably.

One way to reduce the overall radiation dose and to lower the cumulative dose is to reduce the dose in individual patients.¹ All CT manufacturers

have introduced online tube current output modulation systems, also known as automatic exposure control (AEC), with the main intent to decrease radiation dose without compromising image quality. These devices modulate the tube-current output in the x-, y-, and z-directions to maintain a given image noise level appropriate for patient size and volume. Indeed, automatic exposure control algorithms do reduce radiation doses by adjusting tube-current to patient size.^{4,5} However, the scanners without AEC were long in use together the newer devices. On these scanners consideration of patient size mainly depended on the experience and competence of the personnel, and radiation exposure parameters were adjusted only just before the examination.

The cancer patients were mainly studied with two different scanners in our hospital, so we sought to clarify how a device equipped with AEC affects the exposure to radiation of patients with different waist circumferences compared to a non-AEC device.

Patients and methods

The LightSpeed 16 (GE, Wisconsin, United States) and Plus 4 (Siemens, Erlangen, Germany) devices are third-generation CT scanners and they allow helical scanning. The LightSpeed 16 is a multi-slice CT with an adaptive array detector consisting of 24 parallel rows of solid-state detectors. The detectors cover 20 mm in the z-direction at the iso-center. Detectors allow imaging of 16 slices per rotation and 0.63 to 10 mm slices can be reconstructed in the helical mode, depending on the reconstruction method and the selected pitch. The LightSpeed 16 device has an automatic exposure control, which adjusts the tube current to patient size and along the z-axis, but not during rotation. The input value of AEC was the noise index. The Plus 4 device is a single-slice CT with a ceramic detector covering 10 mm in the z-direction at the iso-center. The Plus 4 device can reconstruct 1 to 10 mm slices. It has no automatic tube current control. The main difference between the devices is in current (mA) applications. The Plus 4 uses mainly a current of 150 mA for all patients, but the LightSpeed 16 exploit a wide variation of current (53 to 441 mA) and the baseline is higher. Usually, a voltage of 120 kV was used on both scanners. The Plus 4 used two series with intravenous (IV) contrast and the LightSpeed 16 examined thorax, liver and abdomen separately in order to have better dose modulation, but there

were no other differences on image parameters, when IV contrast agent was used.

The study group consisted of 65 patients who underwent whole-body scanning with the two most frequently used scanners at the Department of Radiology, Turku University Hospital between the years 2000 – 2011. The procedures followed Helsinki declaration and the study was approved by the South-Western Finland Hospital district's Ethical Committee.

The inclusion criteria were testicular cancer and age under 40 years. During this period this group of patients underwent 279 whole-body CT scans, on average 4.3 per patient. IV contrast agent was used on 77.4% of scans. The scanned area usually covered the whole-body from lower neck to the symphysis or mid-thigh; in a few cases it started from the external auditory canal to cover the entire neck.

Details of the imaging studies patients were obtained from the institutional radiology database. The CT-data were collected from each examination for calculation of effective doses and the patient-specific organ doses, where the doses of stomach, urinary bladder, breast, liver, red bone marrow, testicles, colon, lenses, pancreas, lungs and heart were collected. For this, software developed by ImPACT, which uses the NRPB Monte Carlo dose data sets (report SR250), was used.⁶ The tissue-weighting factors from ICRP 103 (2007) were used to calculate the effective dose.⁷ For the calculations the software used voltage, current, rotation time, pitch and scanning length for input, and also tabulated the $CTDI_{air}$ -values, which were dependent on the scanner, voltage and collimation. The patient exposure from the LightSpeed 16, which uses current modulation, was calculated using the highest and lowest current values; the mean of these was then calculated and assumed to be closest to the actual value. The dose calculation has been described in detail by Salminen *et al.*⁸

The waist circumference was measured from one axial CT image with a metric tool (PACS, Carestream Health Inc, New York, USA). The measurement was made at the midpoint between the lowest rib and the iliac crest; the midpoint was identified visually with topogram.

Means and standard deviations (SD) or medians and range of values were used to describe continuous variables. Observations were plotted in a scatter plot and regression lines were created to illustrate the difference between scanners. For non-normally distributed variables group differences were tested with Wilcoxon's Two-Sample Test.

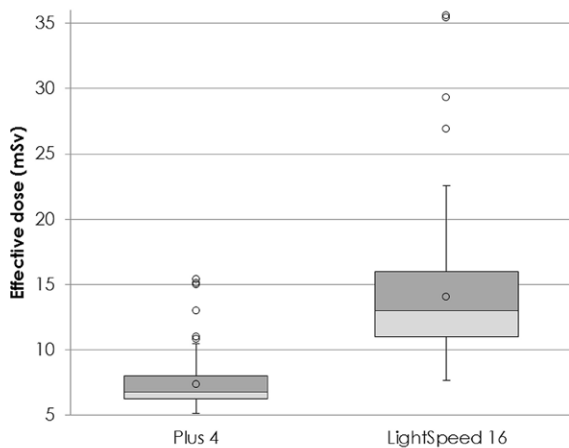


FIGURE 1. Boxplot of effective dose by device. The difference between devices is highly significant ($p < 0.0001$, Wilcoxon's).

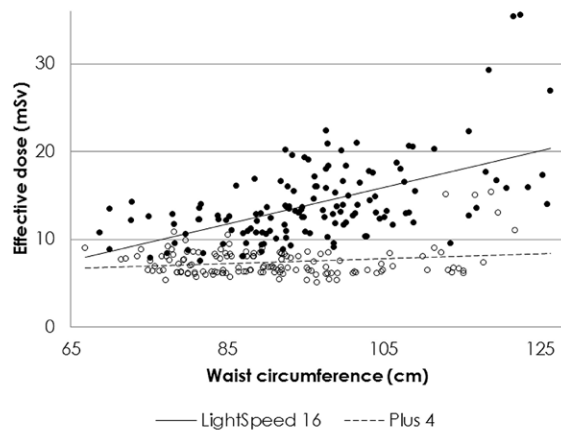


FIGURE 2. Effective dose versus waist circumference by scanner type in whole-body examinations. A wider variation of effective doses is observed for the LightSpeed 16 device.

P-values less than 0.05 were considered statistically significant. The SAS system for Windows, Version 9.3 (SAS Institute Inc, Cary, NC, USA) was used for the statistical calculations.

Results

The mean (SD) age of the patients was 28.3 (6.6) years. Further patient characteristics and number of CTs are presented in Table 1. Figure 1 shows a boxplot comparing effective doses by device. Dose levels were lower and the dose range narrower for the device without an AEC system (Plus 4). The average effective dose delivered was significantly lower for the Plus 4 than the LightSpeed 16 ($p < 0.0001$).

TABLE 1. Patient characteristics at the time of the first whole-body scan

Characteristic	Value
Number of patients	65
Median age (years)	28 (range 16.5-39.4)
Number of patients with seminoma/non-seminoma	26/39
Median waist circumference (cm)†	92.2 (range 66.9-126.3)
Total number of whole-body CTEs	279
Mean number of whole-body CTEs/patient	4.3 (SD 2.6)
Number of whole body CTEs	
-LightSpeed 16	137 (49.1%)
-Plus 4	142 (50.2%)
Number of whole-body CTE with IV contrast	
-LightSpeed 16	104 (75.9)
-Plus 4	112 (78.9)

† The waist circumference was measured midway between the lowest rib and the iliac crest from one axial CT image.

CTE = computed tomography examinations

TABLE 2. Mean effective dose and SD (mSv) by device and waist circumference with and without IV contrast

	LightSpeed 16*		Plus 4**	
	< 100 cm	≥ 100 cm	< 100 cm	≥ 100 cm
Waist circumference	< 100 cm	≥ 100 cm	< 100 cm	≥ 100 cm
With IV	13.6 (3.2)	17.5 (6.1)	7.4 (1.2)	8.5 (3.3)
Without IV	10.7 (2.0)	12.8 (1.9)	6.2 (0.5)	7.7 (2.5)
All	12.8 (3.2)	16.7 (5.9)	7.2 (1.2)	8.2 (3.0)

* The p-value (Wilcoxon two-sample test) between waist circumference over and under 100 cm $p=0.003$

** The p-value (Wilcoxon two-sample test) between waist circumference over and under 100 cm $p=0.003$

When the effective dose was plotted against the in waist circumference (Figure 2) a wider variation was observed for the LightSpeed 16 device, showing that patients with larger waist circumference were exposed to higher doses ($p < 0.0001$). There was a positive association between waist circumference and the dose. The effective dose generated by the LightSpeed 16 device for patients with a waist circumference < 100 cm was 12.8 mSv (SD 3.2) and > 100 cm 16.7 mSv (SD 5.9). With Plus 4 the regression analysis showed that there was no overall statistically significant change in effective dose as the waist circumference increased ($p = 0.41$). However, at a cut point of 100 cm, there was a difference: the effective dose was 7.2 mSv (SD 1.2) when the waist circumference was < 100 cm and 8.2 mSv (SD 3.0) for > 100 cm ($p < 0.025$).

Table 2 shows the mean effective doses by device and waist circumference for imaging stud-

ies with and without IV contrast. The use of IV contrast agent resulted in significantly higher radiation exposure compared to imaging studies with no IV contrast ($p = 0.002$ Plus 4, $p < 0.003$ LightSpeed 16).

The organ doses varied between 0.006 and 65 mGy; the lenses were subjected to the lowest dose, the stomach to the highest. Using LightSpeed 16 device the organ doses tended to increase in pace with the effective doses. For larger patients significantly higher organ doses were received by the breast, lungs, heart, stomach, liver, pancreas, colon, bladder, testicles and red bone marrow, and the doses increased statistically significantly in relation with the waist circumference for imaging studies performed with the LightSpeed 16 device ($p < 0.001$ for all organs). Such an increase in organ doses was not observed for the Plus 4 device.

Discussion

In this study, the effective dose to patients who were imaged because of testicular cancer was, on average, 7 mSv for the Plus 4 device and 12 mSv for the LightSpeed 16 device. The doses were significantly lower for all patients who were imaged with the older device without AEC. Use of the AEC increased the overall exposure, but it varied by patient size: smaller patients received lower doses than larger patients. The principle of AEC is to modify the current for variations in patient size. Still, the baseline level of exposure from the AEC CT-device exceeded the level of non-AEC device, and the exposure was especially high among patients of larger waist circumference. Probably the baseline reset was left on an unnecessarily high level, since the lower level of the non-AEC device was sufficient for producing proper diagnostic results.

Patients, whose waist circumference was over 100 cm, received higher dose on LightSpeed 16, because the scanner used higher current. When the waist circumference increased over 118 cm, the device used the maximum current during the whole examination and the current was not modulating. On LightSpeed 16 the voltage remain unchanged (120 kV) regardless of waist circumference. The reason for higher doses on Plus 4 was the higher voltage (140 kV), which was used, when the waist circumference was over 113 cm.

Comparing procedures performed by devices it should be noted that also the number of series were different. On Plus 4 there were two series, when IV

contrast was used while there were three series on LightSpeed 16. The LightSpeed 16 examined thorax, liver and abdomen separately in order to have better dose modulation. This contributes to higher patient exposure on LightSpeed 16. Basic set up level for LightSpeed 16 was also high, perhaps following the vendor's recommendation rather than being adapted to a departmental protocol.

Based on data available on how patient biometrics should be considered in CT imaging,^{9,10,11} Chan and associates have addressed the question of BMI and abdominal fat. They found that by increasing these variables effective doses from the abdomen and pelvis scans also significantly increased.¹⁰ They observed a potential risk of very high radiation doses to oversized patients when the automatic exposure control system is used. Our results are in concert with this and point out the importance of careful consideration of precise values. A study by Kalra *et al.*¹² reported that a z-axis modulating AEC, if used correctly, can reduce the dose by 34–45%. Optimum use requires an understanding of the importance to reset parameters and of the effect of IV contrast agent on radiation exposure.

The noise index (NI) was used as an input factor in the AEC of the LightSpeed 16 device. The NI is approximately equal to the SD of reconstructed images and allows selecting the amount of noise of images. The NI determines the tube current within the selected range. In our study a higher tube current was used in the LightSpeed 16 device, which implies that the NI was set too low and especially larger patients require selection of a higher NI, because more noise can be moderated on larger patients and a 5% increase in NI is associated with a 10% reduction in radiation dose.¹³ There are also another means to lower the dose in addition to increasing the NI, since all parameters that affect image noise affect indirectly the tube current when an AEC is used.¹⁴

Use of IV contrast increased the radiation dose from both devices further. Paul and associates observed that CTs done with IV contrast agent raises the dose in chest imaging in AEC-equipped CTs.¹⁵ The use of IV contrast agent usually involves multiple imaging steps: first native CT and then contrast-augmented CT. More phases naturally increase the effective dose to the patient. The use of IV contrast agent does not always provide additional diagnostic information and the usefulness of doing both a native and a contrast CT requires further study.^{16,17,18}

The use of already used or refurbished CT scanners is becoming more popular in less privileged

countries. Concerns regarding the poor quality of these devices have been expressed.¹⁹ We voice our concern also for the lag of appropriate and timely maintenance and for the understanding of the importance of protocol details, regardless of the type or age of the device. Even older devices could be used achieving sufficient diagnostic value without increasing patient exposure unnecessarily.

The advantages of the current study include the use of 1-slice and 16-slice CT devices in the same hospital environment. We could collect all data comprehensively since all patients were followed up in the same hospital and scanning was exclusively performed with only two CT devices. The disadvantage of this study was the old fashion devices. However, this is understandable, while the examinations have been done since 2000, when the 16-slice scanners were the state of the art. While 64-slice scanners or more slice scanners are nowadays widely used, it would also be interesting to study the differences between patients with newer devices.

There were significant differences in the amount of radiation exposure to the patients scanned with these two devices. Thus, it is necessary to understand the technical characteristics of each CT device in addition to the scanning protocol, when radiation exposure is determined clinically. The protocol should be adapted to patient biometrics: exposure may be increased only when more radiation is required to improve the quality of the scans. In all clinical radiology, unnecessary exposure must be avoided. Imaging records and protocols should describe in detail when it is allowable to deviate from the pre-assigned imaging protocol regarding radiation dose and use of IV contrast agent. This information is needed for clinical reasons, but importantly also for purposes of reconstructing the estimated amount of radiation exposure to the individual.

Although all imaging studies were done in one hospital, we could not retrospectively establish the reason for why the basic dose levels were higher also for small patients, when the AEC was used compared to previous practice. The reason may reside in the vendor's recommendation. If so, this stands in contrast to the principle of using an AEC: to provide a substantial reduction in radiation dose with similar or improved image quality.²⁰ As the image quality of LightSpeed 16 may have exceeded the image quality needed for clinical decision, there is a need for image quality assessment between these two devices to further explain the differences in doses.

Conclusions

The current results show that there is a need for careful consideration of the set-up of the basic parameters for AEC-equipped CT devices. This need stems from the present observation that patient size and the use of IV contrast media are associated with an excessive risk of unnecessarily high radiation exposure. Proper attention to these circumstances is warranted for improved radiation protection in connection with CT-imaging studies.

Acknowledgements

The study was supported by a government research grant (EVO Foundation) awarded to Turku University Hospital.

References

1. Brenner DJ, Hall EJ. Computed tomography - an increasing source of radiation exposure. *N Engl J Med* 2007; **357**: 2277-84. doi: 10.1056/NEJMra072149
2. Griffey RT, Sodickson A. Cumulative radiation exposure and cancer risk estimates in emergency department patients undergoing repeat or multiple CT. *AJR Am J Roentgenol* 2009; **192**: 887-92. doi:10.2214/AJR.08.1351
3. Brenner DJ, Doll R, Goodhead DT, Hall EJ, Land CE, Little JB, et al. Cancer risks attributable to low doses of ionizing radiation: Assessing what we really know. *Proc Natl Acad Sci U S A* 2003; **100**: 13761-6. doi:10.1073/pnas.2235592100
4. Ghoshhajra BB, Engel LC, Károlyi M, Sidhu MS, Wai B, Barreto M, et al. Cardiac computed tomography angiography with automatic tube potential selection: effects on radiation dose and image quality. *J Thorac Imaging* 2013; **28**: 40-8. doi: 10.1097/RTI.0b013e3182631e8a
5. Lee K, Lee W, Lee J, Lee B, Oh G. Dose reduction and image quality assessment in MDCT using AEC (D-Dom & Z-Dom) and in-plane bismuth shielding. *Radiat Prot Dosim* 2010; **141**: 162-7. doi: 10.1093/rpd/ncq159
6. Shrimpton PC, Jones DG. NRPB-SR250: Normalised organ doses for x-ray computed tomography calculated using Monte Carlo techniques. *Radiat Prot Dosim* 1993; **49**: 241-3.
7. International Commission on Radiological Protection. The 2007 Recommendations of the International Commission on Radiological Protection. ICRP Publication 103 2002; **37** (2-4).
8. Salminen E, Niiniviita H, Kulmala J, Määttänen H, Järvinen H. Radiation dose estimation in computed tomography examinations using NRPB-SR250 software in a retrospective analysis of a patient population. *Radiat Prot Dosim* 2012; **152**: 328-33. doi: 10.1093/rpd/ncs065
9. Sodickson A, Weiss M. Effects of patient size on radiation dose reduction and image quality in low kVp CT pulmonary angiography performed with reduced IV contrast dose. *Emerg Radiol* 2012; **19**: 437-45. doi: 10.1007/s10140-012-1046-z
10. Chan VO, McDermott S, Buckley O, Allen S, Casey M, O'Loaide R, et al. The relationship of body mass index and abdominal fat on the radiation dose received during routine computed tomographic imaging on the abdomen and pelvis. *Can Assoc Radiol J* 2012; **63**: 260-6. doi: 10.1016/j.carj.2011.02.006
11. Alkadhi H, Stolzmann P, Scheffel H, Desbiolles L, Baumüller S, Plass A et al. Radiation dose of cardiac dual-source CT: the effect of tailoring the protocol to patient-specific parameters. *Eur J Radiol* 2008; **68**: 385-91. doi: 10.1016/j.ejrad.2008.08.015

12. Kalra MK, Maher MM, Toht TL, Kamath RS, Halpern EF, Saini S. Comparison of Z-axis automatic tube current modulation technique with fixed tube current CT scanning of abdomen and pelvis. *Radiology* 2004; **232**: 347-53. doi: 10.1148/radiol.2322031304
13. Kalra MK, Naz N, Rizzo S, Blake MA. Computed tomography radiation dose optimization: scanning protocols and clinical applications of automatic exposure control. *Curr Probl Diagn Radiol* 2005; **34**: 171-81. doi: 10.1067/j.cpradiol.2005.06.002
14. Gudjónsdóttir J, Ween B, Olesn DR. Optimal use of AEC in CT: A literature review. *Radiol Tech* 2010; **81**: 309-17.
15. Paul J, Schell B, Kerl JM, Maentele W, Vogl TJ, Bauer RW. Effect of contrast material on image noise and radiation dose in adult chest computed tomography using automatic exposure control: a comparative study between 16-,64- and 128-slice CT. *Eur J Radiol* 2011; **79**: 28-32. doi: 10.1016/j.ejrad.2011.05.012
16. da Costa e Silva EJ, da Silva GA. Elimination unenhanced CT when evaluating abdominal neoplasms in children. *AJR Am J Roentgenol* 2007; **189**: 1211-14. doi:10.2214/AJR.07.2154
17. Patten RM, Byun JY, Freeny PC. CT of hypervascular hepatic tumours: are unenhanced scans necessary for diagnosis. *AJR Am J Roentgenol* 1993; **161**: 979-84. doi: 10.2214/ajr.161.5.8273641
18. Jung SI, Park HS, Kim YJ, Jeon HJ. Multidetector computed tomography for the assessment of adnexal mass: Is unenhanced CT scan necessary. *Korean J Radiol* 2014; **15**: 72-9. doi: 10.3348/kjr.2014.15.1.72
19. Hong JS, Kang HC. Relationship between the use of new or used computed tomography scanners and image retake rates in South Korea. *Acta Radiol* 2013; **54**: 428-34. doi: 10.1258/ar.2012.120290
20. Tack D, De Maertelaer V, Gevenois PA. Dose reduction in multidetector CT using attenuation- based online tube current modulation. *AJR Am J Roentgenol* 2003; **181**: 331-4. doi: 10.2214/ajr.181.2.1810331

Radiol Oncol 2017; 51(2): 121-129.
doi:10.1515/raon-2017-0010

Difuzijsko obteženo slikanje s koeficientom obteženosti gliomov gradus II in III - analiza tumorske infiltracije ob leziji, gradusa in podtipov gliomov

Anna F. Delgado AF, Fahlström M, Nilsson M, Shala G, Berntsson SG, Zetterling M, Libard S, Alafuzoff I, Westen D, Lätt J, Smits A, Larsson EM

Izhodišča. Difuzijsko obteženo slikanje s koeficientom obteženosti (DKI) omogoča oceno difuzije na katero vplivajo mikro-celične strukture. DKI smo analizirali pri bolnikih s sumom na gliom nizke stopnje malignosti pred samo histopatološko analizo. Naš namen je bil raziskati, ali se MR-difuzijski parametri v beli substance normalnega izgleda (BSNI) ob tumorski spremembi razlikujejo od tistih v beli substanci nasproti le-te ter poiskati razlike v DKI med gliomomigradus II in III oz. podtipi gliomov (astrocitomi in oligodendrogliomi).

Bolniki in metode. Osemindeset bolnikov, s sumom na gliom nizke stopnje malignosti, ki so podali pisni pristanek za sodelovanje, smo vključili v raziskavo, ki jo je odobrila etična komisija Univerze. Pri bolnikih smo pred operacijo analizirali DKI izmerjen na MR aparatu jakosti3T. Bolniki, pri katerih je histološka analiza pokazala gliom gradusa II ali III (n=35) so bili vključeni v nadaljevanje raziskave. Na T2 in FLIAR obteženih sekvencah smo določili področja interesa (PI) ter jih poleg tega označili na zemljevidu MR-difuzijskih parametrov. Primerjali smo srednje vrednosti DKI za BSNI ob leziji in nasproti lezije (Studentov t-test za odvisne spremenljivke, Wilcoxonovim testom ujemanja parov). Primerjali smo histograme DKI različnih podtipov gliomov in različnih gradusov (multipla primerjava povprečnih razvrstitev za vse skupine). Sposobnost razlikovanja podtipov in gradusov gliomov s pomočjo DKI smo določili z ROC (receiveroperatingcharacteristics) krivuljami.

Rezultati. Rezultati so pokazali statistično značilne razlike v vseh parametrih DKI med BSNI ob tumorski spremembi in tistimi nasproti le-te. ($p = <0,000$), razen za aksilano sploščenost ($p = 0,099$). Štirinštrideset spremenljivk histograma se je statistično značilno razlikovalo med gliomom gradus II (n = 23) in III (n = 12) ($p = 0,003-0,048$). Deset spremenljivk se je statistično značilno razlikovalo med astroцитom (n = 18) in oligodendrogliomi (n = 17) ($p = 0,011-0,050$). ROC krivulje spremenljivk, ki so pokazale najboljšo razlikovanje so imele AUC (površina pod krivuljo) med 0.657 in 0.815.

Zaključki. Srednje vrednosti spremenljivk DKI v beli substanci normalnega izgleda ob tumorski spremembi se razlikovali od tistih nasproti le-te, kar kaže na spremenjeno mikrostrukturo zaradi tumorske infiltracije, ki pa jo na MR-preiskavi morfološko ne zaznamo. Rezultati analize histogramov DKI so pokazali razlike med podtipi in stopnjo malignosti gliomov.

Radiol Oncol 2017; 51(2): 130-136.
doi:10.1515/raon-2017-0016

Dinamična s kontrastom poudarjena magnetnoresonančna preiskava dojk. Fibrocistične spremembe, ki se izrazijo kot masne lezije in se ne obarvajo ter posnemajo malignost

Milošević ZC, Nadrljanski MM, Milovanović ZM, Gusic NZ, Vučićević SS, Radulović OS

Izhodišča. Namen raziskave je bil analizirati morfološke značilnosti fibrocističnih sprememb v dojkah (neproliferativne lezije, proliferativne lezije brez atipije in proliferativne lezije z atipijo), ki se pri dinamičnih s kontrastom poudarjenih magnetnoresonančnih preiskavah (DCE-MRI) izrazijo kot masne lezije brez obarvanja.

Bolniki in metode. S pomočjo podatkovne slikovne baze za dojke (BI – RADS; *angl. Breast Imaging Reporting and Data System*) smo retrospektivno pregledali 46 bolnikov s histološko dokazanimi fibrocističnimi spremembami. Pred preiskavo DCE-MRI smo na malignost sumljivo enostransko lezijo dojke ugotovili klinično, jo dokazali z mamografijo ali ultrazvokom dojke.

Rezultati. Prevladujoče lastnosti fibrocističnih sprememb, ki so se na preiskavi DCE-MRI izrazile kot masne lezije brez obarvanja, so bile: enostranska regionalna ali difuzna porazdelitev (pri 35 bolnikih ali 76,1 %), heterogen ali gručast notranji vzorec ojačanja (pri 36 bolnikih ali 78,3 %), plato na krivulji odvisnosti časa od intenzivnosti signala (pri 25 bolnikih ali 54,3 %), zmerne ali hitre spremembe (*angl. wash-in*; pri 31 bolnikih ali 67,4 %). Neproliferativne lezije smo odkrili pri 11 bolnikih (24 %), proliferativne lezije brez atipije pri 29 bolnikih (63 %) in lezije z atipijo pri šestih bolnikih (13 %). Pri tem nismo našli statistično pomembnih razlik v morfoloških značilnostih razen združevanja grozdov mikrocist pri proliferativni displaziji brez atipij.

Zaključki. Fibrocistične spremembe, ki se na DCE-MRI preiskavah izrazijo kot masne lezije brez obarvanja, imajo več morfoloških značilnosti, sumljivih za maligno bolezen, zato je potrebna biopsija (BI - RADS 4). Pri večini neproliferativnih lezij, proliferativnih lezij brez atipije in proliferativnih lezij z atipijo najdemo iste predvidljive morfološke značilnosti DCE-MRI.

Radiol Oncol 2017; 51(2): 137-141.
doi:10.1515/raon-2017-0018

Magnetnoresonančno vrednotenje možganskega edema po stereotaktični radiokirurgiji izvedeni na lineranem pospeševalniku

Harat M, Lebioda A, Lasota J, Makarewicz R

Izhodišča. Peritumorski edem je resen in dobro znan zaplet stereotaktične radiokirurgije. Ocenili smo tveganje za nastanek edema po stereotaktični radiokirurgiji ter dinamiko njegovega nastajanja in resolucije.

Bolniki in metode. 107 bolnikov z različnimi diagnozami smo zdravili s stereotaktično radiokirurgijo. Indikacije za zdravljenje so bile: 34 (29 %) arteriovenskih malformacij, 38 (35 %) meningeomov, 16 (15 %) metastatskih tumorjev, 16 (15 %) akustičnih nevromov, 3 (3 %) kavernomov in po 2 (2 %) anaplastična astrocitoma in anaplastična oligoastrocitoma. Področje edema smo visali na sekvenci MRI T2-FLAIR 0, 6, 12, 18, 24, 30, in 38 mesecev po zdravljenju. Lokacijo lezije smo opredelili nad ($n = 80$) ali pod ($n = 32$) „Frankfurtsko modificirano linijo“ (FML).

Rezultati. Pri 17 % bolnikov se je po zdravljenju na novo razvil edem ali pa povečal. Obseg edema je bil največji 6 mesecev po radiokirurgiji (povprečno 7,2 meseca; SD 1,2). Edem po stereotaktični radiokirurgiji je bil 5,1 (1,06–24,53) krat bolj pogost pri bolnikih lezijami nad FML. Povezav med razvojem edema, starostjo, velikostjo planirnega tarčnega volumna (PTV), številom žarkovnih snopov in diagnozo nismo našli ($p = 0,07$).

Zaključki. Z radiokirurgijo povezan edem se je razvil v 6 mesecih po zdravljenju in se nato sčasoma zmanjševal. Nastanek edema je bil močno povezan z lokacijo lezije, njegova prisotnost je bila veliko bolj verjetna, če je lezija ležala nad Frankfurtsko linijo.

Radiol Oncol 2017; 51(2): 142-150.
doi:10.1515/raon-2017-0019

Genetski dejavniki, ki vplivajo na fluorescenco povzročeno s 5-aminolevulinsko kislino med operacijo difuznih gliomov

Saito K, Hirai T, Takeshima H, Kadota Y, Yamashita S, Ivanova A, Yokogami K

Izhodišča. Pri bolnikih z malignim gliomom lahko s fluorescenco povzročeno s 5-aminolevulinsko kislino (5-ALA) usmerjamo operativni poseg. Občasno pa fluorescenco ne vidimo kljub histopatološki diagnozi glioma visoke stopnje. Namen raziskave je bil ugotoviti dejavnike, ki vplivajo na intraoperativno vizualizacijo gliomov s pomočjo fluorescenco povzročene s 5-ALA.

Bolniki in metode. Pregledali smo podatke 60 bolnikov z astrocitnimi ali oligodendrocitnimi tumorji, pri katerih smo tumorje odstranili ob pomoči fluorescenco povzročene s 5-ALA, med januarjem 2014 in decembrom 2015. S pomočjo univariatne in multivariatne statistične analize smo proučili klinične značilnosti bolnikov, ugotovitve predoperativnega slikanja z magnetno resonanco (MRI), histološke diagnoze in genetske profile.

Rezultati. Pri 42 bolnikih (70 %) smo med operacijo opazili fluorescenco povzročeno s 5-ALA. 2 od 8 bolnikov (25 %) sta imela tumor po WHO gradus II, 9 od 17 (53 %) gradus III, in 31 od 35 (89 %) bolnikov tumor gradus IV. Univariatna analiza je pokazala statistično pomembno povezavo med fluorescenco povzročeno s 5-ALA in statusom izocitrat dehidrogenaze 1 (IDH1) ($p < 0,001$), izgubo heterozigotnosti (LOH) 1p19q ($p < 0,003$), proliferacijskim indeksom MIB-1 ($p < 0,007$), tumorskimi robovi ($p < 0,046$), heterogenostjo tumorjev ($p < 0,021$), in privzemom kontrasta pri slikanju z MRI ($p = 0,002$). Multivariatna analiza pa je pokazala, da je status IDH1 edini statistično neodvisen dejavnik, ki vpliva na fluorescenco povzročeno s 5-ALA ($p = 0,009$).

Zaključki. Rezultati raziskave so pokazali, da ima status IDH1 največji vpliv na fluorescenco povzročeno s 5-ALA pri difuznih gliomih.

Radiol Oncol 2017; 51(2): 151-159.
doi:10.1515/raon-2016-0043

Polimorfizmi posameznega nukleotida v genih *MACC1*, *RAD18*, *MMP7* in *SDF-1a* kot napovedni dejavnik pri resektabilnem raku debelega črevesa in danke

Horvat M, Potočnik U, Repnik K, Kavalarič R, Zadnik V, Potrč S, Štabuc B

Izhodišča. Rak debelega črevesa in danke je v svetu med najpogostejšimi raki. Raziskave so pokazale, da funkcionalne spremembe genov (polimorfizmi posameznega nukleotida, SNP) sovpadajo z razsojem in večjo agresivnostjo tumorja ter lahko posledično vplivajo na večjo verjetnost ponovitve bolezni. Namen naše raziskave je bil opredeliti vlogo polimorfizmov izbranih genov kot napovednega dejavnika pri raku debelega črevesa in danke resektabilnih stadijev.

Bolniki in metode. V raziskavo smo vključili bolnike z resektabilnim rakom debelega črevesa in danke stadijev I, II in III, ki smo jim odkrili in zdravili v letu 2007 in prvi polovici leta 2008 v Univerzitetnem kliničnem centru Maribor. Analizirali smo v parafin vpete vzorce tkiva iz arhiva Oddelka za patologijo UKC Maribor in genotipizirali izbrane SNP-je v genih *SDF-1a*, *MMP7*, *RAD18* in *MACC1*. Za genotipizacijo vzorcev DNA smo uporabili metodo verižne reakcije s polimerazo, ki ji je sledila analiza talilne krivulje visoke ločljivosti (PCR-HRM) oziroma reakcija polimorfizmov dolžin restrikcijskih fragmentov (PCR-RFLP).

Rezultati. Ugotovili smo slabše preživetje brez ponovitve bolezni pri bolnikih z genotipom TT SNP-ja rs1990172 na genu *MACC1* ($p = 0,029$). Prav tako smo ugotovili slabše preživetje brez napredovanja bolezni pri bolnikih z genotipom GG SNP-ja rs373572 na genu *RAD18* ($p = 0,020$). Ugotovili smo večjo pogostnost genotipa GG SNP-ja rs11568818 na genu *MMP7* pri bolnikih stadijev T3/T4 ($p = 0,014$), stadijev N1/N2 ($p = 0,041$) in z limfovaskularno invazijo ($p = 0,018$). Prav tako smo ugotovili večjo frekvenco genotipa TT SNP-ja rs1990172 na genu *MACC1* pri bolnikih stadijev T3/T4 ($p = 0,024$). Ugotovili smo večjo frekvenco genotipa GG SNP-ja rs373572 na genu *RAD18* pri bolnikih stadijev T1/T2 s ponovitvijo bolezni ($p = 0,041$).

Zaključki. SNP-ji v genih *MMP7*, *MACC1* in *RAD18* imajo možno vlogo kot napovedni dejavnik pri raku debelega črevesa in danke resektabilnih stadijev.

Radiol Oncol 2017; 51(2): 160-168.

doi:10.1515/raon-2017-0014

Magnetno resonančno slikanje zmanjša variabilnost vrisovanja tarčnega volumna pri bolnicah z rakom dojke brez označevalcev v ležišču tumorja

Al-Hammadi N, Caparrotti P, Divakar S, Riyas M, Halsnad Chandramouli S, Hammoud R, Hayes J, Mc Garry M, Prasad Paloor S, Petric P

Izhodišča. Opustitev vstavitve kovinskih označevalcev oteži vrisovanje kliničnega tarčnega volumna ležišča tumorja (*angl. lumpectomy cavity clinical target volume; CTV_{LC}*) pred obsevanjem. Namen raziskave je bil opredeliti variabilnost in natančnost vrisovanja CTV_{LC} s pomočjo magnetne resonance (MR) in računalniške tomografije (CT).

Bolniki in metode. V raziskavo smo vključili simulatorske slike CT in MR 12 bolnic z rakom dojke, ki smo jih zdravili s kirurško odstranitvijo tumorja in pooperativnim obsevanjem. Pet radioterapevtov je na vse slike vrisalo CTV_{LC} in ocenilo zmožnost vizualizacije kirurške votline (*angl. cavity visualization score; CVS*). Upoštevanje mnenja vseh radioterapevtov je šesti, najizkušenejši radioterapevt, vrisal referenčne (*angl. expert consensus; EC*) obrise CTV_{LC}. Izračunali smo variabilnost velikosti vrisanih tarčnih volumnov in splošni kazalec volumetričnega ujemanja (*ang. generalized conformity index; CI_{gen}*). Odstopanja od EC obrisov smo opredelili z izračunom kazalca natančnosti (*ang. accuracy index; AI*) in razdalj med obrisi (*ang. inter-delineation distance; IDD*).

Rezultati. Povprečen CVS je znašal 3.88 +/- 0.99 oz. 3.05 +/- 1.07 za MR oz. CT ($p = 0.001$). Povprečna prostornina CTV_{LC} je bila podobna med CT in MR: 154 +/- 26 cm³ in 152 +/- 19 cm³. Srednji CI_{gen} in AI sta bila višja pri MR kot CT vrisovanju (CI_{gen}: 0.74 +/- 0.07 proti 0.67 +/- 0.12, $p = 0.007$; AI: 0.81 +/- 0.04 proti 0.76 +/- 0.07; $p = 0.004$). CI_{gen} in AI sta naraščala z naraščanjem CVS. Povprečna IDD je bila 3 mm +/- 1.5 mm oz. 3.6 mm +/- 2.3 mm za vrisovanje na podlagi MR oz. CT ($p = 0.017$).

Zaključki. V primerjavi s CT je MR slikanje izboljšalo opredelitev pooperativnih sprememb, zmanjšalo razlike med obrisi posameznih radioterapevtov in povečalo natančnost vrisovanja CTV_{LC} pri bolnicah brez označevalcev v ležišču tumorja. Za potrditev zgornjih rezultatov so potrebne dodatne raziskave na večjem vzorcu.

Radiol Oncol 2017; 51(2): 169-177.
doi:10.1515/raon-2016-0030

Vpliv dolžine distalnega resekcijskega roba na lokalno ponovitev bolezni in dolgoročno preživetje pri bolnikih z rakom danke zdravljenih s predoperativno radiokemoterapijo in sfinkter - ohranjujočo resekcijo danke

Grosek J, Velenik V, Edhemović I, Omejc M

Izhodišča. Preprečevanje lokalne ponovitve bolezni in zagotavljanje dolgoročnega preživetja sta glavna cilja zdravljenja raka danke. Ustrezna kirurška tehnika, ki sledi predoperativni radiokemoterapiji, omogoča bolnikom z lokalno napredovalim rakom danke najboljše možnosti ozdravljenja. Cilj raziskave je bilo ugotoviti, ali je dolžina distalnega resekcijskega roba povezana z lokalno ponovitvijo bolezni in dolgoročnim preživetjem.

Bolniki in metode. V raziskavo smo vključili 109 bolnikov z lokalno napredovalim nemetastatskim rakom danke, ki smo jih med letoma 2006 in 2010 zdravili s predoperativno radiokemoterapijo in nato sfinkter ohranjujočo resekcijo danke. Dolžine distalnih resekcijskih robov smo izmerili na preparatih, fiksiranih v formalinu. Bolnike smo razdelili v tri skupine glede na dolžino distalnega resekcijskega roba: [1] rob < 8 mm (1. skupina, n = 27); [2] rob 8–20 mm (2. skupina, n = 31) in [3] rob > 20 mm (3. skupina, n = 51). Skupine smo med seboj retrospektivno primerjali in statistično analizirali. Povprečen čas sledenja bolnikov iz 1. skupine je bil 89 mesecev (51–111), iz 2. skupine 83 (57–111) ter 3. skupine 80 (45–116) mesecev (p = 0,326).

Rezultati. Univariatna analiza ni pokazala statistično pomembne povezave dolžine distalnega resekcijskega roba z dolgoročnim preživetjem ali stopnjo lokalne ponovitve bolezni (p > 0,005). Tudi v multivariatnem regresijskem modelu, ob kontroli s patološkim T in N stadijem po operaciji (yT, yN), dolžina distalnega resekcijskega roba ni bila statistično pomembno povezana z dolgoročnim preživetjem.

Zaključek. Pri bolnikih, vključenih v našo raziskavo, dolžina distalnega resekcijskega roba ni bila statistično pomembno povezana z lokalno ponovitvijo bolezni in dolgoročnim preživetjem.

Radiol Oncol 2017; 51(2): 178-186.

doi:10.1515/raon-2017-0015

Rezultati zdravljenja 130 bolnikov, ki so zboleli zaradi primarnih ali sekundarnih pljučnih tumorjev, z robotsko stereotaktično telesno radioterapijo Cyberknife

January ZL, Jansen N, Baart V, Devillers M, Dechambre D, Lenaerts E, Seidel L, Barthelemy N, Berkovic P, Gulyban A, Lakosi F, Horvath Z, Coucke PA

Izhodišča. Avtorji poročajo o rezultatih zdravljenja bolnikov s primarnimi, recidivnimi in metastatičnimi lezijami na pljučih z robotsko stereotaktično telesno radioterapijo (SBRT, ang. *Stereotactic Body RadioTherapy*).

Bolniki in metode. S SBRT ob uporabi Cyberknife smo zdravili 130 bolnikov s 160 lezijami: primarnimi tumorji T1-3 (54 %), recidivnimi tumorji (22 %) in pljučnimi zasevki (24 %). Povprečna biološka ekvivalentna doza (BED_{10Gy}) je bila 151 Gy (72–180 Gy). Srednji predpisani dozi na periferne in centralne lezije sta bili 3 x 20 Gy in 3 x 15 Gy. Poročamo deleže lokalne kontrole, celokupnega preživetja in vzročno-specifičnega preživetja ter zgodnje in kasne toksičnosti. Naredili smo statistično analizo za prepoznavo dejavnikov, ki vplivajo na lokalno kontrolo bolezni.

Rezultati. Srednji čas sledenja je bil 21 mesecev. V univariatni analizi je bila višja doza povezana z boljšo lokalno kontrolo; razmejitevno vrednost smo ugotovili pri $BED_{10Gy} \leq 112,5$ Gy. Za visokodozno in nizkodozno skupino je bil delež lokalne kontrole po 1, 2 in 3 letih 93 % proti 73 %, 80 % proti 61 % in 63 % proti 54 % ($p = 0,0061$, razmerje obojev = 0,384). V multivariatni analizi je bilo povečano tveganje za lokalni recidiv povezano z metastatično naravo lezije, histološko potrditvijo in večjim planirnim tarčnim volumnom (PTV). Deleži 1-, 2- in 3-letnega celokupnega preživetja so bili 85 %, 74 % in 62 %, deleži vzročno-specifičnega preživetja pa 93 %, 89 % in 80 %. Zgodnje in kasno toksičnost stopnje ≥ 3 smo ugotovili pri 3 (2 %) in 6 (5 %) bolnikih.

Zaključki. Spodbudna stopnja lokalne kontrole in preživetja po robotski SBRT ter nizka stopnja hude toksičnosti v naši mešani, neselekcioniirani študijski skupini se sklada s podatki iz literature.

Radiol Oncol 2017; 51(2): 187-194.
doi:10.1515/raon-2017-0013

Genetsko svetovanje, status BRCA1/2 in kliničnopatološke značilnosti pri bolnicah z rakom jajčnikov pred 50. letom

Cvelbar M, Hočevar M, Novaković S, Stegel V, Perhavec A, Krajc M

Izhodišča. V Sloveniji, tako kot v drugih državah, do nedavnega osebne anamneze epitelnega raka jajčnikov nismo vključevali med indikacije za genetsko svetovanje. Nedavne raziskave iz drugih držav so ugotovile delež germinalnih mutacij BRCA1/2 (gBRCA1/2) do 17 % v starostni skupini pod 50 let ob diagnozi. Osnovni namen raziskave je bil povabiti na genetsko svetovanje bolnice z epitelnim rakom jajčnikov pred 45. letom, ponuditi genetsko testiranje z vsemi možnimi implikacijami ter izvesti analizo deleža mutacij gBRCA1/2 in kliničnopatoloških značilnosti. Kasneje smo dodali še podatke predhodno genetsko testiranih bolnic z epitelnim rakom jajčnikov v starosti 45 do 49 let.

Bolniki in metode. Vse klinične podatke smo interpretirali v luči mnogih sprememb, ki so se zgodile na področju epitelnega raka jajčnikov prav v zadnjih nekaj letih: nova histološka klasifikacija stadijev FIGO, nova klasifikacija histoloških tipov in gradusov diferenciacije, nove terapevtske možnosti (uvredba inhibitorjev PARP v klinično prakso tudi v Sloveniji) in nove smerice *National Comprehensive Cancer Network (NCCN)* za genetsko svetovanje bolnicam z epitelnim rakom jajčnikov, kakor tudi nove možnosti, ki jih prinaša sekvenciranje naslednje generacije.

Rezultati. Delež sodelujočih glede na povabljene bolnice je bil 43,1 %. V skupini 27 povabljenih in testiranih bolnic z epitelnim rakom jajčnikov pred 45. letom je bilo najdenih 5 mutacij. Delež gBRCA1/2m je bil 18,5 %. Ugotovljene so bile 4 gBRCA1 in 1 gBRCA2 mutacije. V razširjeni skupini 42 testiranih bolnic z epitelnim rakom jajčnikov pred 50. letom smo našli 14 gBRCA1/2 mutacij. Delež ugotovljenih gBRCA1/2 mutacij v tej razširjeni, delno selekcionirani skupini je bil 33,3 %. Ugotovili smo 11 gBRCA1 mutacij in 3 gBRCA2 mutacije. Klinično je bil prisoten značilno večji delež pozitivne družinske anamneze raka jajčnikov v prvem kolenu pri gBRCA1/2 pozitivnih bolnicah. Povprečna starost ob diagnozi epitelnega raka jajčnikov je bila pri gBRCA1/2 pozitivnih bolnicah značilno višja. Kljub temu pa je bila ugotovljena mutacija gBRCA1/2 pri bolnici stari komaj 24 let. Delež epitelnega raka jajčnikov kot drugega primarnega raka je bil v skupini gBRCA1/2 pozitivnih bolnic značilno višji. Ugotovili smo težnjo večjega deleža prvega stadija epitelnega raka jajčnikov v skupini gBRCA1/2 negativnih bolnic (60,7 % vs. 26,7 % pri pozitivnih; $p = 0,055$). Glede histološkega tipa epitelnega raka jajčnikov ni bilo statistično značilnih razlik med skupinama in delež seroznega tipa je bil skoraj enak (40 % pri BRCA1/2 pozitivnih vs. 46 % pri negativnih). Glede stopnje diferenciacije (gradusa) je bil ugotovljen značilno večji delež visoko gradusnih (G2 in G3) epitelnih raka jajčnikov v gBRCA1/2 pozitivni skupini (66,7 % vs. 21,4 % v negativni skupini; $p = 0,008$). Ugotovljen je bil tudi primer mejno malignega epitelnega tumorja jajčnikov v gBRCA1/2 pozitivni skupini.

Zaključki. Ugotovljeni genetski rezultati so v skladu z nedavnimi raziskavami iz drugih držav in kažejo, da je delež mutacij gBRCA1/2 pri testiranih neizbranih bolnicah z epitelnim rakom jajčnikov pred 50. letom višji kot 10 %, namreč 18,5 %. Prag 10 % verjetnosti mutacije kot kriterij za genetsko testiranje v tej starostni skupini bolnic je dosežen in je genetsko testiranje za to starostno skupino upravičeno. Dodaten razlog so profilaktične implikacije glede raka dojke in implikacije glede njihovih sorodnikov. Upoštevajoč tudi sedanjo neposredno terapevtsko korist testiranja glede na možnost uporabe inhibitorjev PARP za BRCA1/2 pozitivne bolnice z epitelnim rakom jajčnikov obstaja zdaj dvojni razlog za genetsko testiranje vseh bolnic z epitelnim rakom jajčnikov pred 50. letom. Pri kliničnopatoloških podatkih je v vsakodnevni klinični praksi pomembna njihova re-interpretacija, ker ta lahko vpliva na terapevtske možnosti.

Izražanje receptorja za inzulinu podoben rastni faktor 1 pri napredovalem nedrobnoceličnem raku pljuč in njegov vpliv na celokupno preživetje

Humar M, Kern I, Vlačič G, Hadžić V, Čufer T

Izhodišča. Izražanje receptorja za inzulinu podoben rastni faktor (IGF1R) so proučevali kot možen napovedni dejavnik pri nedrobnoceličnem raku pljuč v več raziskavah. Vendar pa povezava med izražanjem IGF1R in napovedjo poteka bolezni teh bolnikov ostaja vprašljiva. Cilja observacijske kohortne raziskave sta bila ocena izražanja IGF1R pri napredovalem nedrobnoceličnem raku pljuč in njegov napovedni pomen; z analizo podskupine pa oceniti vpliv že znane sladkorne bolezni tipa 2 (T2DM) na izražanje IGF1R in celokupno preživetje.

Bolniki in metode. Izražanje IGF1R smo določili pri 167 zaporednih bolnikih z nedrobnoceličnim rakom pljuč, ki smo jih diagnosticirali in zdravili v univerzitetni ustanovi med 2005 in 2010. Vsi bolniki so prejeli vsaj en red standardnega citostatskega zdravljenja. Izražanje IGF1R smo določili imunohistokemijsko in kot pozitivno reakcijo upoštevali vrednost $\geq 1+$. Podatke o osnovnih značilnostih in sledenju bolnikov smo pridobili iz bolnišničnega informacijskega sistema. S χ^2 testom smo primerjali povezave med izražanjem IGF1R in kliničnimi značilnostmi. Celokupno preživetje smo ocenili s Kaplan–Meierjevo metodo in s testom *log-rank* opredelili razlike med podskupinami. Univariatno in multivariatno analizo smo naredili s Coxovim regresijskim modelom sorazmernih tveganj.

Rezultati. Izražanje IGF1R je bilo pozitivno pri 79,6 % bolnikov, statistično značilno pogosteje pri bolnikih s ploščatoceličnim rakom v primerjavi z ne-ploščatoceličnim (88,7 % proti 74,3 %; $P = 0,03$). Pozitivno izražanje IGF1R ni bilo povezano s sladkorno boleznijo ali ostalimi kliničnimi lastnostmi (spol, kadilski status, stanje splošne zmogljivosti). Srednja vrednost celokupnega preživetja je bila primerljiva med IGF1R pozitivno in IGF1R negativno skupino (10,2 proti 8,5 mesecev, $P = 0,168$) in med bolniki z ali brez T2DM (8,7 proti 9,8 mesecev, $P = 0,575$). Izražanje IGF1R in T2DM se nista izkazala kot neodvisna napovednika celokupnega preživetja v Coxovi analizi.

Zaključki. IGF1R ali T2DM nista bila statistično značilno napovedna v raziskovani skupini bolnikov z napredovalim nedrobnoceličnim rakom pljuč, zdravljenim z vsaj enim redom kemoterapije. Tudi povezave med T2DM in izražanjem IGF1R nismo dokazali. Zato so potrebne nadaljnje raziskave v večji skupini bolnikov z napredovalim nedrobnoceličnim rakom pljuč, z ali brez sladkorne bolezni, za opredelitev izražanja IGF1R in njegovega napovednega pomena ter terapevtskega vpliva.

RadiolOncol 2017; 51(2): 203-210.
doi:10.1515/raon-2017-0006

Togost karotidnih arterij, delovanje endotelija prstov rok in kalcinacije koronarnih arterij pri bolnikih z esencialno trombocitozo, brez klinično izražene aterosklerotične bolezni

Vrtovec M, Anžič A, Preložnik Zupan I, Zaletel K, Blinc A

Izhodišča. Bolniki z mieloproliferativnimi neoplazmami (MPN) imajo povečano tveganje za aterotrombotične zaplete. Namen raziskave je bil ugotoviti, ali imajo bolniki z vrsto MPN, esencialno trombocitozo (ET), ki še nimajo klinično izražene ateroskleroze, večjo togost karotidnih arterij, slabše delovanje endotelija in povečano kalcijevo breme koronarnih arterij v primerjavi s kontrolnimi preiskovanci.

Bolniki in metode. V raziskavo smo vključili 40 bolnikov z ET brez klinično izražene žilne bolezni, in 42 navidezno zdravih kontrolnih preiskovancev, ki so bili primerljivi bolnikom po starosti, spolu in srčnožilnem tveganju po framinghamski oceni. Vse preiskovance smo pregledali klinično in laboratorijsko, jim opravili ultrazvočno preiskavo karotidnih arterij, digitalno pletizmografijo z metodo EndoPat in z računalniško tomografijo določili kalcijevo breme koronarnih arterij.

Rezultati. Bolniki z ET in kontrolni preiskovanci se niso razlikovali v točkovanju karotidnih leh [1 (0-1.25) proti 0 (0-2), $p=0.30$], indeksu- β karotidne togosti [7.75 (2.33) proti 8.44 (2.81), $p=0.23$], hitrosti potovanja pulznega vala [6.21 (1.00) proti 6.45 (1.04) m/s; $p=0.46$], indeksu reaktivne hiperemije prstov rok [2.10 (0.57) proti 2.35 (0.62), $p=0.07$], ali v ojačitvenem indeksu [19 (3-30) proti 13 (5-22) %, $p=0.38$]. Celokupno kalcijevo breme koronarnih arterij se med skupinama ni razlikovalo [Agatstonov točkovnik 0.1 (0-16.85) proti 0 (0-8.55), $p=0.26$], značilno več bolnikov z ET pa je imelo povečano kalcijevo breme z vrednostjo Agatstonovega točkovnika >160 [6/40 proti 0/42, $p < 0.01$].

Zaključki. Med skupinama nismo našli značilnih razlik v ultrazvočno merjeni strukturi in funkciji karotidne arterije, v delovanju endotelija prstov rok ali v celokupnem kalcijevem bremenu koronarnih arterij. Značilno več bolnikov z ET kot kontrolnih preiskovancev je imelo povečano koronarno kalcijevo breme z vrednostjo Agatstonovega točkovnika >160 , kar je pomenilo veliko srčnožilno tveganje, ki ga framinghamski točkovnik ni napovedal.

Radiol Oncol 2017; 51(2): 211-220.
doi:10.1515/raon-2016-0016

Povečanje ekspresije CD64 na nevtrofilcih kot pokazatelj okužbe v trebuhu po operaciji debelega črevesa in danke

Kerin Povšič M, Beović B, Ihan A

Izhodišča. Okužbe so pogost zaplet zdravljenja po operaciji debelega črevesa in danke. Zgodnje klinične znake težko razlikujemo od sistemskega vnetnega odziva, ki ga povzroči operativni poseg. Pravočasna diagnoza okužbe lahko pomembno vpliva na preživetje. Zanimalo nas je, kateri biološki kazalec kmalu po operaciji najbolje napove kasnejšo okužbo. V raziskavo smo vključili več bioloških kazalcev in primerjali njihove napovedne vrednosti za okužbo: levkocite, razmerje med nevtrofilnimi granulociti in limfociti (NLR), C-reaktivni protein (CRP), prokalcitonin (PCT) in nov kazalec receptor CD64 na nevtrofilnih levkocitih, izražen kot indeks CD64n (iCD64n).

Metode. V prospektivno raziskavo smo vključili 200 bolnikov z elektivno operacijo raka debelega črevesa ali danke. Vrednosti bioloških kazalcev smo spremljali od prvega do petega pooperativnega dne. Napovedne vrednosti za okužbo smo ugotavljali z analizo ROC (*Receiver Operating Characteristics*). Za oceno napovednih kazalcev smo uporabili model Cox-ove regresije, za analizo preživetja pa metodo Kaplan-Meier.

Rezultati. Povečanje iCD64n po operaciji, izraženo kot razmerje iCD64n po operaciji/pred operacijo je bil boljši napovedni dejavnik za okužbo kot njegova absolutna vrednost. Najboljšo napovedno vrednost za vse okužbe 30 dni po operaciji smo ugotovili za CRP četrtega pooperativnega dne (AUC 0,72; 99 % interval zaupanja [CI] 0,61–0,83) in za NLR petega pooperativnega dne (AUC 0,69; 99 % CI 0,57–0,80). Najboljšo napovedno vrednost za okužbe organov/telesnih votlin 15 dni po operaciji smo ugotovili za razmerje iCD64n prvega pooperativnega dne (AUC 0,72; 99 % CI 0,58–0,86), tretjega pooperativnega dne (AUC 0,73; 99 % CI 0,59–0,87) in CRP tretjega pooperativnega dne (AUC 0,72; 99 % CI 0,57–0,86), četrtega pooperativnega dne (AUC 0,79; 99 % CI 0,64–0,93). Neodvisna dejavnika tveganja za okužbo po operaciji sta bila trajanje operacije in perioperativna transfuzija. Ugotovili smo, da je okužba po operaciji neodvisen negativen napovedni dejavnik za dolgoročno preživetje.

Zaključki. Razmerje iCD64n prvi dan po operaciji je najboljši zgodnji pokazatelj okužbe v trebuhu po operaciji debelega črevesa/danke. CRP napove okužbo z enako napovedno vrednostjo tretji dan po operaciji.

Radiol Oncol 2017; 51(2): 221-227.
doi:10.1515/raon-2016-0021

Pozne posledice na srčno-žilnem sistemu po zdravljenju raka mod

Gugić J, Zdravec Zaletel L, Oblak I

Izhodišča. Rak mod je najbolj pogosta maligna bolezen pri mlajših moških. Upoštevajoč naraščajočo incidenco, izjemno visoko stopnjo ozdravljivosti in dolgo pričakovano življenjsko dobo je ocena poznih posledic pri bolnikih zdravljenih zaradi raka mod zelo pomembna. Zaradi težnje, da bi zmanjšali škodljivost in obenem ohranili visoko učinkovitost zdravljenja, so v zadnjih desetletjih zdravljenje raka mod spreminjali.

Zaključki. Sedanja spoznanja o poznih posledicah zdravljenja temeljijo na uporabi zastarelih načinov zdravljenja. Podatkov o poznih posledicah modernejših načinov zdravljenja, ki so trenutno v uporabi, pa zaradi kratke opazovalne dobe še nimamo. Pozne posledice zdravljenja raka mod na srčno-žilnem sistemu predstavljajo poglavitne življenjsko nevarne zaplete po zdravljenju s platino vsebujočo kemoterapijo ter po obsevanju medpljučja in obsevanju pod prepono.

Radiol Oncol 2017; 228-234.
doi:10.1515/raon-2016-0050

Diozimetrični kazalci limfopenije, povzročene s paliativnim obsevanjem. Napovedna vrednost dozno-volumskih parametrov, ki temeljijo na telesnem obodu

Saito T, Toya R, Matsuyama T, Semba A, Oya N

Izhodišča. Z obsevanjem povezana limfopenija je združena s slabšim preživetjem bolnikov. Namen raziskave je bil opredeliti kazalce za limfopenijo po paliativni radioterapiji, s poudarkom na dozno-volumskih parametrih.

Bolniki in metode. Za potrebe retrospektivne analize bolnikov z različnimi raki, ki smo jih zdravili s paliativno radioterapijo, smo označili tri rizične organe: volumen, zamejen s telesnim obodom (telo A); volumen, ki je ostal po izključitvi zraka, plevralnega izliva, ascitesa, žolča, urina in črevesne vsebine (telo B); in volumen kostnega mozga. Ugotavljali smo absolutni volumen treh rizičnih organov, ki je prejel dozo 5–30 Gy in ocenili napovedno vrednosti za nastanek limfopenije stopnje 3 ali več (LP3+) po zdravljenju.

Rezultati. LP3+ je imelo 23 (43 %) izmed 54 bolnikov. Univariatna logistična regresijska analiza je pokazala, da so telo A V5, telo A V10, telo B V5, telo B V10, število frakcij in obsevanje vranice statistično pomembni napovedovalci LP3+ ($p < 0.05$). V multivariatni analizi so statistično značilnost ($p < 0,05$) zadržali telo A V5, telo A V10, telo B V5, telo B V10 in število frakcij. Dozno-volumski parametri kostnega mozga niso napovedovali limfopenije.

Zaključki. Višji dozno-volumski parametri, telo A in telo B ter število frakcij bi lahko bili kazalci za napoved hude limfopenije po paliativni radioterapiji.

Radiol Oncol 2017; 51(2): 235-240.
doi:10.1515/raon-2017-0012

Breme sevanja za mlade bolnike z rakom testisov pri slikanju z računalniško tomografijo ter z uporabo avtomatske kontrole izpostavljenosti in z kontrastnimi sredstvi

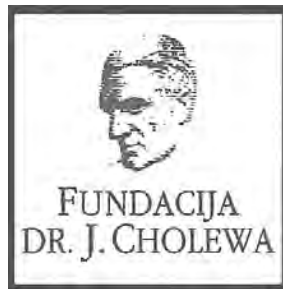
Niiniviita H, Kulmala J, Pölönen T, Heli Määttänen H, Järvinen H, Salminen E

Izhodišča. Namen raziskave je bil oceniti dozo, ki jo prejme bolnik pri slikanju celotnega telesa s računalniško tomografijo (CT) ter ugotoviti odvisnost te doze od velikosti bolnika, uporabe avtomatske kontrole izpostavljenosti (AKI) in intravenske aplikacije kontrastnega sredstva.

Bolniki in metode. Od aprila 2000 do aprila 2011 smo pri petinšestdesetih bolnikih z rakom testisov (povprečne starosti 28 let) naredili 279 slikanj celotnega telesa s CT. Povprečno število ponovnih slikanj je bilo 4,3. Za slikanja smo uporabili aparaturo GE Lightspeed 16 opremljeni z AKI in CT aparat Siemens Plus 4. Slikanje celega telesa smo v 216 primerih izvedli z intravensko apliciranim kontrastnim sredstvom, v 63 primerih pa brez njega. Efektivno dozo in dozo na posamezne organe smo določili s pomočjo programske opreme ImPACT.

Rezultati. Pri uporabi naprave Plus 4 je bila doza na bolnika neodvisna od velikosti bolnika (srednja vrednost 7,4 mSv, SD 1,7 mSv; $p < 0,41$). Pri slikanju z Lightspeed 16 z AKI pa se je doza statistično značilno povečala (srednja vrednost 14 mSv, SD 4,6 mSv; $p < 0,001$) z obsegom pasu. Slikanje s intravensko apliciranim kontrastnim sredstvom je povzročilo statistično značilno višjo izpostavljenost v primerjavi s slikanji brez uporabe kontrastnega sredstva (13 % pri slikanju s Plus4 v primerjavi s 35 % pri slikanju z Lightspeed 16; $p < 0,001$).

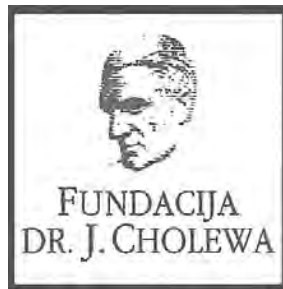
Zaključki. Da bi se izognili pretirani izpostavljenosti sevanju pri slikanju celotnega telesa mladih bolnikov z aparatom CT, je potrebna previdnost zlasti pri uporabi intravensko apliciranih kontrastnih sredstev, poleg tega pa je priporočljivo skrbno spremljanje parametrov AKI.



FUNDACIJA "DOCENT DR. J. CHOLEWA"
JE NEPROFITNO, NEINSTITUCIONALNO IN NESTRANKARSKO
ZDRUŽENJE POSAMEZNIKOV, USTANOV IN ORGANIZACIJ, KI ŽELIJO
MATERIALNO SPODBUJATI IN POGLABLJATI RAZISKOVALNO
DEJAVNOST V ONKOLOGIJI.

DUNAJSKA 106
1000 LJUBLJANA

IBAN: SI56 0203 3001 7879 431



Activity of "Dr. J. Cholewa" Foundation for Cancer Research and Education - a report for the second quarter of 2017

Dr. Josip Cholewa Foundation for cancer research and education continues with its planned activities in the second quarter of 2017. Its primary focus remains the provision of grants and scholarships and other forms of financial assistance for basic, clinical and public health research in the field of oncology. In parallel, it also makes efforts to provide financial and other support for the organisation of congresses, symposia and other forms of meetings to spread the knowledge about prevention and treatment of cancer, and finally about rehabilitation for cancer patients. In Foundation's strategy the spread of knowledge should not be restricted only to the professionals that treat cancer patients, but also to the patients themselves and to the general public.

The Foundation continues to provide support for »Radiology and Oncology«, a quarterly scientific magazine with a respectable impact factor that publishes research and review articles about all aspects of cancer. The magazine is edited and published in Ljubljana, Slovenia. »Radiology and Oncology« is an open access journal available to everyone free of charge. Its long tradition represents a guarantee for the continuity of international exchange of ideas and research results in the field of oncology for all in Slovenia that are interested and involved in helping people affected by many different aspects of cancer.

The Foundation will continue with its activities in the future, especially since the problems associated with cancer affect more and more people in Slovenia and elsewhere. Ever more successful treatment results in longer survival in many patients with previously incurable cancer conditions, thus adding many new dimensions in life of cancer survivors and their families.

Viljem Kovač M.D., Ph.D.
Borut Štabuc, M.D., Ph.D.
Tomaž Benulič, M.D.
Andrej Plesničar, M.D., M.Sc.



Iclusig® (ponatinib)

Ključ do učinkovitega zdravljenja bolnikov s KML in Ph + ALL



Zdravilo Iclusig® je peroralni zaviralec tirozin-kinaze (TKI) za doziranje enkrat dnevno z učinkovitim delovanjem pri odraslih bolnikih s KML in Ph+ ALL¹



Za bolnike s kronično mieloidno levkemijo (KML) v kronični, pospešeni ali blastni fazi, ki:

- so odporni na dasatinib ali nilotinib **ali**
- ne prenašajo dasatiniba ali nilotiniba in pri katerih nadaljnje zdravljenje z imatinibom ni klinično ustrezno **ali**
- imajo mutacijo T315I

Za bolnike z akutno limfoblastno levkemijo s prisotnim kromosomom Philadelphia (Ph+ ALL), ki:

- so odporni na dasatinib **ali**
- ne prenašajo dasatiniba in pri katerih nadaljnje zdravljenje z imatinibom ni klinično ustrezno **ali**
- imajo mutacijo T315I

SKRAJŠAN POVZETEK GLAVNIH ZNAČILNOSTI ZDRAVILA Iclusig 15 mg, 30 mg in 45 mg filmsko obložene tablete

Pred predpisovanjem natančno preberite celoten Povzetek glavnih značilnosti zdravila.

Samo za strokovno javnost.

▼ Za to zdravilo se izvaja dodatno spremljanje varnosti. Tako bodo hitreje na voljo nove informacije o njegovi varnosti. Zdravstvene delavce naprošamo, da poročajo o katerih koli domnevno neželenih učinkih zdravila.

Sestava: Ena filmsko obložena tableta vsebuje 15mg, 30mg ali 45 mg ponatiniba (v obliki ponatinibijevoga klorida). Indikacije: Zdravilo Iclusig je indicirano pri odraslih bolnikih s kronično mieloidno levkemijo (KML) v kronični fazi, pospešeni fazi ali blastni fazi, ki so odporni na dasatinib ali nilotinib; ki ne prenašajo dasatiniba ali nilotiniba in pri katerih nadaljnje zdravljenje z imatinibom ni klinično ustrezno; ali ki imajo mutacijo T315I ter pri odraslih bolnikih z akutno limfoblastno levkemijo s prisotnim kromosomom Philadelphia (Ph+ ALL), ki so odporni na dasatinib; ki ne prenašajo dasatiniba in pri katerih nadaljnje zdravljenje z imatinibom ni klinično ustrezno; ali ki imajo mutacijo T315I. Odmerjanje in način uporabe: Terapijo mora uvesti zdravnik z izkušnjami v diagnosticiranju in zdravljenju bolnikov z levkemijo. Med zdravljenjem se lahko bolniku nudi hematološka podpora, če je to klinično indicirano. Pred začetkom zdravljenja s ponatinibom je treba oceniti kardiovaskularni status bolnika, vključno z anamnezo in telesnim pregledom, in aktivno obravnavati kardiovaskularne dejavnike tveganja. Kardiovaskularni status je treba še naprej spremljati in med zdravljenjem s ponatinibom optimizirati zdravljenje z zdravili in podporno zdravljenje stanj, ki prispevajo h kardiovaskularnim tveganjem.

Odmerjanje: Priporočeni začetni odmerak ponatiniba je 45 mg enkrat na dan. Potrebno je razmisлити o ukinitvi ponatiniba, če v 3 mesecih ni celovitega hematološkega odgovora. Z zdravljenjem je treba prenehati, če se pojavijo znaki napredovane bolezn ali v primeru hudih neželenih učinkov. Prilagoditev odmerjanja: tveganje za žilni okluzivni dogodek je verjetno povezano z odmerkom. Zdravljenje z zdravilom Iclusig je treba pri sumu, da se je pri bolniku razvil arterijski ali venski okluzivni dogodek, takoj prekiniti. Ko se dogodek razreši, je treba pri odločitvi o ponovni uvedbi zdravljenja upoštevati oceno koristi in tveganj. Pri obravnavi hematoloških in nehematoloških težavstev je treba razmisлити o prilagoditvi ali prekinitvi odmerjanja. V primeru hudih neželenih učinkov je treba z zdravljenjem prekiniti. Prilagoditev odmerka je priporočljiva v primeru navrtopenje ali trombotičnega, ki nista povezani z levkemijo, pri pankreatitisu in zvišani ravni lipaze/amilaze. Način uporabe: tablete je treba pogoltniti cele, ne sme se jih drobiti ali razpustiti, lahko pa se jih jamlje s hrano ali brez nje. Kontraindikacije: Preobčutljivost na ponatinib ali katero koli pomožno snov. Posebna opozorila in previdnostni ukrepi: *Milozosupresija* – Zdravilo Iclusig je povezano s hudo trombotičnostjo, navrtopenjem in anemijo. Prve 3 mesece je treba vsaka 2 tedna opraviti pregled celotne krvne slike, nato pa mesečno ali kot je klinično indicirano. *Žilna okluzija* – Pojavili so se arterijski in venska tromboza in okluzija, vključno s smrtim miokardnim infarktom, možgansko kapjo, nezalna žilna okluzija, v nekaterih primerih povezana s trajno okvaro vida ali slepoto, stenozo velikih arterijskih žil v možganih, hudo periferno žilno boleznijo in potrebo po nujnem postopku revaskularizacije.

Zdravilo Iclusig se ne sme uporabljati pri bolnikih z miokardnim infarktom, predhodno revaskularizacijo ali možgansko kapjo v anamnezi, razen če so močno koristi zdravljenja večje od možnih tveganj. Med zdravljenjem s ponatinibom je treba spremljati znake trombotične in žilne okluzije in zdravljenje je treba takoj prekiniti, če se pojavi žilna okluzija. V primeru, da se pojavi poslabšanje vida ali zamegljen vid, je treba opraviti oftalmološki pregled (vključno s funduskopijo). *Hipertenzija* – Pri zdravljenju z zdravilom Iclusig se je pojavila z zdravljenjem povezana hipertenzija (vključno s hipertenzivno krizo), ki lahko pripelje k tveganju arterijskih trombotičnih dogodkov. Zato je treba ob vsakem obisku zdravnika spremljati krvni tlak. Zdravljenje z zdravilom Iclusig je treba prekiniti, če hipertenzija ni pod zdravniškim nadzorom. *Kongestivno srčno popuščanje* – Pojavilo se je smirno in neno srčno popuščanje ter dogodki, povezani s predhodnimi vaskularnimi okluzivnimi dogodki. Bolnika je treba spremljati in jih zdraviti, kot je klinično ustrezno, vključno s prekinitvijo zdravljenja z zdravilom Iclusig. Pri bolnikih, pri katerih se razvije neno srčno popuščanje, je treba razmisлити o ukinitvi ponatiniba. *Pankreatitis in serumska lipaza* – Pogostnost pojava pankreatitisa je večja prva 2 meseca uporabe. Prva 2 meseca vsaka 2 tedna preverjajte serumsko lipazo, nato pa periodično. Morda bo treba odmerak prekiniti ali zmanjšati. Če zvišanje ravni lipaz spremljajo abdominalni simptomi, je treba z uporabo zdravila Iclusig prenehati in preveriti, ali ima bolnik pankreatitis. Pri bolnikih s pankreatitisom ali zlorabe alkohola v anamnezi se pripravite na prehodnost. Bolnikas hudo ali zelo hudo hipertrioglobulinemijo je treba ustrezno obravnavati. *Laktaza* – Zdravilo Iclusig vsebuje laktazo monohidrat. Bolniki z rednimi dihalnimi težavami neprimerne galaktose, laktosne oblike zmanjšane aktivnosti laktaze ali slabo absorpcijo glukoze-galaktose ne smejo jemati tega zdravila. *Podajanje intervala QT* – Klinično pomembnih učinkov na interval QT ni mogoče izključiti. *Hepatotoksičnost* – Lahko se zvišajo ravni ALT, AST, bilirubina in alkalne fosfataze. Opazilno jetrno odpoved (vključno s smrtim izdomom). Teste delovanja jeter je treba opraviti pred uvedbo zdravljenja in nato periodično, kot je klinično indicirano. *Krvavitve* – Pojavili so se smirni ter resni hemoragični dogodki. Pri resni ali hudi krvavitvi je treba zdravljenje z zdravilom Iclusig prekiniti. *Okvara jeter* – Pri bolnikih s hudo okvaro jeter se pripravite na prehodnost. *Okvara ledvic* – Pri bolnikih z ocenjenim odstotkom kreatinina < 50 ml/min ali ledvično boleznijo v zadnjem stadiju se pripravite na prehodnost. *Starjši bolniki* – Verjetnost neželenih učinkov je večja. *Podatkovna populacija* – Varnost in učinkovitost zdravila Iclusig pri bolnikih starih do 18 let, se nista bili dokazani. *Medsebojno delovanje z drugimi zdravili in druge oblike interakcije*: Sočasni uporabi zdravila Iclusig z močnimi induktorji CYP3A4 se je treba izogniti; pri sočasni uporabi močnih zaviralcev CYP3A4 je potrebna previdnost, razmisлити pa je treba tudi o uporabi zdravila Iclusig z začetnim odmerkom 30 mg, potrebna je previdnost pri sočasno uporabljenih substratih P-glikoproteina (P-gp) ali baljalkovne resistance za raka dojke (BCRP). Pri sočasni uporabi ponatiniba z zdravili proti stitjuvanju krvi pri bolnikih, pri katerih obstaja tveganje za krvavitve, je potrebna previdnost. *Ploščnost, nespečnost in dojenje*: Znanjem v rodni dobi je treba svetovati, da naj v času zdravljenja z zdravilom Iclusig ne zasnojo, možnim pa, da naj v času zdravljenja ne zplodijo otroka. Med zdravljenjem je treba uporabljati

alternativno ali dodatno metodo kontracepcije. Ni zadostnih podatkov o uporabi zdravila Iclusig pri nosečnicah. Studije na živalih so pokazale vpliv na sposobnost razmnoževanja. Če se zdravilo uporablja med nosečnostjo, je treba bolnico obvestiti o možnih tveganjih za plod. Z dojenjem je treba med zdravljenjem z zdravilom Iclusig prenehati. Vpliv na sposobnost vožnje in upravljanja s stroji: Pri vožnji ali upravljanju strojev je potrebna previdnost. Neželeni učinki: Zelo pogosti (> 1/10): okužba zgornjih dihal, nespečnost, anamija, zmanjšanje števila trombocitov, zmanjšanje števila nevtrofilcev, zmanjšanje apetita, glavobol, omotica, hipertenzija, dispneja, kašelj, bolečina v trebuhu, driska, bruhanje, zaprtje, navzea, zvišanje ravni lipaz, zvišanje ravni alanin aminotransferaze, zvišanje ravni aspartat-aminotransferaze, izpuščaji suha koža, bolečina v kosteh, artralgijs, mialgija, bolečina v okončinah, bolečina v hrbtu, mišični krči, utrujenost, astenija, periferni edem, preleptja, bolečina. Pogosti (> 1/100 do < 1/10): pljučnica, sepsa, folikulitis, pancitopenija, febrilna navrtopenja, zmanjšanje števila levkocitov, dehidracija, zastajanje tekočine, hipokalciemija, hiperkalemija, hiperurkemija, hipofosfatemija, hiperglicemija, hipokalcemija, zmanjšanje telesne mase, cerebrovaskularni dogodki, cerebralni infarkt, periferna navrtopenja, letargija, migrena, hiperparatiroidizem, hipoestezija, parestezija, prehodni ishemični napad, zamegljen vid, suha oči, periorbitalni edem, odem veke, srčno popuščanje, miokardni infarkt, kongestivno srčno popuščanje, bolezen koronarnih arterij, angina pektoris, perikardni izliv, atrijska fibrilacija, zmanjšanje telesnega debla, periferna arterijska okluzivna bolezen, periferna ishemijska stenozna periferna arterija, intermitentna kladivacija, globoka venska tromboza, vročinski obliki, zaprtost, pljučna embolija, pljučni tili, epistaksa, disfonija, pljučna hipertenzija, pankreatitis, zvišanje amilaz v krvi, gastrogogačna refluksna bolezen, stomatitis, dispepsija, trebušna distenzija, nelagodje v trebuhu, suha usta, zvišanje ravni bilirubina v krvi, zvišanje ravni alkalne fosfataze v krvi, zvišanje ravni gama-glutamyltransferaze, pruritični izpuščaji, ekfoliativni izpuščaji, eritem, alopecija, parutis, ekfoliacija kože, nočno potenje, hiperhidroza, petahije, ekhimoza, boleča koža, ekfoliativni dermatitis, mišično-skeletna bolečina, bolečina v vratu, mišično-skeletna bolečina v prsnem košu, arektna disfunkcija, mrzlica, grip podobna bolezen, nekardogena bolečina v prsnem košu, tujli vozki, obrabni edem. Občasni (> 1/1000 do < 1/100): sindrom tumorske lize, cerebralna arterijska stenozna, tromboza mrežične vene, okluzija mrežične vene, okluzija mrežične arterije, okvara vida, miokardna ishemijska, akutni koronarni sindrom, kardialno nelagodje, ishemična kardiomiopatija, spazem koronarnih arterij, disfunkcija levega prekata, atrjska undulacija, slaba periferna cirkulacija, vranski infarkt, venska embolija, venska tromboza, hipertenzivna kriza, krvavitve v želodcu, hepatotoksičnost, odpoved jeter, zatratnica. Različni izdelki zdravila: Predpisovanje in izdaja zdravila je la na recept. Imenik dovoljenja za promet z zdravilom: ARIAD Pharma Ltd., Riverbridge House, Guilford Road, Leatherhead, Surrey KT22 9AD, Velika Britanija. Zadeja revizija besedila: marec 2016. Informacija pripravljena: april 2016. Podrobnejše informacije o zdravilu Iclusig so na voljo pri predstavniku imetnika dovoljenja za promet z zdravilom: Angalini Pharma d.o.o., Kopska ulica 108A, 1000 Ljubljana, Tel.: +386 1 544 65 79, E-pošta: info@angalini.si



Predstavniki:
Angelini Pharma d.o.o.
Kopska ulica 108 A, Ljubljana

➤ PRVA REGISTRIRANA TERAPIJA
V 2. LINIJI ZA ZDRAVLJENJE
ADENOKARCINOMA ŽELODCA ALI
GASTRO-EZOFAGEALNEGA PREHODA¹


CYRAMZA™
(ramucirumab)

UKREPAJTE ZDAJ



**USPOSOBLJENI
ZA SPREMEMBE,
ZA NEPRIMERLJIVE
IZKUŠNJE**

Skrajšan povzetek glavnih značilnosti zdravila

▼ Za to zdravilo se izvaja dodatno spremljanje varnosti. Tako bodo hitreje na voljo nove informacije o njegovi varnosti. Zdravstvene delavce naprošamo, da poročajo o katerem koli domnevnem neželenem učinku zdravila.

Cyramza 10 mg/ml koncentrat za raztopino za infundiranje

En mililiter koncentrata za raztopino za infundiranje vsebuje 10 mg ramucirumaba. Ena 10-mililitrska viala vsebuje 100 mg ramucirumaba. **Terapevtske indikacije** Zdravilo Cyramza je v kombinaciji s paklitakselom indicirano za zdravljenje odraslih bolnikov z napredovalim rakom želodca ali adenokarcinomom gastro-efozagealnega prehoda z napredovalo boleznijo po predhodni kemoterapiji, ki je vključevala platino in fluoropirimidin. Monoterapija z zdravilom Cyramza je indicirana za zdravljenje odraslih bolnikov z napredovalim rakom želodca ali adenokarcinomom gastro-efozagealnega prehoda z napredovalo boleznijo po predhodni kemoterapiji s platino ali fluoropirimidinom, za katere zdravljenje v kombinaciji s paklitakselom ni primerno. Zdravilo Cyramza je v kombinaciji s shemo FOLFIRI indicirano za zdravljenje odraslih bolnikov z metastatskim kolorektalnim rakom (mCRC), z napredovanjem bolezni ob ali po predhodnem zdravljenju z bevacizumabom, oksaliplatinom in fluoropirimidino. Zdravilo Cyramza je v kombinaciji z docetakselom indicirano za zdravljenje odraslih bolnikov z lokalno napredovalim ali metastatskim nedrobnoceličnim pljučnim rakom, z napredovanjem bolezni po kemoterapiji na osnovi platine. **Odmernanje in način uporabe** Zdravljenje z ramucirumabom morajo uvesti in nadzirati zdravniki z izkušnjami onkologiji. **Odmernanje Rak želodca in adenokarcinomom gastro-efozagealnega prehoda** Priporočeni odmerek ramucirumaba je 8 mg/kg 1. in 15. dan 28-dnevnega cikla, pred infuzijo paklitakselata. Priporočeni odmerek paklitakselata je 80 mg/m² in se daje z intravenskim infundiranjem, ki traja približno 60 minut, 1., 8. in 15. dan 28-dnevnega cikla. Pred vsakim infundiranjem paklitakselata je treba pri bolnikih pregledati celotno krvno sliko in izvide kemičnih preiskav krvi, da se oceni delovanje jeter. Priporočeni odmerek ramucirumaba kot monoterapije je 8 mg/kg vsaka 2 tedna. **Kolorektalni rak** Priporočeni odmerek ramucirumaba je 8 mg/kg vsaka 2 tedna, dan z intravensko infuzijo pred dajanjem sheme FOLFIRI. Pred kemoterapijo je treba bolnikom odvzeti kri za popolno krvno sliko. **Nedrobnocelični pljučni rak (NSCLC)** Priporočeni odmerek ramucirumaba je 10 mg/kg na 1. dan 21-dnevnega cikla, pred infuzijo docetakselata. Priporočeni odmerek docetakselata je 75 mg/m², dan z intravensko infuzijo približno 60 minut na 1. dan 21-dnevnega cikla. **Premedikacija** Pred infundiranjem ramucirumaba je priporočljiva premedikacija z antagonistom histaminskih receptorjev H1. **Način uporabe** Po redčenju se zdravilo Cyramza daje kot intravenska infuzija v približno 60 minutah. Zdravila ne dajajte v obliki intravenskega bolusa ali hitre intravenske injekcije. Da boste dosegli zahtevano trajanje infundiranja približno 60 minut, največja hitrost infundiranja ne sme preseči 25 ml/minuto, saj morate sicer podaljšati trajanje infundiranja. Bolnika je med infundiranjem treba spremljati glede znakov reakcij, povezanih z infuzijo, zagotoviti pa je treba tudi razpoložljivost ustrezne opreme za oživiljanje. **Kontraindikacije** Pri bolnikih z NSCLC je ramucirumab kontraindiciran, kjer gre za kavitacijo tumorja ali prepletenost tumorja z glavnimi žilami. **Posebna opozorila in previdnostni ukrepi** Trajno prekinite zdravljenje z ramucirumabom pri bolnikih, pri katerih se pojavijo resni arterijski tromboembolični dogodki, gastrointestinalne perforacije, krvavitve stopnje 3 ali 4, če zdravstveno pomembne hipertenzije ni mogoče nadzirati z antihipertenzivnim zdravljenjem ali če se pojavi fistula, raven beljakovin v urinu > 3 g/24 ur ali v primeru nefrotskega sindroma. Pri bolnikih z neuravnavano hipertenzijo zdravljenje z ramucirumabom ne sme uvesti, dokler oziroma v kolikor obstoječa hipertenzija ni uravnavana. Pri bolnikih s ploščatocelično histologijo obstaja večje tveganje za razvoj resnih pljučnih krvavitev. Če se pri bolniku med zdravljenjem razvijejo zapleti v zvezi s celjenjem rane, prekinite zdravljenje z ramucirumabom, dokler rana ni povsem zaceljena. V primeru pojava stomatitisa je treba takoj uvesti simptomatsko zdravljenje. Pri bolnikih, ki so prejeli ramucirumab in docetaksel za zdravljenje napredovalnega NSCLC z napredovanjem bolezni po kemoterapiji na osnovi platine, so opazili trend manjše učinkovitosti naraščajočo starostjo. **Plodnost, nosečnost in dojenje** Ženskam v rodni dobi je treba svetovati, naj se izognejo zanositvi med zdravljenjem z zdravilom Cyramza in jih je treba seznaniti z možnim tveganjem za nosečnost in plod. Ni znano, ali se ramucirumab izloča v materino mleko. **Neželeni učinki** **Želo pogosti** ($\geq 1/10$) nevtropenija, levkopenija, trombocitopenija, hipoalbuminemija, hipertenzija, epistaksa, gastrointestinalne krvavitve, stomatitis, driska, proteinurija, utrujenost/astenija, periferni edem, bolečina v trebuhu. **Pogosti** ($\geq 1/100$ do $< 1/10$) hipokaliemija, hiponatriemija, glavobol. **Rok uporabnosti** 3 leta. **Posebna navodila za shranjevanje** Shranjujte v hladilniku (2 °C–8 °C). Ne zamrzujte. Vialo shranjujte v zunanji ovojnini, da zagotovite zaščito pred svetlobo. **Pakiranje** 2 viali z 10 ml. **IMETNK BOV OLJENJA ZA PROMET Z ZDRAVILOM** Eli Lilly Nederland B.V., Papendorpseweg 83, 3528 BJ Utrecht, Nizozemska. **DATUM ZADNJE REVIZIJE BESEDILA** 25.01.2016

Režim izdaje: Predpisovanje in izdaja zdravila je le na recept, z zdravilo pa se uporablja samo v bolnišnicah.

Pomembno obvestilo:

Pričujoče gradivo je namenjeno samo za strokovno javnost. Zdravilo Cyramza se izdaja le na recept. Pred predpisovanjem zdravila Cyramza vas v ljudno prosimo, da preberete celotni Povzetek glavnih značilnosti zdravila Cyramza. Podrobnejše informacije o zdravilu Cyramza in o zadnji reviziji besedila Povzetka glavnih značilnosti zdravila so na voljo na sedežu podjetja Eli Lilly (naslov podjetja in kontaktni podatki spodaj) in na spletni strani European Medicines Agency (EMA): www.ema.europa.eu. In na spletni strani European Commission <http://ec.europa.eu/health/documents/community-register/html/alfregister.htm>.

Eli Lilly farmacevtska družba, d.o.o., Dunajska cesta 167, 1000 Ljubljana, telefon: (01) 5800 010, faks: (01) 5691 705

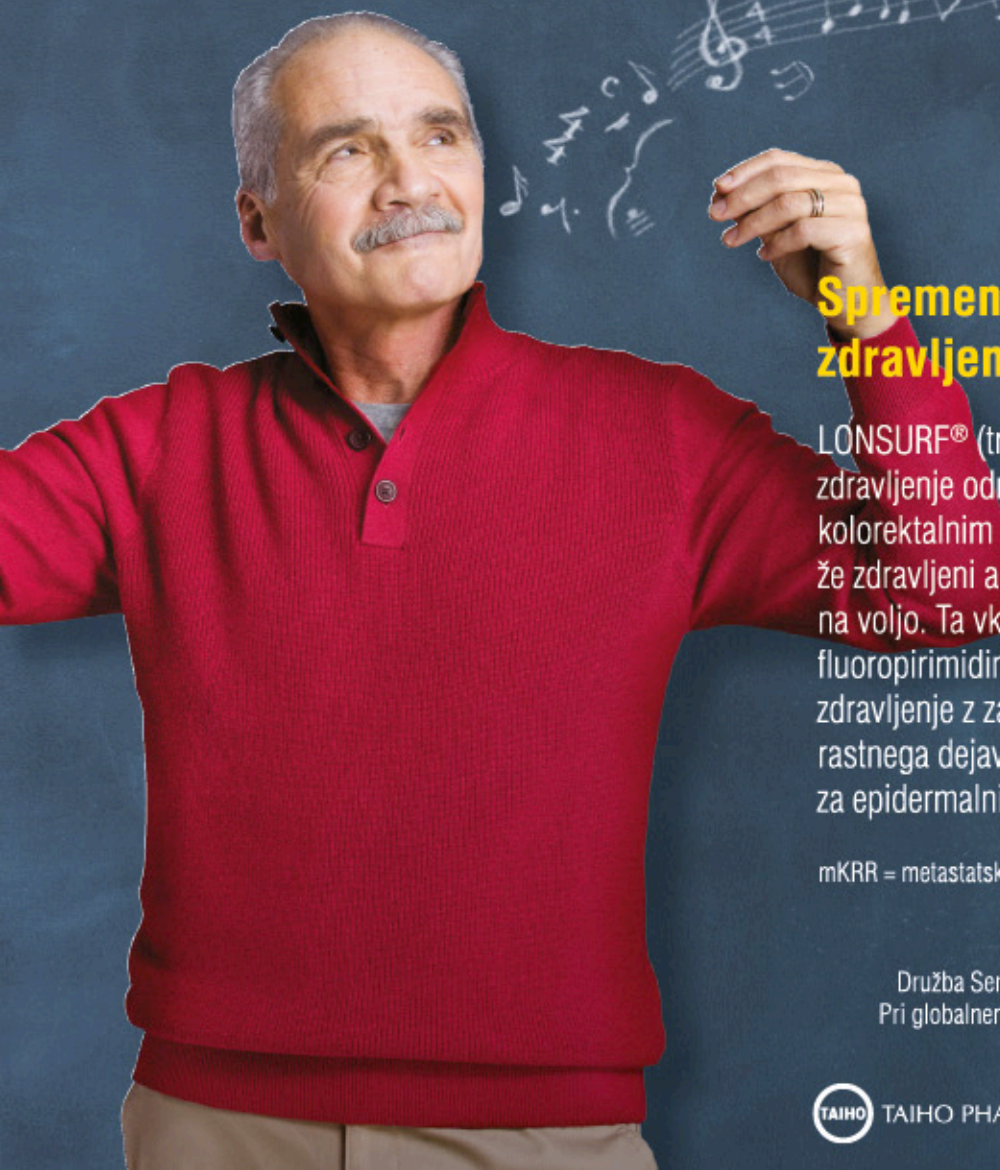
Referenca: 1. Cyramza, Povzetek glavnih značilnosti zdravila, zadnja odobrena verzija.

EERA W00010a, 12.02.2016.



Zdravilo za predhodno že zdravljene bolnike z mKRR

Več časa za trenutke, ki štejejo



Lonsurf
trifluridin/tipiracil

Spremeni zgodbo predhodno že zdravljenih bolnikov z mKRR

LONSURF® (trifluridin/tipiracil) je indiciran za zdravljenje odraslih bolnikov z metastatskim kolorektalnim rakom (mKRR), ki so bili predhodno že zdravljeni ali niso primerni za zdravljenja, ki so na voljo. Ta vključuje kemoterapijo na osnovi fluoropirimidina, oksaliplatina in irinotekana, zdravljenje z zaviralci žilnega endotelijskega rastnega dejavnika (VEGF) in zaviralci receptorjev za epidermalni rastni dejavnik (EGFR).

mKRR = metastatski kolorektalni rak

Družba Servier ima licenco družbe Taiho za zdravilo Lonsurf®. Pri globalnem razvoju zdravila sodelujeta obe družbi in ga tržita v svojih določenih področjih.



TAIHO PHARMACEUTICAL CO., LTD.



Skratizni povzetek glavnih značilnosti zdravila: Lonsurf 15 mg/6,14 mg filmsko obložene tablete in Lonsurf 20 mg/8,19 mg filmsko obložene tablete

▼ Za to zdravilo se izvaja dodatno spremljanje varnosti. **SESTAVA:** Lonsurf 15 mg/6,14 mg: Ena filmsko obložena tableta vsebuje 15 mg trifluridina in 6,14 mg tipiracila (v obliki klorida). Lonsurf 20 mg/8,19 mg: Ena filmsko obložena tableta vsebuje 20 mg trifluridina in 8,19 mg tipiracila (v obliki klorida). **TERAPEVTSKE INDIKACIJE:** Zdravilo Lonsurf je indicirano za zdravljenje odraslih bolnikov z metastatskim kolorektalnim rakom, ki so bili predhodno že zdravljeni ali niso primerni za zdravljenja, ki so na voljo. Ta vključuje kemoterapijo na osnovi fluoropirimidina, oksaliplatina in irinotekana, zdravljenje z zaviralci žilnega endotelijskega rastnega dejavnika (VEGF - Vascular Endothelial Growth Factor) in zaviralci receptorjev za epidermalni rastni dejavnik (EGFR - Epidermal Growth Factor Receptor). **ODMERJANJE IN NAČIN UPORABE:** Odrmerjanje: Priporočeni dnevni odmerek zdravila Lonsurf pri odraslih je 35 mg/m² odmerek peroralno dvakrat dnevno na 1. do 5. dan in 8. do 12. dan vsakega 28-dnevnega cikla zdravljenja, najpozneje 1 ura po zaključku jutranjega in večernega obroka. Odrmerjanje, uračunano glede na telesno površino, ne sme presegati 80 mg/odmerek. Močne prilagoditve odmerka glede na varnost in prenašanje zdravila: dovoljena so največ 3 zmanjšanja odmerka na najmanjši odmerek 20 mg/m² dvakrat dnevno. Polem ko je bil odmerek zmanjšan, povečanje ni dovoljeno. **KONTRAINDIKACIJE:** Preobčutljivost na zdravilni učinkovini ali kateri koli pomožni snov. **OPOMBUJENA IN PREVIDNOSTNI UKREPI:** Supresija kostnega mozga: Pred uvedbo zdravljenja, pred vsakim ciklom zdravljenja in po potrebi je treba pregledati celotno krvno sliko. Zdravljenje ne sme začeti, če je absolutno število nevtrifilov < 1,5 x 10⁹/l, če je število trombocitov < 75 x 10⁹/l ali če se je pri bolniku zaradi predhodnih zdravljenj pojavila klinična sprememba nehematološke toksičnosti 3. ali 4. stopnje, ki še traja. Bolnike je treba skrbno spremljati zaradi morebitnih okužb, uvedbi je treba ustrezne ukrepe, kot je klinično indicirano. Toksičnost za prebavila: Potrebna je uporaba antiemetikov, antiidiaroidov ter drugih ukrepov, kot je klinično indicirano. Če je potrebno, prilagodite odmerke. Ledvična okvara: Zdravilo Lonsurf ni primerno za uporabo pri bolnikih s hudo ledvično okvaro ali karčno stopnjo ledvične okvare. Bolnike z zmerno ledvično okvaro je treba zaradi hematološke toksičnosti bolj pogosto spremljati. Jetna okvara: Uporaba zdravila Lonsurf pri bolnikih z obstoječo zmerno ali hudo jetno okvaro ni priporočljiva. Preležanine: Pred začetkom zdravljenja in med njim je priporočljiva spremljanje preležanine z urinskimi testnimi lističi. Pomožne snovi: Vsebujejo laktozo. **INTERAKCIJE:** Zdravila, ki medsebojno delujejo z nukleozidnimi prenosilci CNT1, ENT1 in ENT2, zaviralci OCT2 ali MATE1, substrati humane timidin-kinaze (npr. zidovudinom), hormonskimi kontraceptivi. **PLODNOST, NOSEČNOST IN DOJENJE:** Ni priporočljiva. **KONTRACELIJA:** Ženske in moški morajo uporabljati učinkovito metodo kontracepcije med zdravljenjem in do 6 mesecev po zaključku zdravljenja. **VPLIV NA SPOSOBNOST VOŽNJE IN UPRAVLJANJA S STROJI:** Med zdravljenjem se lahko pojavijo utrujenost, omotica ali splošno slabo počutje. **NEŽELENI UČINKI:** Zelo pogosti: nevropatija, levkopanija, anemija, trombocitopenija, eritropenija, zmanjšan apetit, diareja, navzea, bruhanje, utrujenost. Pogosti: okužba spodnjih dihal, okužba zgornjih dihal, febrilna nevropatija, limfopenija, monocitopenija, hipoburimija, nespečnost, disgeuzija, periferna nevropatija, omotica, glavobol, vročinski oblivi, dispneja, kašelj, bolečina v trebuhu, zaprtje, stomatitis, bolezi ustne votline, hiperbilirubinemija, sindrom palmarne plantarne eritrodizestezije, izgubljanje, alopecija, pruritus, suha koža, preležanine, piroksija, edem, vnetje sluznice, splošno slabo počutje, zvišanje jetrnih encimov, zvišanje alkalne fosfatase v krvi, zmanjšanje telesne mase. Občasni: sepični šok, infekcijski enteritis, pljučnica, okužba žolčevoda, gripa, okužba soč, vnetje ušesa, herpes zoster, tinea pedis, kardialna, bakterijska okužba, okužba, bolečina zaradi raka, pancitopenija, granulocitopenija, monocitopenija, eritropenija, levkocitoza, dehidracija, hiperglikemija, hipokalemija, hipokalcemija, hipotenzija, hipermagnezija, hiponatremija, hiponatriemija, hipokalcemija, profin, anksioznost, nevrotoksičnost, disestezija, hiperestezija, hipostezijska, sindroma, parestezija, pekoč občutek, letargija, zmanjšane ostrine vida, zamajen vid, diplopija, katarakta, konjunktivitis, suho oko, vrtoglavica, neugodje v ušesu, angina pektoris, aritmija, papilacija, embolija, hiperterzija, hipotenzija, pljučna embolija, pleuralni izliv, izcedek iz nosu, distonija, ortostatska bolečina, epistaksa, hemoragični enterokolitis, krvavitev v prebavilih, akutni pankreatitis, ascites, ileus, subileus, kolitis, gastritis, refluksni gastritis, ezofagitis, meleno praznjenje želodca, abdominalna distenzija, analno vnetje, razjede v ustih, dispagija, gastrozofagealna refleksna bolezen, proktalgija, bukalni polip, krvavitve dlesni, glositis, parodontalna bolezen, bolezen zob, siljenje na bruhanje, flatulenca, slab zadah, hepatotoksičnost, razširitev žolčnih vodov, luščenje kože, urtikarija, preobčutljive reakcije na svetlobo, eritem, akne, hiperhidroza, žulj, bolni natož, otekanje sklepov, atrofija, bolečina, hemoragični enterokolitis, bolečina v kosteh, mialgija, mišično-skeletna bolečina, mišična oslabilost, mišični krči, bolečina v okončinah, občutek teže, ledvična odpoved, nefritični cistitis, močne mikcije, hematurija, levkopanija, močne menstruacije, poslabšanje splošnega zdravstvenega stanja, bolečina, občutek spremembe telesne temperature, kserozna, zvišanje kreatinina v krvi, podaljšanje intervala QT na elektrokardiogramu, povečanje mednarodnega umernega razmerja (INR), podaljšanje aktiviranega parcialnega trombotičnega časa (aPTC), zvišanje sečnine v krvi, zvišanje lokalne dihidrogenaze v krvi, znižanje celokupnih proteinov, zvišanje C-reaktivnega proteina, zmanjšan hematokrit. **Post-marketske okužbe:** pri bolnikih, zdravljenih z zdravilom Lonsurf na Japonskem, so poročali o arimih intersticijske bolezni slije. **PREVELIKO ODMERJANJE:** Neželeni učinki, o katerih so poročali v povezavi s prevelikim odmerjanjem, so bili v skladu z uveljavljenim vznosnim profilom. Glavni pričakovani zaplet prevelikega odmerjanja je supresija kostnega mozga. **FARMAKODINAMIČNE LASTNOSTI:** Farmakoterapevtska skupina: zdravila z delovanjem na novotvorbo, aritmeličarji, oznaka ATC: L01BC59. Zdravilo Lonsurf sestavlja antineoplastični timidinski nukleozidni analog, trifluridin, in zaviralec timidin-raztopilaze (TPase), tipiraciljev klorid. Po pripravi v rakave celice timidin-kinaza fosforilira trifluridin. Ta se v celicah nato presnovi v substrat deoksiribonukleotidske kisline (DNA), ki se vgradi neposredno v DNA ter tako preprečuje celično proliferacijo. TPase hitro razgradi trifluridin in njegova presnove po peroralni uporabi je hitra zaradi učinkovitega prehoda, zato je v zdravilo vključen zaviralec TPase, tipiraciljev klorid. **PAKIRANJE:** 20 filmsko obloženih tablet. **NAČIN PREDPISOVANJA IN IZDAJANJA ZDRAVILA:** Rp/Spec. **Imetnik dovoljenja za promet z zdravilom:** Les Laboratoires Servier, 50, rue Carnot, 92284 Guresnes cedex, Francija. **Številka dovoljenja za promet z zdravilom:** EU/1/16/1096/001 (Lonsurf 15 mg/6,14 mg), EU/1/16/1096/004 (Lonsurf 20 mg/8,19 mg). * Pred predpisovanjem preberite celoten povzetek glavnih značilnosti zdravila. Datum zadnje revizije besedila: marec 2017. **Celoten povzetek glavnih značilnosti zdravila in podrobnejše informacije so na voljo pri: Servier Pharma d.o.o., tel: 01 563 48 11, www.servier.si.**

Datum priprave informacije: april 2017.
LNF16/17C2A02 Samo za strokovno javnost.



**THE MOST ADVANCED
ELECTROPORATION TECHNOLOGY**
for treatment of tumour nodules located to the
skin, subcutaneous tissue, parenchyma and bone.

Instructions for authors

The editorial policy

Radiology and Oncology is a multidisciplinary journal devoted to the publishing original and high quality scientific papers and review articles, pertinent to diagnostic and interventional radiology, computerized tomography, magnetic resonance, ultrasound, nuclear medicine, radiotherapy, clinical and experimental oncology, radiobiology, radiophysics and radiation protection. Therefore, the scope of the journal is to cover beside radiology the diagnostic and therapeutic aspects in oncology, which distinguishes it from other journals in the field.

The Editorial Board requires that the paper has not been published or submitted for publication elsewhere; the authors are responsible for all statements in their papers. Accepted articles become the property of the journal and, therefore cannot be published elsewhere without the written permission of the editors.

Submission of the manuscript

The manuscript written in English should be submitted to the journal via online submission system Editorial Manager available for this journal at: www.radioloncol.com.

In case of problems, please contact Sašo Trupej at saso.trupej@computing.si or the Editor of this journal at gsera@onko-i.si

All articles are subjected to the editorial review and when the articles are appropriated they are reviewed by independent referees. In the cover letter, which must accompany the article, the authors are requested to suggest 3-4 researchers, competent to review their manuscript. However, please note that this will be treated only as a suggestion; the final selection of reviewers is exclusively the Editor's decision. The authors' names are revealed to the referees, but not vice versa.

Manuscripts which do not comply with the technical requirements stated herein will be returned to the authors for the correction before peer-review. The editorial board reserves the right to ask authors to make appropriate changes of the contents as well as grammatical and stylistic corrections when necessary. Page charges will be charged for manuscripts exceeding the recommended length, as well as additional editorial work and requests for printed reprints.

Articles are published printed and on-line as the open access (www.degruyter.com/view/j/raon).

All articles are subject to 700 EUR + VAT publication fee. Exceptionally, waiver of payment may be negotiated with editorial office, upon lack of funds.

Manuscripts submitted under multiple authorship are reviewed on the assumption that all listed authors concur in the submission and are responsible for its content; they must have agreed to its publication and have given the corresponding author the authority to act on their behalf in all matters pertaining to publication. The corresponding author is responsible for informing the coauthors of the manuscript status throughout the submission, review, and production process.

Preparation of manuscripts

Radiology and Oncology will consider manuscripts prepared according to the Uniform Requirements for Manuscripts Submitted to Biomedical Journals by International Committee of Medical Journal Editors (www.icmje.org). The manuscript should be written in grammatically and stylistically correct language. Abbreviations should be avoided. If their use is necessary, they should be explained at the first time mentioned. The technical data should conform to the SI system. The manuscript, excluding the references, tables, figures and figure legends, must not exceed 5000 words, and the number of figures and tables is limited to 8. Organize the text so that it includes: Introduction, Materials and methods, Results and Discussion. Exceptionally, the results and discussion can be combined in a single section. Start each section on a new page, and number each page consecutively with Arabic numerals.

The Title page should include a concise and informative title, followed by the full name(s) of the author(s); the institutional affiliation of each author; the name and address of the corresponding author (including telephone, fax and E-mail), and an abbreviated title (not exceeding 60 characters). This should be followed by the abstract page, summarizing in less than 250 words the reasons for the study, experimental approach, the major findings (with specific data if possible), and the principal conclusions, and providing 3-6 key words for indexing purposes. Structured abstracts are required. Slovene authors are requested to provide title and the abstract in Slovene language in a separate file. The text of the research article should then proceed as follows:

Introduction should summarize the rationale for the study or observation, citing only the essential references and stating the aim of the study.

Materials and methods should provide enough information to enable experiments to be repeated. New methods should be described in details.

Results should be presented clearly and concisely without repeating the data in the figures and tables. Emphasis should be on clear and precise presentation of results and their significance in relation to the aim of the investigation.

Discussion should explain the results rather than simply repeating them and interpret their significance and draw conclusions. It should discuss the results of the study in the light of previously published work.

Charts, Illustrations, Images and Tables

Charts, Illustrations, Images and Tables must be numbered and referred to in the text, with the appropriate location indicated. Charts, Illustrations and Images, provided electronically, should be of appropriate quality for good reproduction. Illustrations and charts must be vector image, created in CMYK color space, preferred font "Century Gothic", and saved as .AI, .EPS or .PDF format. Color charts, illustrations and Images are encouraged, and are published without additional charge. Image size must be 2.000 pixels on the longer side and saved as .JPG (maximum quality) format. In Images, mask the identities of the patients. Tables should be typed double-spaced, with a descriptive title and, if appropriate, units of numerical measurements included in the column heading. The files with the figures and tables can be uploaded as separate files.

References

References must be numbered in the order in which they appear in the text and their corresponding numbers quoted in the text. Authors are responsible for the accuracy of their references. References to the Abstracts and Letters to the Editor must be identified as such. Citation of papers in preparation or submitted for publication, unpublished observations, and personal communications should not be included in the reference list. If essential, such material may be incorporated in the appropriate place in the text. References follow the style of Index Medicus, DOI number (if exists) should be included.

All authors should be listed when their number does not exceed six; when there are seven or more authors, the first six listed are followed by "et al.". The following are some examples of references from articles, books and book chapters:

Dent RAG, Cole P. In vitro maturation of monocytes in squamous carcinoma of the lung. *Br J Cancer* 1981; **43**: 486-95. doi:10.1038/bjc.1981.71

Chapman S, Nakielnny R. *A guide to radiological procedures*. London: Bailliere Tindall; 1986.

Evans R, Alexander P. Mechanisms of extracellular killing of nucleated mammalian cells by macrophages. In: Nelson DS, editor. *Immunobiology of macrophage*. New York: Academic Press; 1976. p. 45-74.

Authorization for the use of human subjects or experimental animals

When reporting experiments on human subjects, authors should state whether the procedures followed the Helsinki Declaration. Patients have the right to privacy; therefore the identifying information (patient's names, hospital unit numbers) should not be published unless it is essential. In such cases the patient's informed consent for publication is needed, and should appear as an appropriate statement in the article. Institutional approval and Clinical Trial registration number is required. Retrospective clinical studies must be approved by the accredited Institutional Review Board/Committee for Medical Ethics or other equivalent body. These statements should appear in the Materials and methods section.

The research using animal subjects should be conducted according to the EU Directive 2010/63/EU and following the Guidelines for the welfare and use of animals in cancer research (*Br J Cancer* 2010; **102**: 1555 – 77). Authors must state the committee approving the experiments, and must confirm that all experiments were performed in accordance with relevant regulations.

These statements should appear in the Materials and methods section (or for contributions without this section, within the main text or in the captions of relevant figures or tables).

Transfer of copyright agreement

For the publication of accepted articles, authors are required to send the License to Publish to the publisher on the address of the editorial office. A properly completed License to Publish, signed by the Corresponding Author on behalf of all the authors, must be provided for each submitted manuscript.

The non-commercial use of each article will be governed by the Creative Commons Attribution-NonCommercial-NoDerivs license.

Conflict of interest

When the manuscript is submitted for publication, the authors are expected to disclose any relationship that might pose real, apparent or potential conflict of interest with respect to the results reported in that manuscript. Potential conflicts of interest include not only financial relationships but also other, non-financial relationships. In the Acknowledgement section the source of funding support should be mentioned. The Editors will make effort to ensure that conflicts of interest will not compromise the evaluation process of the submitted manuscripts; potential editors and reviewers will exempt themselves from review process when such conflict of interest exists. The statement of disclosure must be in the Cover letter accompanying the manuscript or submitted on the form available on www.icmje.org/coi_disclosure.pdf

Page proofs

Page proofs will be sent by E-mail to the corresponding author. It is their responsibility to check the proofs carefully and return a list of essential corrections to the editorial office within three days of receipt. Only grammatical corrections are acceptable at that time.

Open access

Papers are published electronically as open access on www.degruyter.com/view/j/raon, also papers accepted for publication as E-ahead of print.



XALKORI® - prvi zaviralec ALK, odobren za I. linijo zdravljenja napredovalega, ALK pozitivnega nedrobnoceličnega pljučnega raka¹

ALK = anaplastično limfomsko krczo

BISTVENI PODATKI IZ POVZETKA GLAVNIH ZNAČILNOSTI ZDRAVILA

XALKORI 200 mg, 250 mg trde kapsule

▼ Za to zdravilo se izvaja dodatno spremljanje varnosti. Tako bodo hitreje na voljo nove informacije o njegovi varnosti. Zdravstvene delavce naprošamo, da poročajo o katerikoli domnevnem neželenem učinku zdravila. Glejte poglavje 4.8 povzetka glavnih značilnosti zdravila, kako poročati o neželenih učinkih. **Sestava in oblika zdravila:** Ena kapsula vsebuje 200 mg ali 250 mg krizotiniba. **Indikacije:** Prva linija zdravljenja odraslih bolnikov z napredovalim nedrobnoceličnim pljučnim rakom (NSCLC - Non-Small Cell Lung Cancer), ki je ALK (anaplastična limfomska krcza) pozitiven. Zdravljenje odraslih bolnikov s predhodno zdravljenim, napredovalim NSCLC, ki je ALK pozitiven. Zdravljenje odraslih bolnikov z napredovalim NSCLC, ki je ROS1 pozitiven. **Odmerjanje in način uporabe:** Zdravljenje mora uvesti in nadzorovati zdravnik z izkušnjami z uporabo zdravil za zdravljenje rakavih bolezni. **Preverjanje prisotnosti ALK in ROS1:** Pri izbiri bolnikov za zdravljenje je treba pred zdravljenjem opraviti točno in validirano preverjanje prisotnosti ALK ali ROS1. **Odmerjanje:** Priporočeni odmerek je 250 mg dvakrat na dan (500 mg na dan), bolniki pa morajo zdravilo jemati brez prekinitev. Če bolnik pozabi vzeti odmerek, ga mora vzeti takoj, ko se spomni, razen če do naslednjega odmerka manjka manj kot 6 ur. V tem primeru bolnik pozabljenega odmerka ne sme vzeti. **Prilagoditve odmerka:** Glede na varnost uporabe zdravila pri posameznem bolniku in kako bolnik zdravljenje prenaša, utegne biti potrebno prekinitev in/ali zmanjšanje odmerka zdravila na 200 mg dvakrat na dan. Če je potrebno še nadaljnje zmanjšanje, pa znaša odmerek 250 mg enkrat na dan. Za prilagoditve odmerkov pri hematološki in nehematološki (povečanje vrednosti AST, ALT, bilirubina, ILD/pnevmonitis; podaljšanje intervala QTc, bradikardija, boleznin oči) toksičnosti glejte poglavje 4.8 v povzetku glavnih značilnosti zdravila. **Oviro jeter:** Pri blagi in zmerni oviri je zdravljenje treba izvajati previdno, pri hudi oviri se zdravila ne sme uporabljati. **Oviro ledvic:** Pri blagi in zmerni oviri prilagajanje začetnega odmerka ni priporočeno. Pri hudi oviri ledvic (ki ne zahteva peritonealne dialize ali hemodialize) je začetni odmerek 250 mg peroralno enkrat na dan; po vsaj 4 tednih zdravljenja se lahko poveča na 200 mg dvakrat na dan. **Starejši bolniki (U 65 let):** Prilagajanje začetnega odmerka ni potrebno. **Pediatrična populacija:** Varnost in učinkovitost nista bili dokazani. Način uporabe: Kapsule je treba pogoltni cele, z nekaj vode, s hrano ali brez nje. Ne sme se jih zdrobiti, razstaviti ali odpreti. Izogibati se je treba uživanju grenik, grenikinega soka ter uporabi šentjanževke. **Kontraindikacije:** Neobčutljivost na krizotinib ali katerikoli pomožni snov. Huda ovira jeter. **Posebna opozorila in previdnostni ukrepi:** Določanje statusa ALK in ROS1: Pomembno je izbrati dobro validirano in robustno metodologijo, da se izognemo lažno negativnim ali lažno pozitivnim rezultatom. **Hepatotoksičnost:** V kliničnih študijah so poročali o hepatotoksičnosti, ki jo je povzročilo zdravilo (vključno s primeri s smrtnim izidom). Delovanje jeter, vključno z ALT, AST in skupnim bilirubinom, je treba preveriti enkrat na teden v prvih 2 mesecih zdravljenja, nato pa enkrat na mesec in kot je klinično indicirano. Ponovni preverjanj morajo biti pogostejši pri povečani vrednosti stopnje 2, 3 ali 4. **Interakcijska bolezen pljuč (ILD)/pnevmonitis:** Lahko se pojavi huda, življenjsko nevarna ali smrtna ILD/pnevmonitis. Bolnike s simptomi ILD/pnevmonitisa, je treba spremljati, zdravljenje pa prekiniti ob sumu na ILD/pnevmonitis. **Podaljšanje intervala QTc:**

Opazili so podaljšanje intervala QTc. Pri bolnikih z obstoječo bradikardijo, podaljšanjem intervala QTc v anamnezi ali pred izpolnjenimi znanji, pri bolnikih, ki jemljejo antiaritmike ali druga zdravila, ki podaljšujejo interval QT, ter pri bolnikih s pomembno obstoječo srčno boleznijo in/ali motnjami elektrolitov je treba krizotinib uporabljati previdno; potrebno je redno spremljanje EKG, elektrolitov in delovanja ledvic; preskavi EKG in elektrolitov je treba opraviti čim bližje uporabi prvega odmerka, potem se priprava redno spremljanje. Če se interval QTc podaljša za 60 ms ali več, je treba zdravljenje s krizotinibom začasno prekiniti in se posvetovati s kardiologom. Bradikardija: Lahko se pojavi simptomatska bradikardija (lahko se razvije več tednov po začetku zdravljenja); izogibati se je treba uporabi krizotiniba v kombinaciji z drugimi zdravili, ki povzročajo bradikardijo; pri simptomatski bradikardiji je treba prilagoditi odmerek. **Srčno popuščanje:** Poročali so o hudih, življenjsko nevarnih ali smrtnih neželenih učinkih srčnega popuščanja. Bolnike je treba spremljati glede pojavov znakov in simptomov srčnega popuščanja in ob pojavu simptomov zmanjšati odmerjanje ali prekiniti zdravljenje. **Nevtropenija in levkopenija:** V kliničnih študijah so poročali o nevtropeniji, levkopeniji in febrilni nevtropeniji; spremljati je treba popolno krvno sliko (pogostejše preskave, če se opazijo abnormalnosti stopnje 3 ali 4 ali če se pojavi povišana telesna temperatura ali okužba). **Perforacija v prebavilih:** V kliničnih študijah so poročali o perforacijah v prebavilih, v obdobju trženja pa o smrtnih primerih perforacij v prebavilih. Krizotinib je treba pri bolnikih s tveganjem za nastanek perforacije v prebavilih uporabljati previdno; bolniki, pri katerih se razvije perforacija v prebavilih, se morajo prenehati zdraviti s krizotinibom; bolnike je treba poučiti o prvih znakih perforacije in jim svetovati, naj se nemudoma posvetujejo z zdravnikom. **Vplivi na ledvice:** V kliničnih študijah so opazili zvišanje ravni kreatinina v krvi in zmanjšanje očistka kreatinina. V kliničnih študijah in v obdobju trženja so poročali tudi o odpovedi ledvic, akutni odpovedi ledvic, primerih s smrtnim izidom, primerih, ki so zahtevali hemodializo in hiperkalemiji stopnje 4. **Vplivi na vid:** V kliničnih študijah so poročali o izgubi vidnega polja stopnje 4 z izgubo vida. Če se na novo pojavi huda izguba vida, je treba zdravljenje prekiniti in opraviti oftalmološki pregled, če so motnje vida trdovratne ali se poslabšajo, je priporočljivo oftalmološki pregled. **Histološka preskava, ki ne nakazuje adenokarcinoma:** Na voljo so le omejeni podatki pri NSCLC, ki je ALK in ROS1 pozitiven in ima histološke značilnosti, ki ne nakazujejo adenokarcinoma, vključno s ploščatoceličnim karcinomom (SCC). **Medsebojno delovanje z drugimi zdravili in druge oblike interakcij:** Zdravilo, ki lahko poveča koncentracije krizotiniba v plazmi (močni zaviralci CYP3A4, npr. atazanavir, indinavir, neflavinir, ritonavir, sakvinavir, itakonazol, letkolonazol, vorikonazol, klaritromicin, telitromicin, toleandomicin), tudi grenivke in grenikvin sok. Zdravila, ki lahko zmanjšajo koncentracije krizotiniba v plazmi (močni induktorji CYP3A4, npr. karbamazepin, fenobarbital, fenitoin, rifampicin, šentjanževka). **Zmerni induktorji CYP3A4, npr. efavirenz in rifabutin.** Zdravila, katerih koncentracije v plazmi lahko krizotinib spremeni (midazolam, alfentanil, cisaprid, ciklosporin, derivati ergot alkaloidov, fentanil, pimozid, kinidin, sirolimus, takrolimus, bupropion, efavirenz, peroralni kontraceptivi, raltegravir, inotekan, morfin, nalokson, digoksin, dabigatran, kolhicin, prazosin, mefloformin, prokinamid). Zdravila, ki podaljšujejo interval QT ali ki lahko



povzročijo Torsades de pointes (antiaritmiki skupine IA (kinidin, disopiramid), antiaritmiki skupine III (amiodaron, sotalol, dofetilid, ibutilid), metadon, cisaprid, moksifloksacin, antipsihotiki). Zdravila, ki povzročajo bradikardijo (nedihidropiridinski zaviralci kalcijevih kanalčkov (verapamil, diltiazem), antagonist adrenergičnih receptorjev beta, klonidin, guanfacin, digoksin, meflokin, antiholinesteraze, pilokarpin). **Plodnost, nosečnost in dojenje:** Ženske v rodni dobi se morajo izogibati zanositvi. Med zdravljenjem in najmanj 90 dni po njem je treba uporabljati ustrezno kontracepcijo (velja tudi za moške). Zdravilo lahko škoduje plodu in se ga med nosečnostjo ne sme uporabljati, razen če klinično stanje matere ne zahteva takega zdravljenja. Matere naj se med jemanjem zdravila dojenja izogibajo. Zdravilo lahko zmanjša plodnost moških in žensk. **Vpliv na sposobnost vožnje in upravljanja strojev:** Lahko se pojavijo simptomatska bradikardija (npr. sinkopa, omotica, hipotenzija), motnje vida ali utrujenost; potrebna je previdnost. **Neželeni učinki:** Najnevarnejši neželeni učinki so bili hepatotoksičnost, ILD/pnevmonitis, nevtropenija in podaljšanje intervala QT. Najpogostejši neželeni učinki (U 25 %) so bili motnje vida, navzea, diareja, bruhanje, edem, zaprtje, povečane vrednosti transaminaz, utrujenost, pomanjkanje apetita, omotica in nevropatija. Ostali veliki pogosti (U 1/10 bolnikov) neželeni učinki so: nevtropenija, anemija, levkopenija, disgeuzija, bradikardija, bolečina v trebuhu in izpuščaji. **Način in režim izdaje:** Predpisovanje in izdaja zdravila je le na recept, zdravilo pa se uporablja samo v bolnišnicah. Izjemoma se lahko uporablja pri nadaljevanju zdravljenja na domu ob odpuštu iz bolnišnice in nadaljnjem zdravljenju. **Imetnik dovoljenja za promet:** Pfizer Limited, Ramsgate Road, Sandwich, Kent CT13 9NJ, Velika Britanija. **Da tam zadnje revizije be se dil:** 11.11.2016 **Pred predpisovanjem se seznanite s celotnim povzetkom glavnih značilnosti zdravila.**

Vir: 1. Povzetek glavnih značilnosti zdravila Xalkori, 11.11.2016



Pfizer Luxembourg SARI, GRAND DUCHY OF LUXEMBOURG, 51, Avenue J.F. Kennedy, L-1855, Pfizer podružnica Ljubljana, Letališka cesta 3c, 1000 Ljubljana

